# Investigations of Cross Section Model and Near Detector Choices for DUNE.

Jake Calcutt[1], Joshua Hignight[1], and Kendall Mahn[1]

[1]Michigan State University

## 1 Executive Summary

As part of the DUNE ND Taskforce, we have studied if the neutrino interaction model could affect any of DUNE's goals. To do this, we have looked at how different interaction models, used here as proxies for uncertainties, couple to different NDs and the FD. This was done by using three different event generators, GENIE, NEUT, and NuWro, which all have different FSI and 2p2h models. While it is not guaranteed that the physics of nature corresponds to any of these software packages, the different choices made by the generators can act as a proxy for possible variations in the neutrino interaction model. Using these three event generators, we have studied their impact on a number of different physics parameters which could affect DUNE's results. Currently we have looked at the sufficiency of the QE and 2p2h parameterization in the DUNE ND taskforce. We have also investigated the role of neutrons and protons in the reconstructed neutrino energy to the three ND configurations.

We first consider a "perfect" ND and FD without any efficiencies applied, and then look what changes as we consider the three different configurations of the ND and a simple LAr efficiency in the FD. Currently, only full efficiency information is know for the Fine-Grained Tracker. For the High Pressure Gaseous Argon TPC and Liquid Argon TPC, only simple efficiencies with a proton threshold of 100 MeV/c and 200 MeV/c, respectively, have been applied.

From these studies we have concluded that even though the pure-$Q^2$ parameterization and the binning developed by VALOR would cover model variations for $\nu_\mu$ and $\overline{\nu}_\mu$ CCQE events, there are some discrepancies at high-$Q^2$. This is an example of how the choice of the ND configuration can couple to model uncertainties. The 2p2h $\nu_\mu$ and $\overline{\nu}_\mu$ events appear to be covered by the current 1-bin parameterization, but this approach may neglect some of the physics present in the models studied.

There are large differences across generators in the neutron multiplicity predicted for all processes. However, this difference between the generators is not seen once a ND to FD extrapolation is taken into account. Neutrons still remain important in energy reconstruction, though, because as much as 50% of the energy can be taken away by the neutron in CCQE events. The proton multiplicity vs momentum does show differences in the near to far extrapolation. Despite this, the overall proton threshold does not seem to be of concern for the ND.

This is only a first pass of our investigations in to how neutrino interaction models could affect DUNE. For future work we would like to further investigate: the origins of high-$Q^2$ variations in CCQE, extend all studies to include the LAr and GAr efficiency and acceptance information when available, include pions when efficiencies are available, study the ability for GENIE FSI errors to cover differences between generators and final state energy, and study the effect on the reconstructed neutrino energy of applying efficiencies to each final state particle independently. For full details on how this study was done and how we came to the conclusion, please see [?] for the details.

# 2 Overview

The Deep Underground Neutrino Experiment (DUNE) is a next-generation long baseline neutrino experiment designed to search for CP violation and establish the neutrino mass hierarchy. It consists of both a near and far detector (ND and FD) separated by 1300km and uses a neutrino beam created at Fermilab.[1]. While the design of the far detector has been decided to be Liquid Argon, there are still ongoing efforts in deciding the configuration of the near detector. The main ND design includes a Fine-Grained Tracker (FGT) with possible inclusion of additional detectors. Under consideration for these additional detectors are a Liquid (LArTPC) or High Pressure Gaseous Argon TPC (GArTPC). DUNE's physics goals require systematic uncertainties in the interaction model to be below the 2% limit after a near to far extrapolation[2]. The focus of this document is to quantify how the neutrino interaction model could affect DUNE's goals. This work was done concurrent with the DUNE ND Taskforce (NDTF), and so the studies investigate possible weaknesses and limitations of the current parameterization of neutrino interaction uncertainties. The studies also explore how different interaction models, used as proxies for variations in a given model, couple to the different NDs and the FD.

Below is a list of the studies we have conducted for this work.

- Choice of parameterization.
  - The sufficiency of a pure-$Q^2$ parameterization in a near to far extrapolation. Are variations in CCQE and 2p2h models covered in this parameterization? Does the $Q^2$ parameterization ignore additional physics as represented as variations in $q_0$ - $q_3$?
- The different abilities of the three ND configurations to reconstruct the neutrino energy.
  - The energy lost to neutrons.
  - How do different ND configurations couple to model differences in variations in proton and pion multiplicity and momentum?

– Difference from true neutrino energy. How do the above effects couple to reconstructed energy?

# 3 Methods

## 3.1 Monte Carlo Generators

Neutrino interaction modeling is of great interest to current and future oscillation experiments. Currently, there are a few different neutrino interaction software packages, referred to here as "generator". While it is not guaranteed that the physics of nature corresponds to any of these software packages, the different choices made by the generators can act as a proxy for possible variations in the neutrino interaction model. The models considered span a range of different "vertex-level" interaction models (e.g. CCQE, 2p2h) and Final State Interaction (FSI) models. These are given in Table 1.

## 3.2 Generating Events

Sets of $\nu$ and $\overline{\nu}$ events with an Argon-40 target are produced with these generators according to the 2015 DUNE CDR fluxes [7], shown in Figure 1 for $\nu_\mu$ at the ND and FD. The oscillation parameters used for the FD fluxes are included in Table 2. Note that the $\nu_\mu$ and $\overline{\nu}_\mu$ flux correspond to the Forward and Reverse Horn Current (FHC and RHC) modes, respectively. No "wrong-sign" studies, where there are $\overline{\nu}_\mu$ within the primary $\nu_\mu$ beam, are considered in this work. The various data sets are then passed through the NUISANCE[6] software to reduce the outputs to a common format, in turn saving all final state particle information for each event. Various event types are studied separately. These event types are true-CCQE, true-2p2h, CC0$\pi$, CC1$\pi$, and CCOther and are defined in Table 3. Note that for CCQE and 2p2h, though these are based on generator-level reaction modes, they are defined by 1 reconstructed lepton in the final state if efficiencies are applied.

| Generator | Version | Model |
|---|---|---|
| GENIE[3] | 2.10 | RFG |
| NEUT[4] | 5.3.6 | Nieves et. al RPA+2p2h/MEC ($M_A = 1.01$) |
| NuWro[5] | 11 | LFG + RPA + Nieves et. al |

Table 1: The various Monte Carlo event generators used for this work.

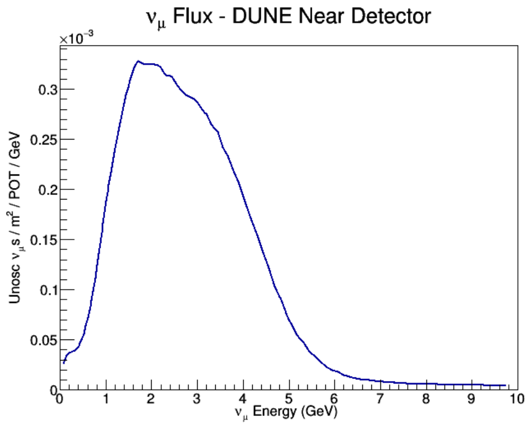


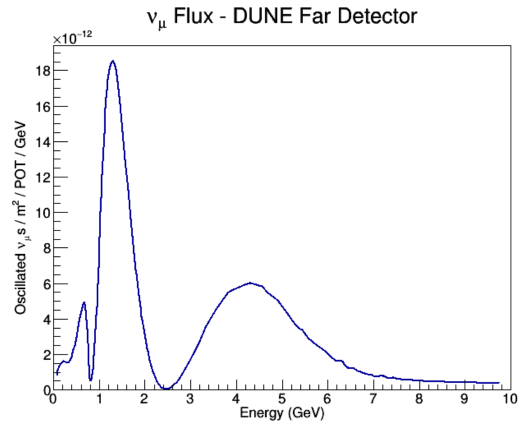


Figure 1: $\nu_\mu$ flux at DUNE ND (Left) and FD (Right)

| Parameter | Central Value | Relative Uncertainty |
|---|---|---|
| $\theta_{12}$ | 0.5843 | 2.3% |
| $\theta_{23}$ (NH) | 0.738 | 5.9% |
| $\theta_{23}$ (IH) | 0.864 | 4.9% |
| $\theta_{13}$ | 0.148 | 2.5% |
| $\Delta m^2_{21}$ | $7.5 \times 10^{-5}\text{eV}^2$ | 2.4% |
| $\Delta m^2_{31}$ (NH) | $2.457 \times 10^{-3}\text{eV}^2$ | 2.0% |
| $\Delta m^2_{31}$ (IH) | $-2.449 \times 10^{-3}\text{eV}^2$ | 1.9% |

Table 2: Oscillation parameters used for FD fluxes.

| Event Type | Definition |
|---|---|
| True-CCQE | MC-level CCQE mode |
| True-2p2h | MC-level 2p2h mode |
| CC0$\pi$ | 0 $\pi^\pm$, 1 lepton, any number of protons and $\pi^0$ in final state. |
| CC1$\pi$ | 1 $\pi^\pm$, 1 lepton, any number of protons and $\pi^0$ in final state. |
| CCOther | 1 lepton, any number of $\pi^\pm$, protons, and $\pi^0$ in final state. |

Table 3: Definitions of various event types distinguished within our studies. Note that CCQE and 2p2h are based on MC-level reaction mode, but must also have 1 lepton in the final state if efficiencies are applied.

## 3.3 Near to Far Flux Comparisons

The various studies regarding near to far extrapolations are explored using the following procedure. Ratios of either NEUT or NuWro to GENIE, referred to as "single ratios", separately at the ND and FD are taken. NEUT and NuWro are both normalized to GENIE to highlight shape differences rather than overall normalization effects. These offer insight into model variations and how the dependence of ND configuration couple to these variations. The effect of a near to far extrapolation is approximated by taking a "double ratio" between the near and far single ratios. To be explicit, these are defined in Equations 1 and 2, where "Other MC" refers to either NEUT or NuWro and "near" can be replaced by "far" in the single ratio. We note this is a crude approximation to give intuition about the problem for just a single reaction process; a fit to the ND spectrum will have multiple reactions in a given topology which can complicate the determination of physics effects for a single reaction.

$$\text{ND Single Ratio} = \frac{(\text{Other MC @ Near Detector})}{(\text{GENIE @ Near Detector})} \tag{1}$$

$$\text{Double Ratio} = \frac{(\text{ND Single Ratio})}{(\text{FD Single Ratio})} \tag{2}$$

Note that the studies in Section 5.1 use a slightly different near to far ratio, where the rates for a single generator is compared between ND and FD as in Figure 13.

## 3.4 Detector Configurations and Efficiencies

These studies highlight the effect of applying efficiencies of the various detectors. We first consider a "perfect" ND and FD without any efficiencies applied, and then look what changes as we consider the three different configurations of the ND and a simple LAr efficiency in the FD.

Efficiency information is included with the following procedure. Each particle is randomly accepted or rejected by throwing a random number and checking against the efficiency according to the particle's momentum. No angular efficiencies have yet been taken into account for this work, but a brief check with the FGT showed almost full angular efficiency due to track-quality cuts. At the time of this writing, only a full description of the FGT efficiency according to NDTF samples is available, but other configurations will be added to subsequent versions of this note. An example of the efficiency for protons in the FGT is given in Figure 2; FGT efficiencies for other particles are included in Appendix **??**. We also lack knowledge of the efficiencies for $\pi^0$ in the FGT, so we accept all of these in this configuration. Because we do not have the efficiencies for the LAr and GAr, simple thresholds for protons are applied for the GAr, 100 MeV/c, and LAr ND and FD, 200 MeV/c. We also make no assumptions for the efficiencies of $\mu$, $\pi^{+,-}$, and $\pi^0$ in the simple descriptions, and so all of these types of particles are accepted in the LAr and GAr.

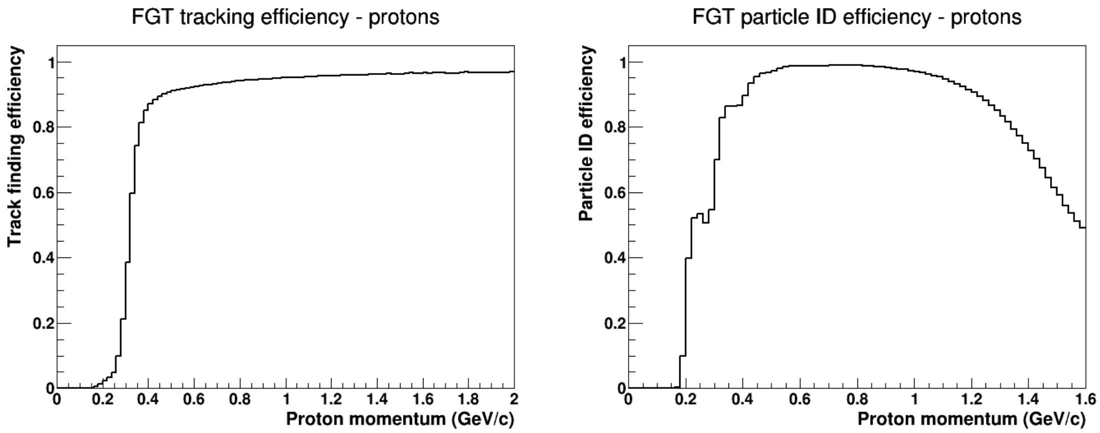


Figure 2: Left: Tracking efficiency for protons in FGT. Right: PID efficiency for protons in FGT. Total efficiency for a given proton momentum is given by the product of the two efficiencies.

# 4 Parameterization

The VALOR software package has been used on multiple T2K oscillation analyses, and has recently been used to study the DUNE near detector configurations. The VALOR group has contributed to optimization studies for DUNE[8], and has defined a $Q^2$ parameterization, used to parametrize uncertainties according to model variations, for neutrinos and anti-neutrinos as:

- CCQE $\nu_\mu$ with $Q^2$ bins {0 - 0.20, 0.20 - 0.55, >0.55} GeV$^2$
- CCQE $\overline{\nu}_\mu$ with $Q^2$ bins {0 - 0.20, 0.20 - 0.55, >0.55} GeV$^2$
- 2p2h $\nu_\mu$ with 1 $Q^2$ bin
- 2p2h $\overline{\nu}_\mu$ with 1 $Q^2$ bin

This portion of the work seeks to determine if variations in CCQE and 2p2h models are well represented by these parameterizations in $Q^2$. It also serves to highlight the behavior of the models as they couple to FSI and detector effect as we use a reconstructed $Q^2$ when efficiencies are applied. The variations are also studied in $q_0$ vs. $q_3$ to check if a pure-$Q^2$ parameterization is sufficient.

## 4.1 $Q^2$ Parameterization

The single and double ratio procedure described in Section 3.3 is conducted using events created by all three generators at the ND and FD and distributed according to $Q^2$. This is done separately with and without efficiencies, for both $\nu_\mu$ and $\overline{\nu}_\mu$, and for true-CCQE and true-2p2h. Applying efficiencies allows us to investigate how the interaction model can couple to detector effects. For distributions without efficiencies, the MC-level $Q^2$ quantity is used, giving us insight into the interaction model uncertainties. However, when including efficiencies, $Q^2$ becomes a reconstructed quantity, as it is calculated from the final state particles that are accepted after efficiencies are applied. This is highlighted in Equations 3 - 6. Though we call it "reconstructed", it is calculated using the true energies and momentums without smearing applied, so it is not truly reconstructed in the usual sense of the word. Using this reconstructed quantity reveals how interaction/FSI variations, and detector acceptance effects couple together.

$$Q^2 = |q_0^2 - q_3^2|, \tag{3}$$

$$q_0^2 = (E_{reco} - E_{lep})^2, \tag{4}$$

$$q_3^2 = (\vec{P}_{reco} - \vec{P}_{lep})^2 \tag{5}$$

$$E_{reco} = E_{lep} + \Sigma E_\pi + \Sigma(E_{prot} - M_{prot}) \tag{6}$$

Conclusions are drawn from the double ratios according to the following prescription. as a crude approximation, we look for if the ratio is flat, i.e. if a horizontal line is within the statistical error bars, in a given bin of the parameterization.

For $\nu_\mu$ CCQE events, both NEUT's and NuWro's models differ significantly from GENIE's model in $Q^2$ distributions, as seen in the single ratios in Figure 3. Despite this, the double ratios for both NEUT to GENIE and NuWro to GENIE remain relatively flat and close to 1, with small amounts of variation in the higher $Q^2$ region.

For double ratios with FGT efficiencies applied to the ND and simple LAr efficiencies applied to the FD, shape variations are greater above ~1.25 GeV$^2$ as seen in Figure 4. This is an example of how the choice of ND configuration can couple to model uncertainties. These studies will be expanded in the future to increase statistics and determine the origin of the variation in this region. We suspect that the loss if low momentum muons could be the reason.

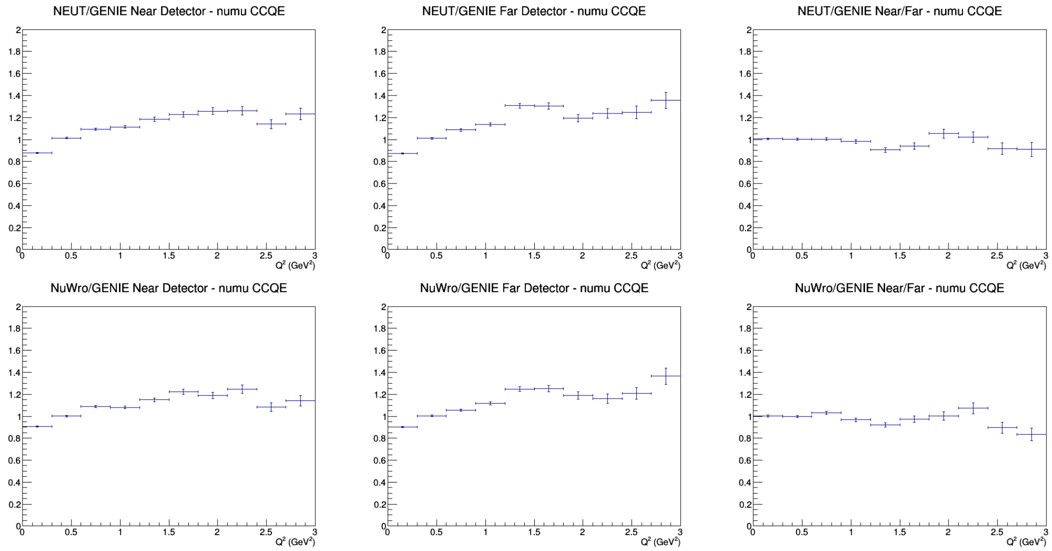


Figure 3: MC-level $Q^2$ distributed $\nu_\mu$ events using DUNE flux, no efficiencies applied to ND or FD. Top: Ratios of NEUT to GENIE. Bottom: Ratios of NuWro to GENIE. Left to Right: Single ratio at ND, single ratio at FD, double ratio near/far. Of note is the relative flatness throughout the double ratio compared to the single ratio at the ND. Note that the VALOR binning is separated by lower bin edges of (0, 0.20, and 0.55) $\text{GeV}^2$

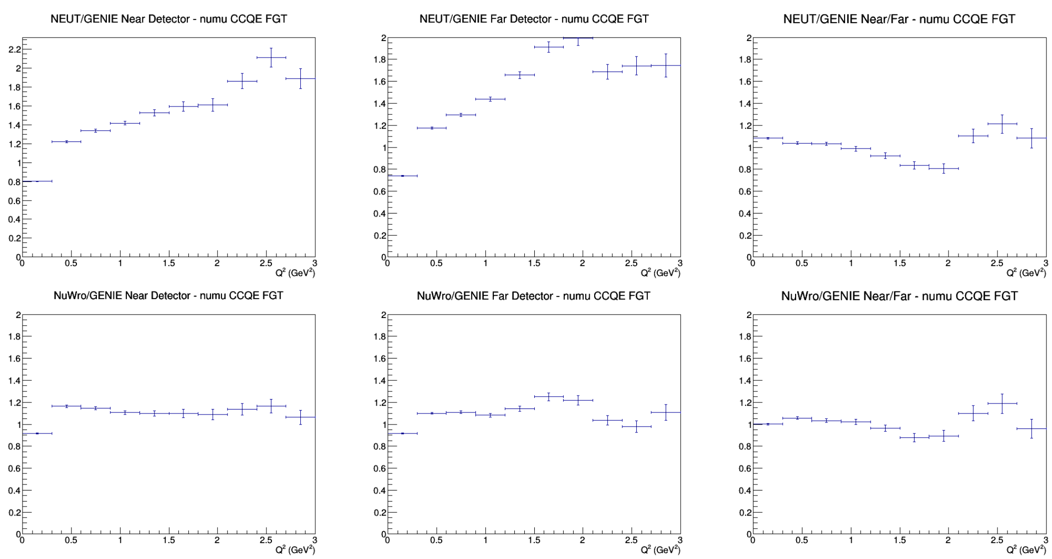


Figure 4: Reconstructed $Q^2$ distributed $\nu_\mu$ events using DUNE flux, FGT efficiencies applied to ND and simple LAr efficiencies applied to FD. Top: Ratios of NEUT to GENIE. Bottom: Ratios of NuWro to GENIE. Left to Right: Single ratio at ND, single ratio at FD, double ratio near/far. More shape variations do arise above ~1.25 $\text{GeV}^2$ in the double ratios. Note that the current VALOR binning is separated by lower bin edges of (0, 0.20, and 0.55) $\text{GeV}^2$.

However, for $\overline{\nu}_\mu$ CCQE events, we observe distortions in the $Q^2$ distribution even in the double ratios. This is true without efficiencies for both NEUT to GENIE and NuWro to GENIE ratios. This is displayed in Figure 5. The variations again arise above 1.5 GeV$^2$ for the double ratios, supporting the addition of a bin between .55 and 1.25 GeV$^2$. This appears without efficiencies, and points to variations in the CCQE interaction model being responsible for this effect rather than FSI variations or detector effects.

We run into trouble extending the $\overline{\nu}_\mu$ CCQE study with efficiencies applied, as this leaves the high $Q^2$ region with very low statistics, preventing us from drawing any meaningful conclusions. These plots are included in Appendix **??** for completeness.

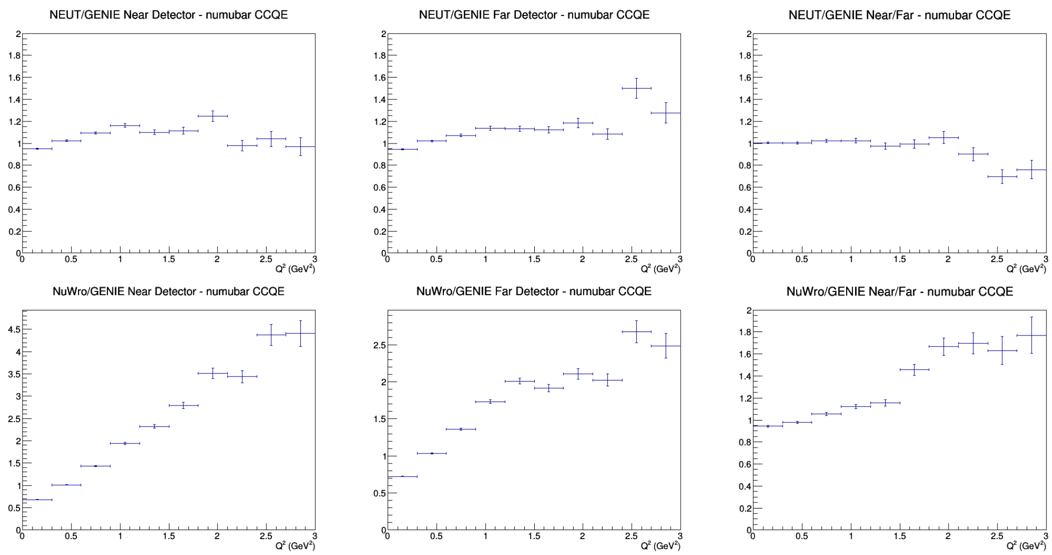


Figure 5: MC-level $Q^2$ distributed $\overline{\nu}_\mu$ CCQE events using DUNE flux. Top: Ratios of NEUT to GENIE. Bottom: Ratios of NuWro to GENIE. Left to Right: Single ratio at ND, single ratio at FD, double ratio near/far. Large amounts of variations in the region above 1.5 GeV$^2$ in both double ratios. This differs from $\nu_\mu$ CCQE, where this arose in the ratios after efficiencies are added. Here, it exists without any efficiencies. This points to variations in the CCQE model, rather than FSI or detector effects, not being covered by the parameterization. Note that the VALOR binning is separated by lower bin edges of (0, 0.20, and 0.55) GeV$^2$.

For 2p2h $\nu_\mu$ and $\overline{\nu}_\mu$ events, the double ratios from both NEUT and NuWro remain centered close to or around 1 below about 1 GeV$^2$ without efficiencies applied, as seen in Figure 6 and 7. Above 1 GeV$^2$, the statistics are again low. At this moment, the currently-proposed 1-bin normalization appears sufficient in the region below 1 GeV$^2$.

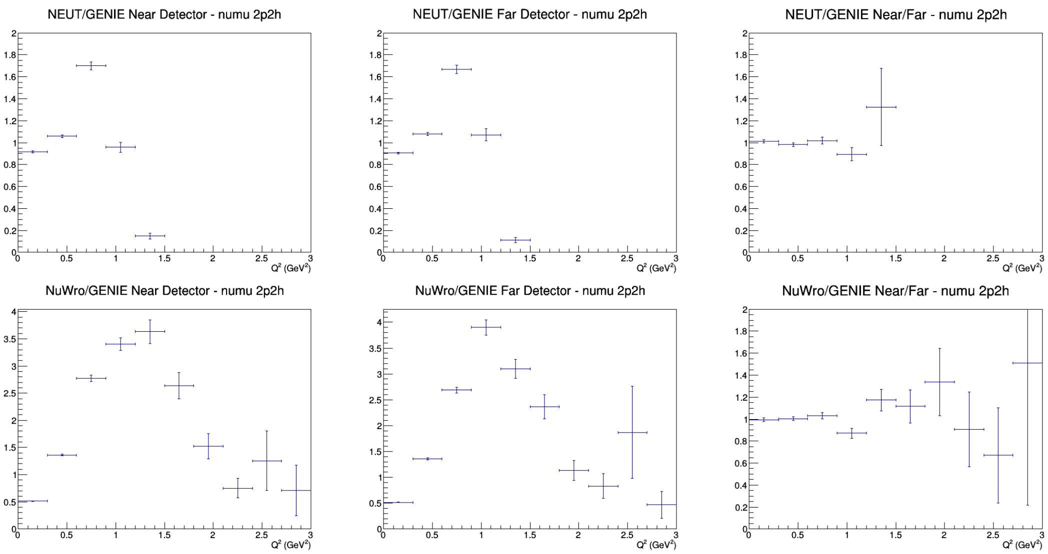


Figure 6: $Q^2$ distributed $\overline{\nu}_\mu$ 2p2h events using DUNE flux. Top: Ratios of NEUT to GENIE. Bottom: Ratios of NuWro to GENIE. Left to Right: Single ratio at ND, single ratio at FD, double ratio near/far. Large amounts of variations are present resulting from low statistics in the higher end of all distributions, but the lower end holds close to 1. Note that the VALOR binning is separated by lower bin edges of (0, 0.20, and 0.55) GeV$^2$.

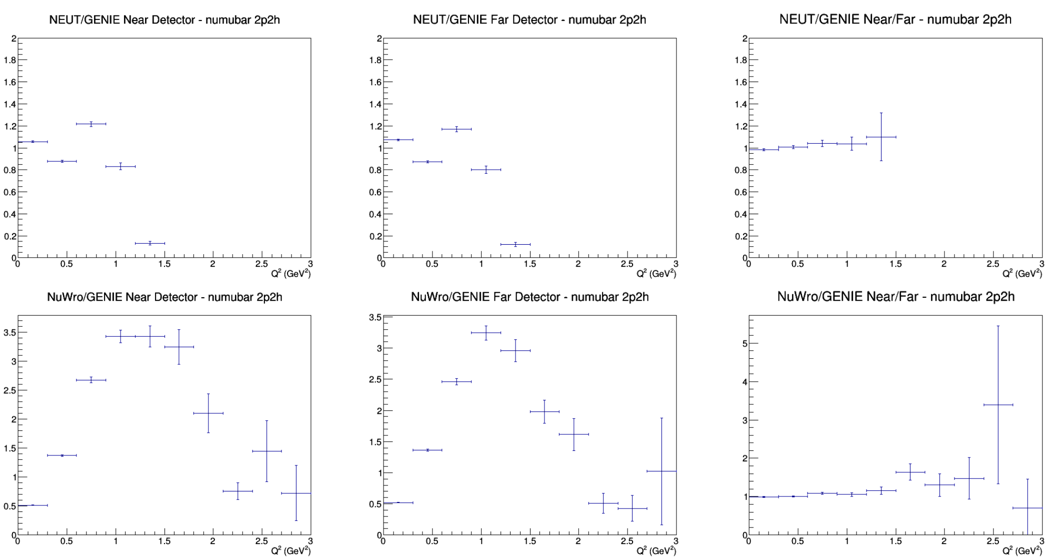


Figure 7: $Q^2$ distributed $\overline{\nu}_\mu$ 2p2h events using DUNE flux. Top: No efficiencies, Bottom: FGT efficiencies applied to ND, LAr efficiencies applied to FD. Left to right: NEUT to GENIE double ratio, NuWro to GENIE double ratio. Large amounts of deviations from 1 throughout distributions with efficiencies applied. Note that the VALOR binning is separated by lower bin edges of (0, 0.20, and 0.55) GeV$^2$.

We currently find an additional bin in the region (.55, ~1.25) will account for uncertainties in both $\nu_\mu$ and $\overline{\nu}_\mu$ CCQE. For $\nu_\mu$ and $\overline{\nu}_\mu$ 2p2h, the overall normalization currently appears sufficient from these studies. Investigations into the origin of the variation in the high $Q^2$ region of CCQE will be conducted as this work is furthered. Additional statistics and more complete efficiency descriptions for the LAr and GAr are required, and will be conducted at a later date.

## 4.2 $q_0$ vs. $q_3$ Variations

In addition to studying the $Q^2$ ratios, the ratios in $q_0$ - $q_3$ were also investigated to explore the possibility that variations arise when changing the parameterization from $Q^2$ to $q_0$ - $q_3$. The $Q^2$ parameterization assumes the variations are purely functions of $Q^2$. Under this assumption, the double ratios should be flat in $q_0$ - $q_3$ regions corresponding to the $Q^2$-binned parameterization. If this is not the case, a pure-$Q^2$ parameterization cannot sufficiently account for CCQE and 2p2h variations.

These studies were done in the exact same way as those in the previous section, only with the events and ratios distributed in $q_0$ - $q_3$ bins. Note: to be symmetric around 1, the scale extends from 0 to 2, but the variations in those bins can actually be greater than 2. Again, the quantities are MC-level truth information in the distributions without efficiencies, but are reconstructed in those with efficiencies applied, as described in Equations 3 - 6.

For $\nu_\mu$ CCQE, the double ratios without efficiencies appear flat for both NEUT to GENIE and NuWro to GENIE double ratios, as seen in Figure 8. There is distortion in the upper right region, consistent with the high $Q^2$ regions in Figure 3. This binning proves to be a problem for creating reliable conclusions once efficiencies are applied, as statistics for each individual bin become quite low. These are included in Appendix **??**. Higher statistics will be achieved for future work.

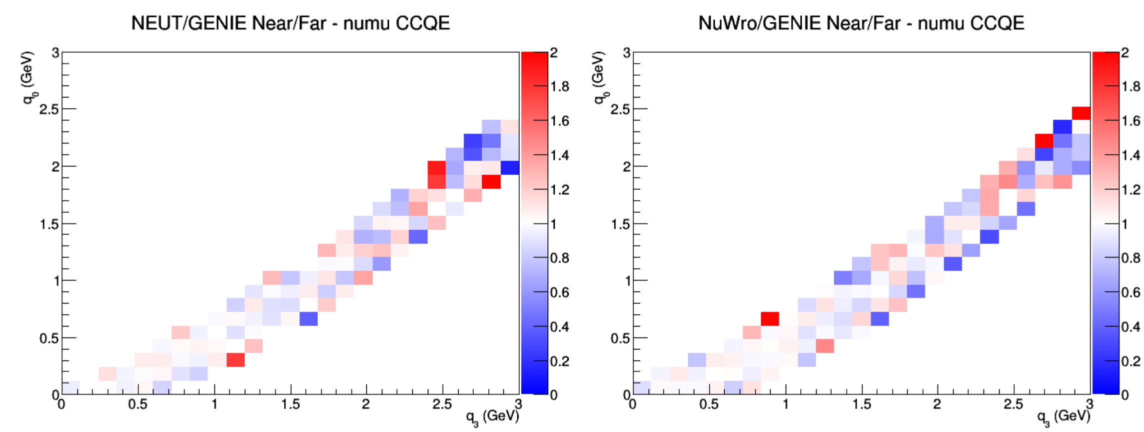


Figure 8: MC-level $q_0$ - $q_3$ distributed $\nu_\mu$ CCQE events using DUNE flux without efficiencies applied. Left: Double ratio of NEUT to GENIE, Right: Double ratio of NuWro to GENIE. Relatively flat distributions, but with bin-to-bin variations arising from low statistics. Consistent with corresponding $Q^2$ ratios

For $\overline{\nu}_\mu$ CCQE, the large variations in the high $Q^2$ region are present in the corresponding $q_0$ - $q_3$ region. As shown in Figure 9, the upper right region of both double ratios are consistent with the corresponding double ratios in Figure 5. Here again, the NuWro to GENIE double ratio is consistently higher in this region, while the NEUT to GENIE double ratio is slightly lower.

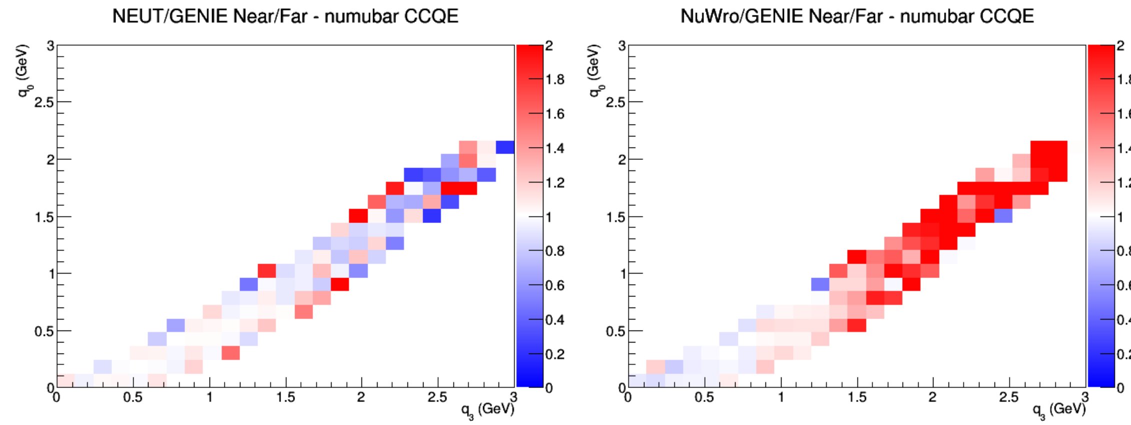


Figure 9: $q_0$ - $q_3$ distributed $\overline{\nu}_\mu$ CCQE events using DUNE flux without efficiencies applied. Left: Double ratio of NEUT to GENIE, Right: Double ratio of NuWro to GENIE. Variations in upper right region are consistent with corresponding $Q^2$ ratios.

Each of the three generators have very different behavior for 2p2h $\nu_\mu$ and $\overline{\nu}_\mu$ events with no efficiencies applied, as can be seen in Figure 10. This contains the raw event rate for 2p2h, and is shown to highlight the drastic shape difference. This causes very restricted phase space in the double ratios in $q_0$ - $q_3$, and so double ratios are not shown here, however they are included in Appendix **??**. The shape differences suggest that an overall binning in $Q^2$ cannot cover uncertainties, and reweighting events according to $q_0$ - $q_3$ shape should be considered.

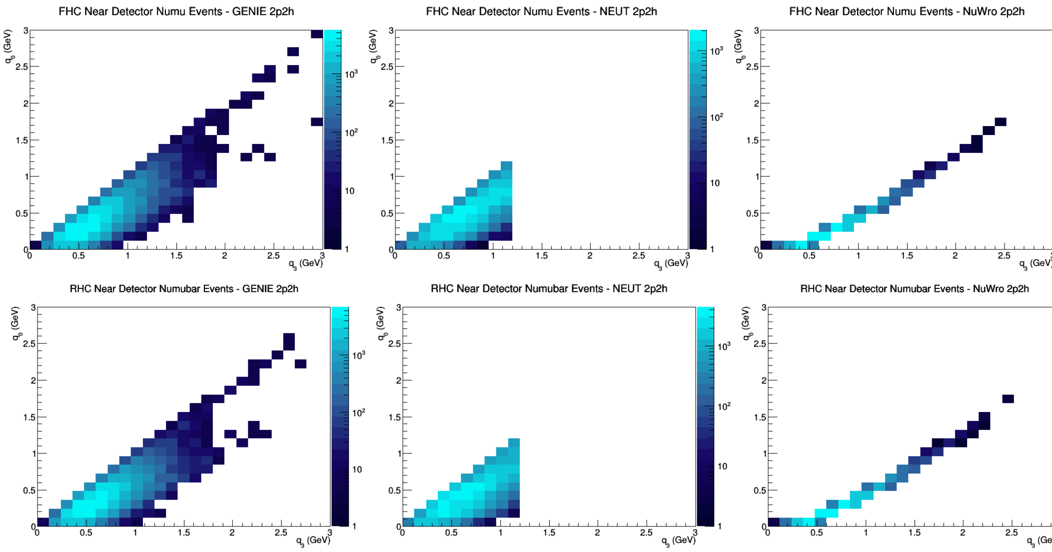


Figure 10: MC-level $q_0$ - $q_3$ distributed 2p2h events using DUNE flux with no efficiencies applied. Top: $\nu_\mu$ events, Bottom: $\overline{\nu}_\mu$ events. Right to Left: GENIE events distribution, NEUT events distribution, NuWro events distribution. The phase spaces are very different without efficiencies, and restrict the coverage of the double ratios in $q_0$ - $q_3$. This suggests the use of 1 $Q^2$ is insufficient bin to cover uncertainties.

# 5 Reconstructed Energy

A framework for investigating variations in reconstructed energy calculations between different generators and ND configurations has been developed. Currently, the estimate for the incident neutrino energy is calculated by summing the total energy from final state leptons and pions (all charges) and the kinetic energy of final state protons after passing efficiencies through the data sets. All neutrons are assumed undetectable. This can be summed up in Equation 6: where $E_{lep}$ is the energy of the outgoing lepton, $E_\pi$ is the energy of the pion, and $E_{prot}$ and $M_{prot}$ are the energy and mass of the proton.

## 5.1 Neutron Multiplicities and Energy

Differences between models in the number of final state neutrons and the total energy into final state neutrons can affect reconstruction of neutrino energy. Large variations in reconstructed energy can arise due to missing energy caused by the inability to detect neutrons in the various models.

To investigate this, we have looked at GENIE, NEUT, and NuWro to see if the different models showed a large difference in the neutron energy and multiplicity. This was done for CCQE, CC1$\pi$, 2p2h, and everything else ("Other"') interactions and neutrinos as well as anti-neutrinos. In all cases, the generators agreed rather well with each other even though there were some differences in the neutron multiplicity. These differences only account for a small fraction of the events, generally less than 10%, as can be seen in Table 11. Figure 12 shows an example of this for 2p2h neutrino

| Generator & Interaction | $N_N > 3(\%)$ ND | $E_N > 600MeV/c(\%)$ ND | $N_N > 3(\%)$ FD | $E_N > 600MeV/c(\%)$ FD |
|---|---|---|---|---|
| GENIE-CCQE | 13 | 2 | 13 | 2 |
| GENIE-2p2h | 28 | 1 | 29 | 2 |
| GENIE-CC1$\pi$ | 17 | 21 | 18 | 25 |
| GENIE-CCOther | 24 | 17 | 24 | 19 |
| NEUT-CCQE | 1 | 0.8 | 1 | 0.7 |
| NEUT-2p2h | 8 | 4 | 8 | 4 |
| NEUT-CC1$\pi$ | 9 | 21 | 9 | 23 |
| NEUT-CCOther | 9 | 18 | 11 | 21 |
| NuWro-CCQE | 4 | 2 | 3 | 2 |
| NuWro-2p2h | 3 | 0.3 | 3 | 0.2 |
| NuWro-CC1$\pi$ | 30 | 22 | 34 | 27 |
| NuWro-CCOther | 33 | 20 | 38 | 26 |

Figure 11: Percentage of events with $N_{neutron} > 3$ and $E_{neutron} > 600MeV/c$, broken down by generator and event type. These cut offs where chosen to encompass most of the GENIE sample.

events, while the other interaction modes can be found in Appendix **??**.

Furthermore, the difference in the multiplicities between the generators becomes irrelevant after a ND to FD extraction, as can be seen in Figure 13. Here, the region where the most energy is lost agrees very well between the ND and FD for all generators and interaction types. The areas with low statistics do show a disagreement, but very few events fall into this area.

Care should still be taken when calculating the neutrino energy of the event if only a calorimetric approach is used, as is the case in this document. This is because as much as 50% of the energy can be taken away by the neutron in CCQE events. Even for 2p2h events, as shown in Figure 14, it can be as high as 30%. The other interaction modes and anti-neutrino events can also be found in Appendix **??** and have a smaller fraction.

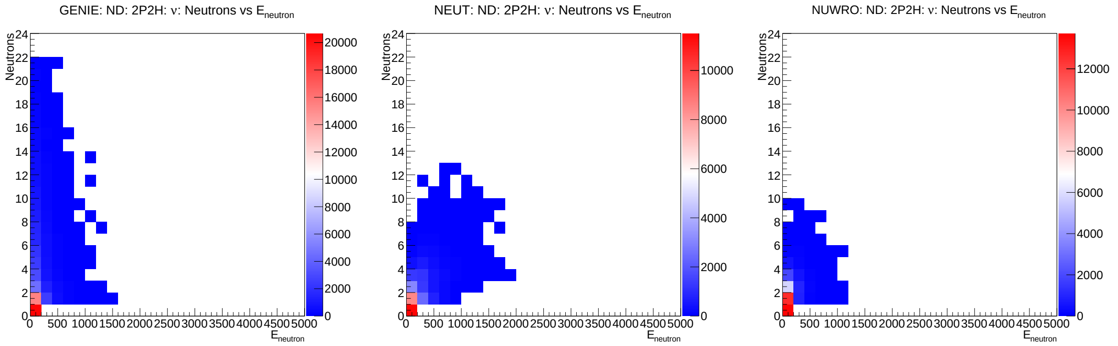


Figure 12: The neutron multiplicity vs total neutron energy for 2p2h interactions for GENIE, NEUT, and NuWro, respectively. Even though they do show a different phase-space for the neutron multiplicity, they all agree where most of the energy lost to neutrons should be. This is similar for other interaction types as well.

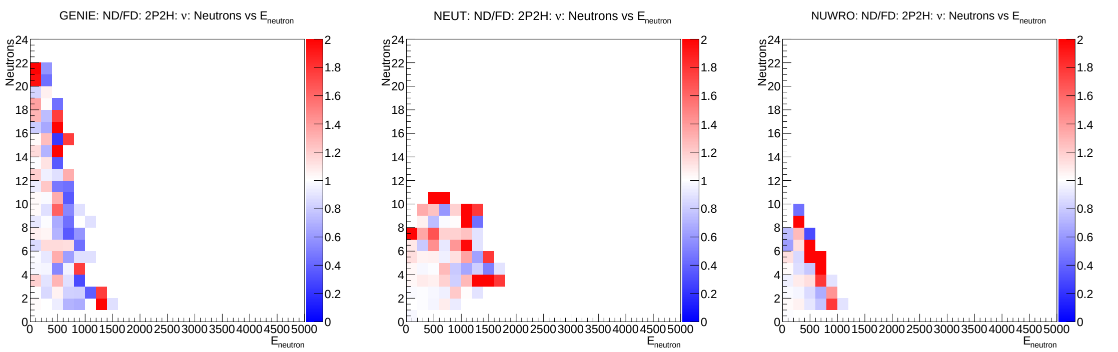


Figure 13: The ratio of the ND to the FD for neutron multiplicity vs total neutron energy for 2p2h interactions for GENIE, NEUT, and NuWro, respectively. In the area where the largest amount of energy is lost to neutrons, low multiplicity and low energy, the agreement between the ND and FD is almost perfect.

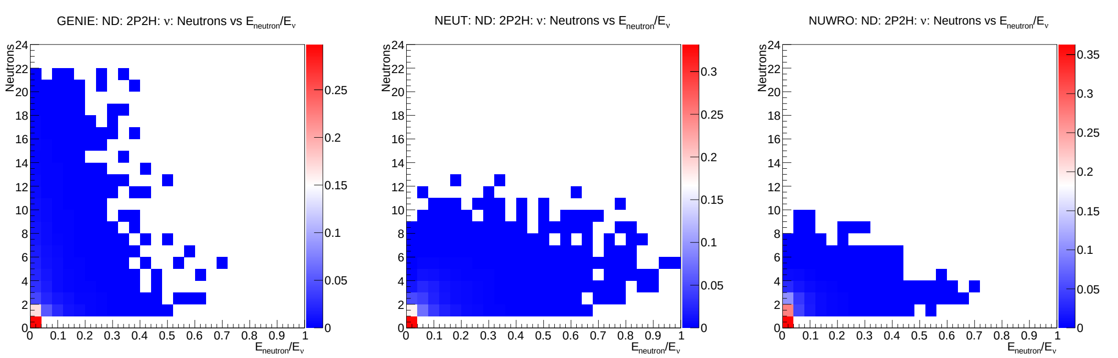


Figure 14: Neutron multiplicity vs total neutron energy divide by the neutrino energy for 2p2h interactions from GENIE, NEUT, and NuWro, respectively. For low multiplicity, the neutron carries away a significant fraction of the neutrino energy.

Missing neutrons can effect the neutrino energy reconstruction, which is especially important for neutrino oscillation studies which require an exact energy. However, much of the effect of these missing neutrons can be taken into account with the near to far extrapolation. At the moment, the difference between the models seem to be OK for these analyses given a near to far ratio. Future work will investigate to see if the FSI errors in GENIE can cover the differences between the models.

## 5.2 Proton/Pion Multiplicity and Momentum

Similar to the neutron multiplicity and energy studies, proton and pion multiplicities offer insight into the coupling of the detector configurations with variations in FSI models as well as the energy reconstruction capabilities of the different detector configurations. The total momentum of the particles gives us a proxy for the energy into the final state protons or pions as well as a direct link to detector efficiency effects. For these studies, the 3-momentum of the final state protons are summed. The magnitude is then plotted against the multiplicity for the specific particle type. This was done for the final state particles in true-CCQE, true-2p2h, CC0$\pi$, CC1$\pi$, and CCOther. It was first done without efficiencies applied so we can look at the effects of the FSI models. It was also done with all three ND configuration efficiencies and the LAr FD efficiencies so we can investigate the effects of the different ND configurations and how they couple to the FD. As the efficiencies for pions are currently unknown for the LAr and GAr, we will only consider the protons in the current iteration of this note.

To show the difference in the FSI models, Figure 15 shows the proton multiplicity vs total proton momentum for 2p2h interactions. 2p2h models where chosen as they have the smallest phase space in this projection and therefore show the differences the best, but all interaction types have been investigated and can be found in Appendix ??. From this, one can see that there is a difference between the FSI models. Particularly, GENIE prefers to have more proton multiplicity compared to NEUT and NuWro. It also has lower total momentum for these protons when compared to the other two.

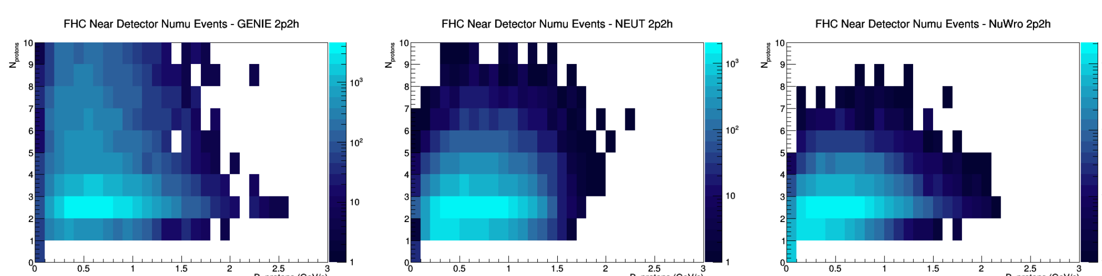


Figure 15: The proton multiplicity as a function of total proton momentum for 2p2h interaction in GENIE, NEUT, and NuWro, respectively. There is a clear difference in phase space with GENIE having both higher proton multiplicity and lower total momentum.

Unlike with the neutron multiplicity, the differences between the models is important as the a near to far extrapolation does not hold. Figure 16 shows this with variations of 20-30% in the regions where the most events are. The exact reason for this discrepancy is unclear. It could be attributed to the plot only includes the total momentum of all protons, with it being possible that one or two protons take away the most energy and the highest momentum protons would agree between the two detectors. This is something that will be looked at in the future.

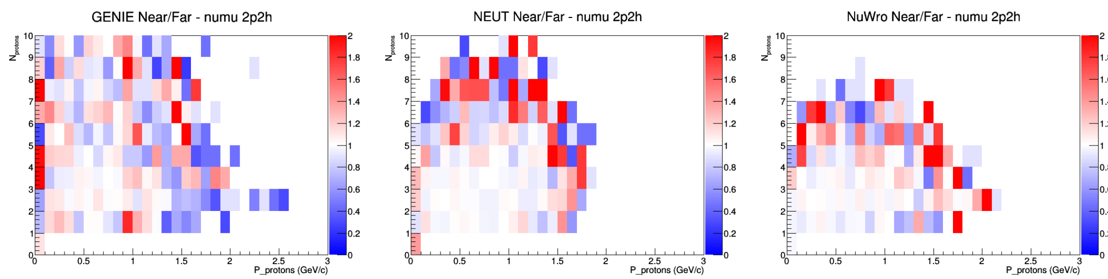


Figure 16: The ND/FD of proton multiplicity as a function of total proton momentum for 2p2h interaction in GENIE, NEUT, and NuWro, respectively. In the region with the most events, there are variations of up to 20%

Once detector efficiencies are added in, there is an even greater difference in the near to far ratio. Figure 17 shows these striking differences. The top row shows the near to far ratio for the FGT to a LAr far detector. In the region of interest the differences are 100% and greater. The middle row shows the high pressure GAr TPC, with differences again ranging from 20-100%. The last row shows the LAr TPC, and unsurprisingly, gives the best agreement. Even then though, differences of up to 20% exist, arising most likely due to the different flux at each detector.

These plots show the importance of not just the FSI model in use but also the detector's threshold to measure protons. The FGT, which has the most realistic thresholds and therefore the ones most unlike the LAr far detector, shows just how important this can be. It is expected pions will have an even larger impact than the protons due to there re-interactions with the nucleus. This needs to be confirmed and will be shown in updates to this document.

## 5.3 Difference from True Neutrino Energy

The studies in Sections 5.1 and 5.2 highlight the differences in the generators' FSI behavior as well as the different abilities of the various detector configurations to reconstruct final state energy. This section studies the overall change we see to $E_{reco}$, defined in Equation 6, as we apply detector efficiencies. To do this, the difference between true and reconstructed neutrino energy from each generator is plotted. This is first done for a "perfect" near detector, one in which we assume all particles except neutrons are accepted. Next, it is done for each ND configuration, FGT, simple LAr, and simple GAr. Each distribution is normalized to 1 so the y-axis serves as the relative event rate.

For $\nu_\mu$, all three generators behave similarly in the perfect ND for CCQE, 2p2h, CC0$\pi$, and CC1$\pi$. This is shown for CCQE in the left plot of Figure 18. Meanwhile,

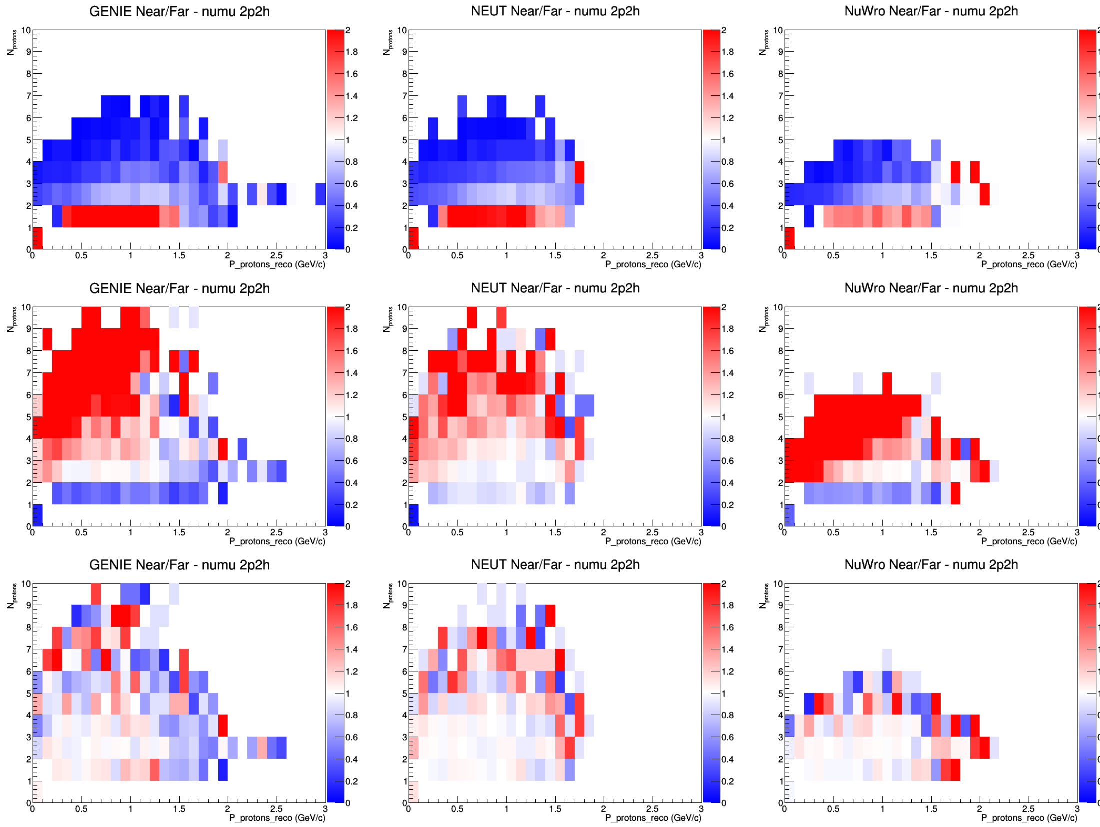


Figure 17: The ND/FD of proton multiplicity as a function of total proton momentum for 2p2h interactions. The left hand columns show GENIE, and middle column shows NEUT, and the right hand column shows NuWro. The top row has the FGT efficiencies applied for the ND, the middle row has the high pressure GAr TPC efficiencies, while the last row has the LAr TPC efficiencies for the ND. All of these use LAr efficiencies for the FD.

NuWro CCOther is slightly different to NEUT and GENIE, as seen in the right plot of the same figure. The other reactions can be found in Appendix **??**.

However, for $\overline{\nu}_\mu$ in the perfect ND, NuWro now differs significantly from NEUT and GENIE for CCQE, 2p2h, and CC0$\pi$, while all three generators behave similarly for CC1$\pi$ and CCOther. This is shown for 2p2h and CCOther in Figure 19.

Future work will be conducted to determine if GENIE FSI errors are able to cover the variations between these generators within the perfect ND.

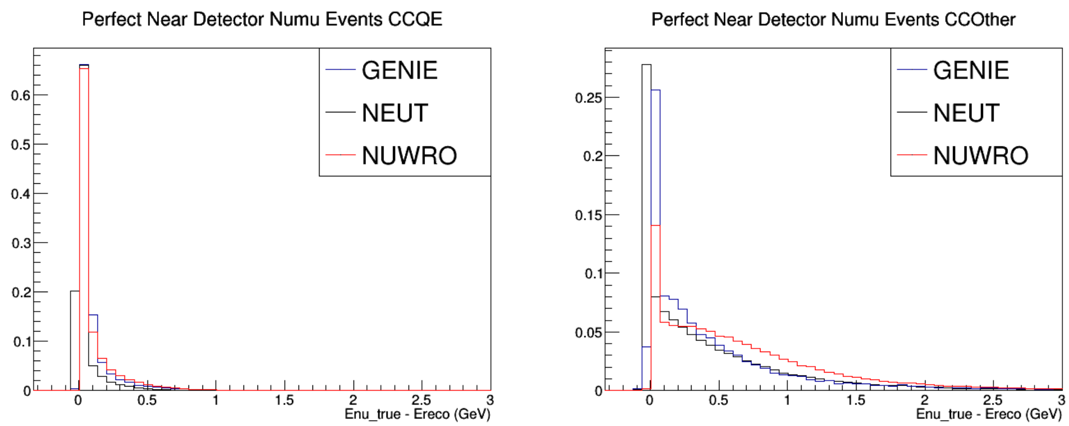


Figure 18: Difference between true and reconstructed neutrino energy in the "perfect" ND. Left: $\nu_\mu$ CCQE, Right: CCOther. All three generators behave similarly for CCQE. For CCOther, NEUT and GENIE have similar behavior, while NuWro slightly differs.

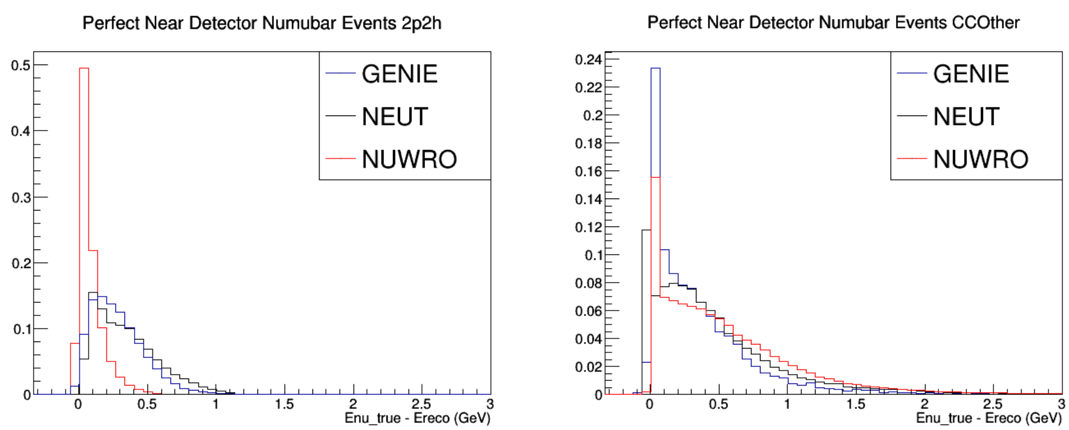


Figure 19: Difference between true and reconstructed neutrino energy in the "perfect" ND. Left: 2p2h $\overline{\nu}_\mu$, Right: CCOther. NuWro differs from NEUT and GENIE in 2p2h, while all generators are similar for CCOther.

After applying detector efficiencies, the discrepancy between true and reconstructed neutrino energy changes only slightly as seen in Figure 20. Here, we show the $\nu_\mu$ 2p2h distributions with the perfect, simple LAr, simple GAr, and FGT ND. The other reaction modes can be found in Appendix **??**. Keeping in mind that the simple GAr and LAr only include thresholds (100 and 200 MeV respectively) for protons, comparing these configurations to the perfect ND shows that a simple proton threshold has little effect on the ability to reconstruct the true neutrino energy despite the effect seen when looking at the multiplicity and momentum distributions. Future work will include a more reasonable description of the proton efficiencies, as well as efficiency descriptions for the other final state particles, within these two detectors to see if any larger effect arises.

Applying the FGT efficiencies has a slightly more noticeable effect, as can be seen in the bottom right plot of Figure 20. This motivates further investigation into both the relative effect of applying a more complete description of proton efficiencies and including efficiencies for other final state particles. Additional studies include applying the FGT efficiencies for each particle individually in order to see each effect independently.

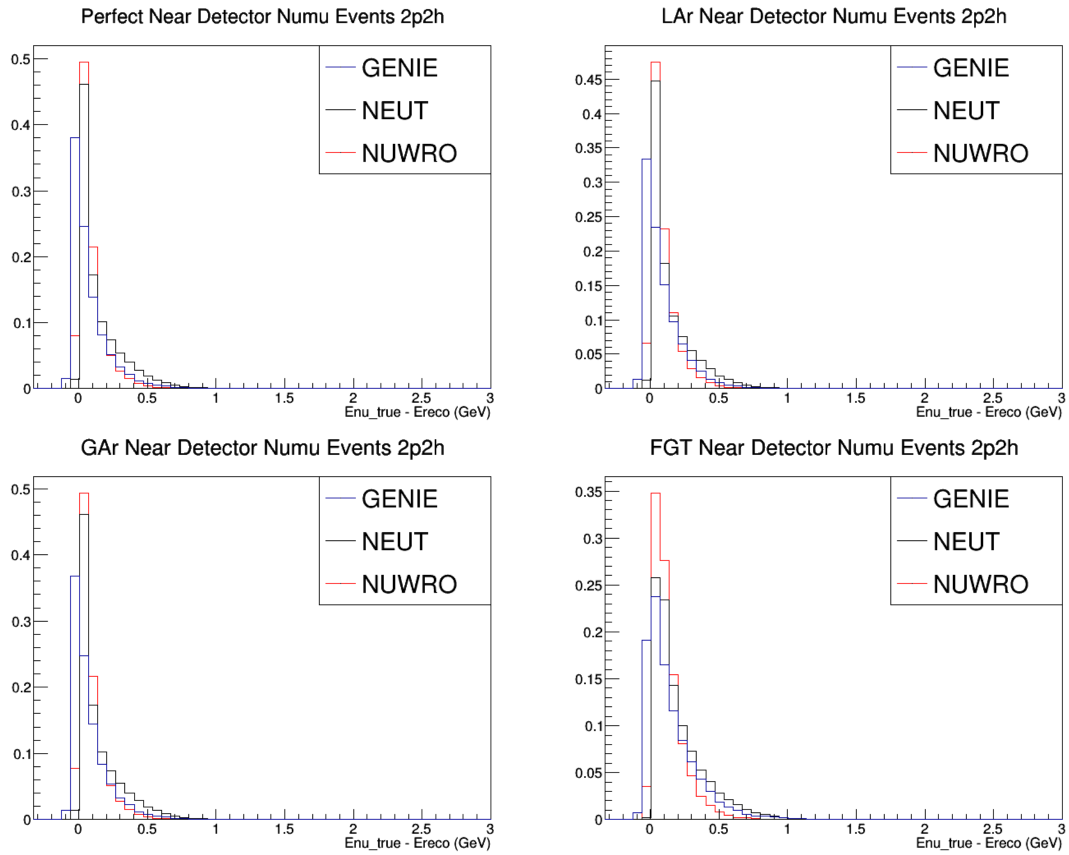


Figure 20: Difference between true and reconstructed neutrino energy for $\nu_\mu$ 2p2h. Top Left: Perfect ND, Top Right: Simple LAr ND. Bottom Left: Simple GAr ND, Bottom Right: FGT ND. There exists only small differences when applying simple LAr and GAr proton thresholds. There is a slightly more noticeable effect when applying a more complete FGT description.

# 6 Future Work

The above studies need to be furthered and expanded upon to successfully arrive at useful conclusions on ND configuration choice.

- Improved statistics: this can be easily and quickly achieved.
- Investigate origins of high-$Q^2$ variations
  - Is this FSI or detector effects?
- Extend studies to include LAr and GAr efficiency and acceptance information when available.
- Extend final state studies into proton multiplicity vs. energy, and include pions when efficiencies are available.

- Study the ability for GENIE FSI errors to cover differences between generators and final state energy.
- Study the effect of particle thresholds on the reconstructed neutrino energy by applying thresholds final state particles individually.

# A Efficiencies

This appendix includes all the ND efficiency plots not shown in Section 3.4.

## A.1 FGT

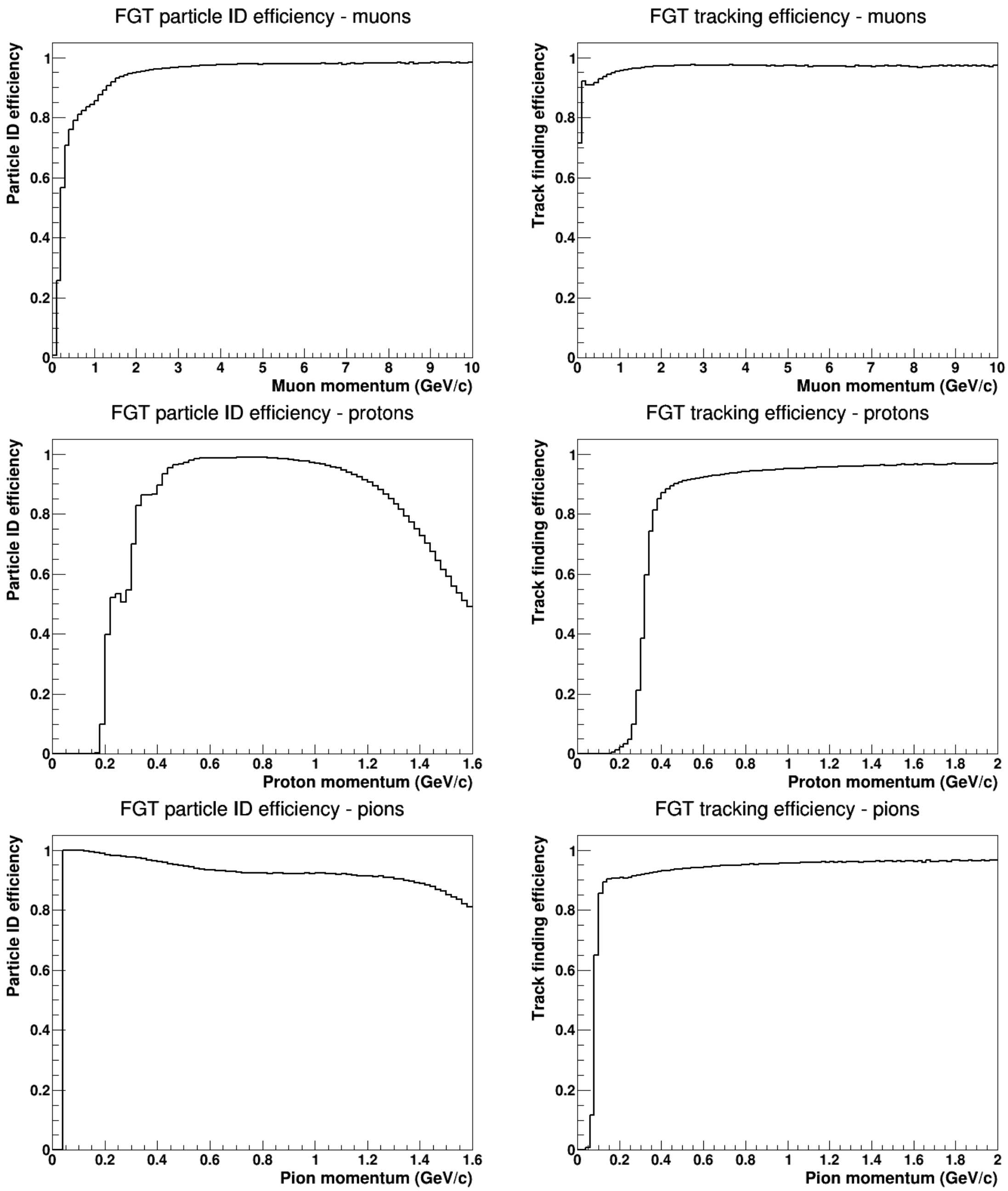

FGT particle ID efficiency - muons
Particle ID efficiency
Muon momentum (GeV/c)
FGT tracking efficiency - muons
Track finding efficiency
Muon momentum (GeV/c)
FGT particle ID efficiency - protons
Particle ID efficiency
Proton momentum (GeV/c)
FGT tracking efficiency - protons
Track finding efficiency
Proton momentum (GeV/c)
FGT particle ID efficiency - pions
Particle ID efficiency
Pion momentum (GeV/c)
FGT tracking efficiency - pions
Track finding efficiency
Pion momentum (GeV/c)

# B $Q^2$ Plots

This appendix includes all the plots not show in Section 4.1. For full description of the files, please make reference to that section. The plots will be put in the same order as before.

## B.1 numu CCQE no efficiencies

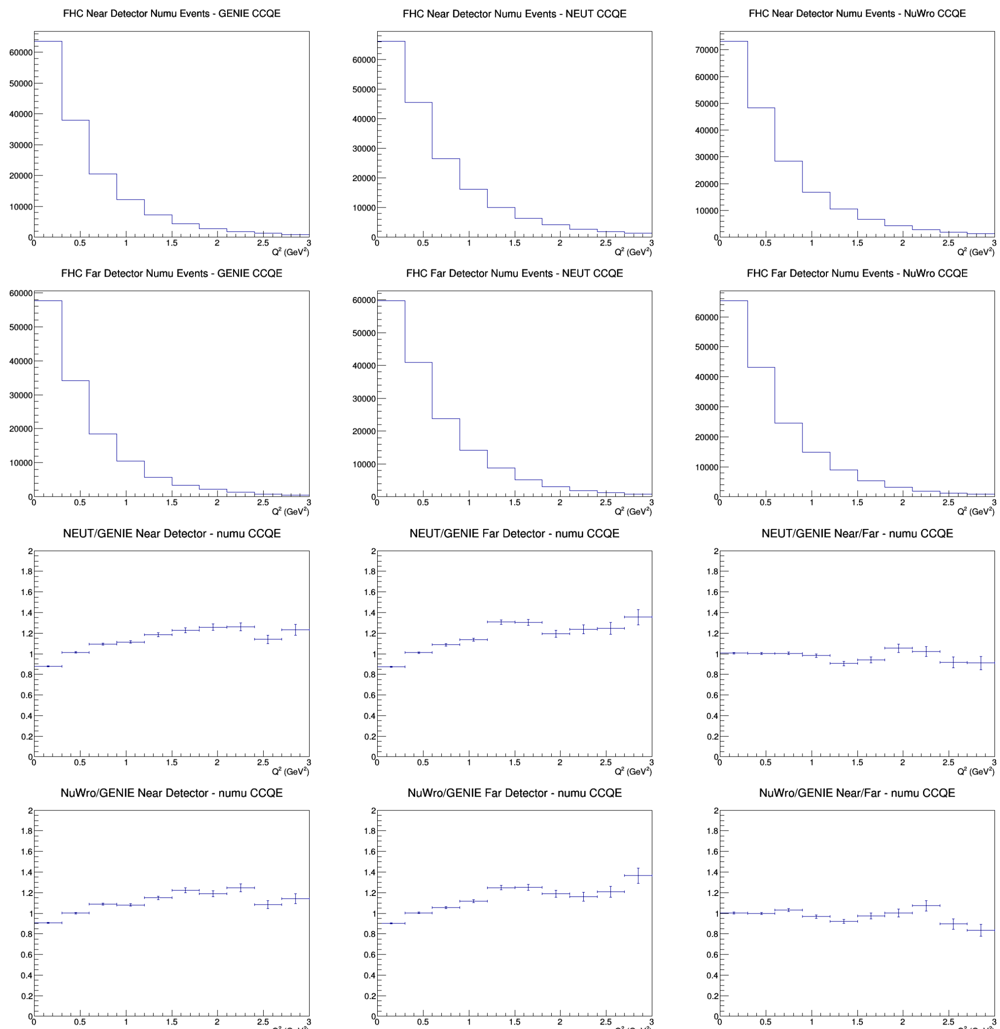

## B.2 numu CCQE FGT efficiencies

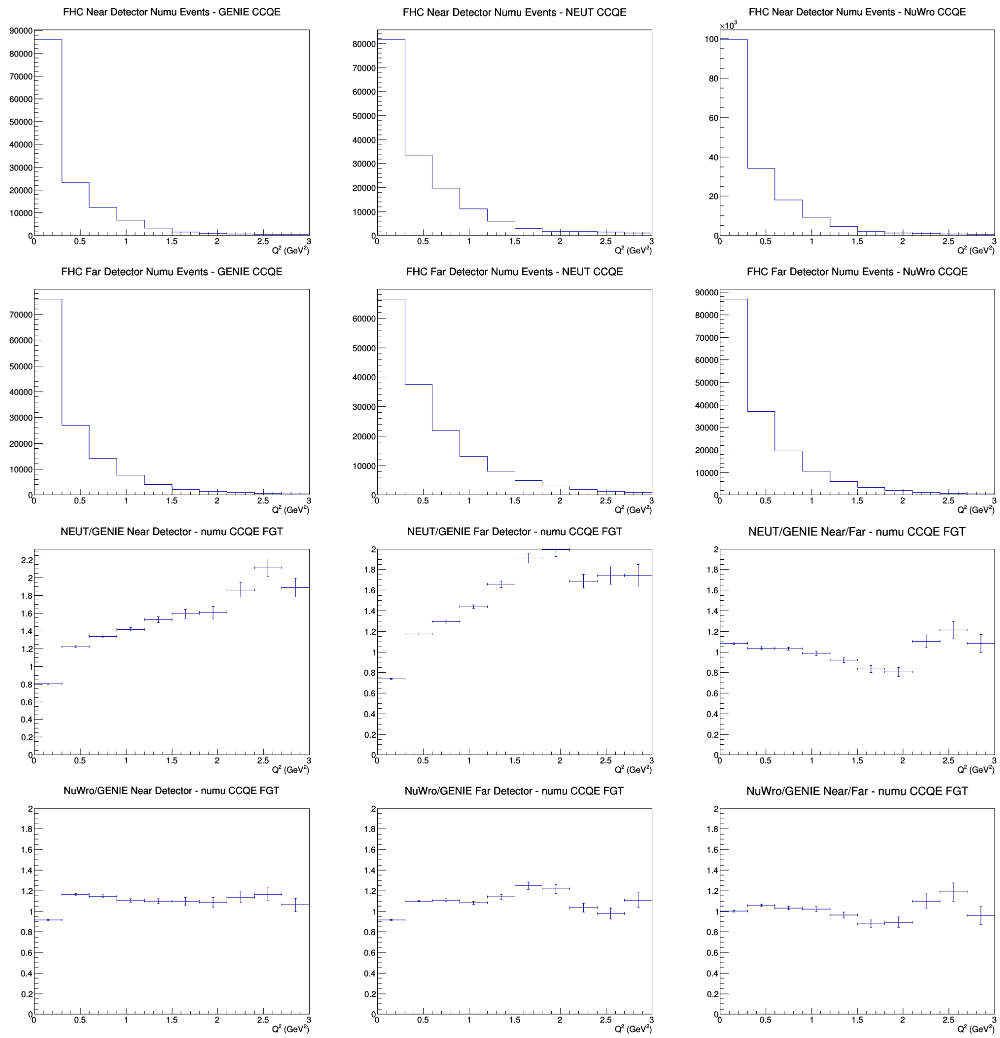

## B.3 numu CCQE LAr efficiencies

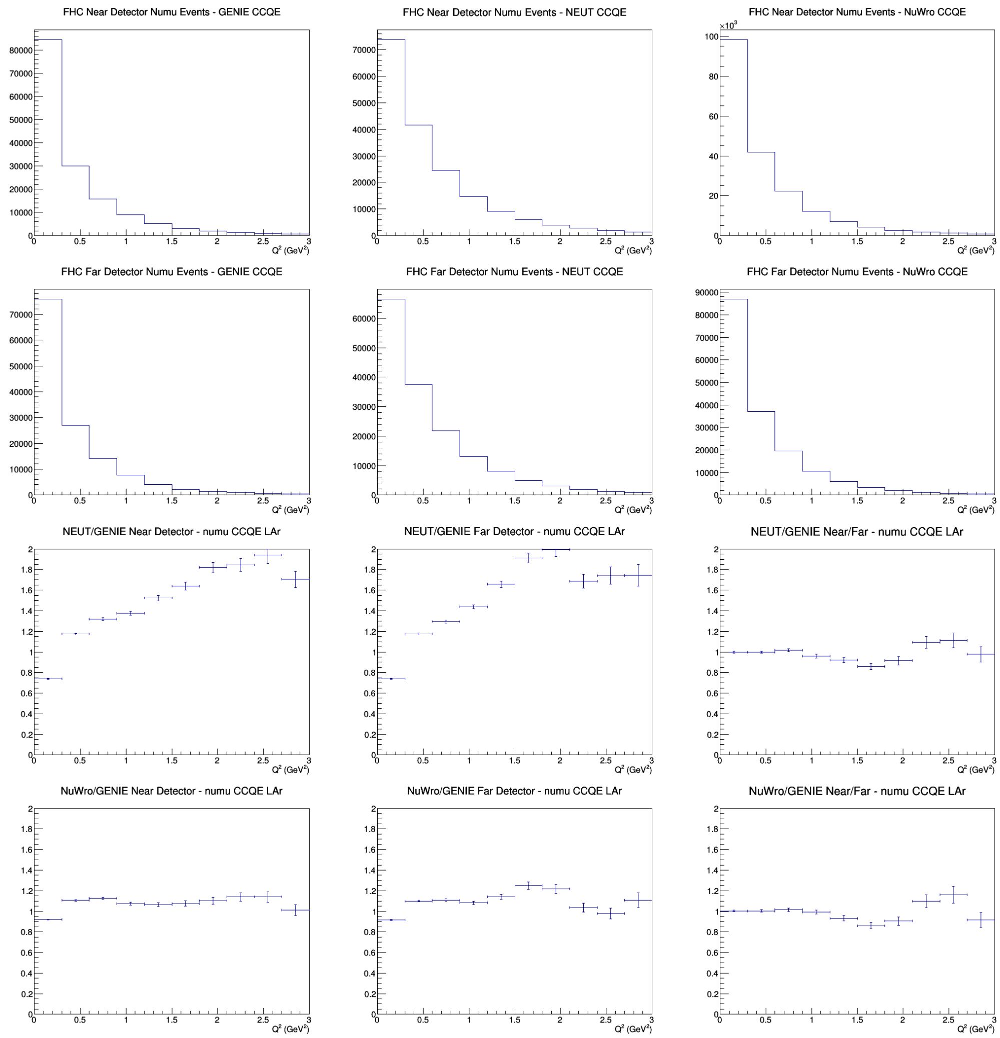

## B.4 numu CCQE GAr efficiencies

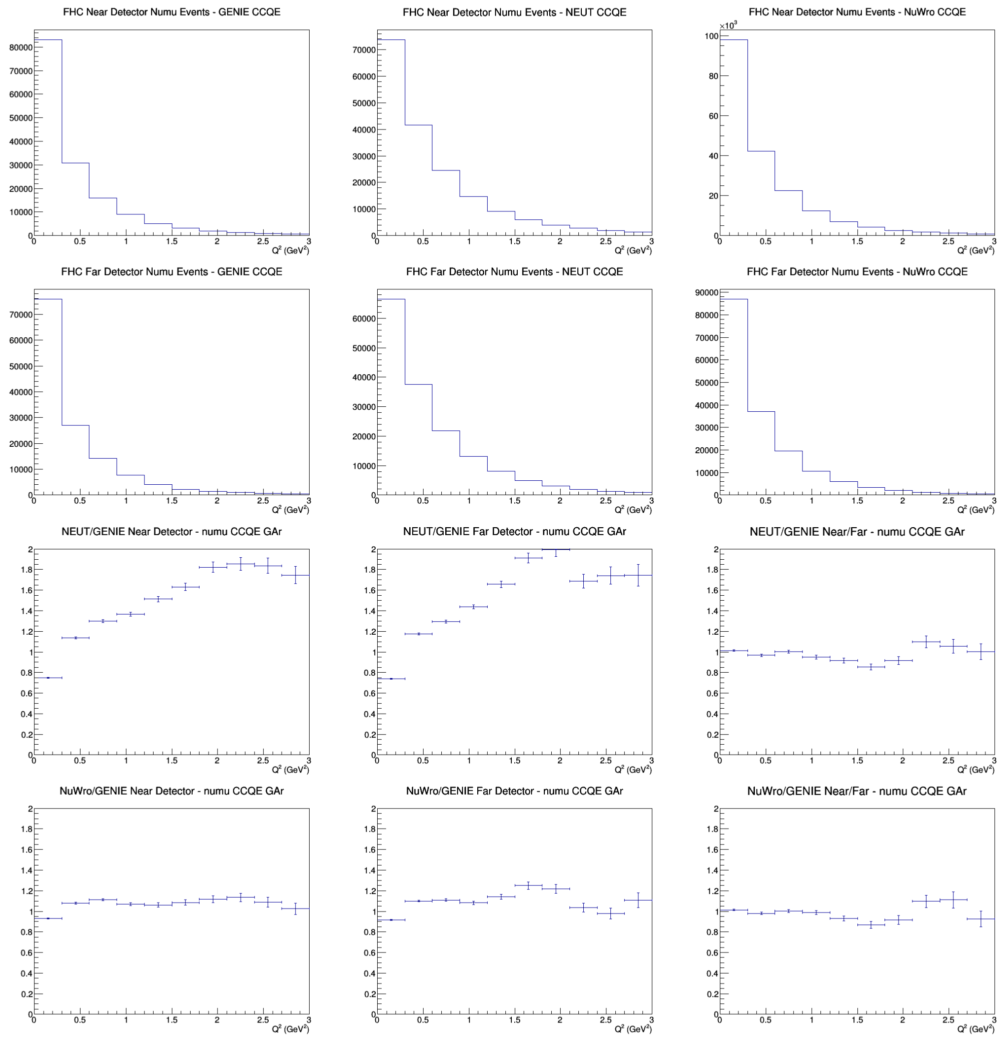

## B.5 numubar CCQE no efficiencies

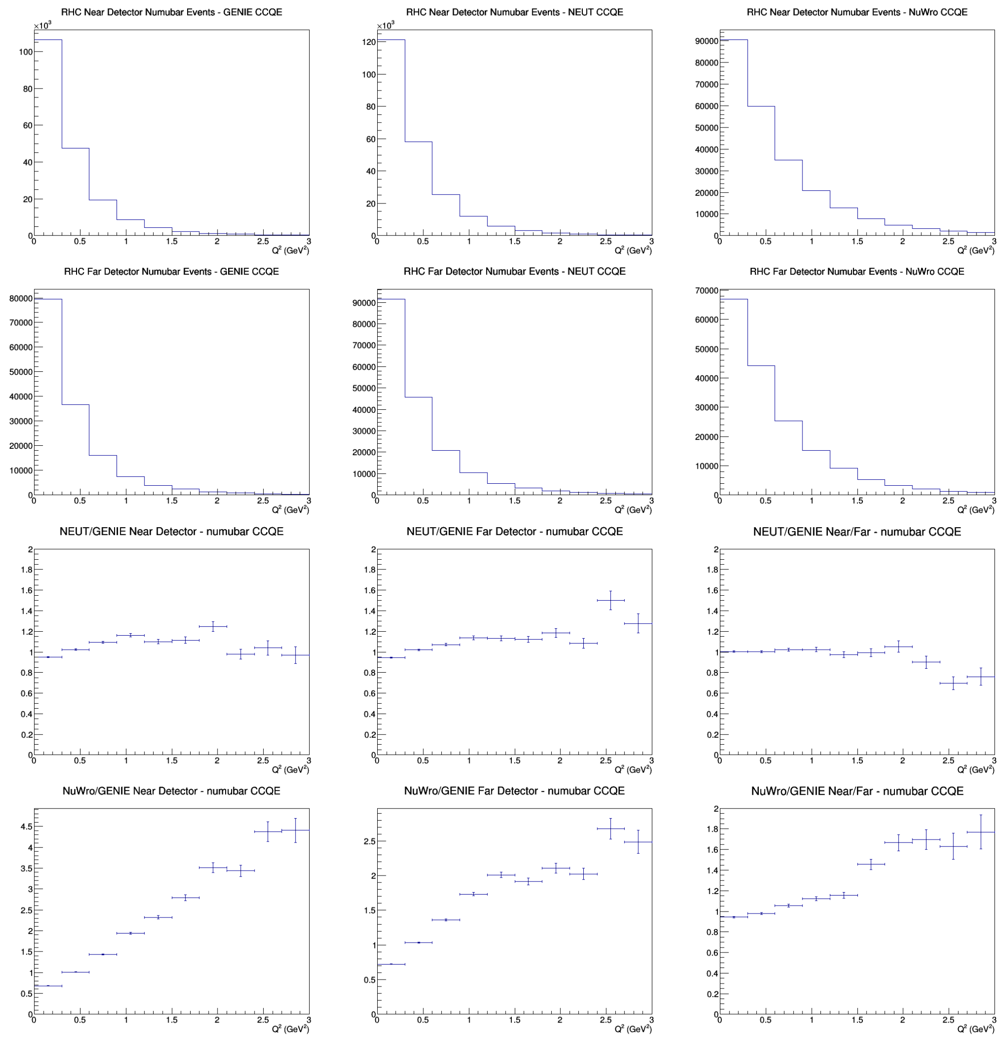

## B.6 numubar CCQE FGT efficiencies

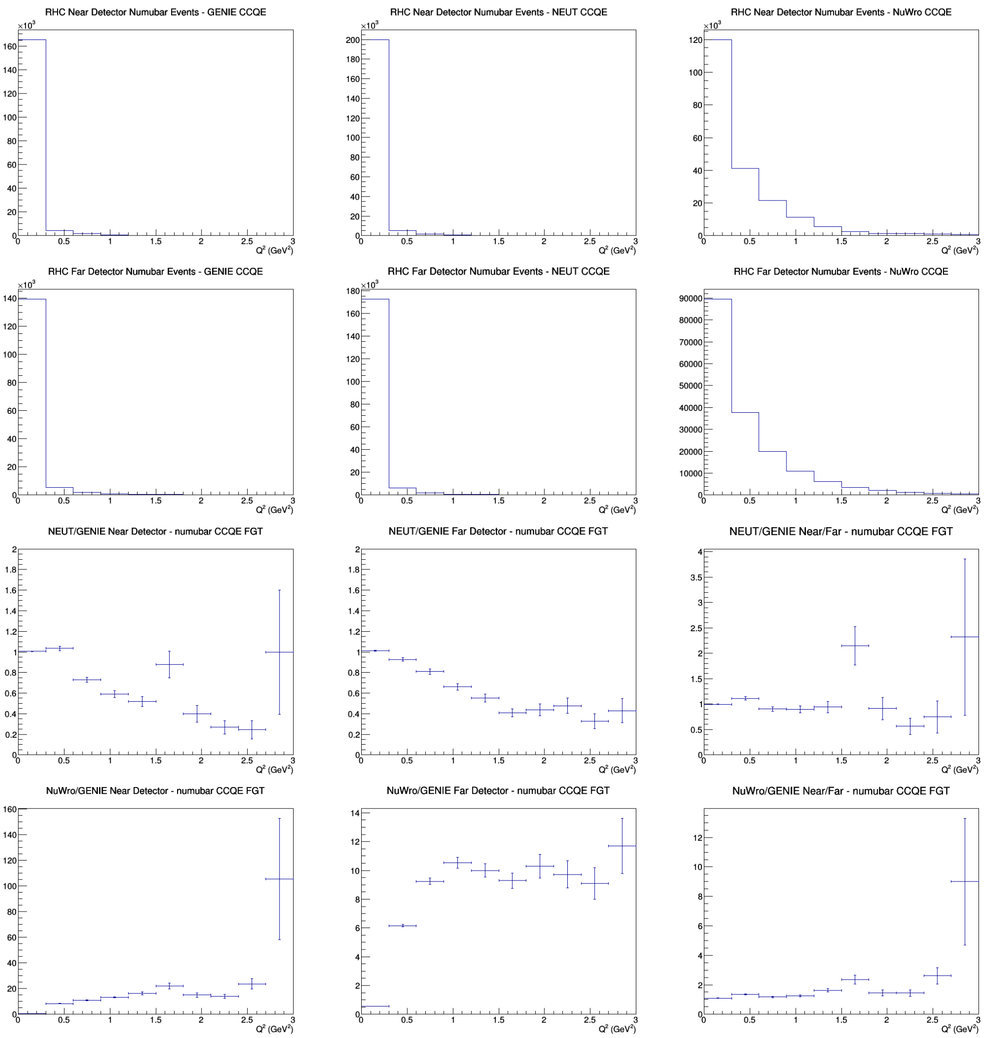

## B.7 numubar CCQE LAr efficiencies

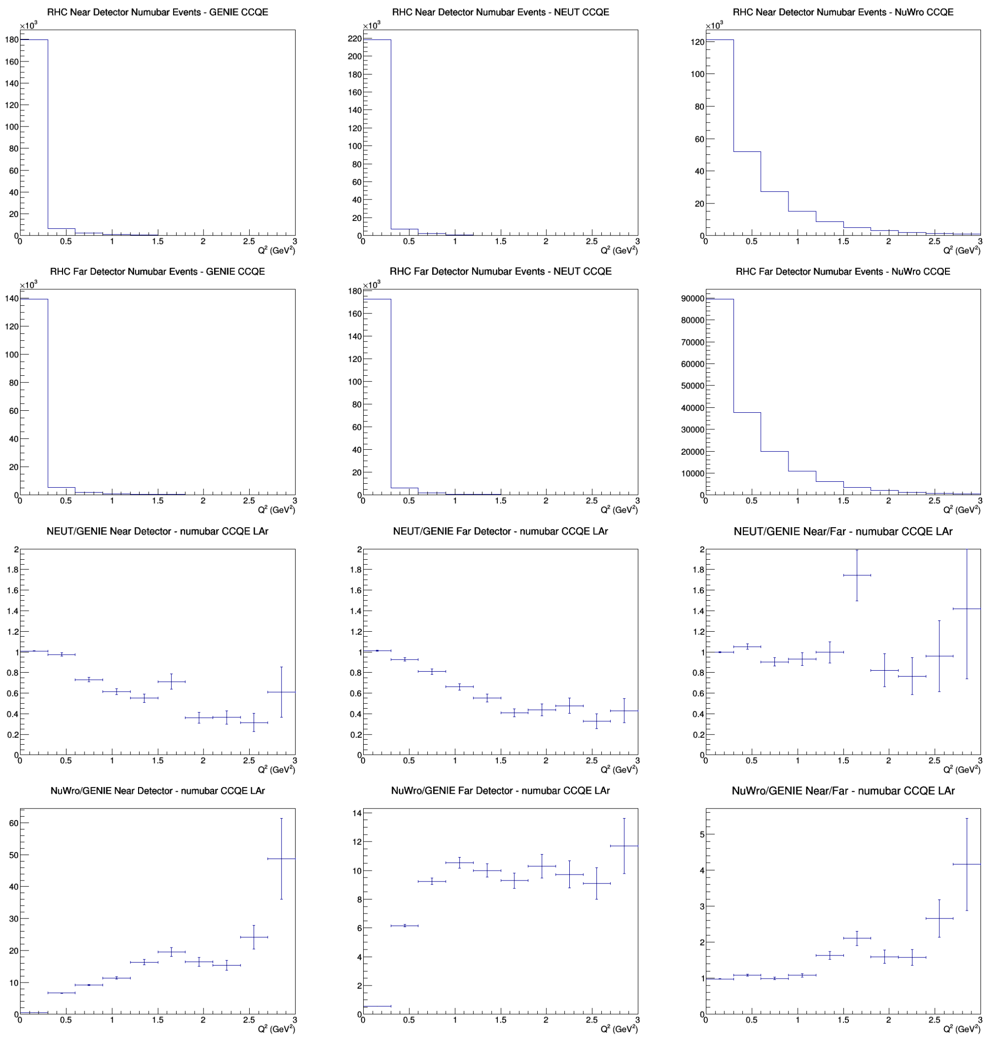

## B.8 numubar CCQE GAr efficiencies

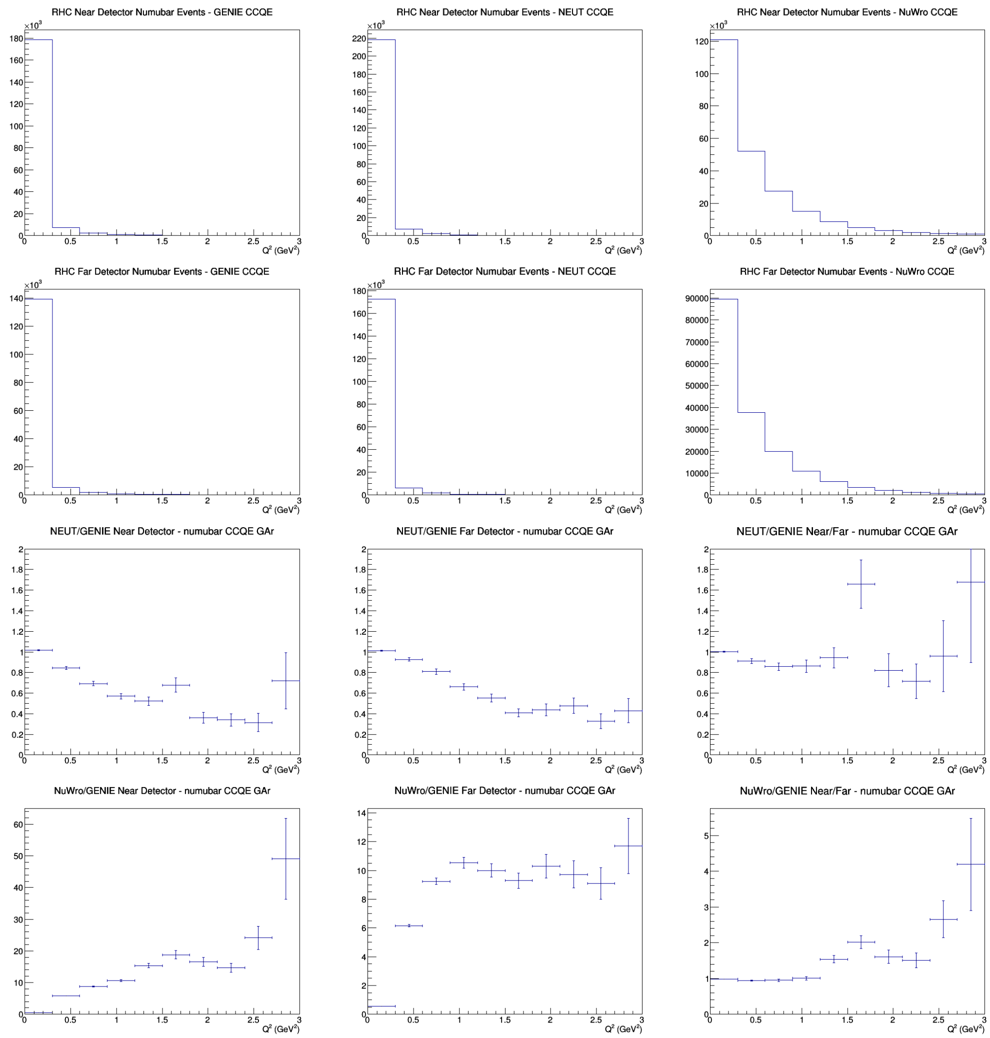

## B.9 numu 2p2h no efficiencies

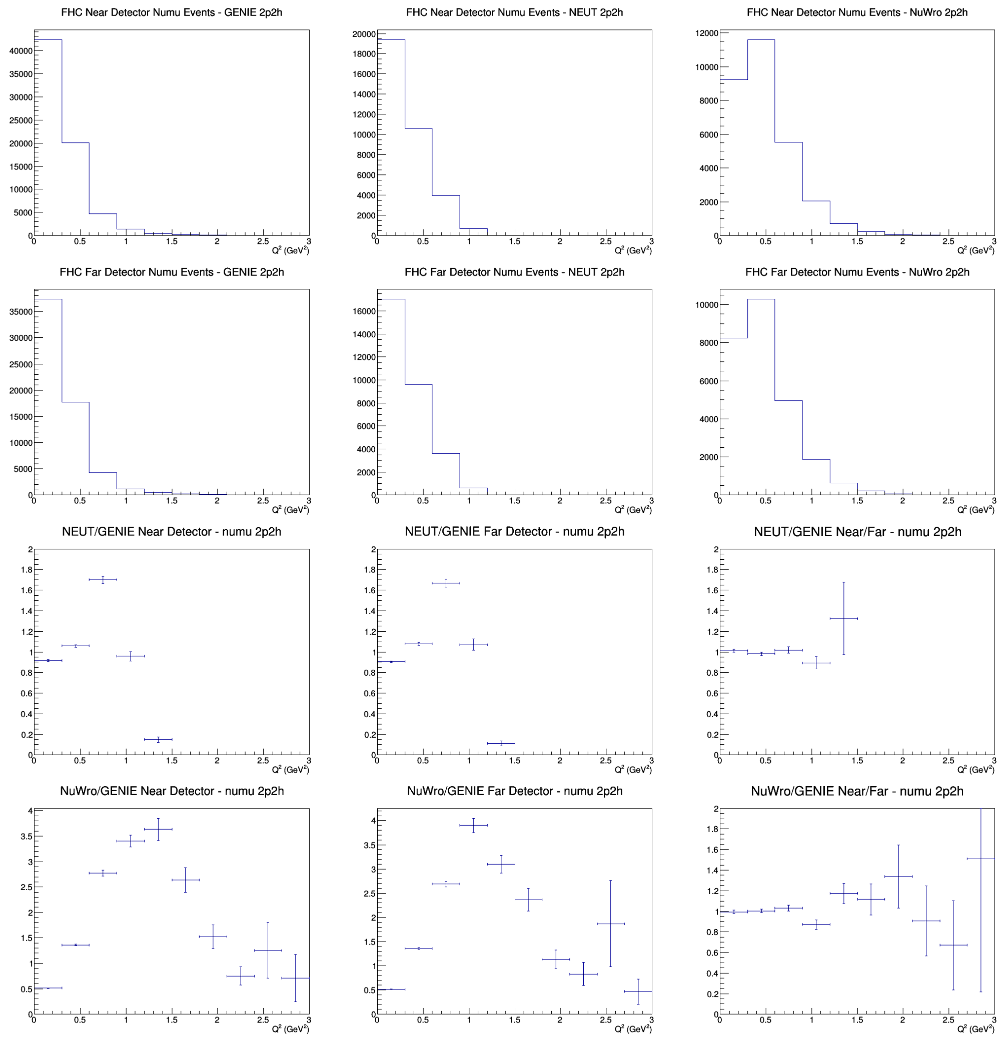

## B.10 numu 2p2h FGT efficiencies

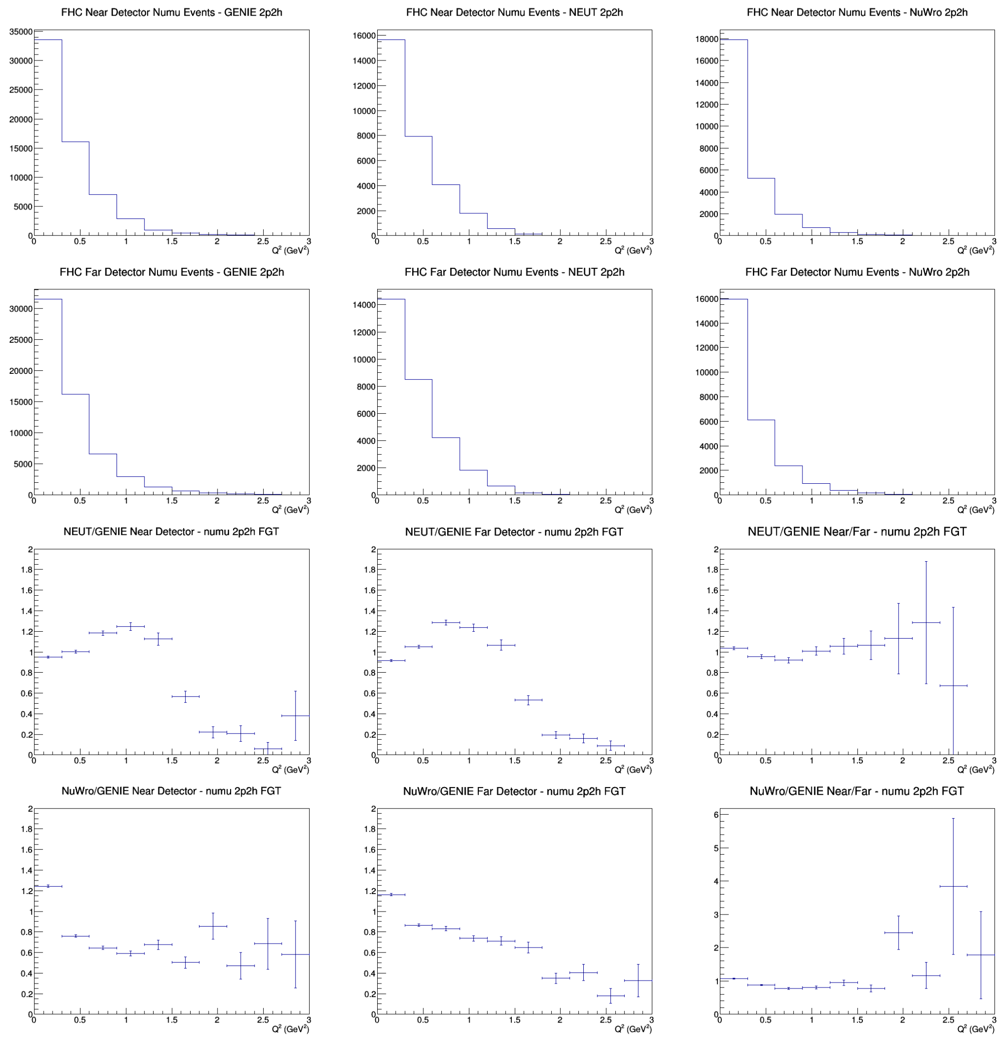

## B.11 numu 2p2h LAr efficiencies

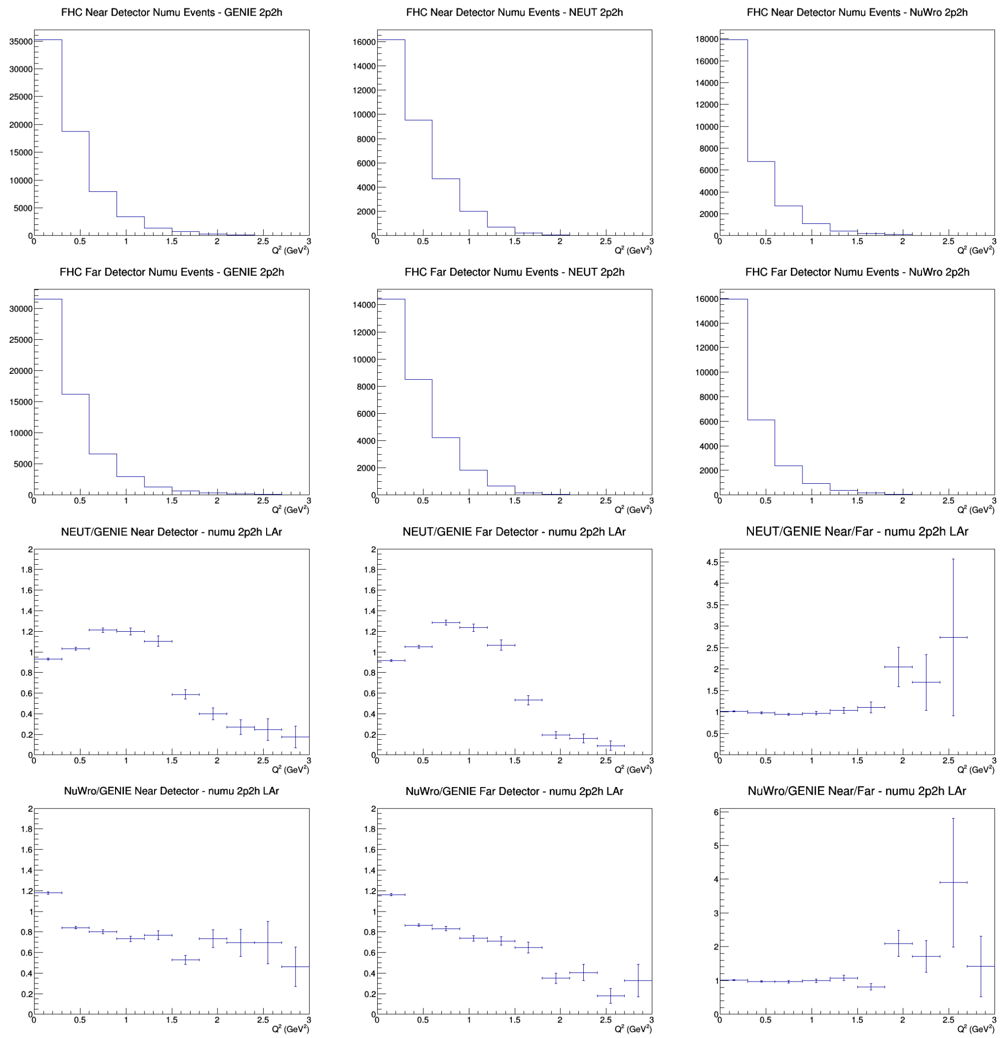

## B.12 numu 2p2h GAr efficiencies

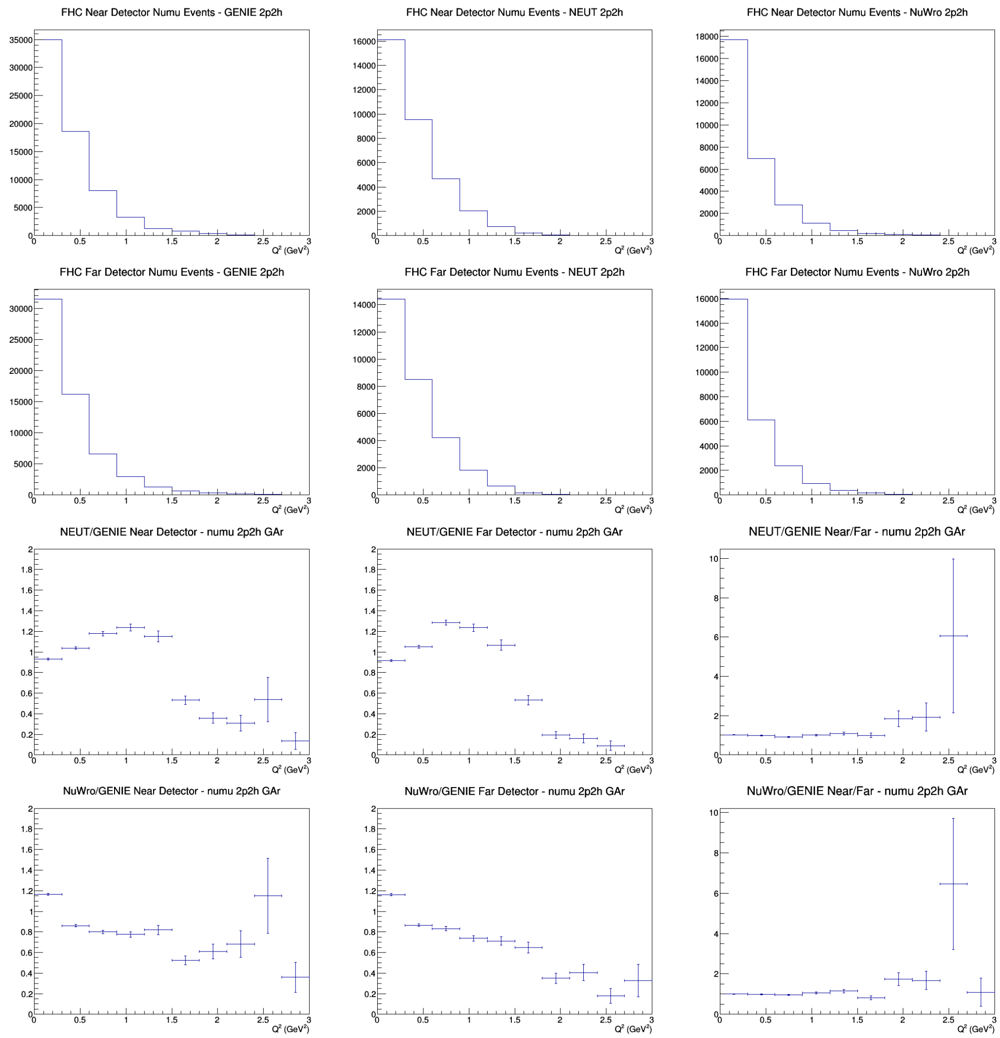

## B.13 numubar 2p2h no efficiencies

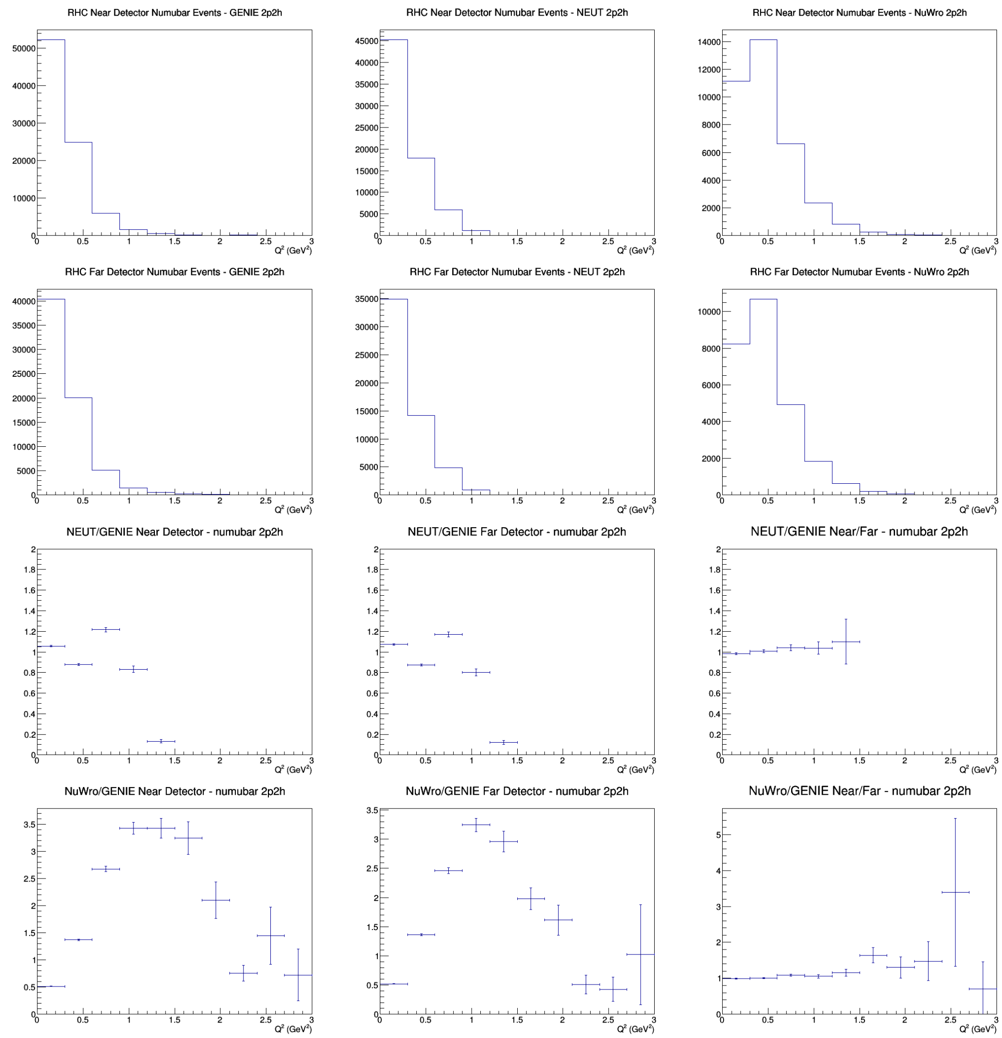

## B.14 numubar 2p2h FGT efficiencies

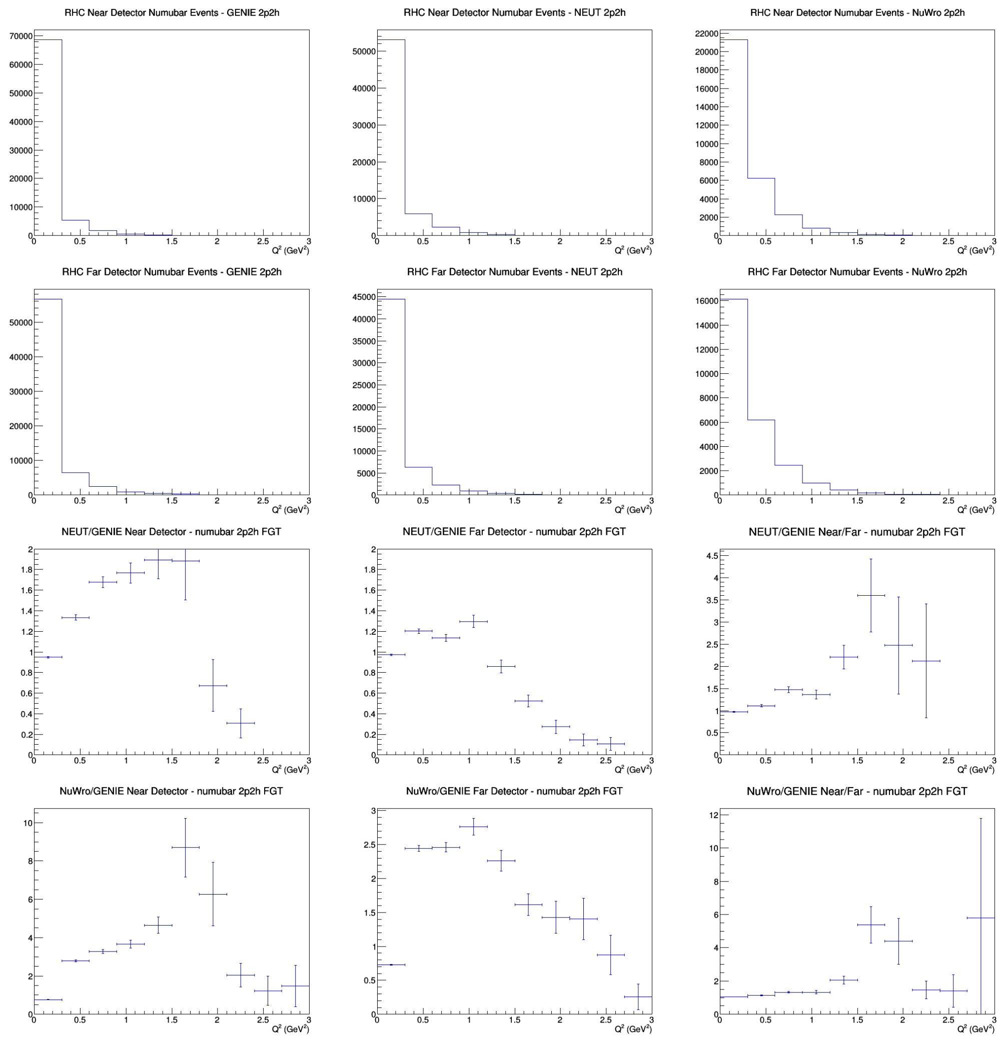

## B.15 numubar 2p2h LAr efficiencies

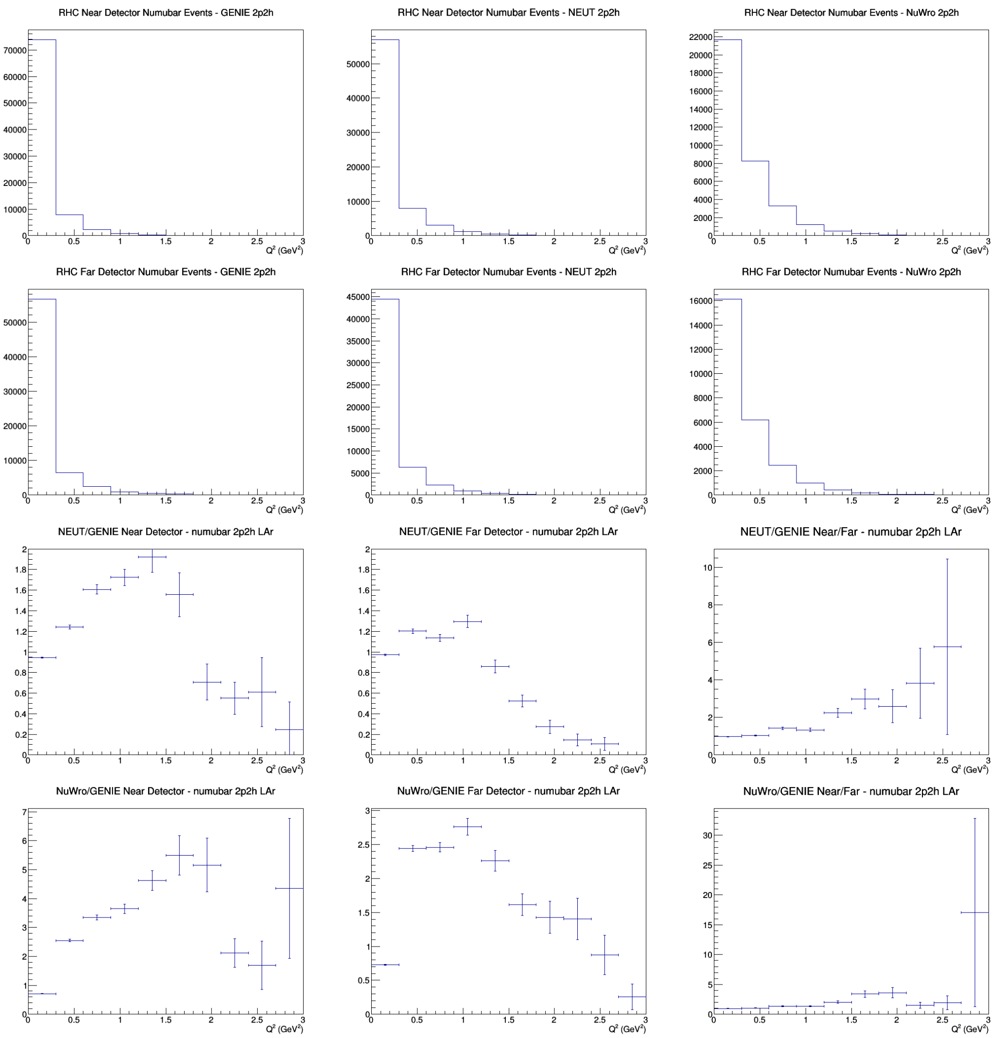

## B.16 numubar 2p2h GAr efficiencies

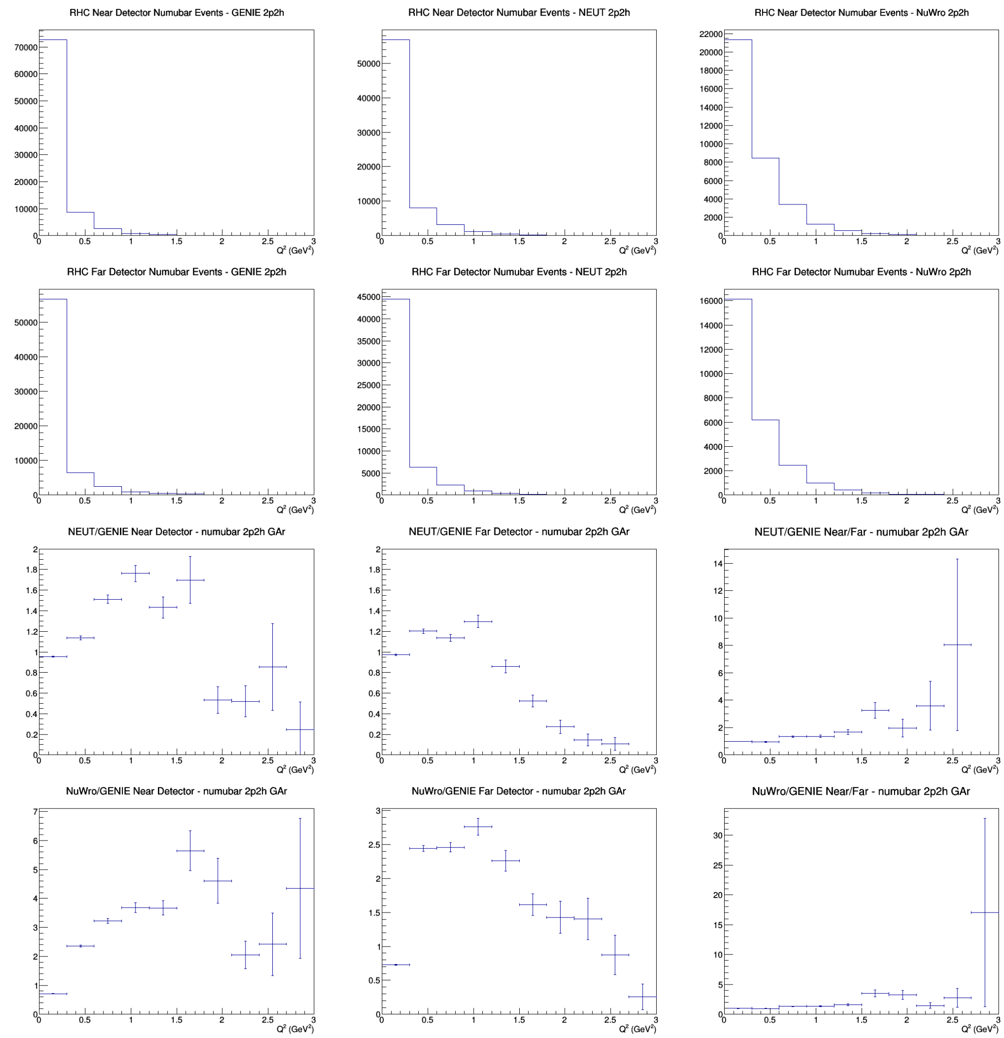

## B.17 numu CC0Pi no efficiencies

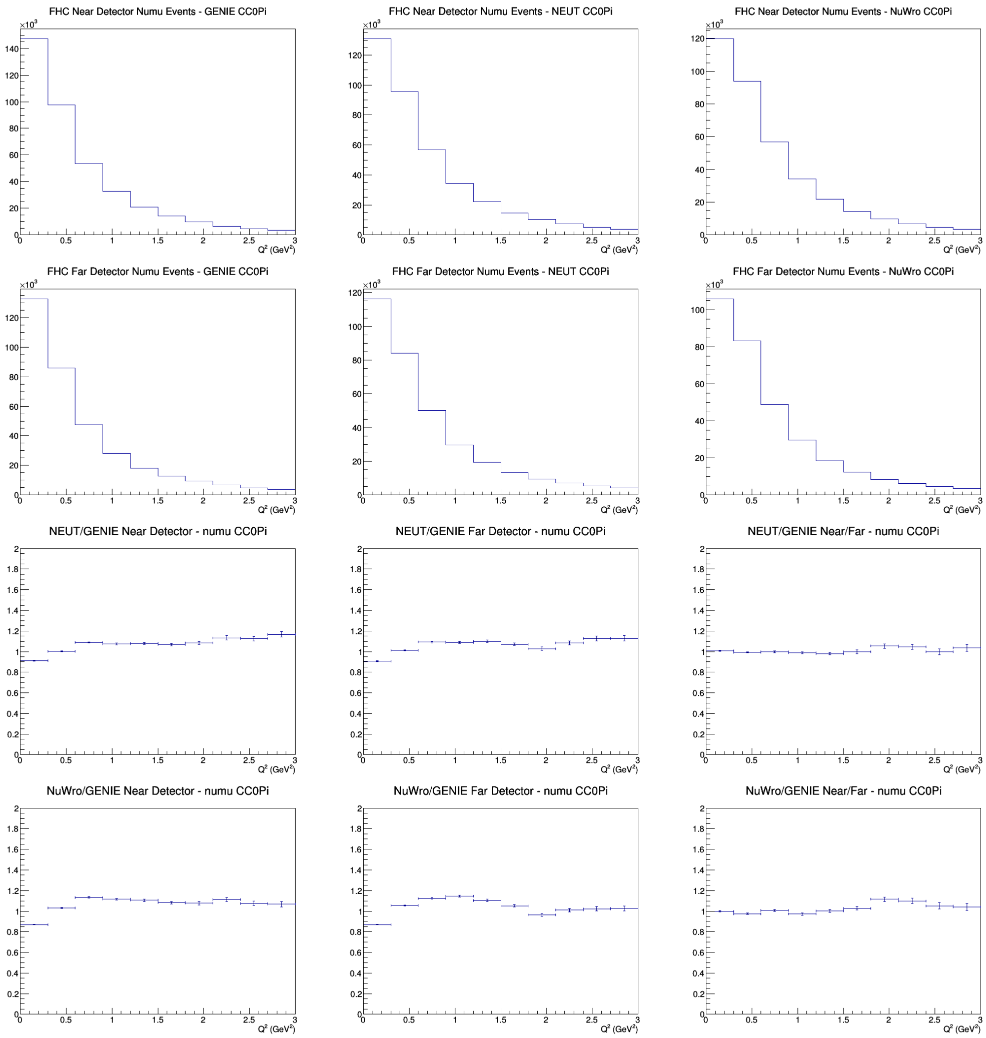

## B.18 numu CC0Pi FGT efficiencies

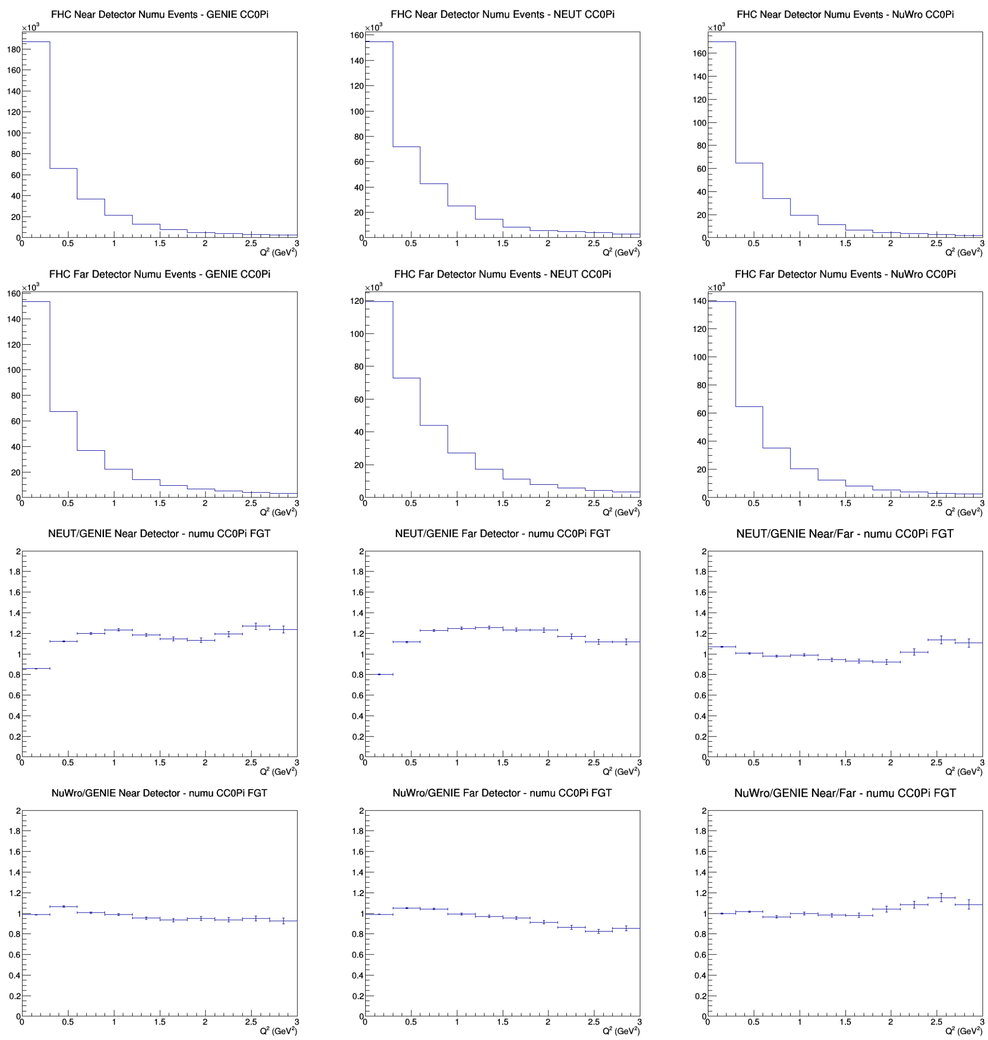

## B.19 numu CC0Pi LAr efficiencies

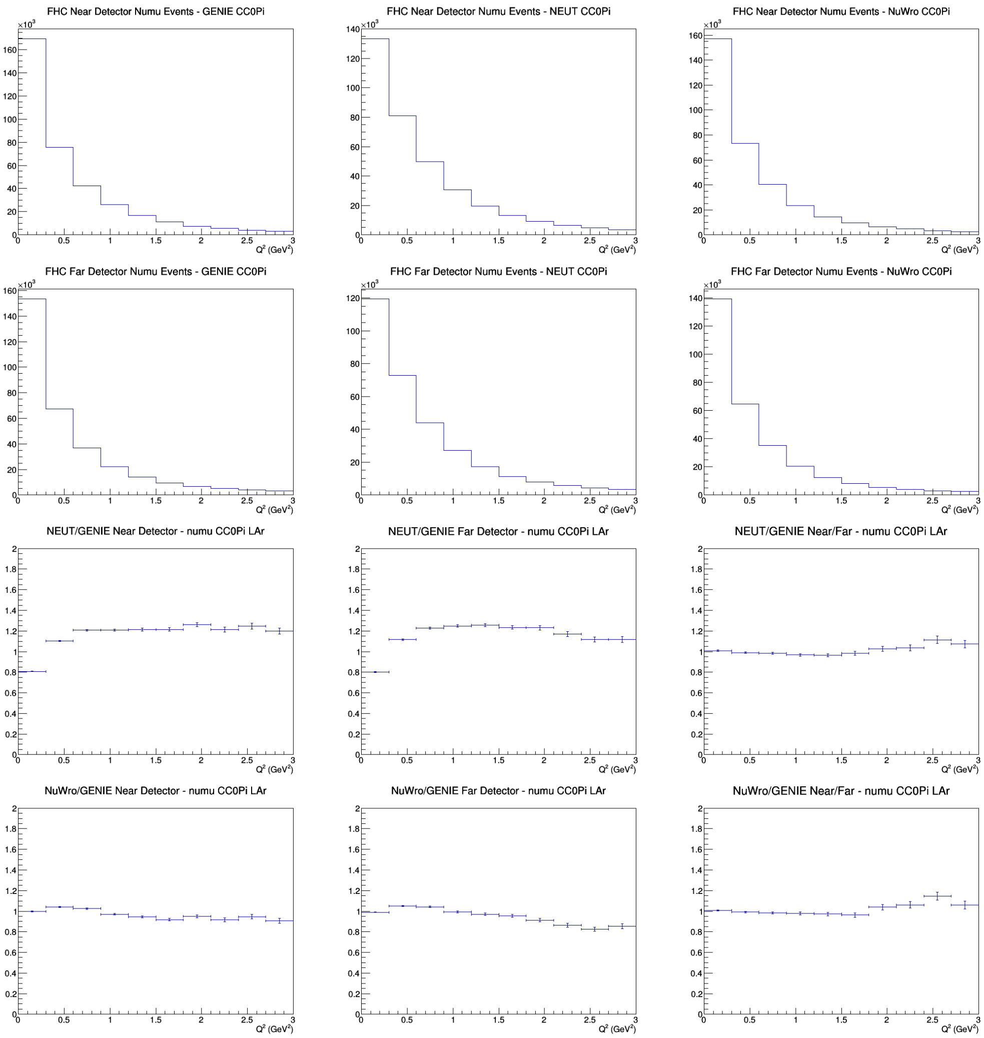

## B.20 numu CC0Pi GAr efficiencies

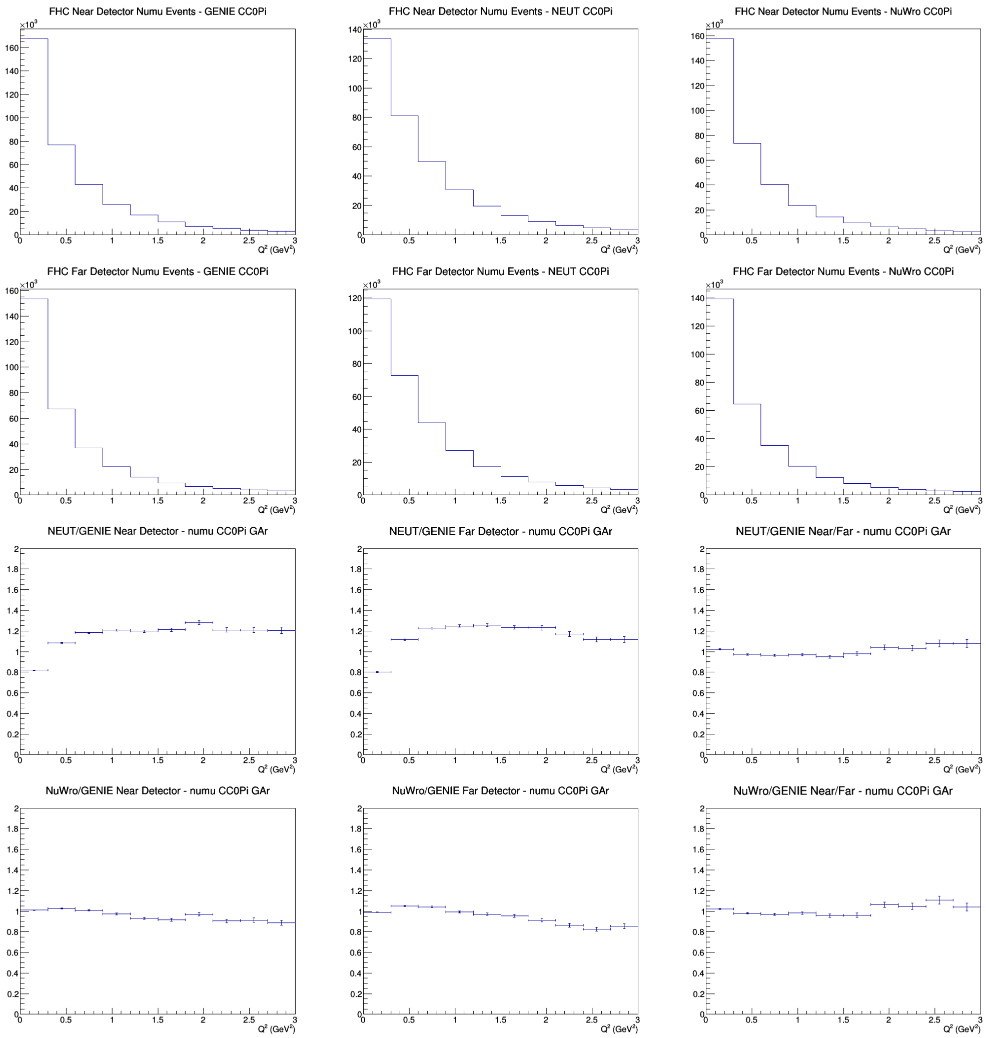

## B.21 numubar CC0Pi no efficiencies

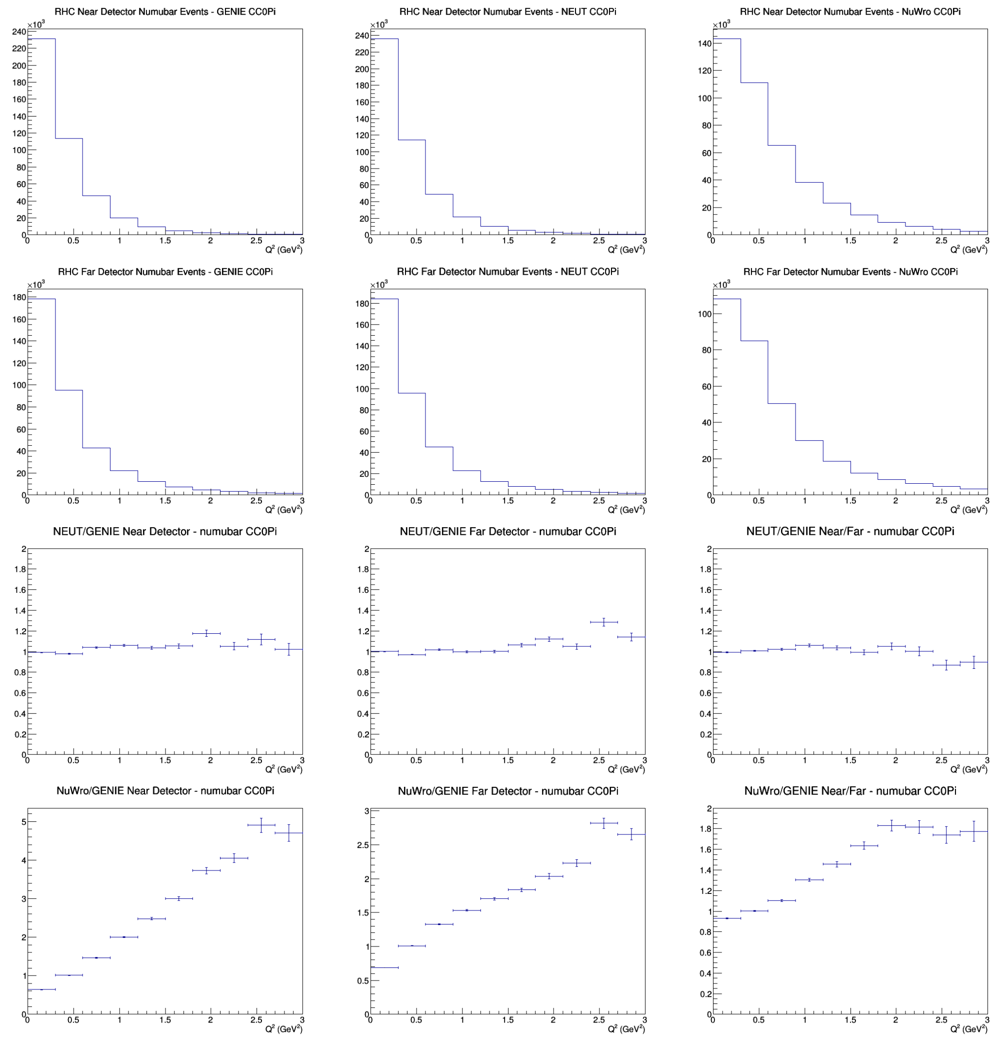

## B.22 numubar CC0Pi FGT efficiencies

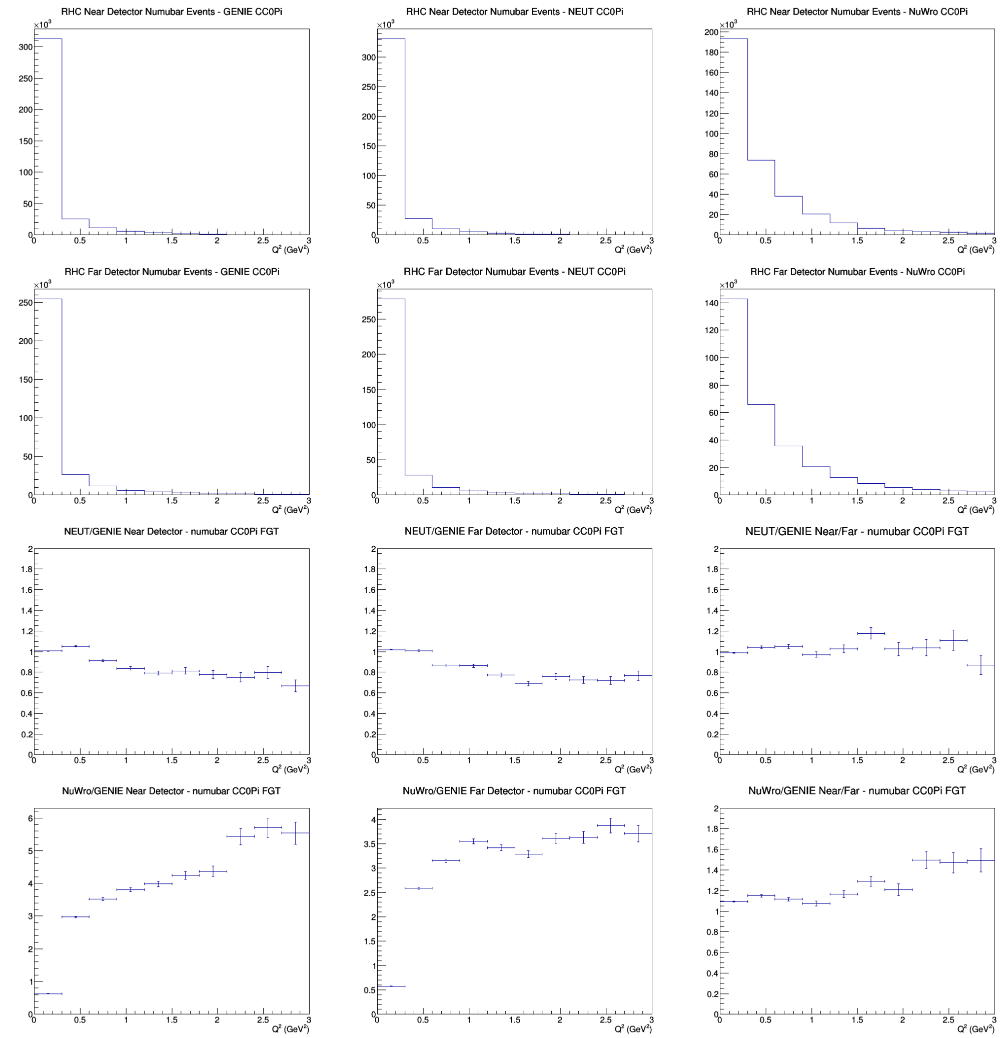

## B.23 numubar CC0Pi LAr efficiencies

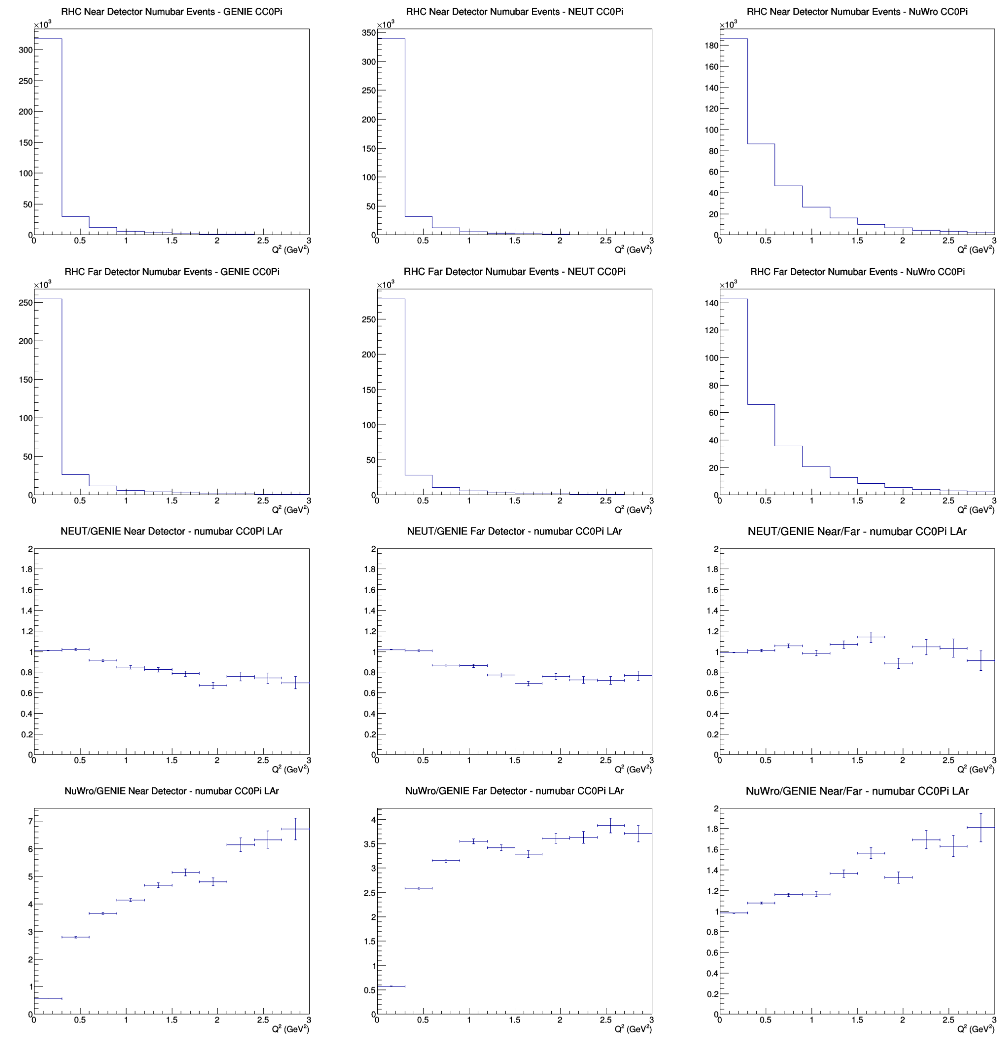

## B.24 numubar CC0Pi GAr efficiencies

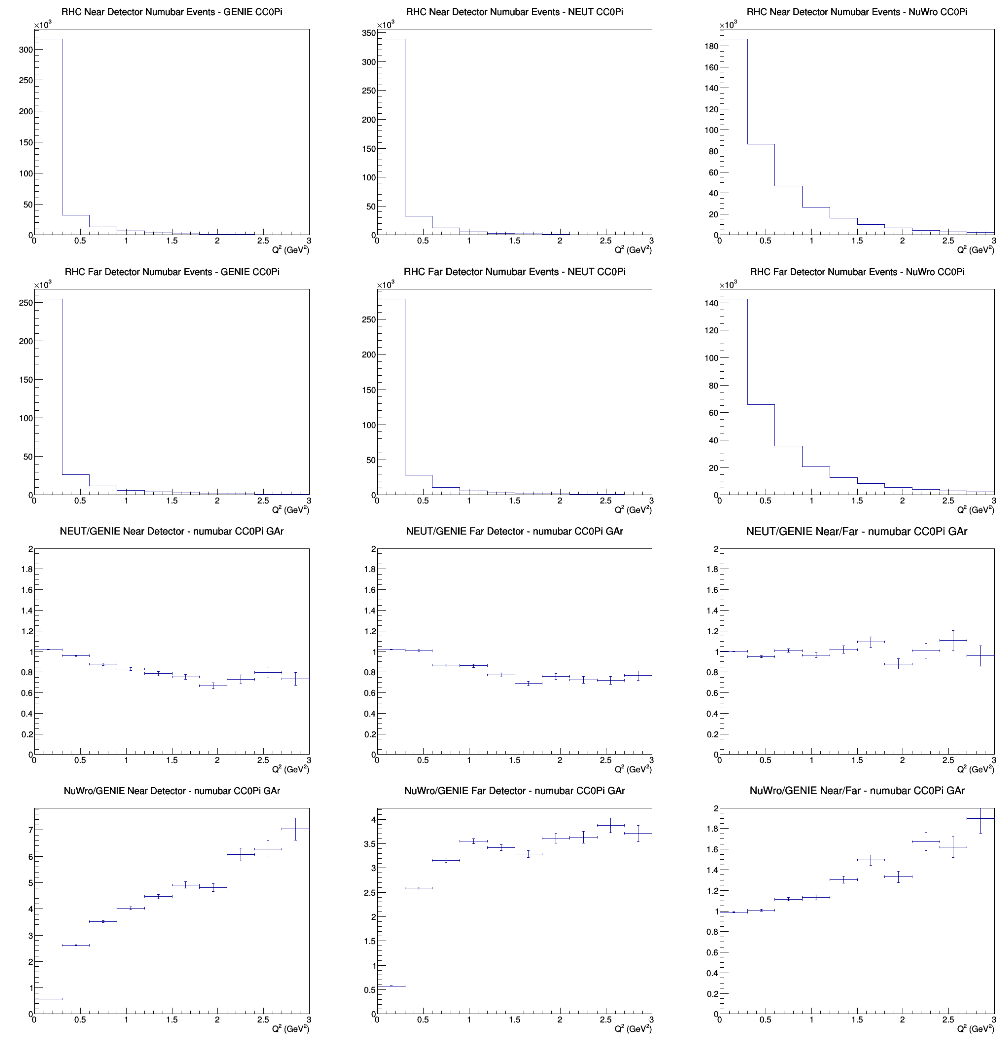

## B.25 numu CC1Pi no efficiencies

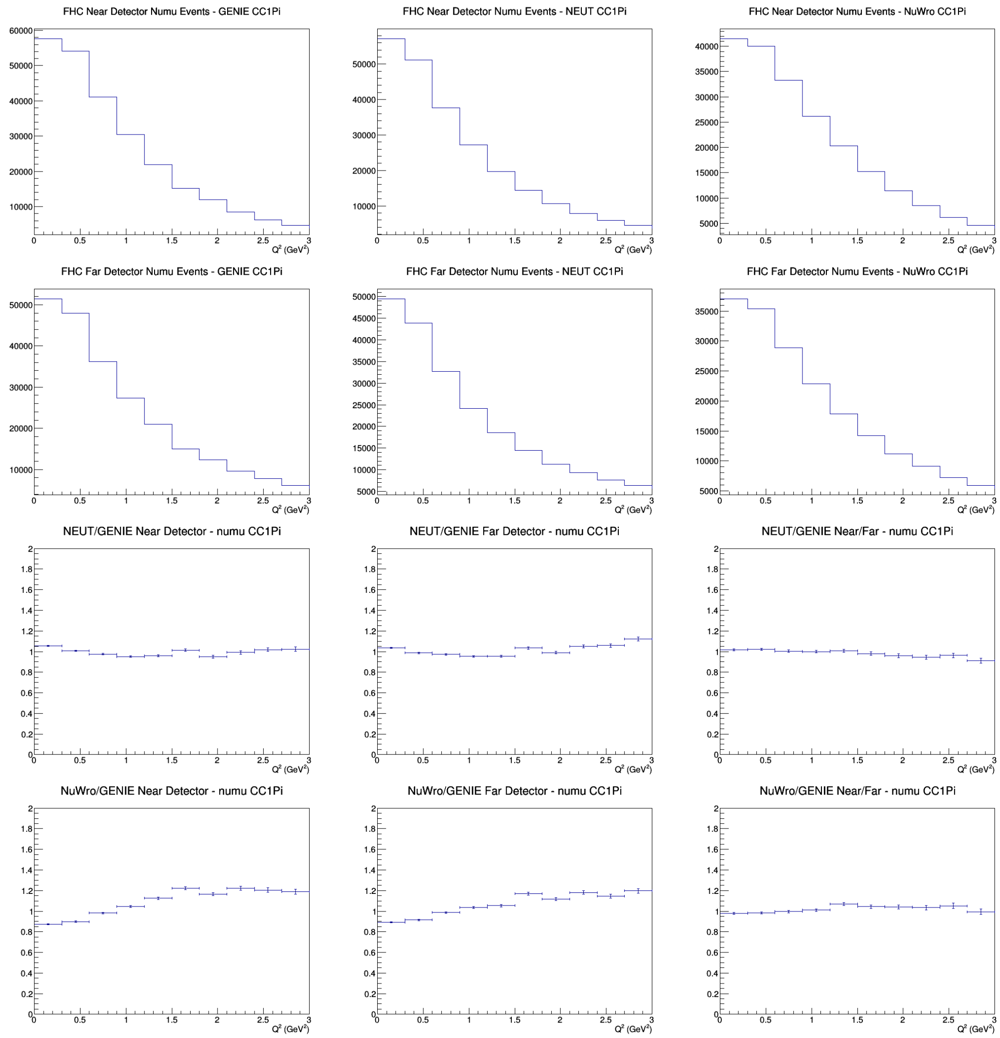

## B.26 numu CC1Pi FGT efficiencies

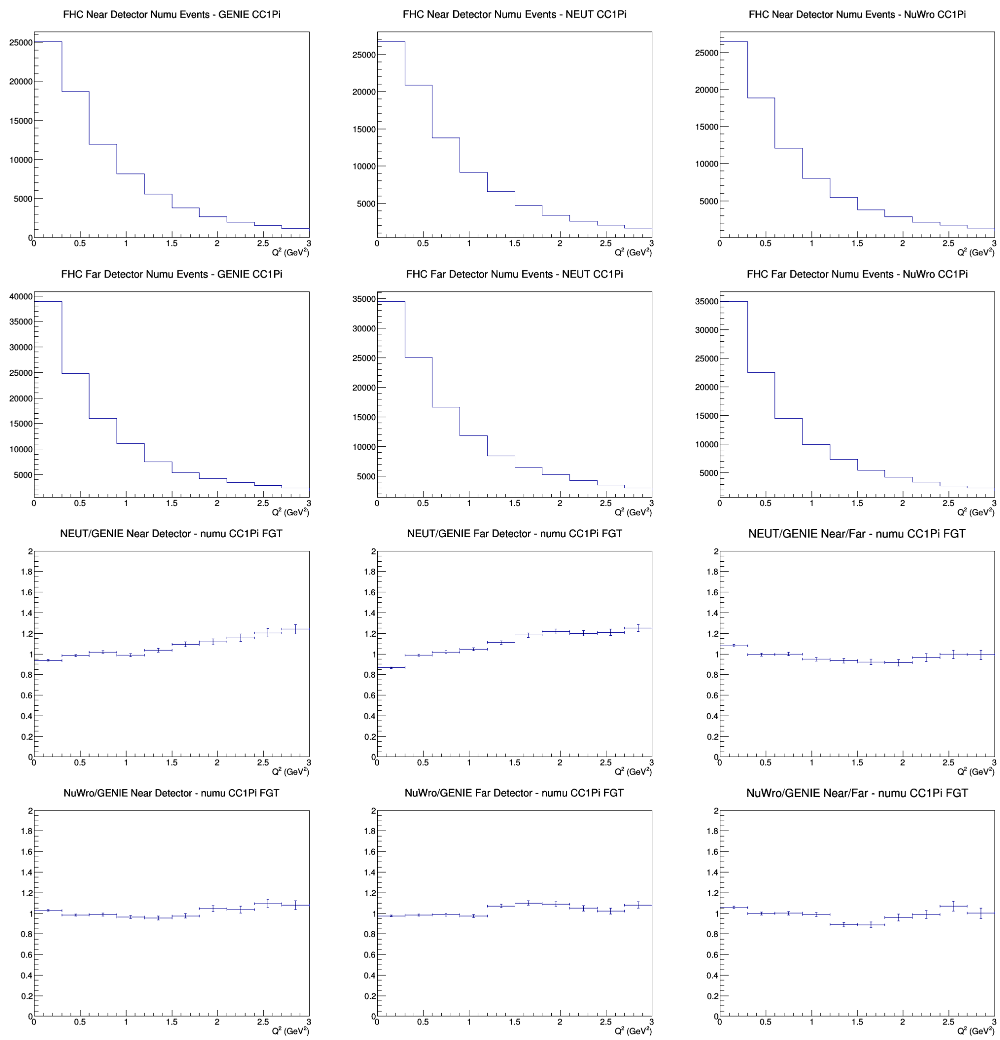

## B.27 numu CC1Pi LAr efficiencies

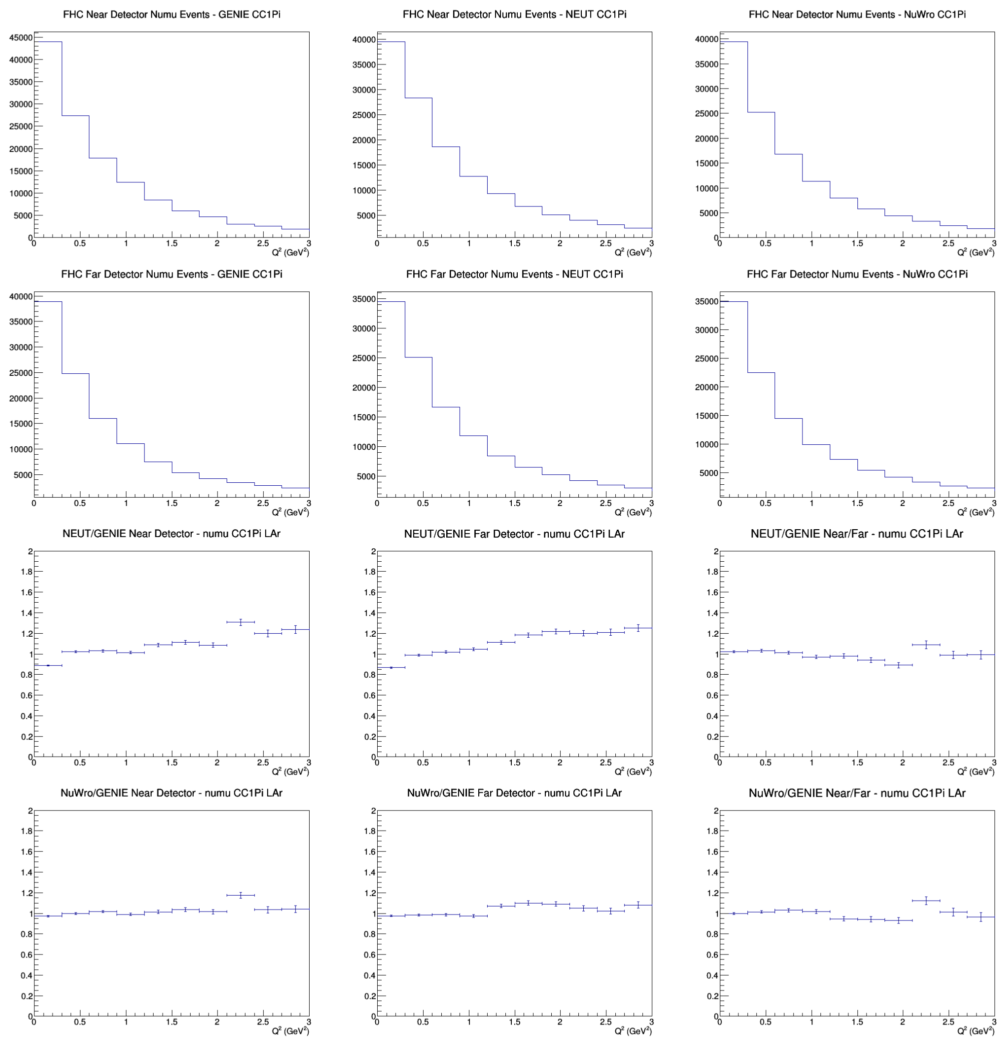

## B.28 numu CC1Pi GAr efficiencies

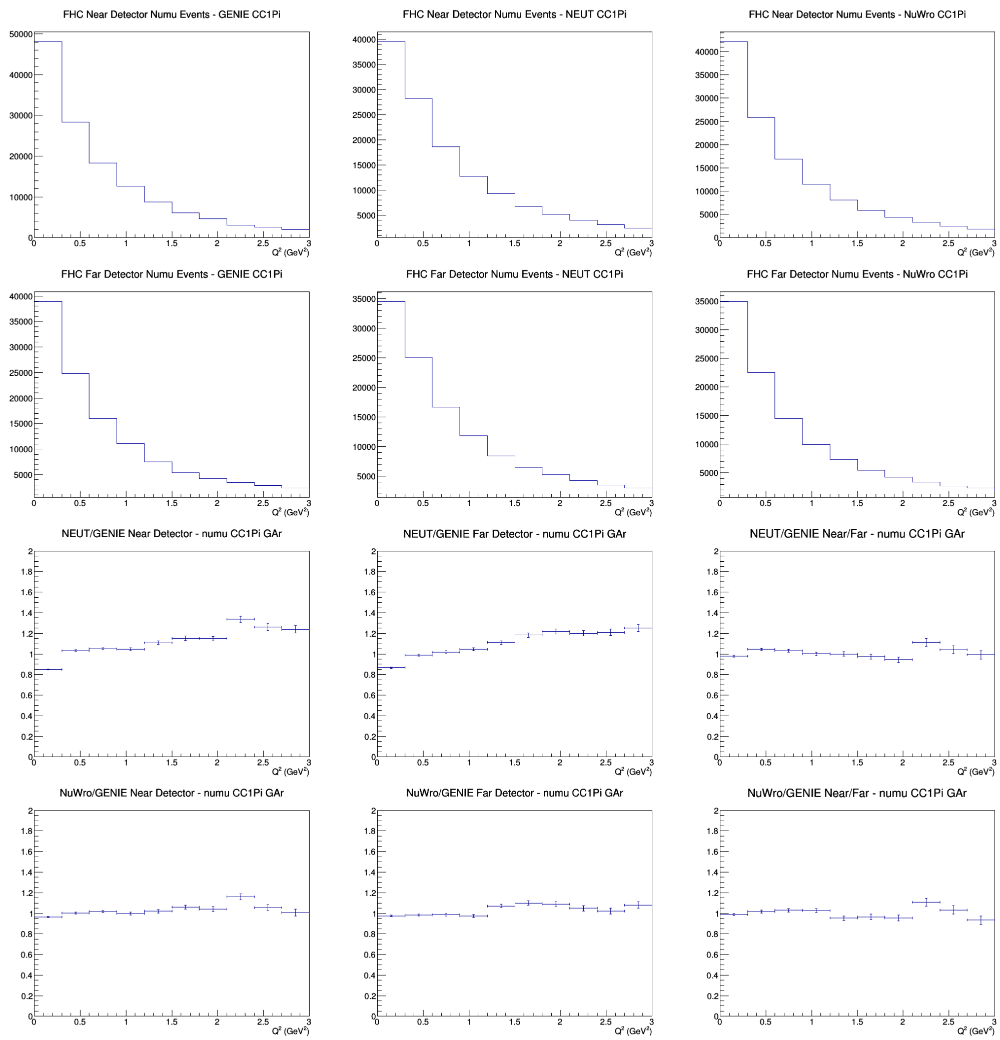

## B.29 numubar CC1Pi no efficiencies

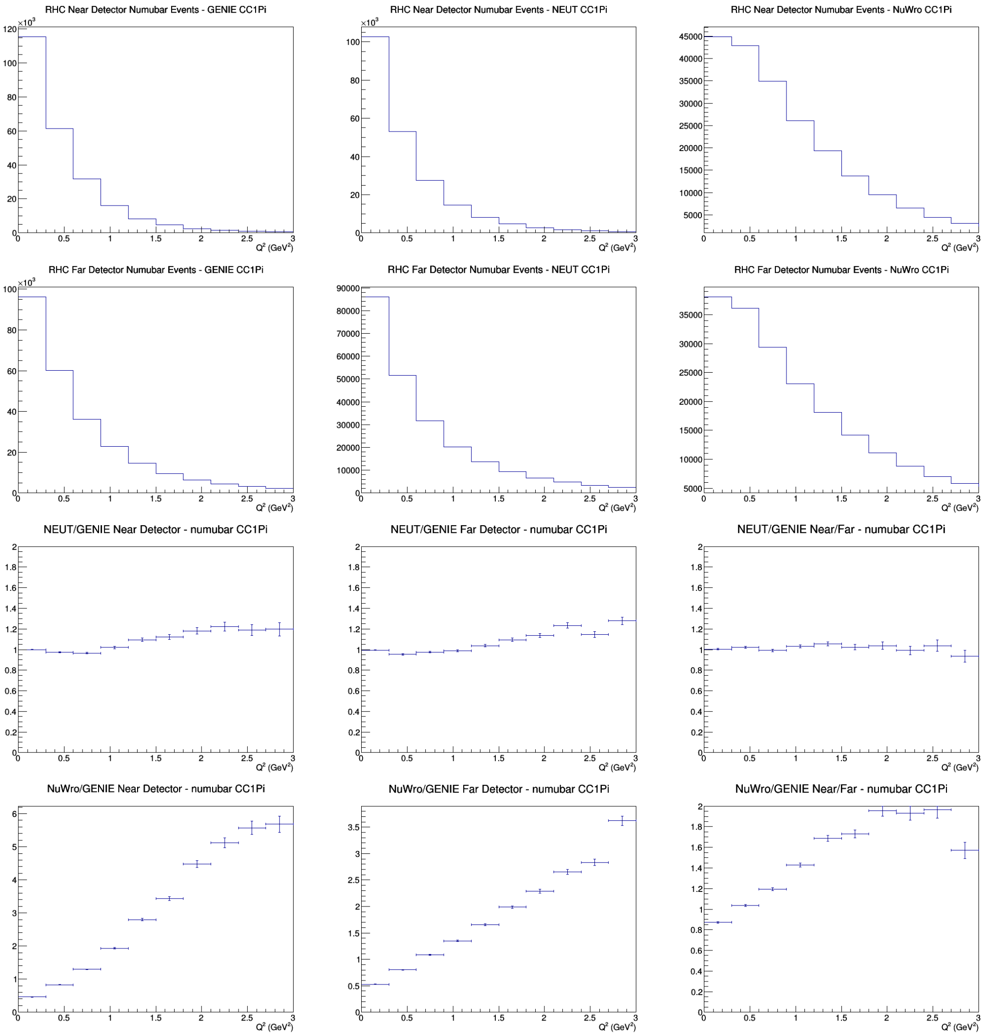

## B.30 numubar CC1Pi FGT efficiencies

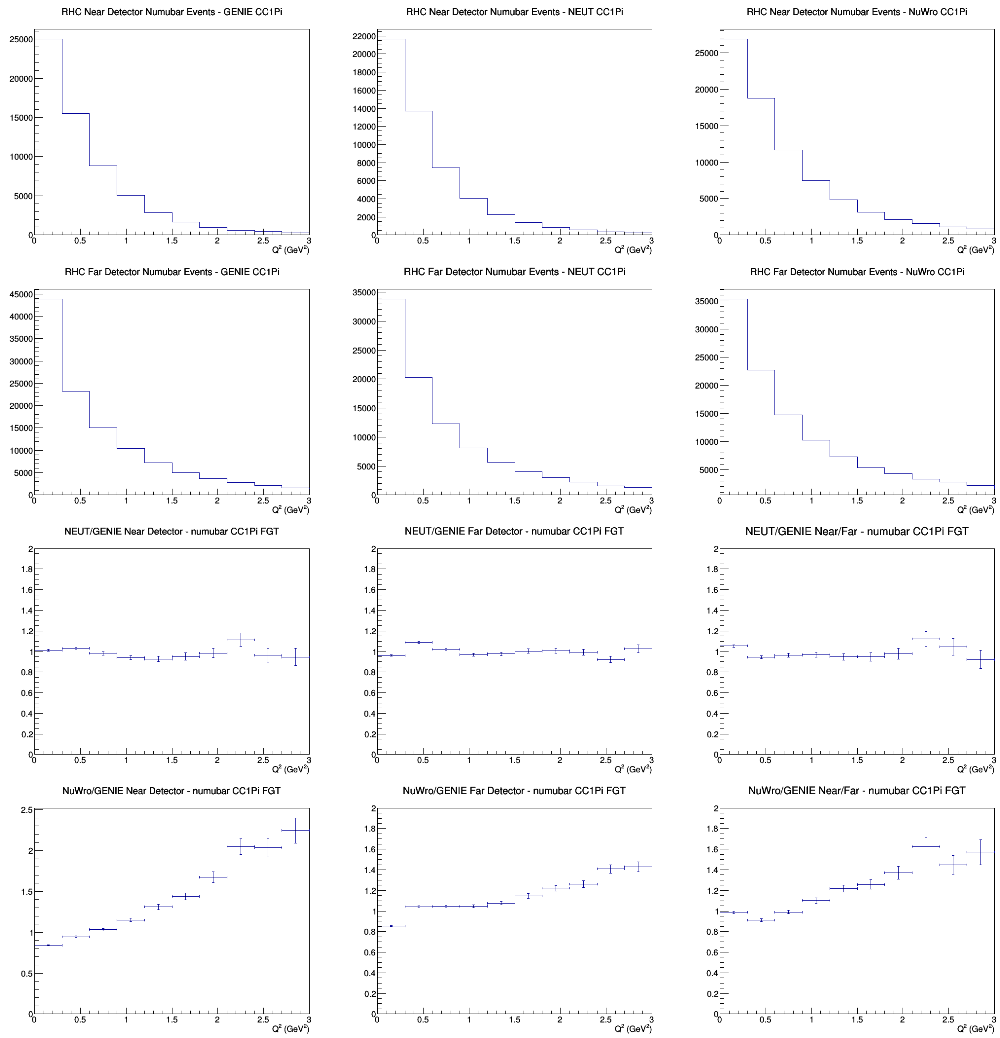

## B.31 numubar CC1Pi LAr efficiencies

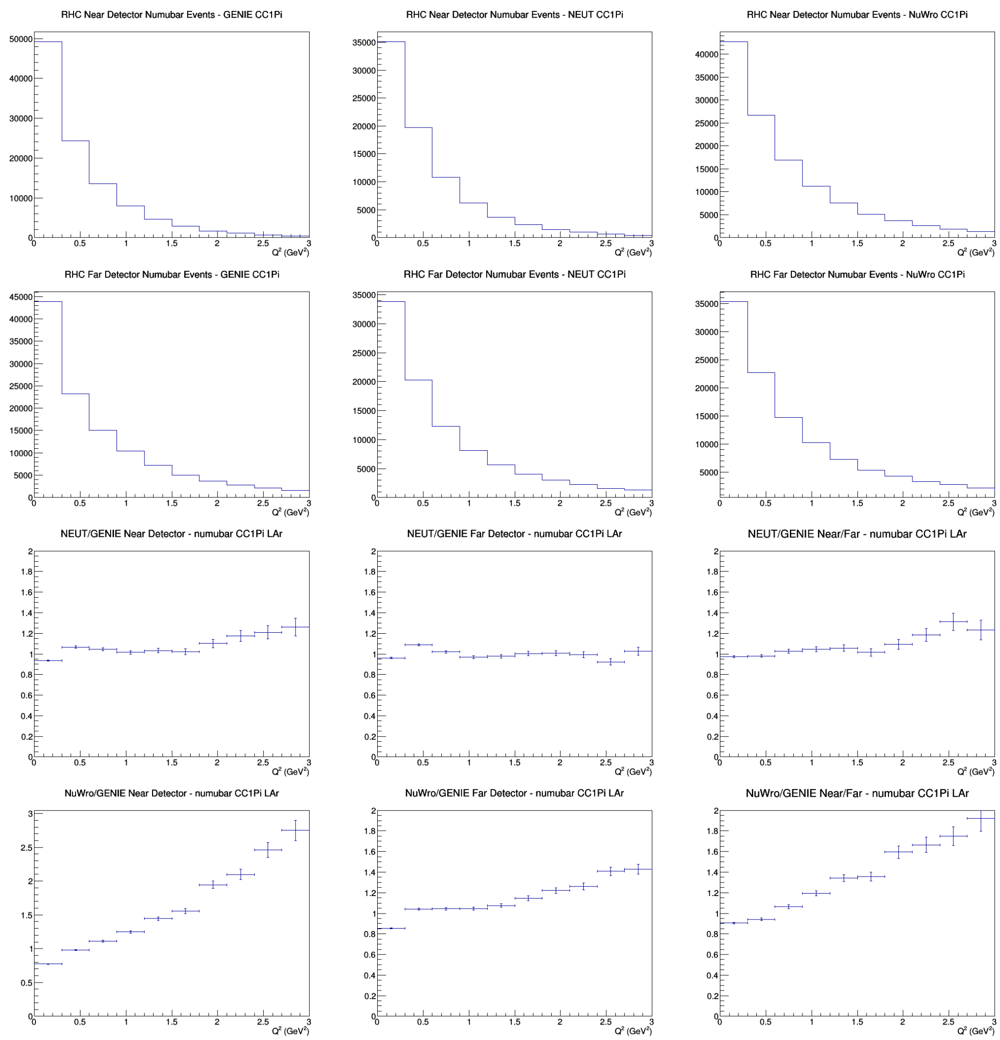

## B.32 numubar CC1Pi GAr efficiencies

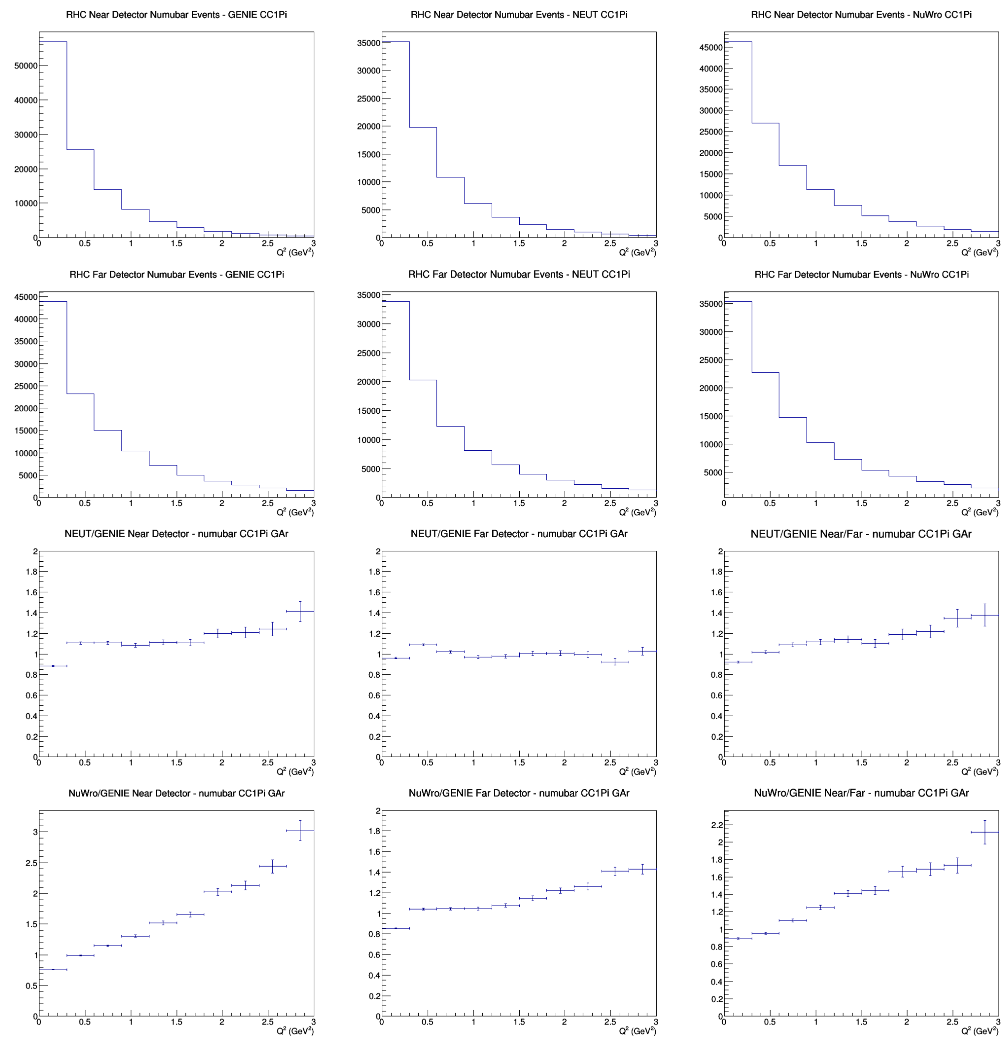

## B.33 numu CCOther no efficiencies

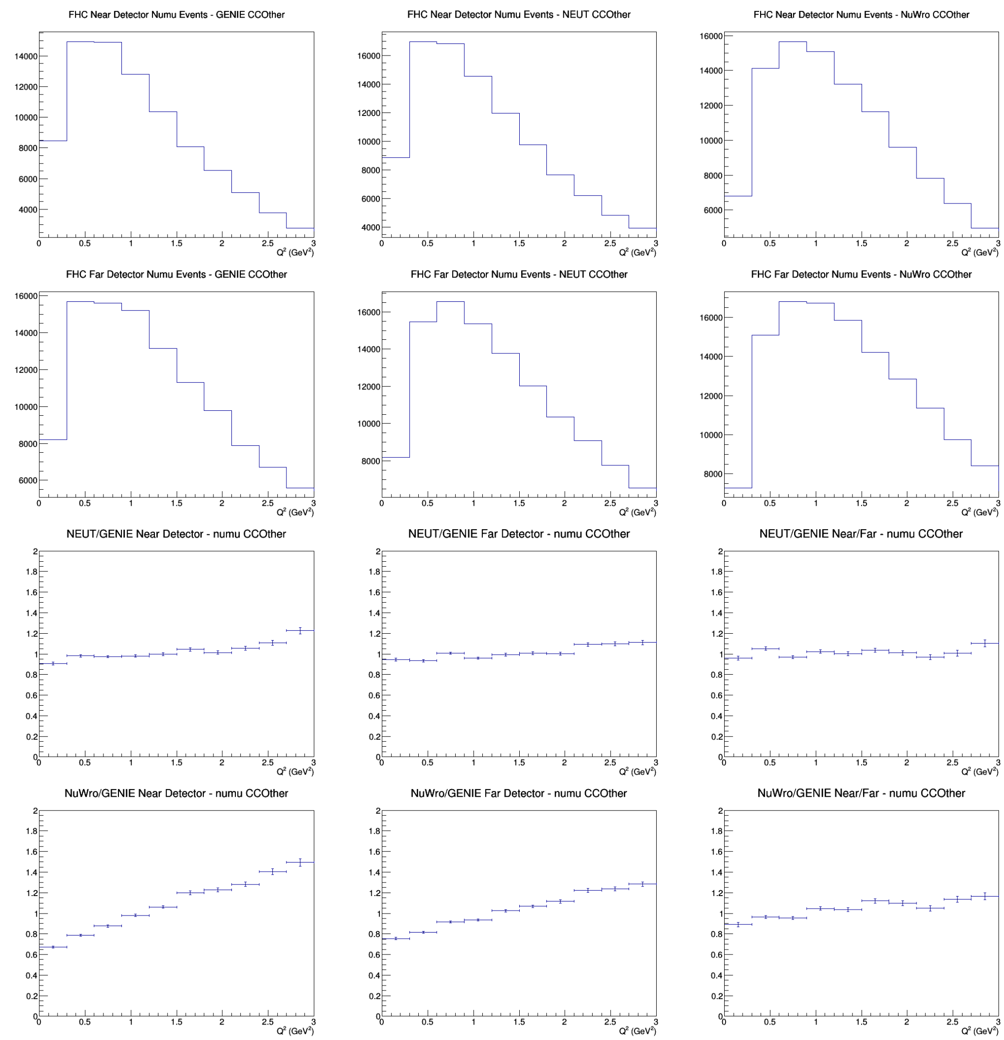

## B.34 numu CCOther FGT efficiencies

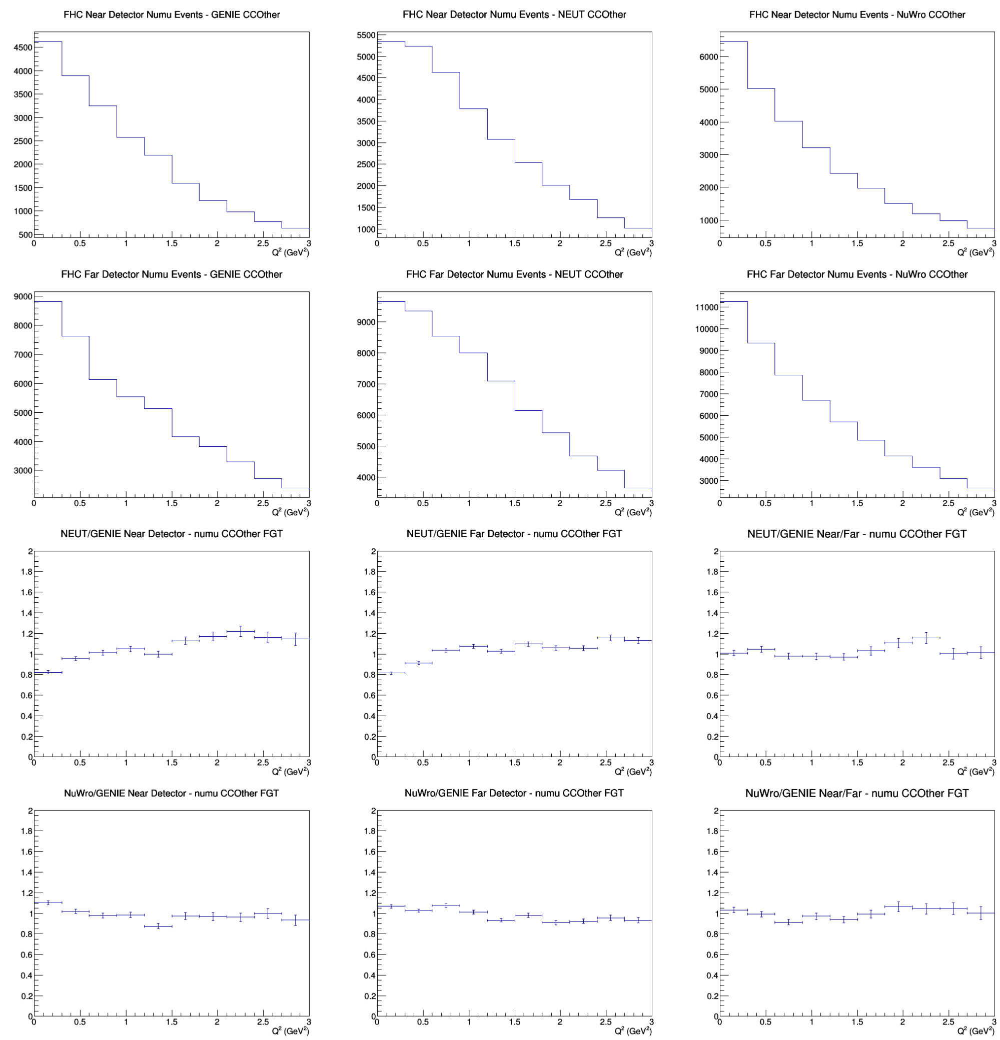

## B.35 numu CCOther LAr efficiencies

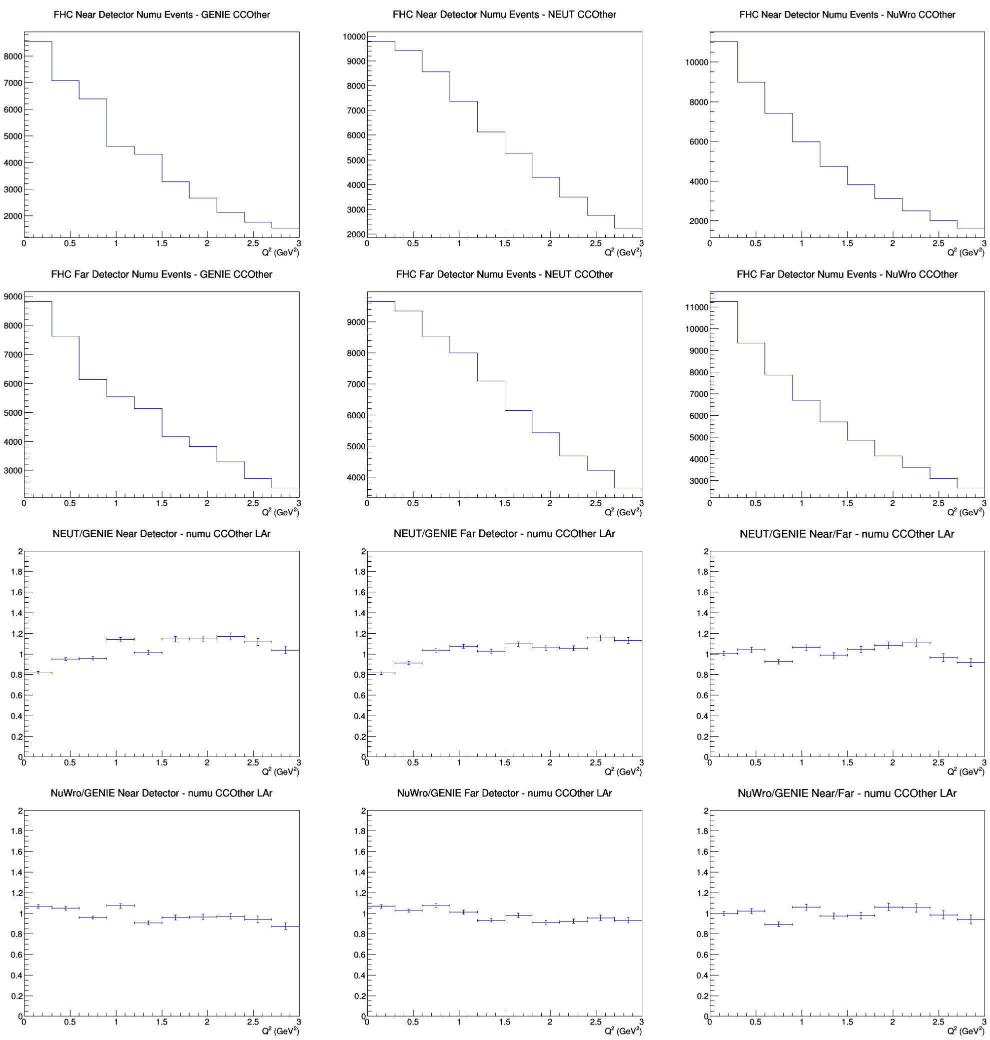

## B.36 numu CCOther GAr efficiencies

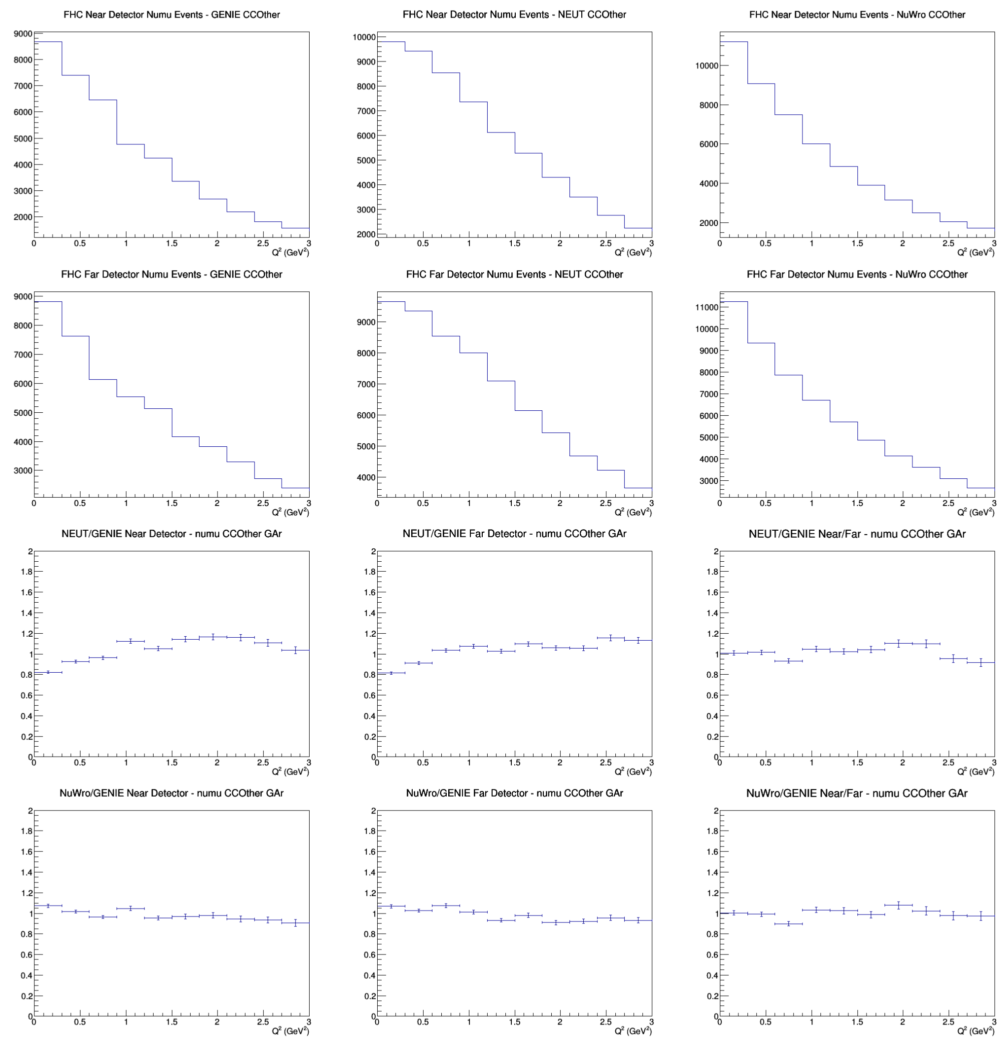

## B.37 numubar CCOther no efficiencies

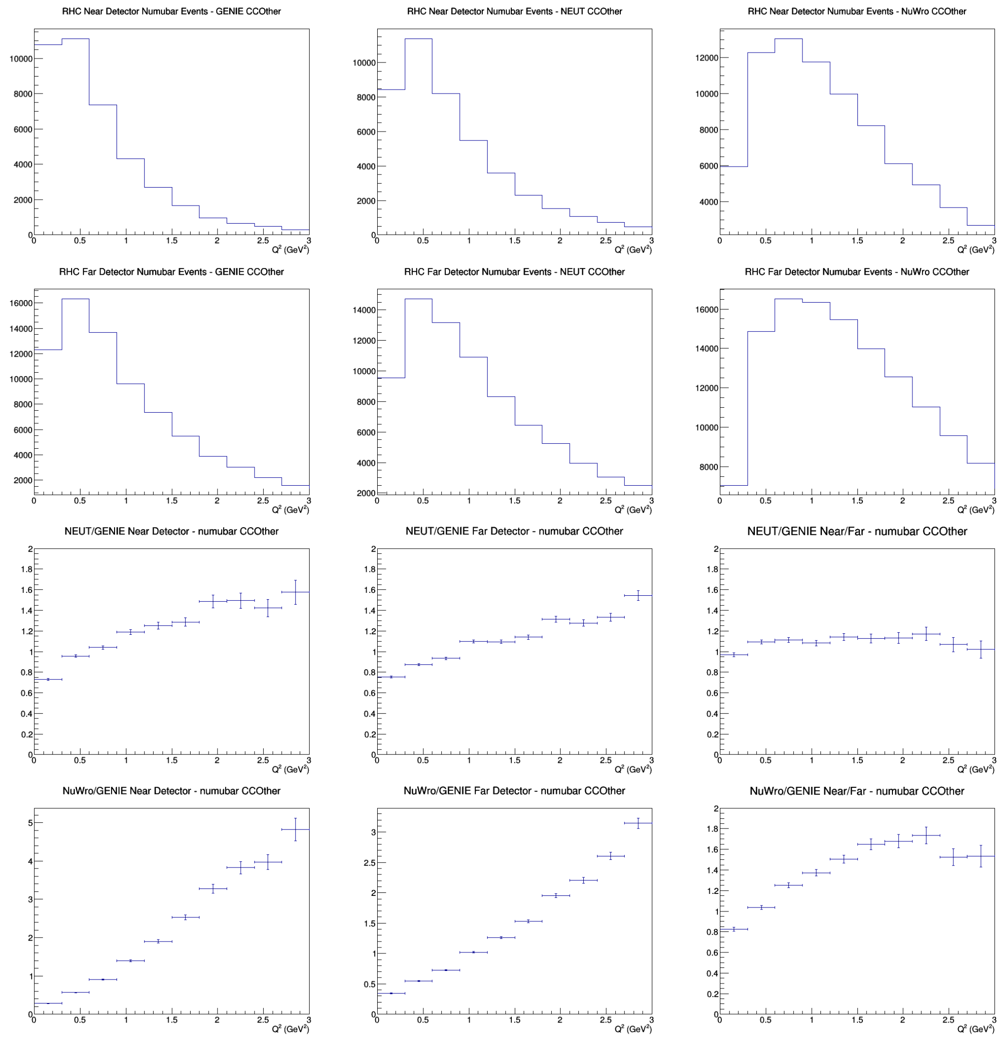

## B.38 numubar CCOther FGT efficiencies

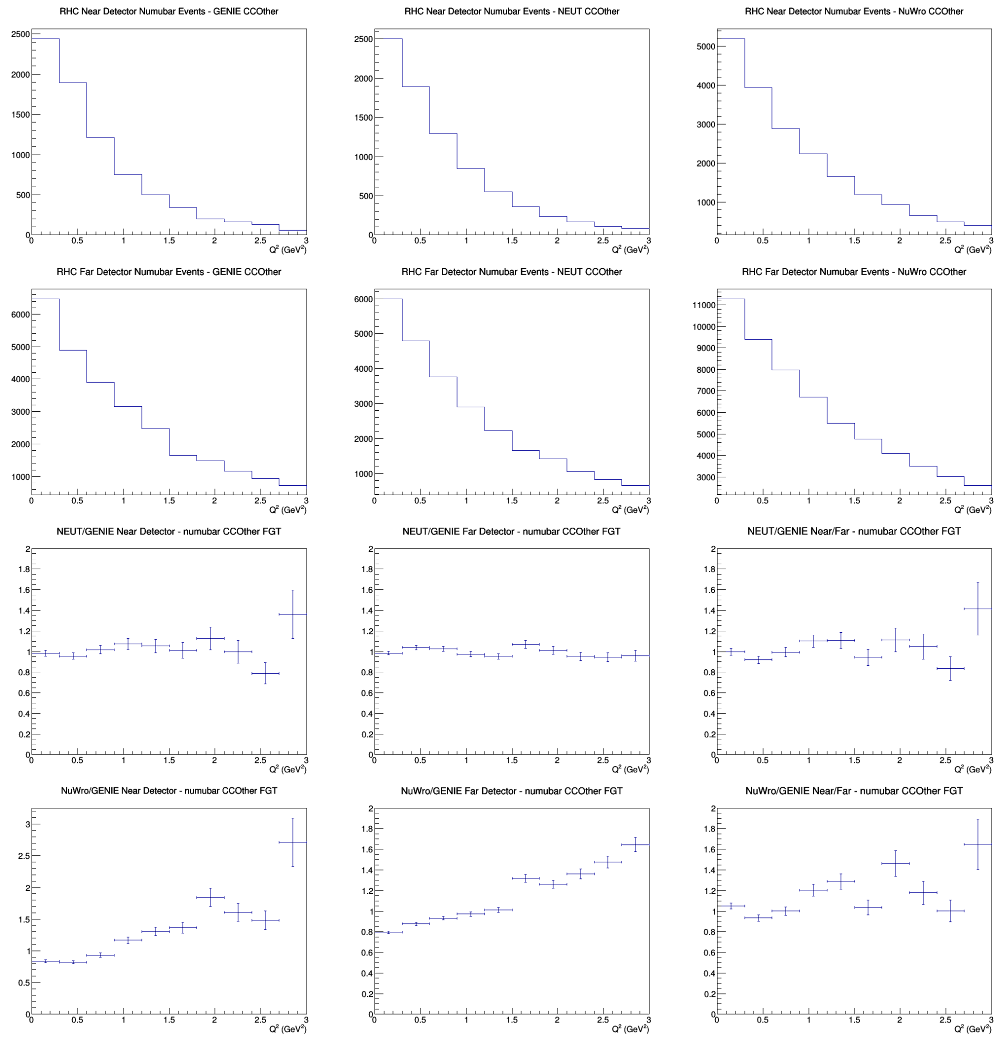

## B.39 numubar CCOther LAr efficiencies

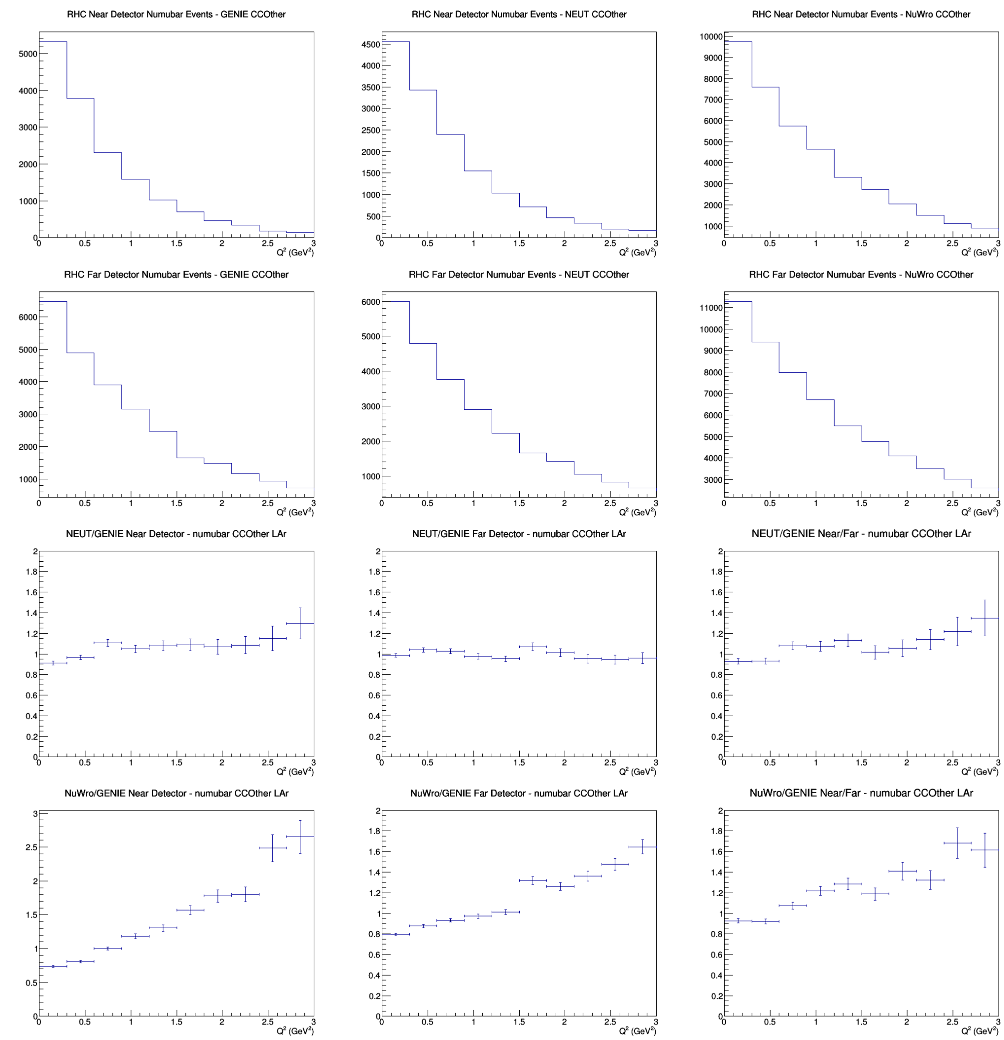

## B.40 numubar CCOther GAr efficiencies

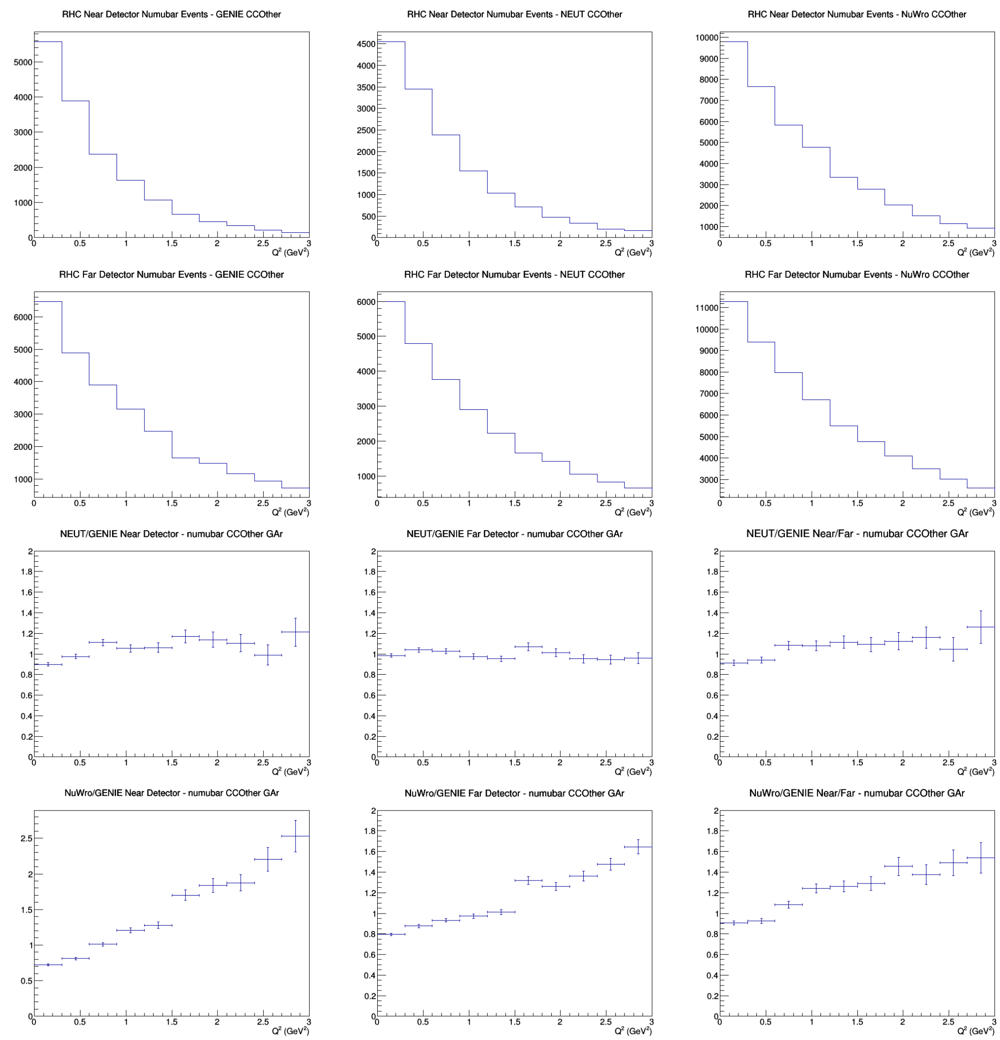

# C $q_0$ vs. $q_3$ Plots

This appendix includes all the plots not show in Section 4.2. For full description of the files, please make reference to that section. The plots will be put in the same order as before.

## C.1 numu CCQE no efficiencies

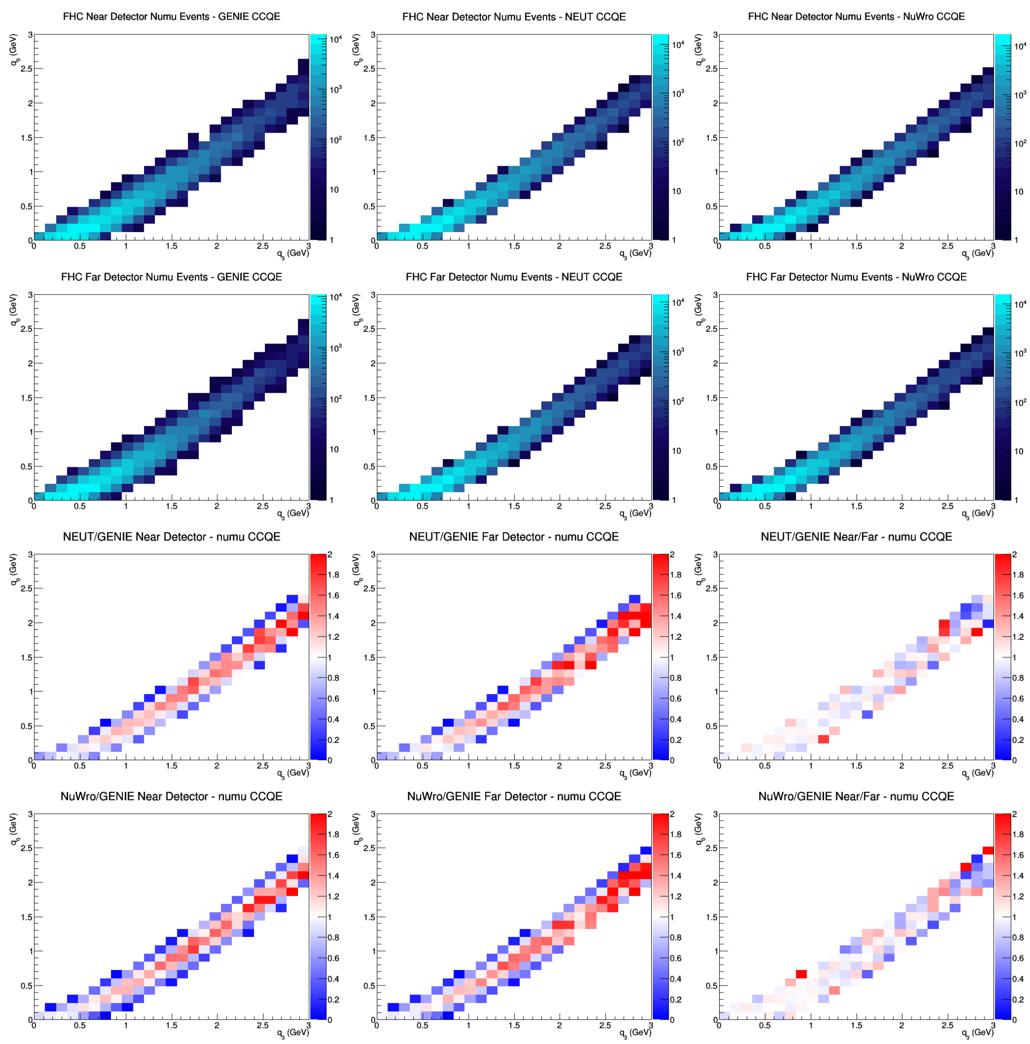

## C.2 numu CCQE FGT efficiencies

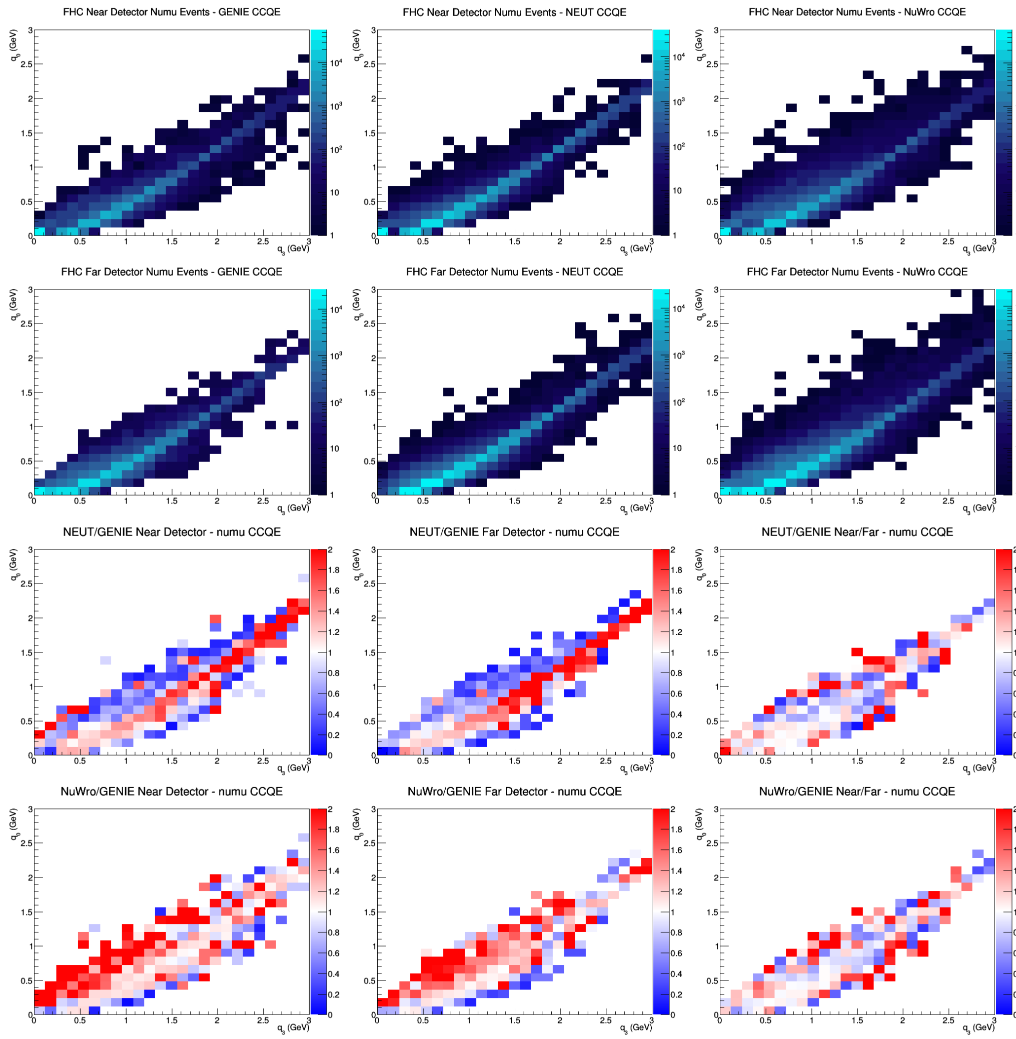

## C.3 numu CCQE LAr efficiencies

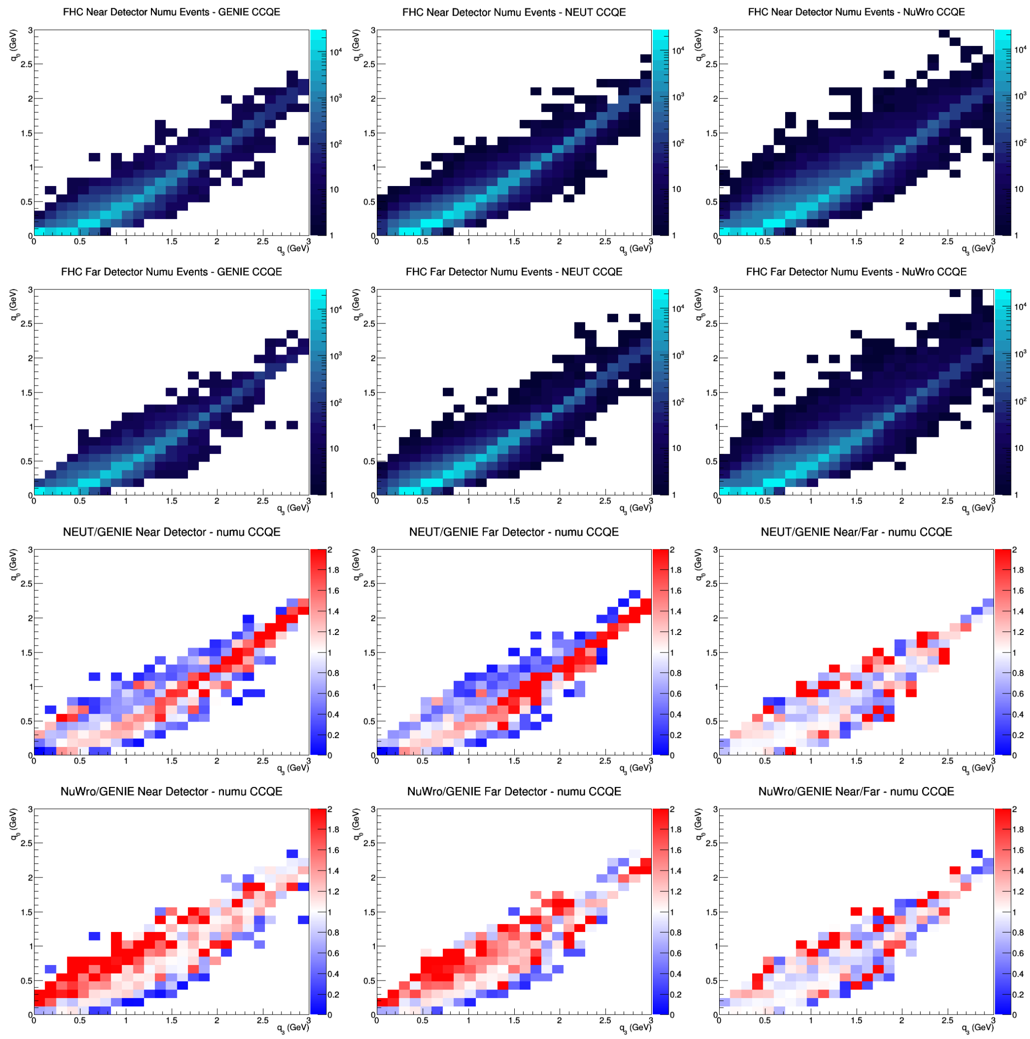

## C.4 numu CCQE GAr efficiencies

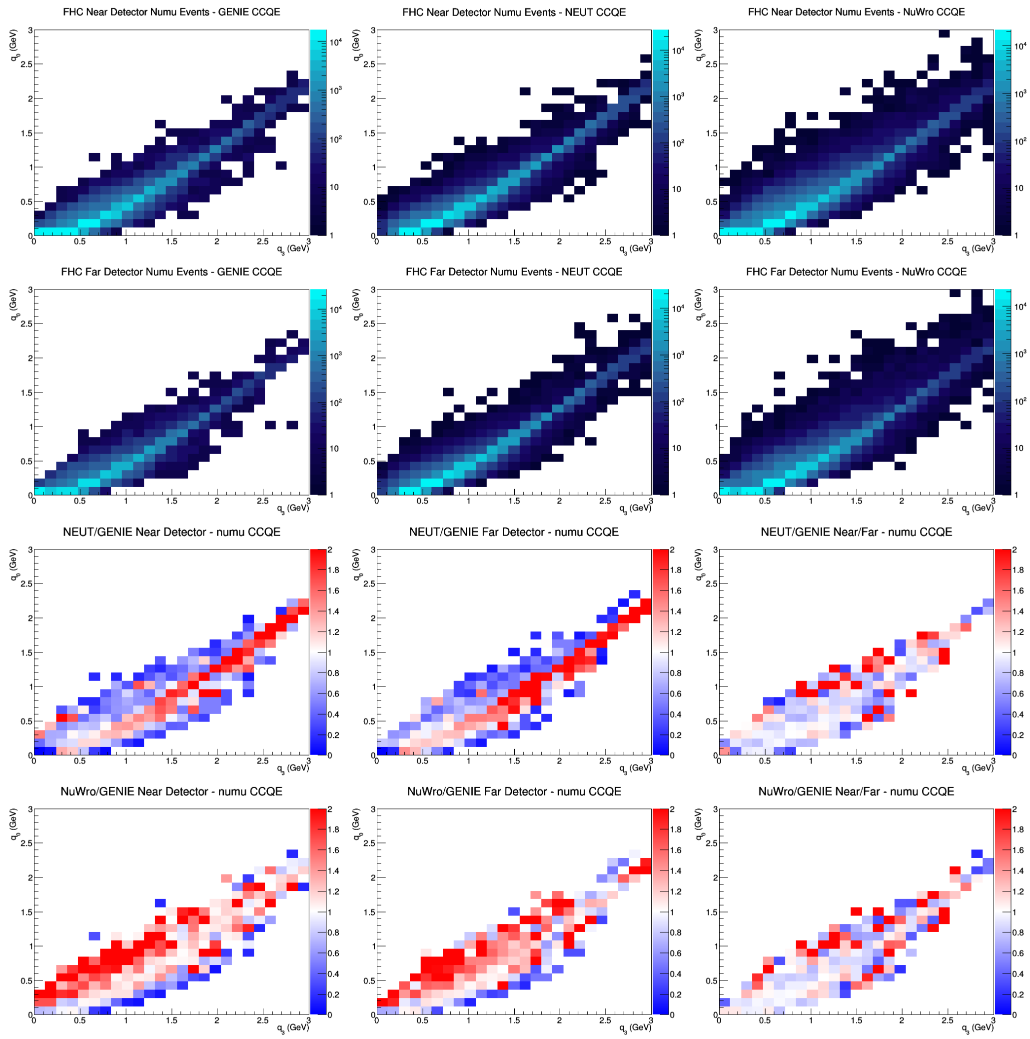

## C.5 numubar CCQE no efficiencies

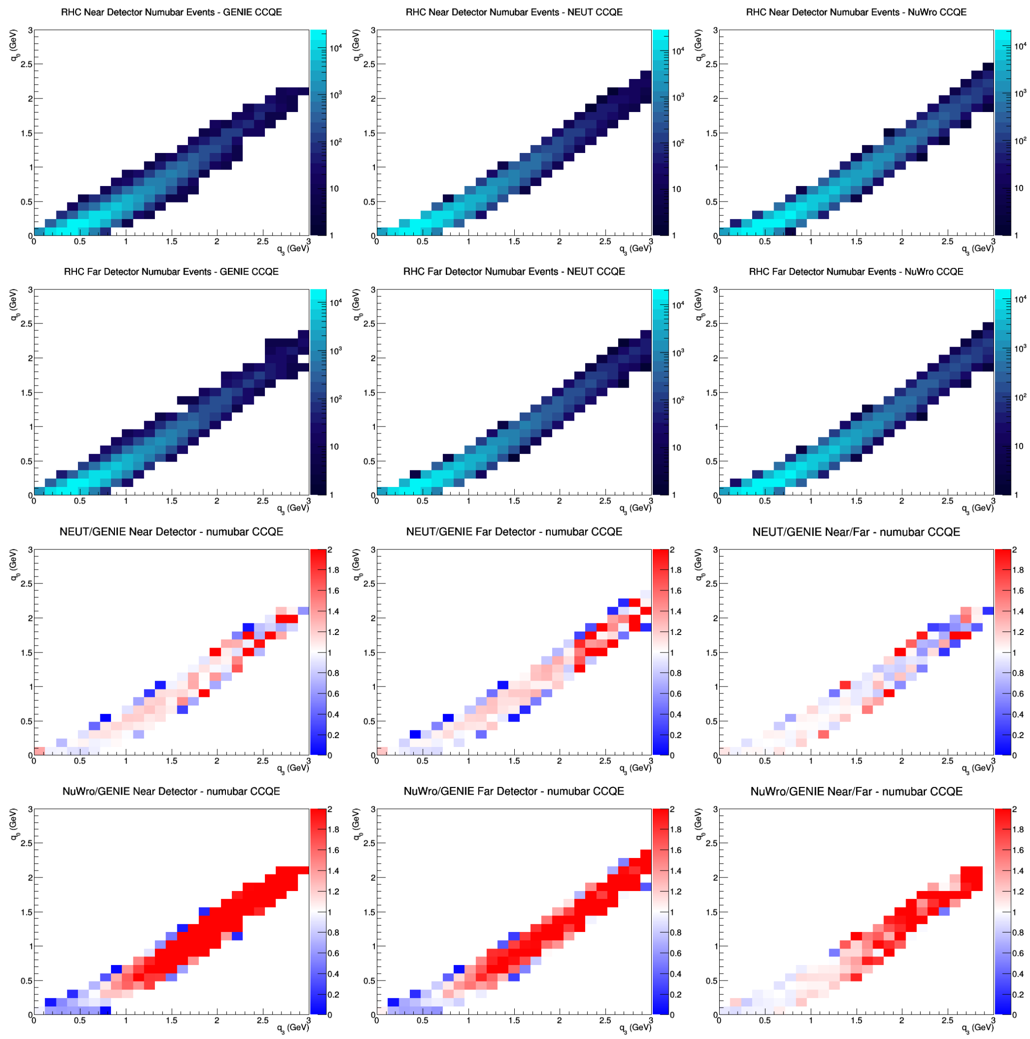

## C.6 numubar CCQE FGT efficiencies

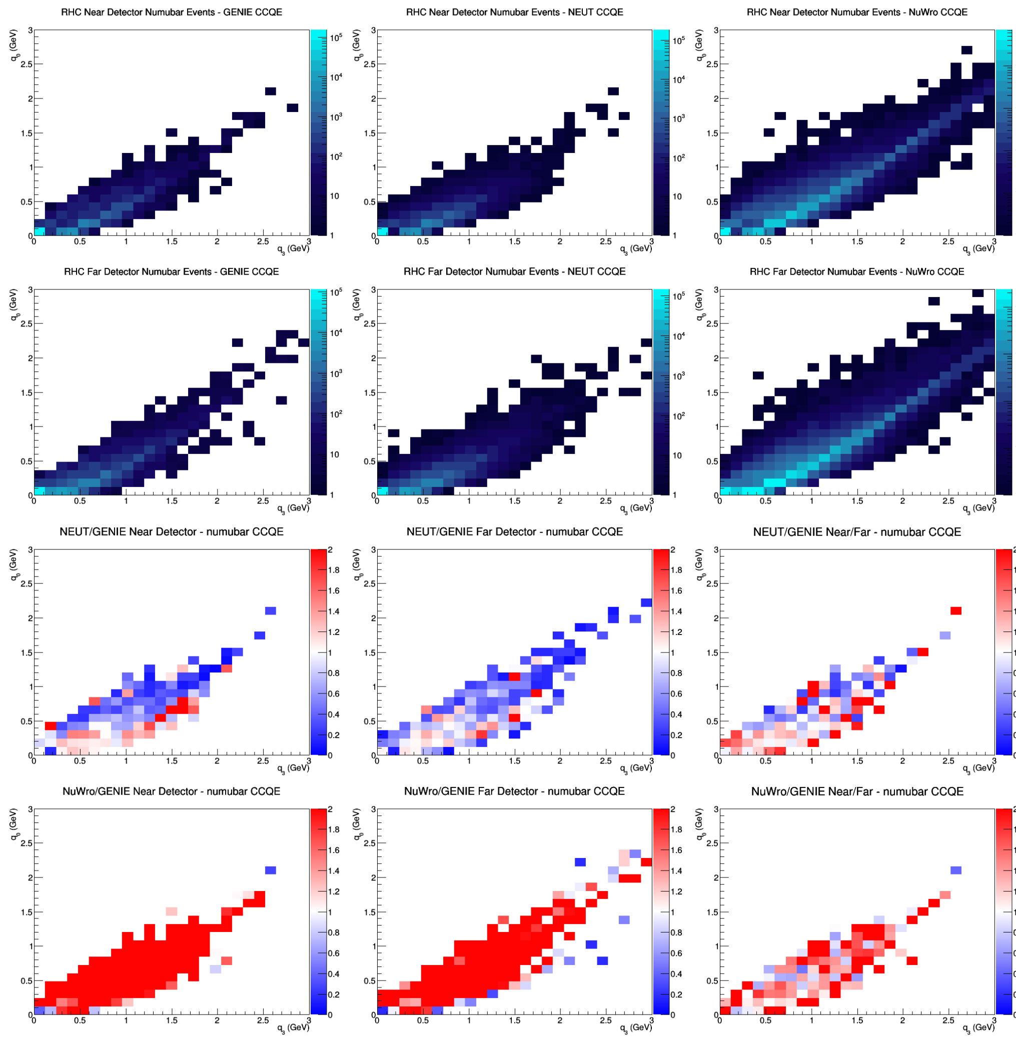

## C.7 numubar CCQE LAr efficiencies

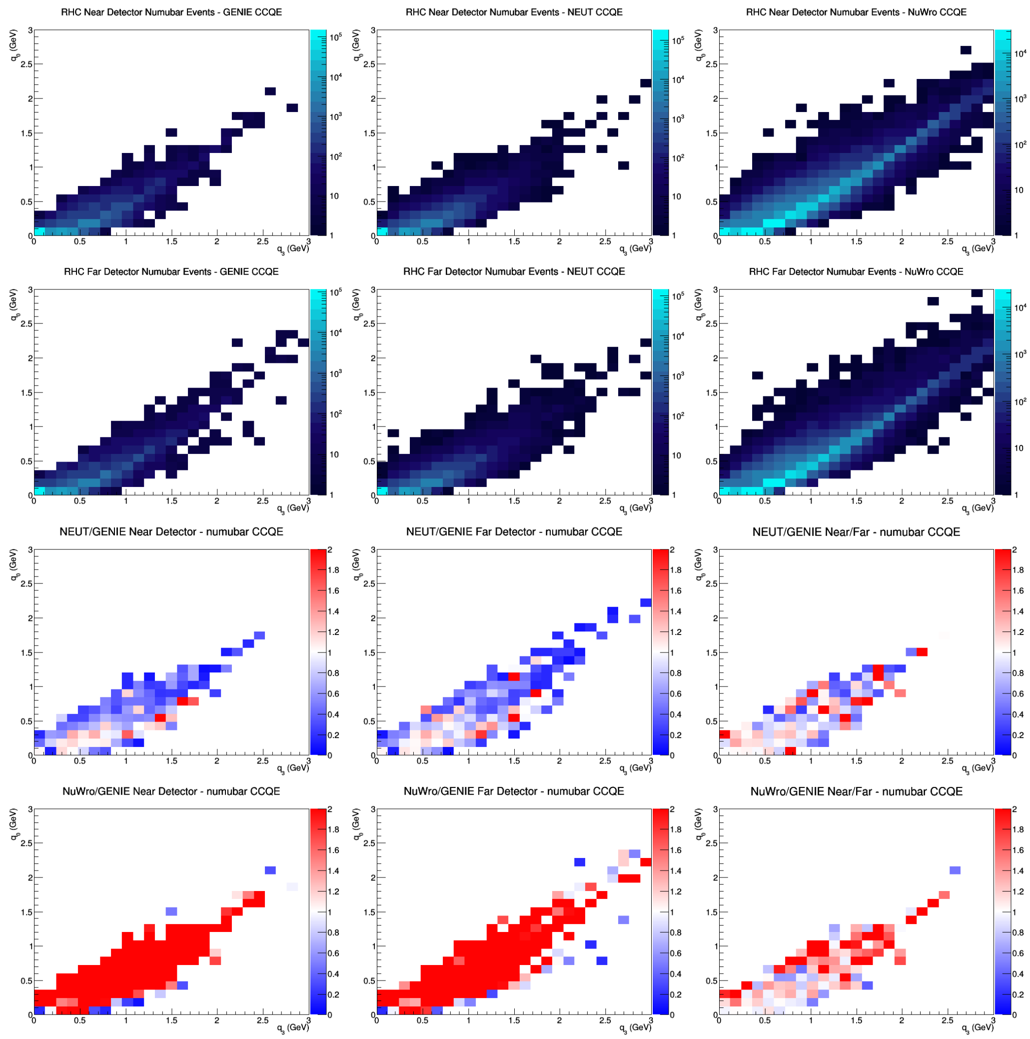

## C.8 numubar CCQE GAr efficiencies

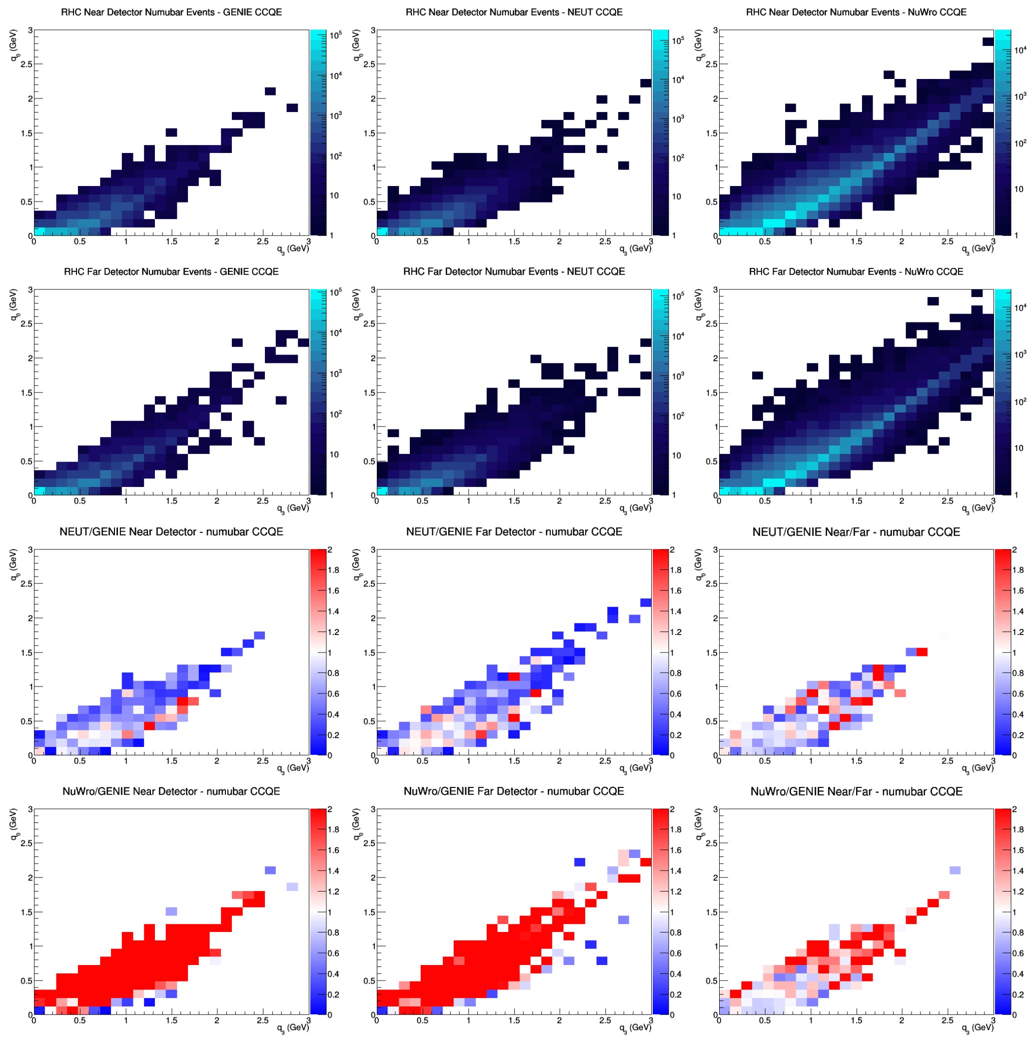

## C.9 numu 2p2h no efficiencies

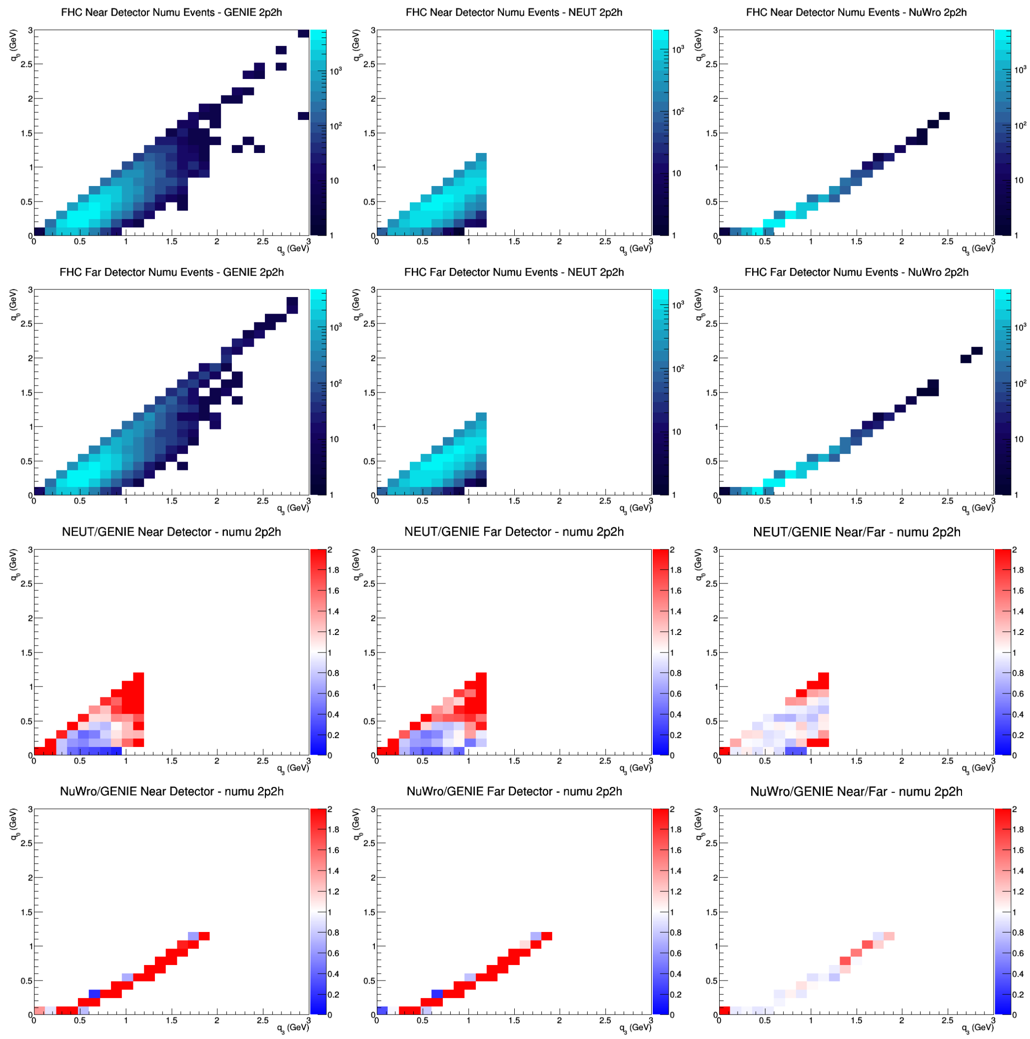

## C.10 numu 2p2h FGT efficiencies

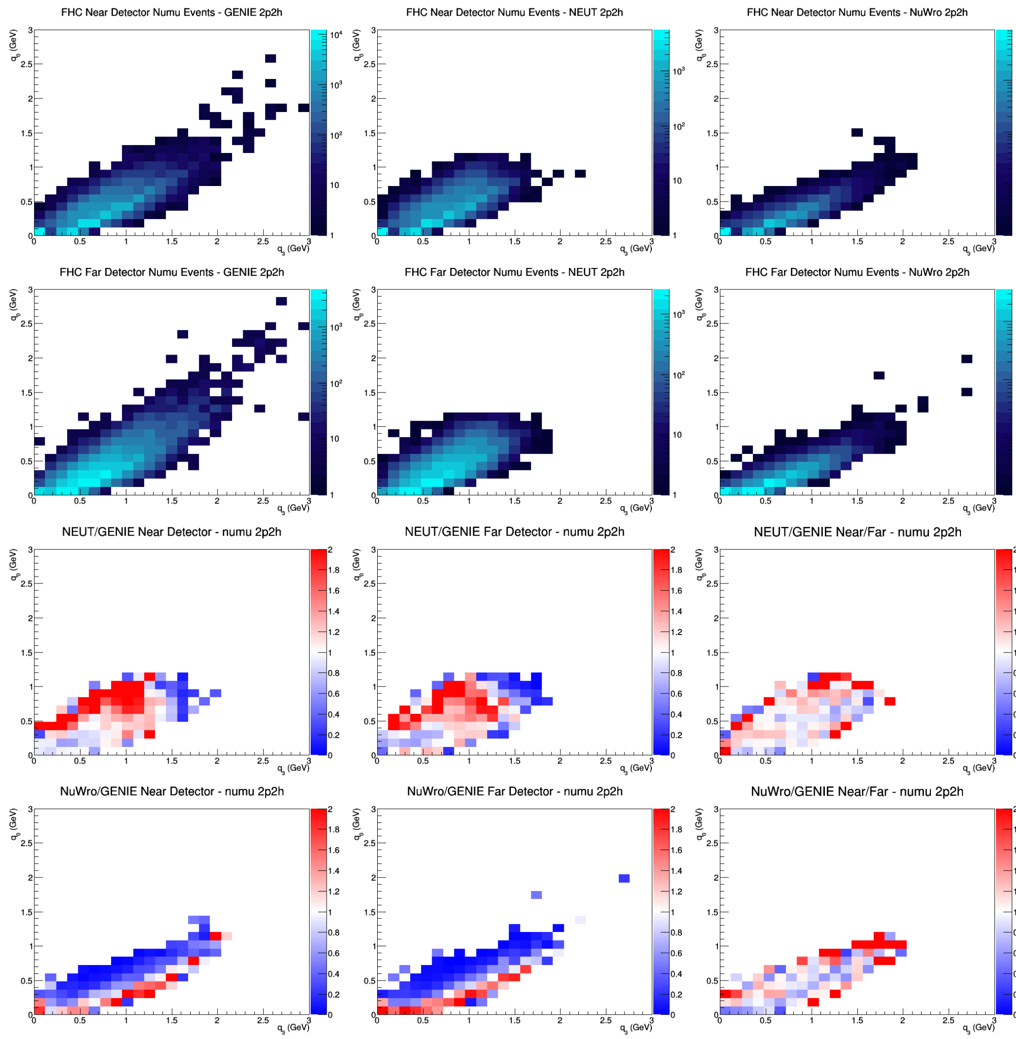

## C.11 numu 2p2h LAr efficiencies

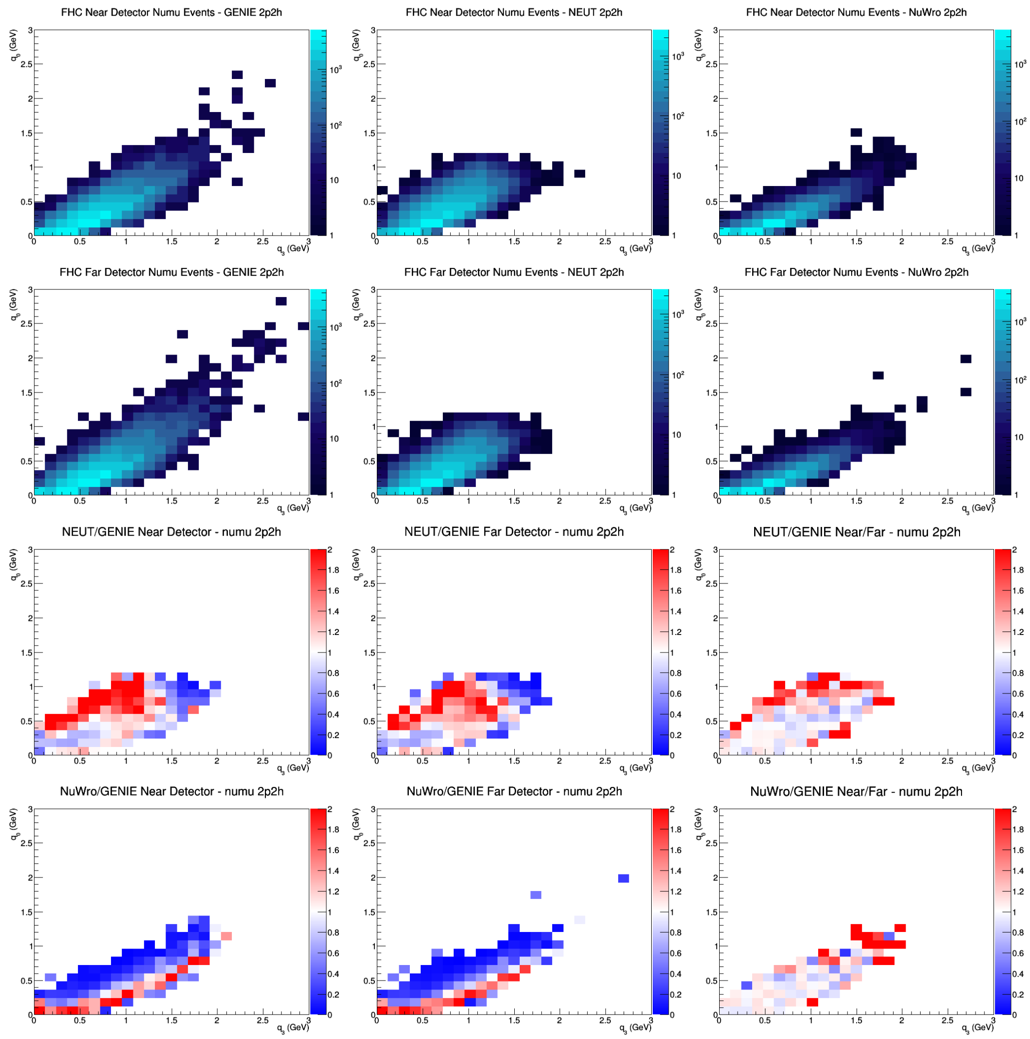

## C.12 numu 2p2h GAr efficiencies

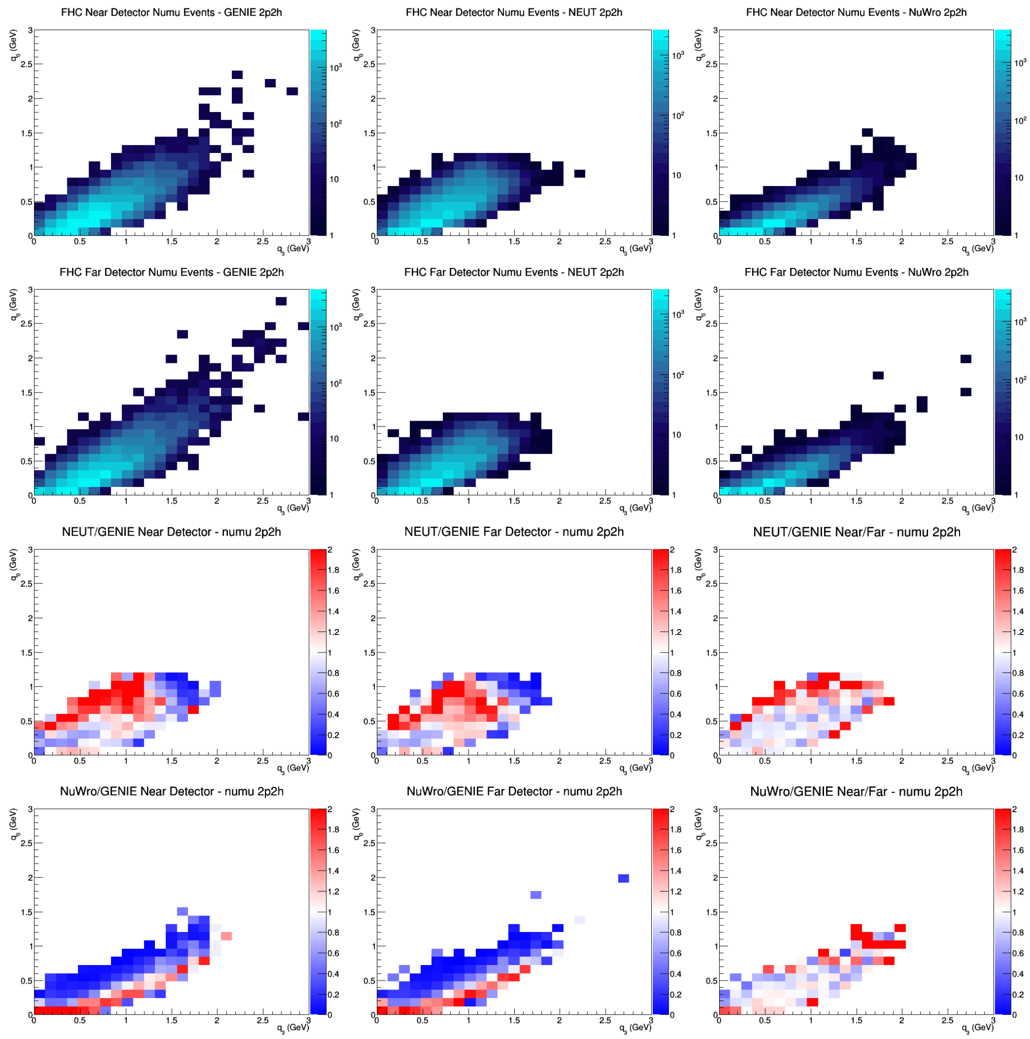

## C.13 numubar 2p2h no efficiencies

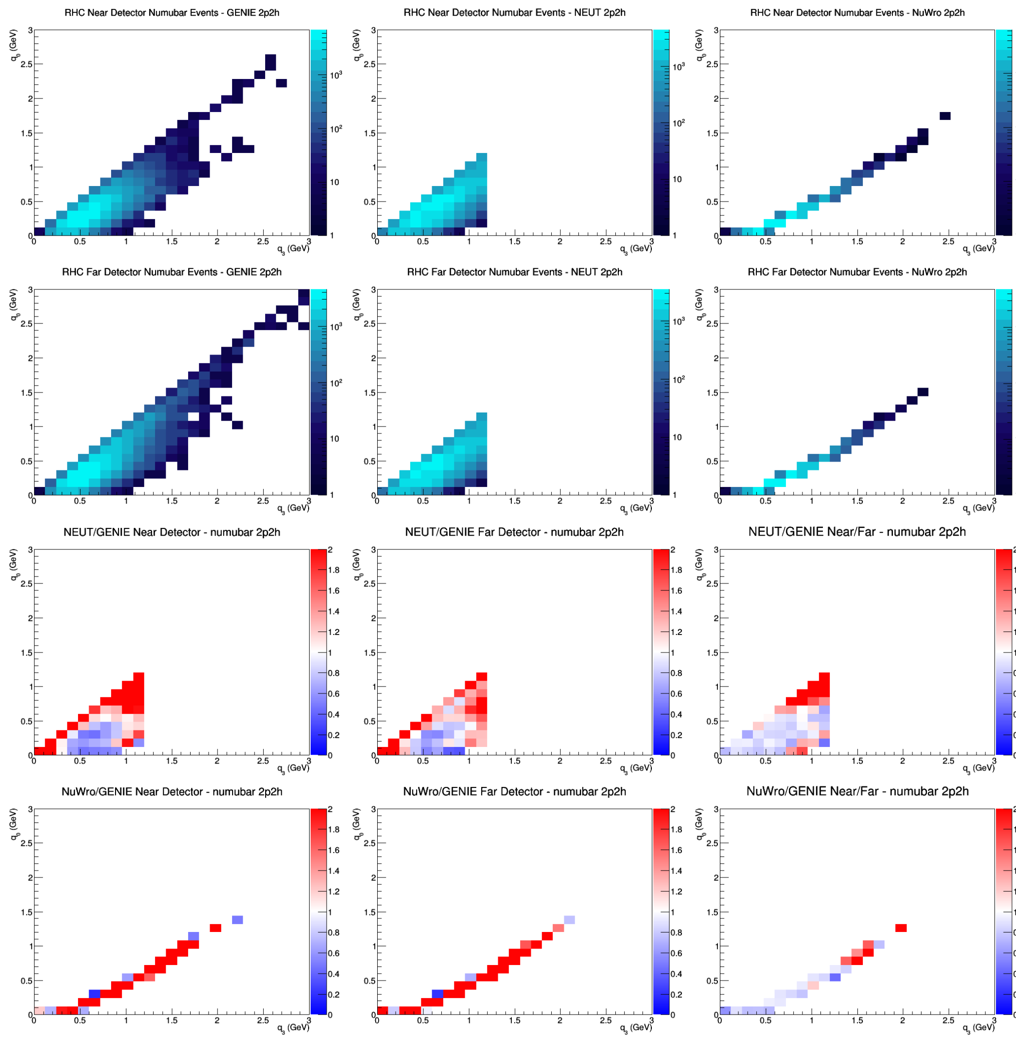

## C.14 numubar 2p2h FGT efficiencies

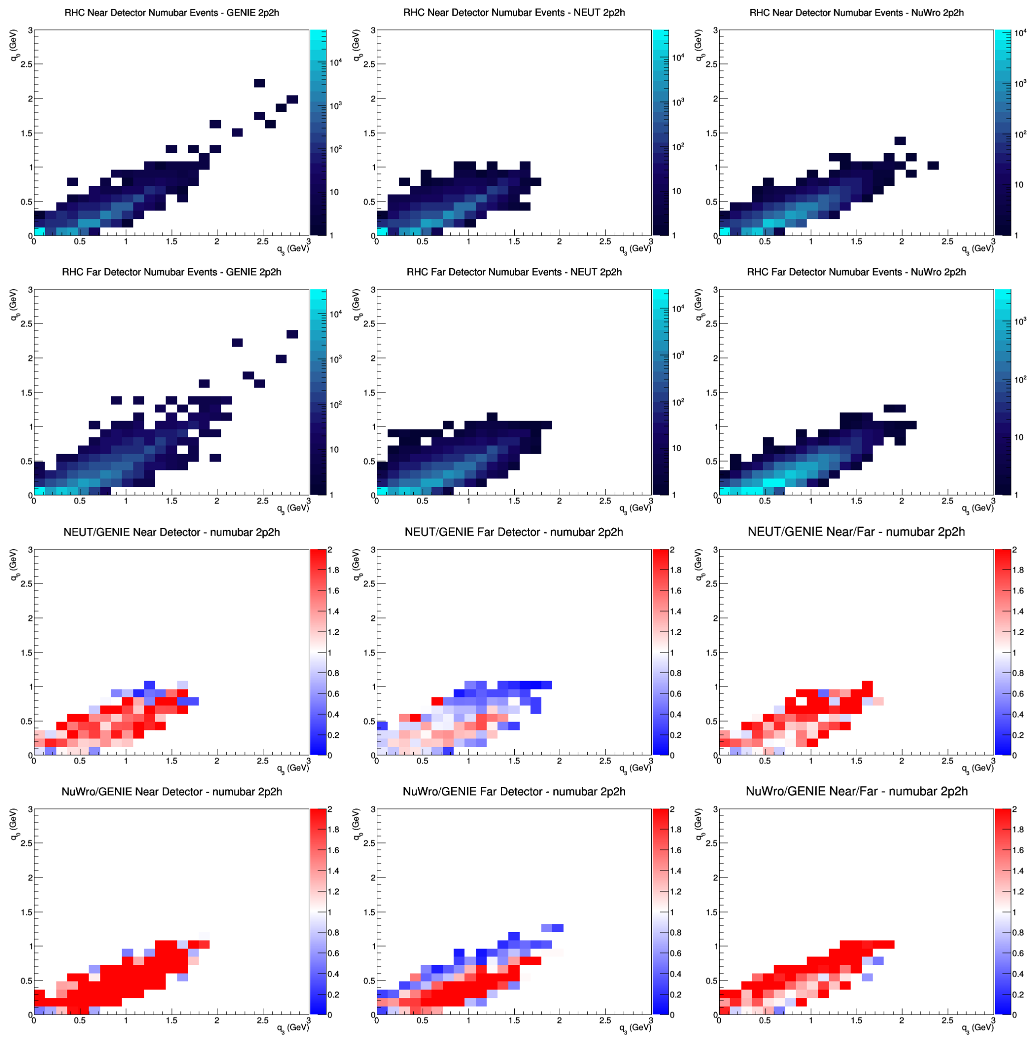

## C.15 numubar 2p2h LAr efficiencies

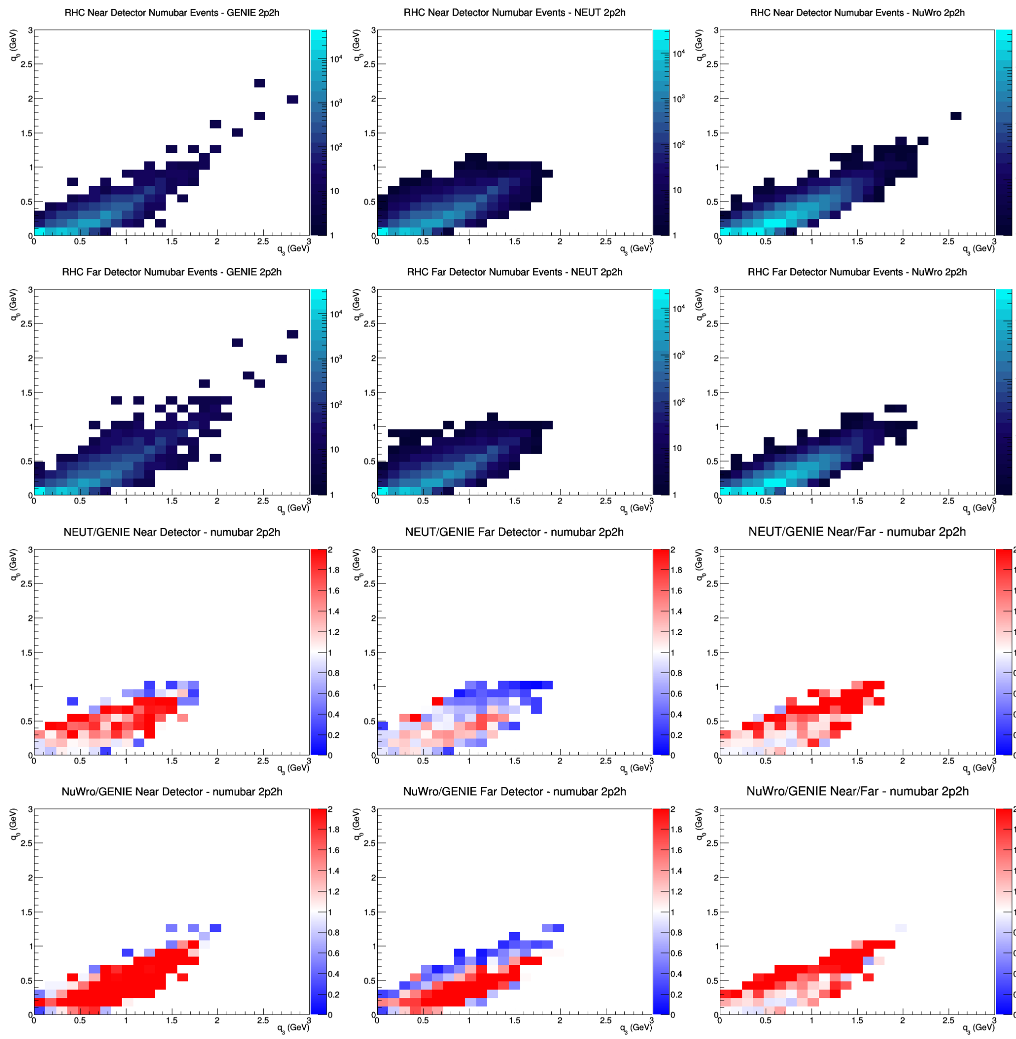

## C.16 numubar 2p2h GAr efficiencies

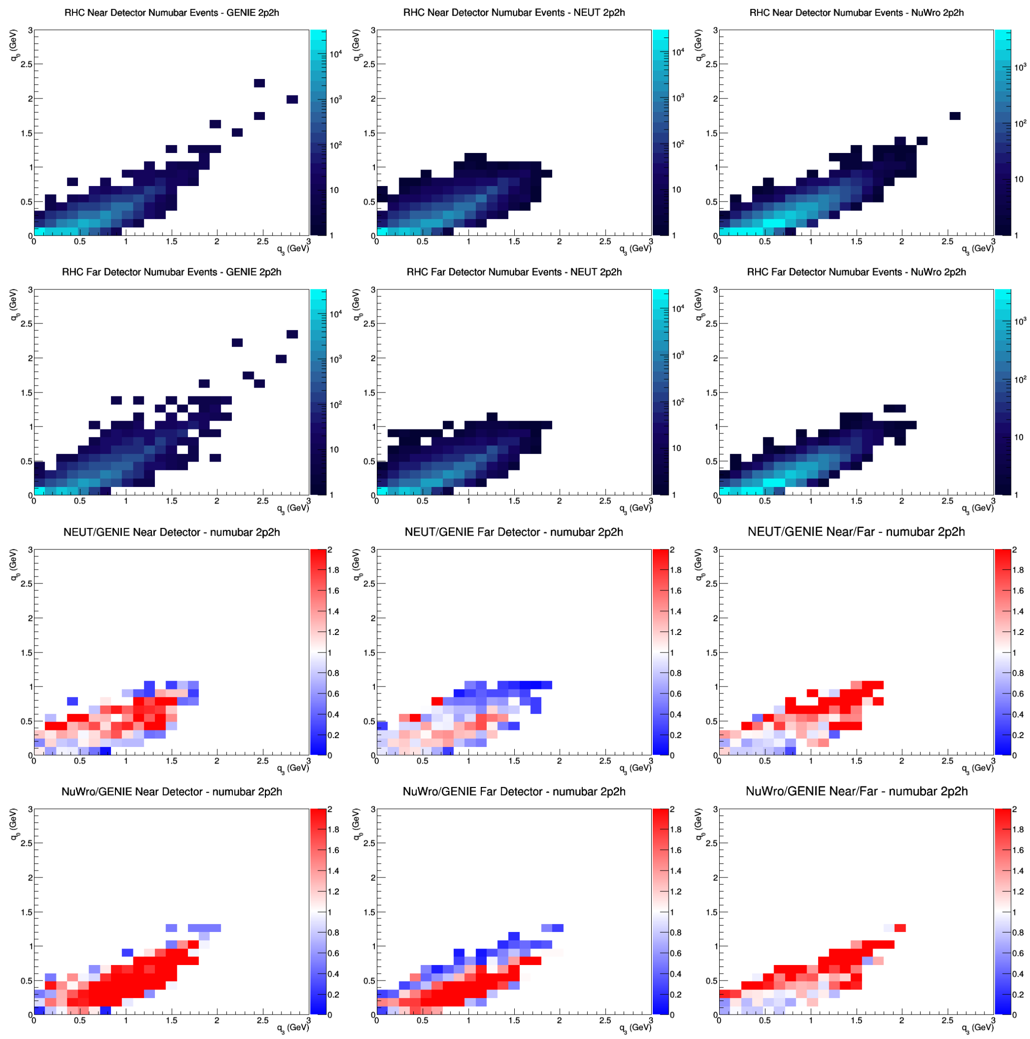

## C.17 numu CC0Pi no efficiencies

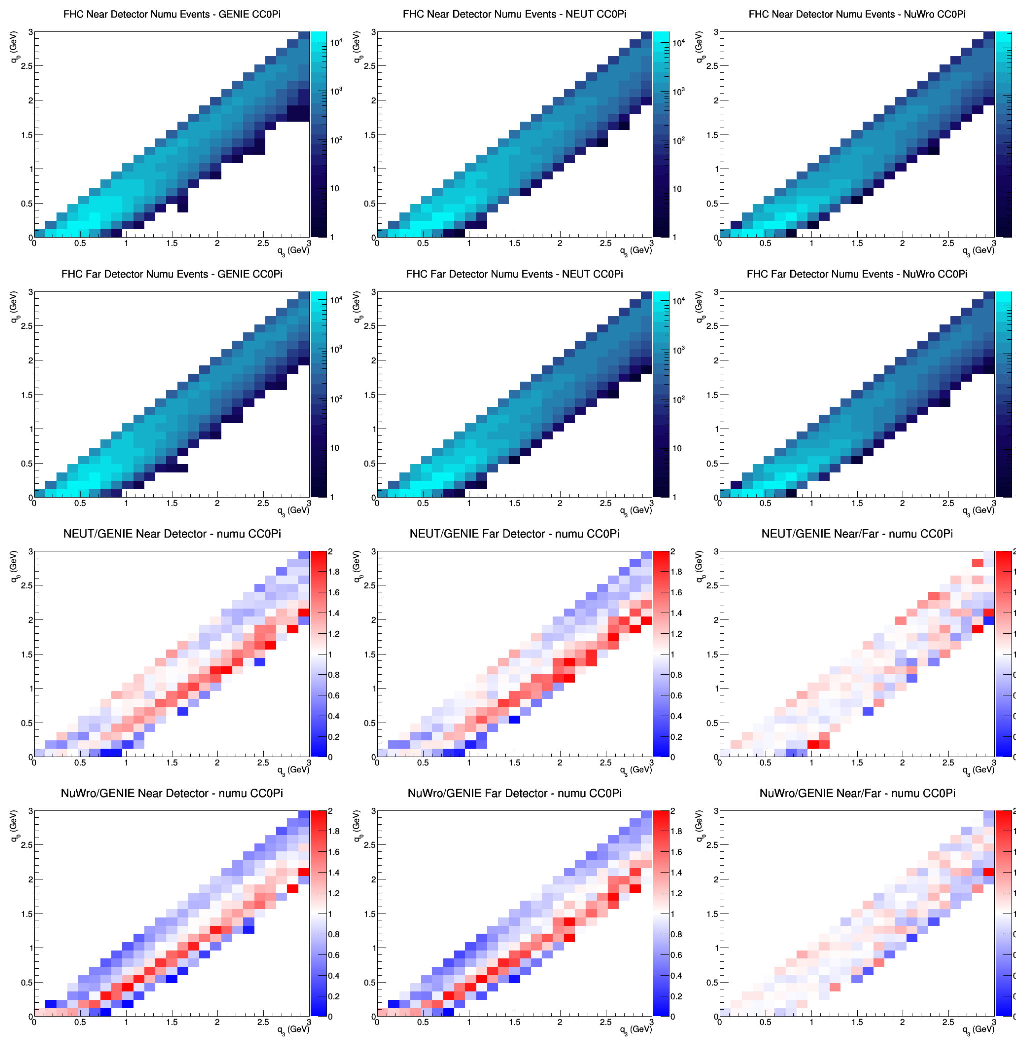

## C.18 numu CC0Pi FGT efficiencies

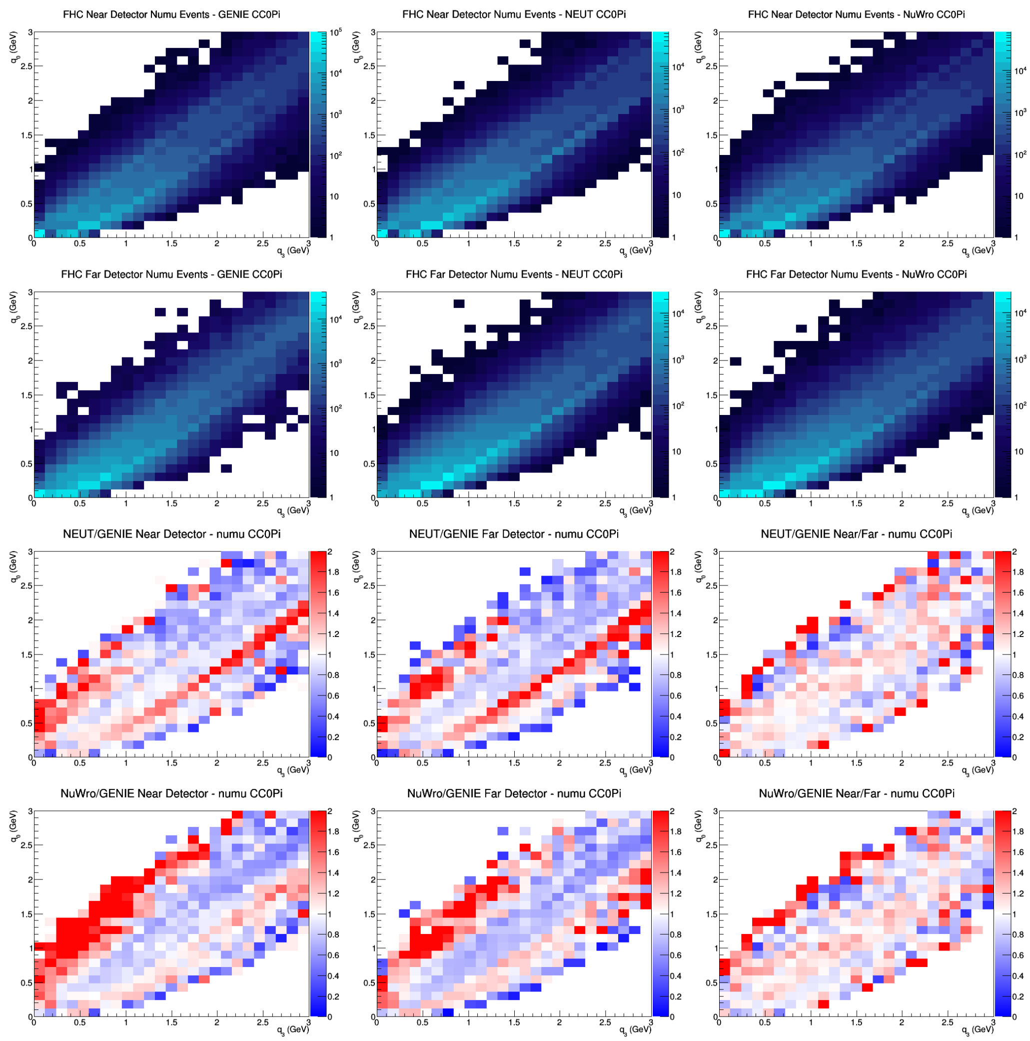

## C.19 numu CC0Pi LAr efficiencies

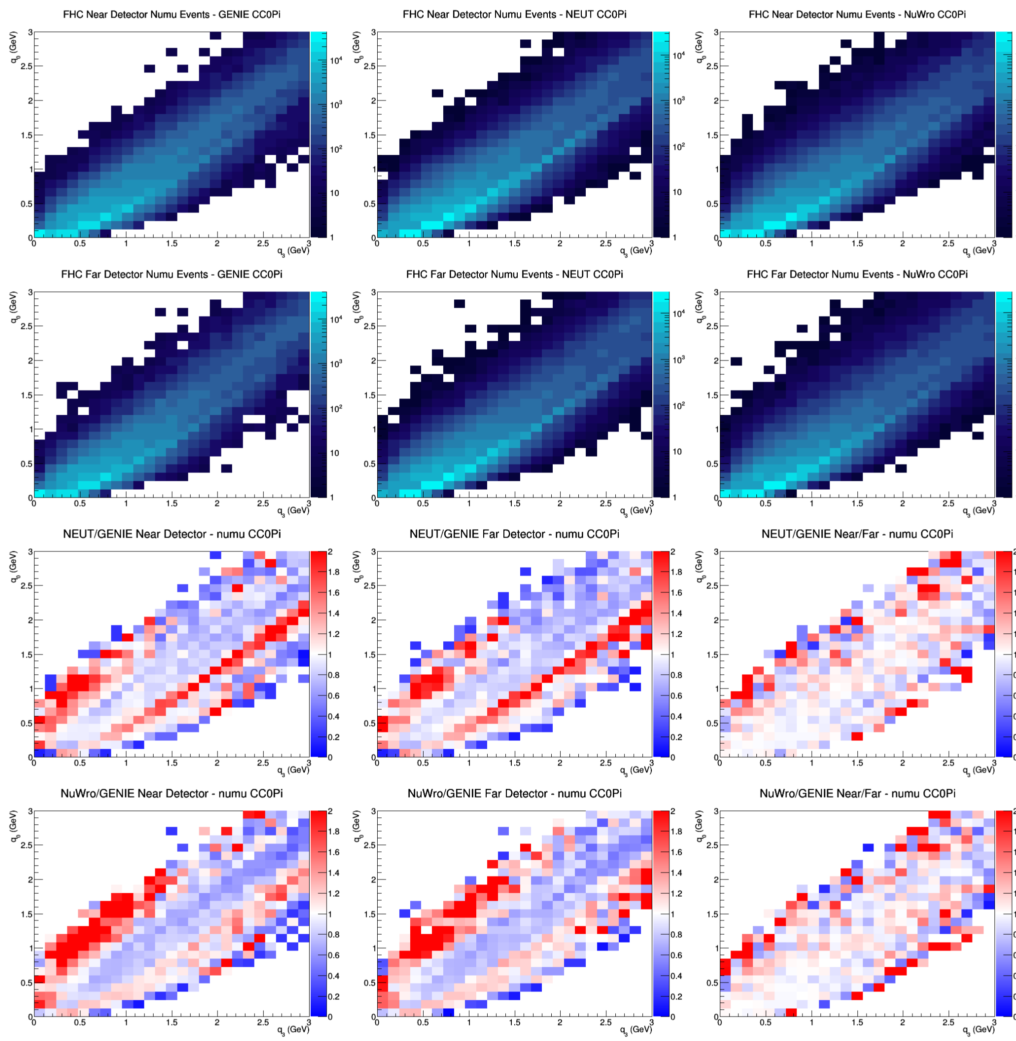

## C.20 numu CC0Pi GAr efficiencies

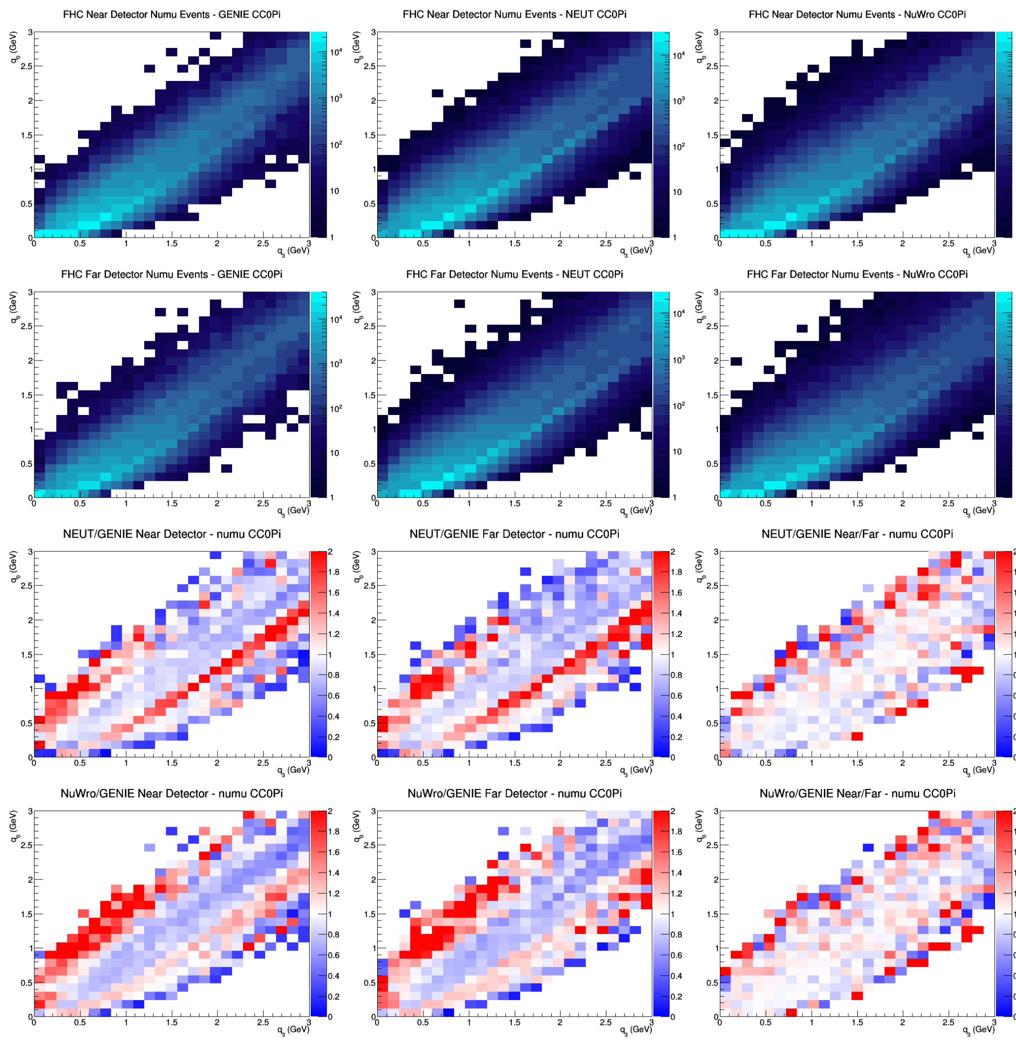

## C.21 numubar CC0Pi no efficiencies

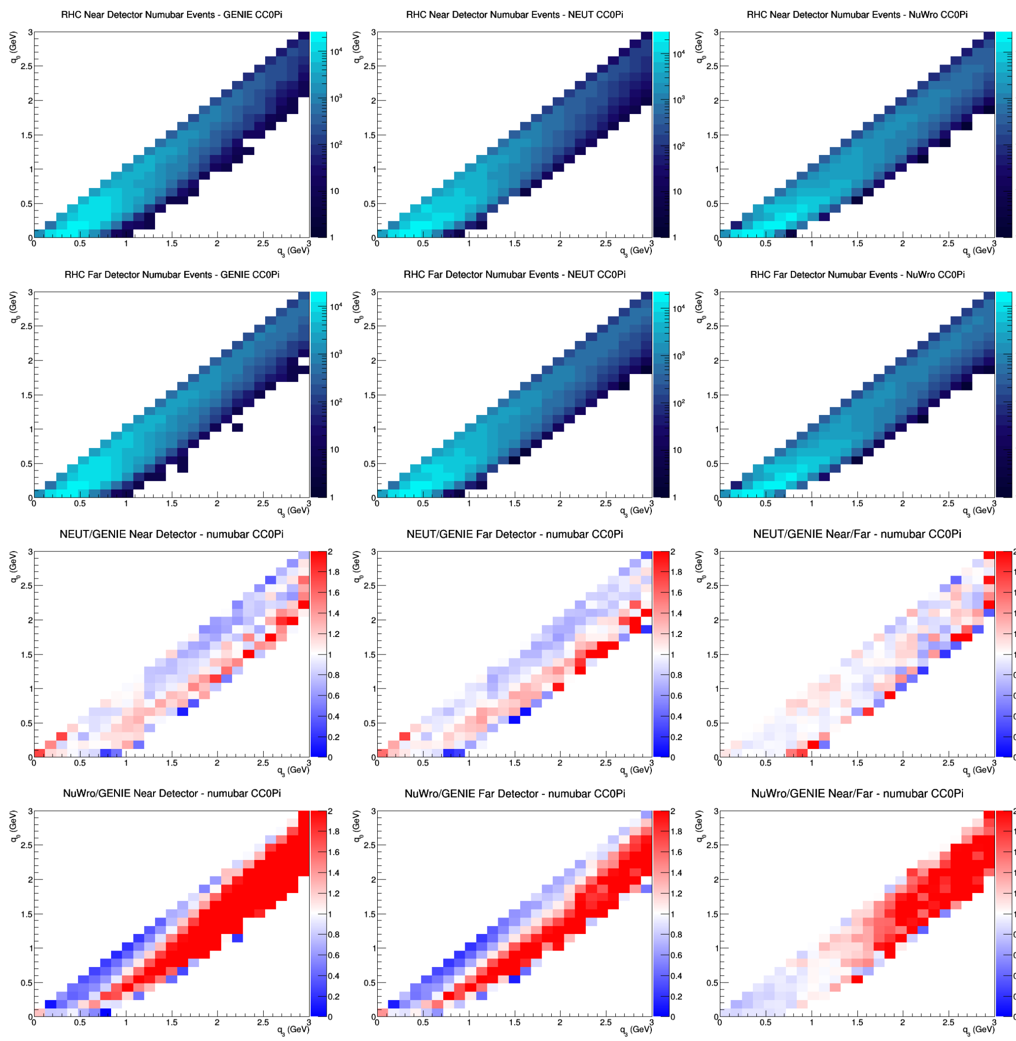

## C.22 numubar CC0Pi FGT efficiencies

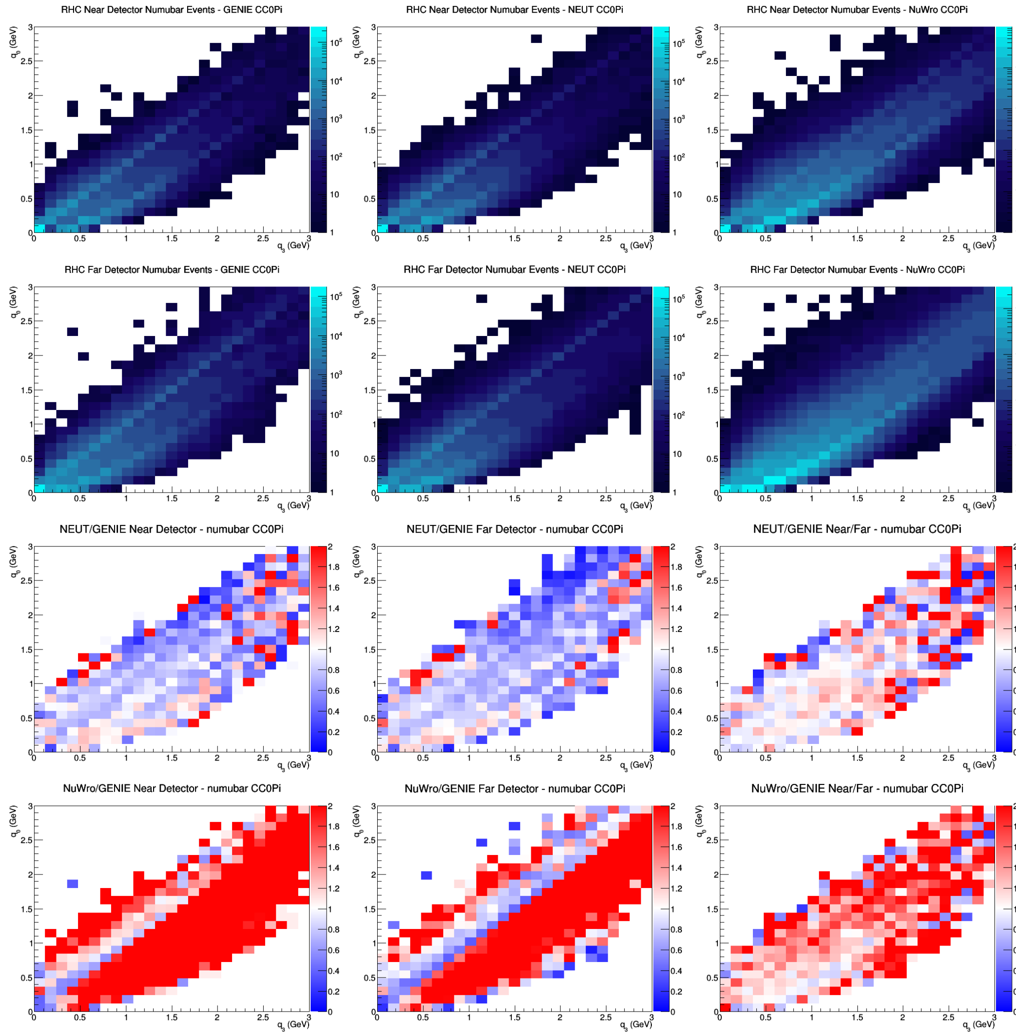

## C.23 numubar CC0Pi LAr efficiencies

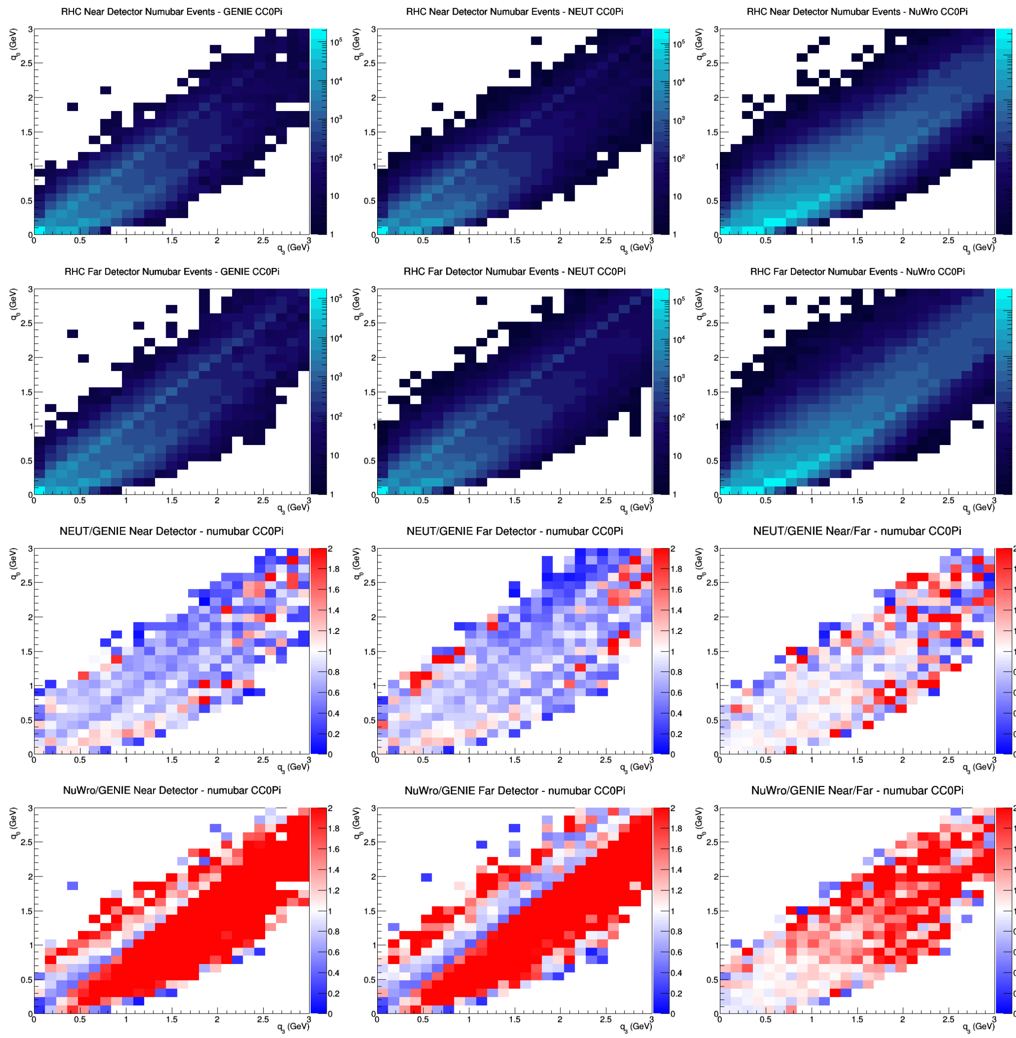

## C.24 numubar CC0Pi GAr efficiencies

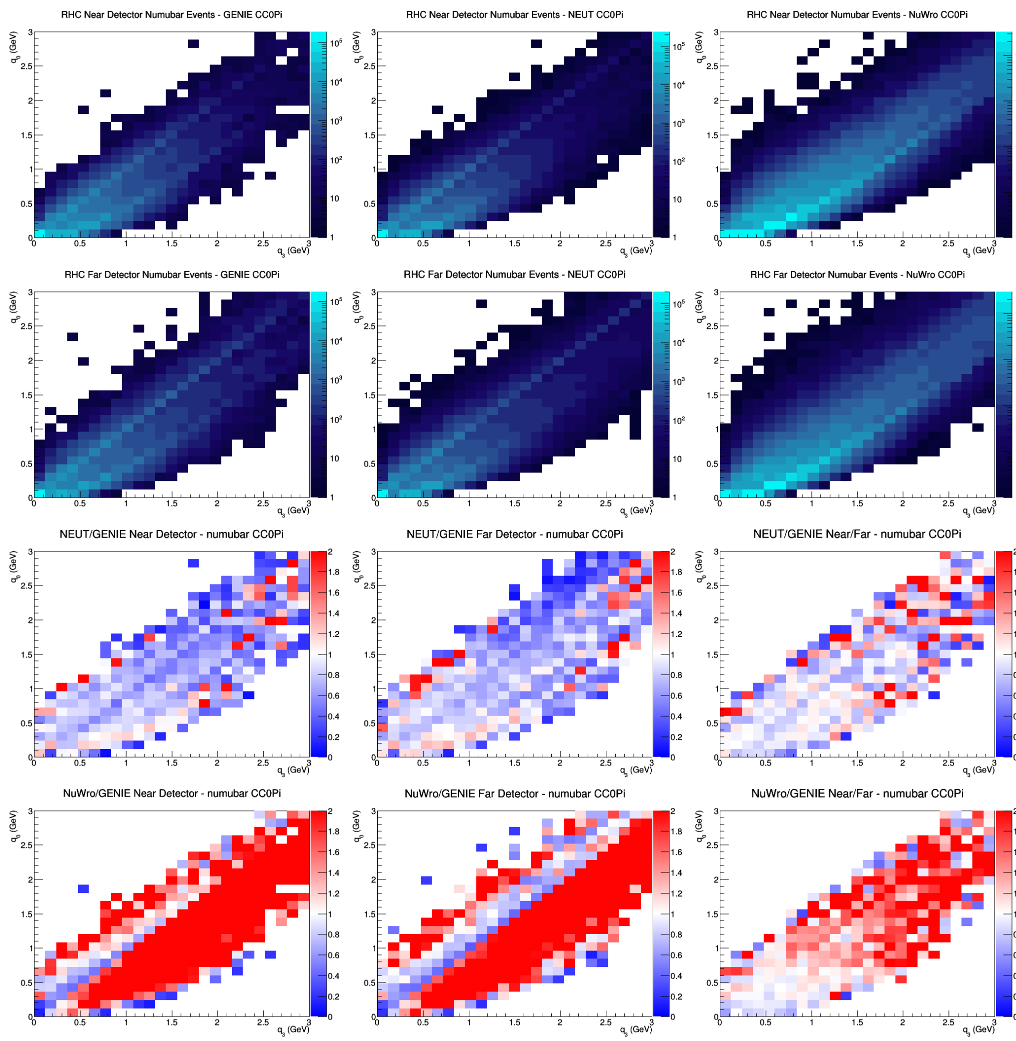

## C.25 numu CC1Pi no efficiencies

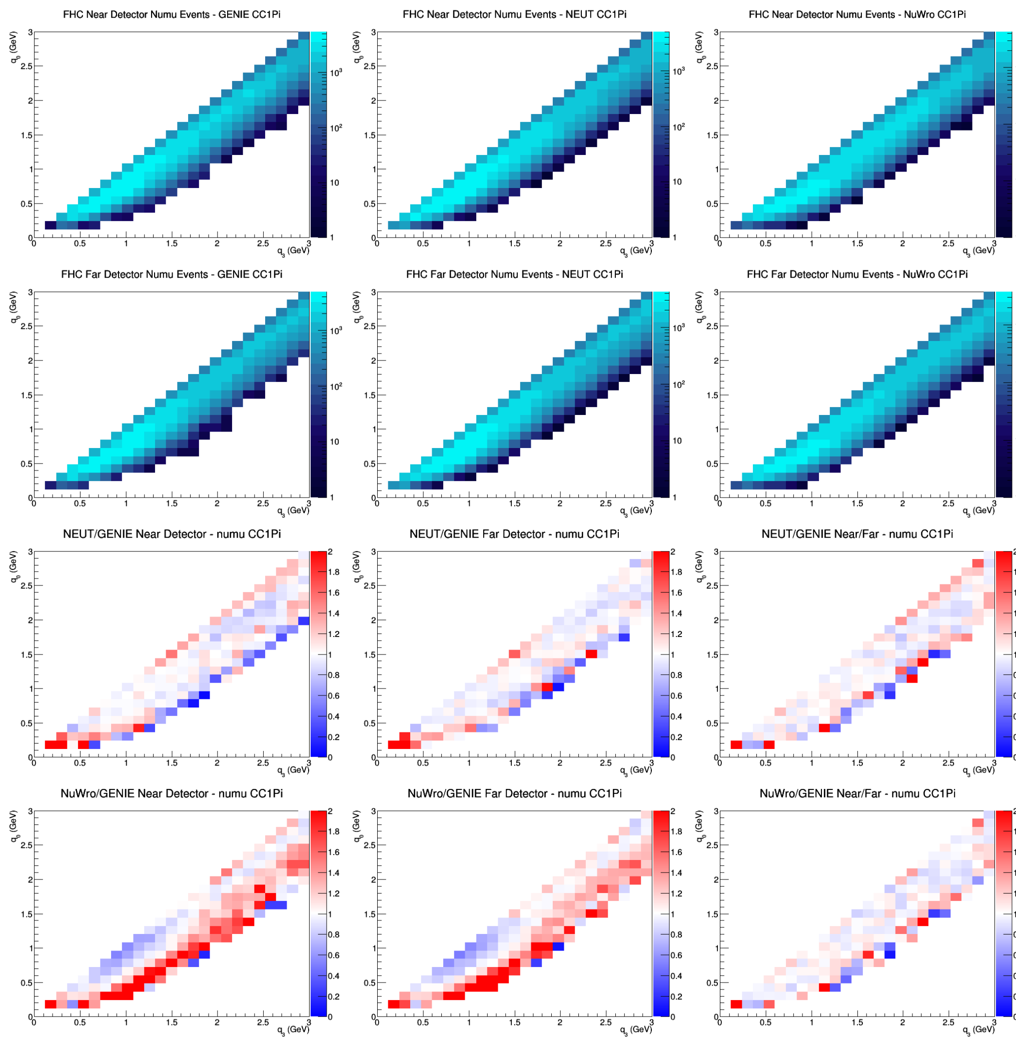

## C.26 numu CC1Pi FGT efficiencies

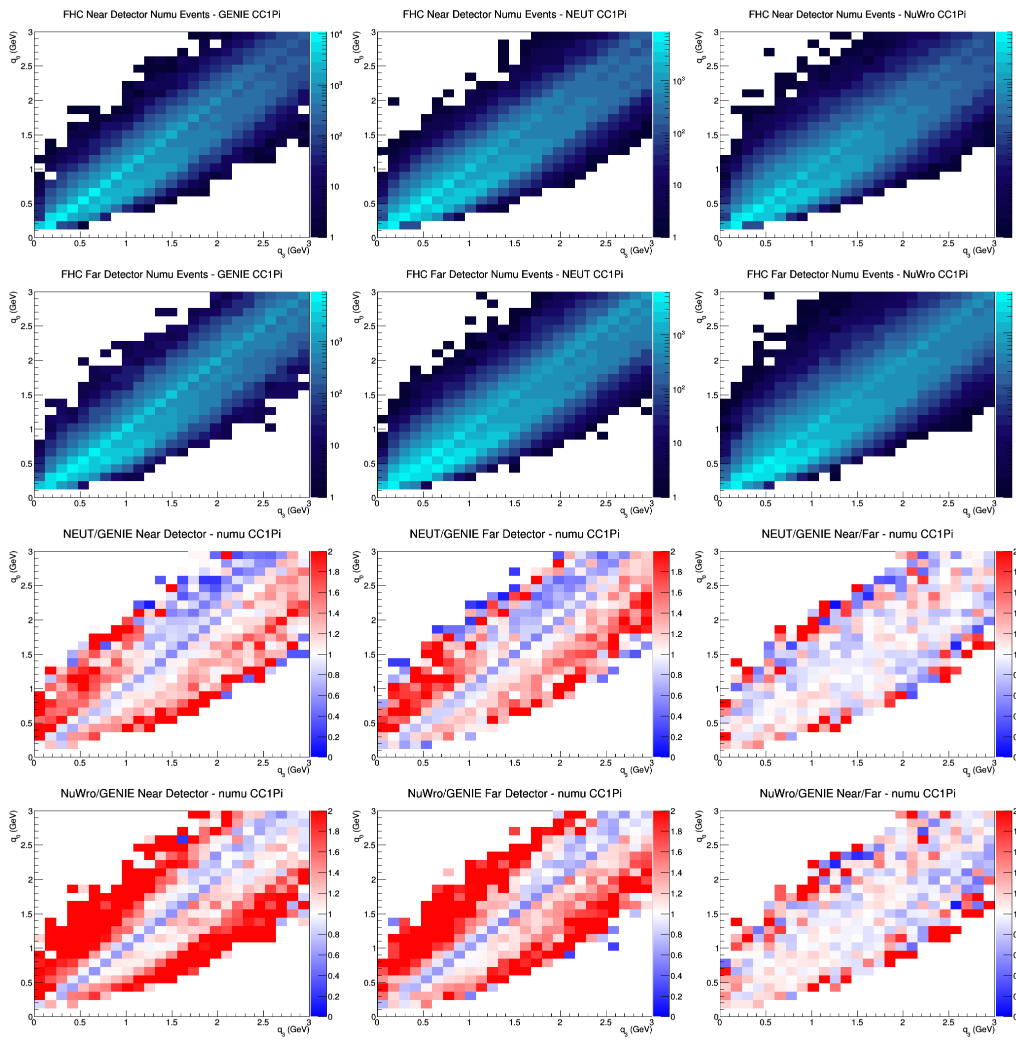

## C.27 numu CC1Pi LAr efficiencies

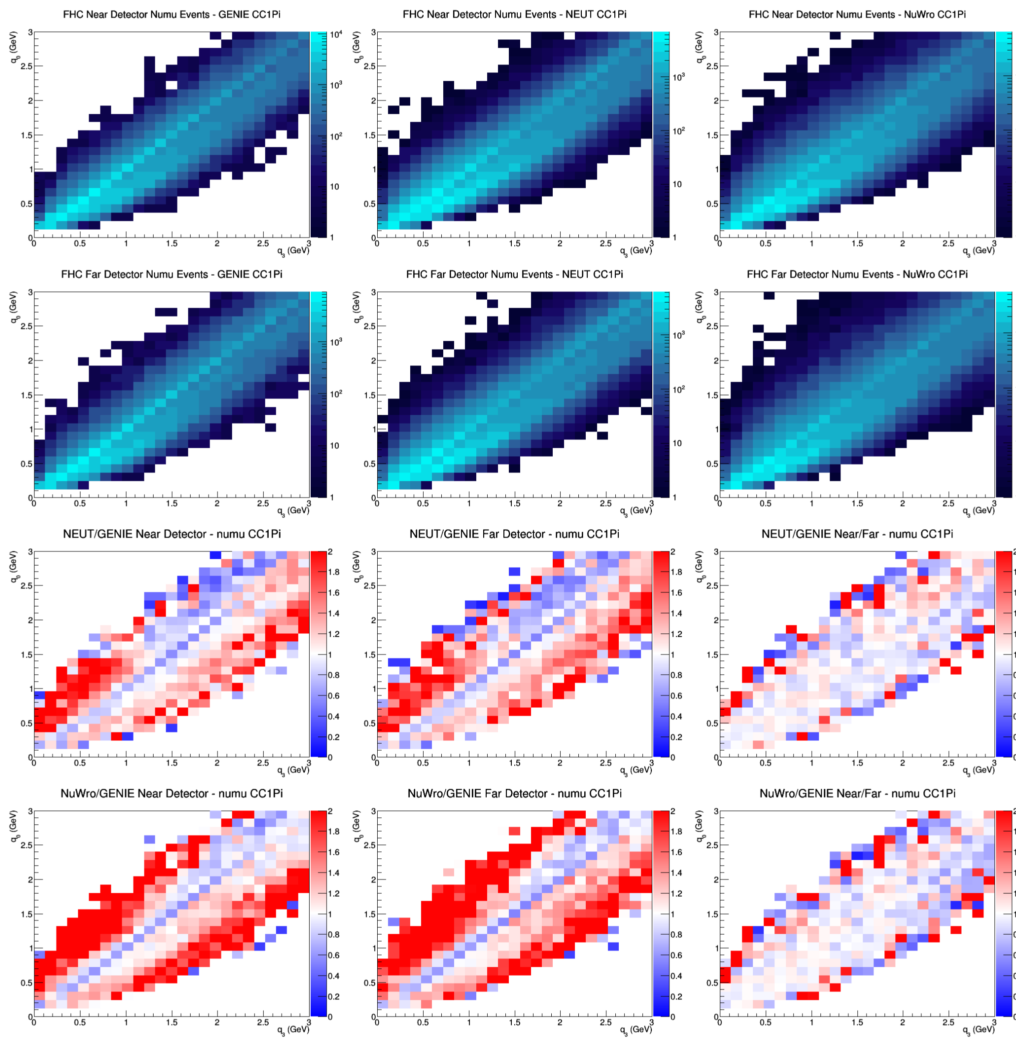

## C.28 numu CC1Pi GAr efficiencies

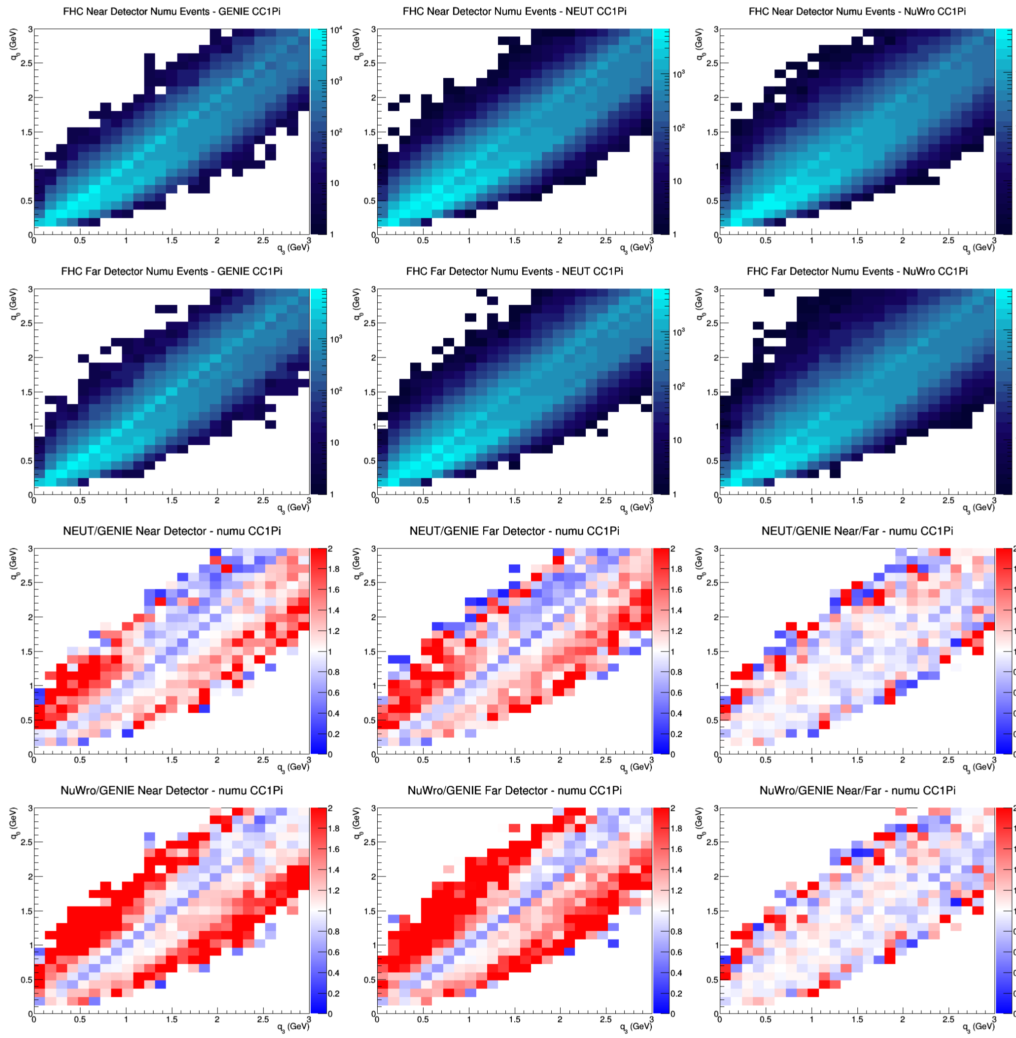

## C.29 numubar CC1Pi no efficiencies

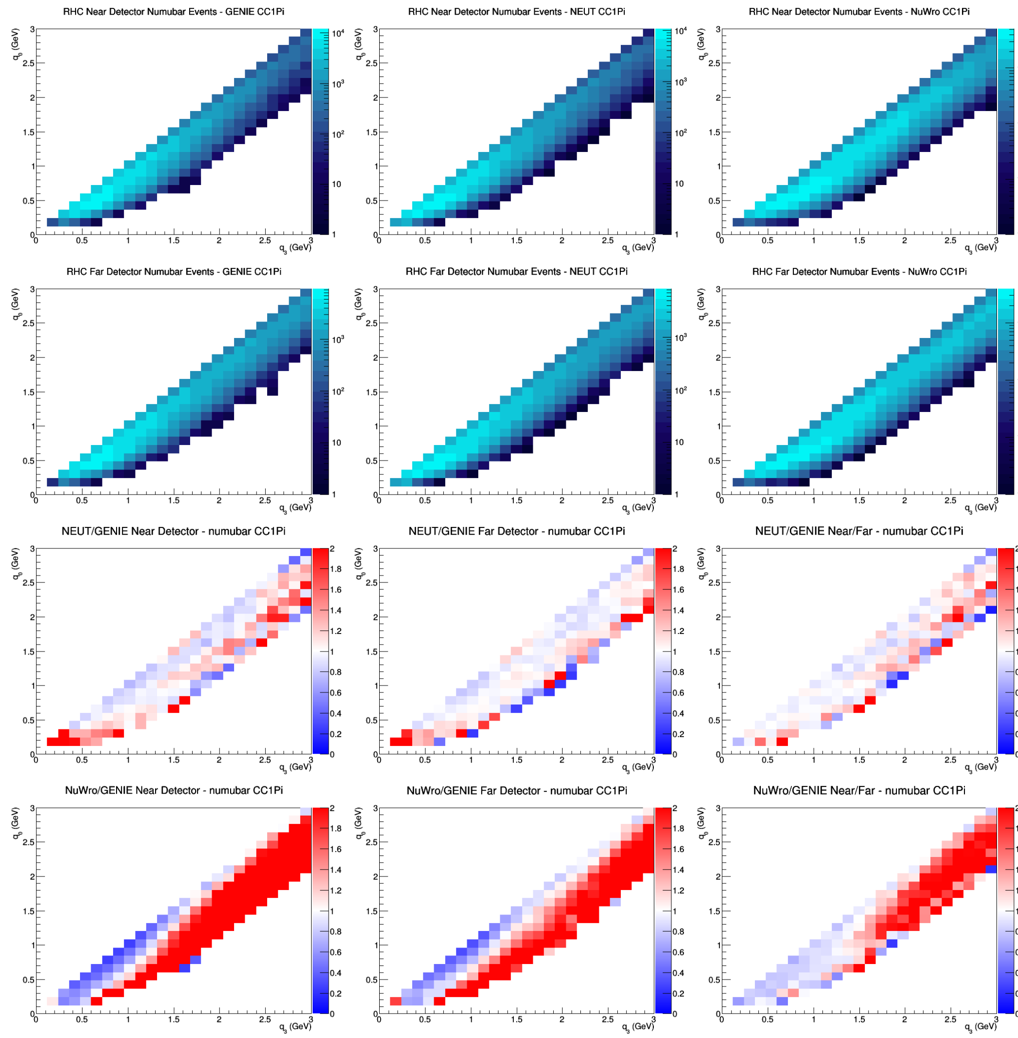

## C.30 numubar CC1Pi FGT efficiencies

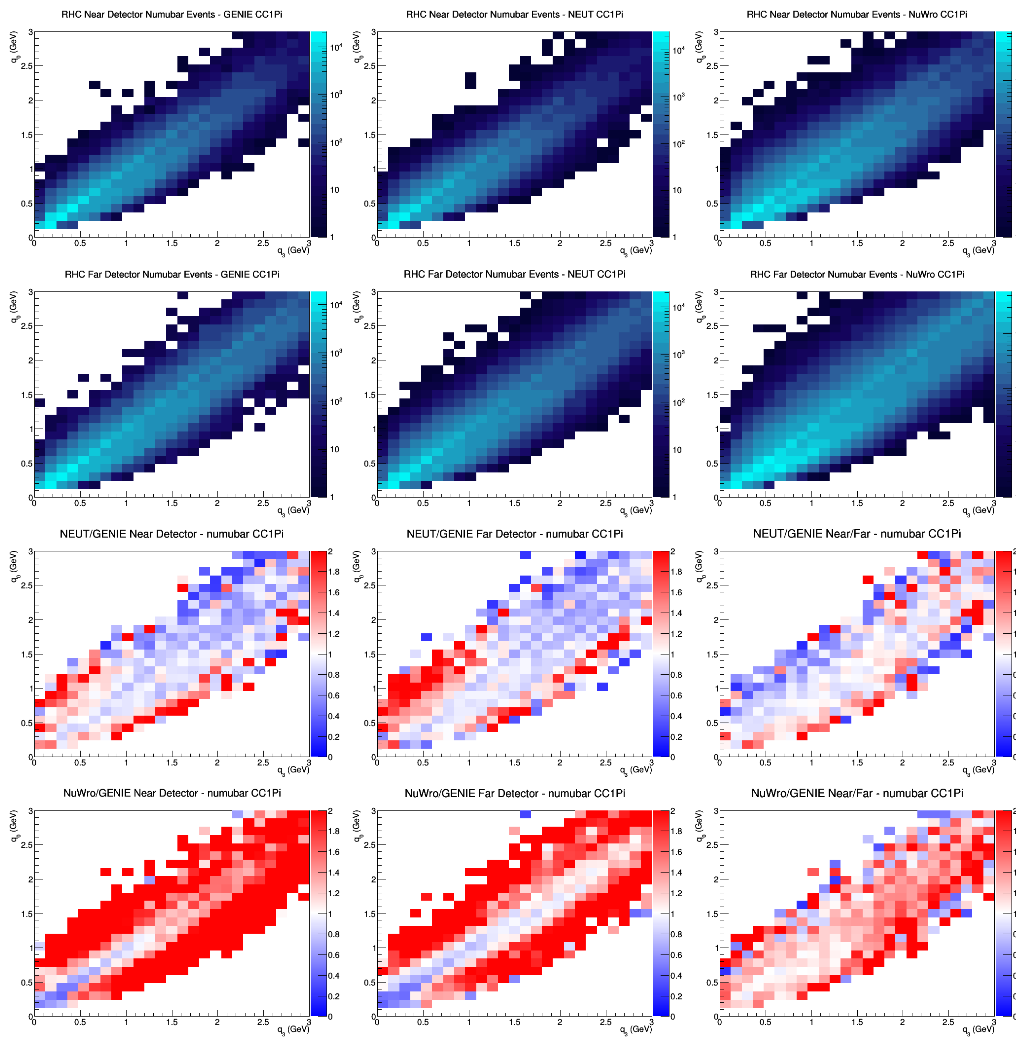

## C.31 numubar CC1Pi LAr efficiencies

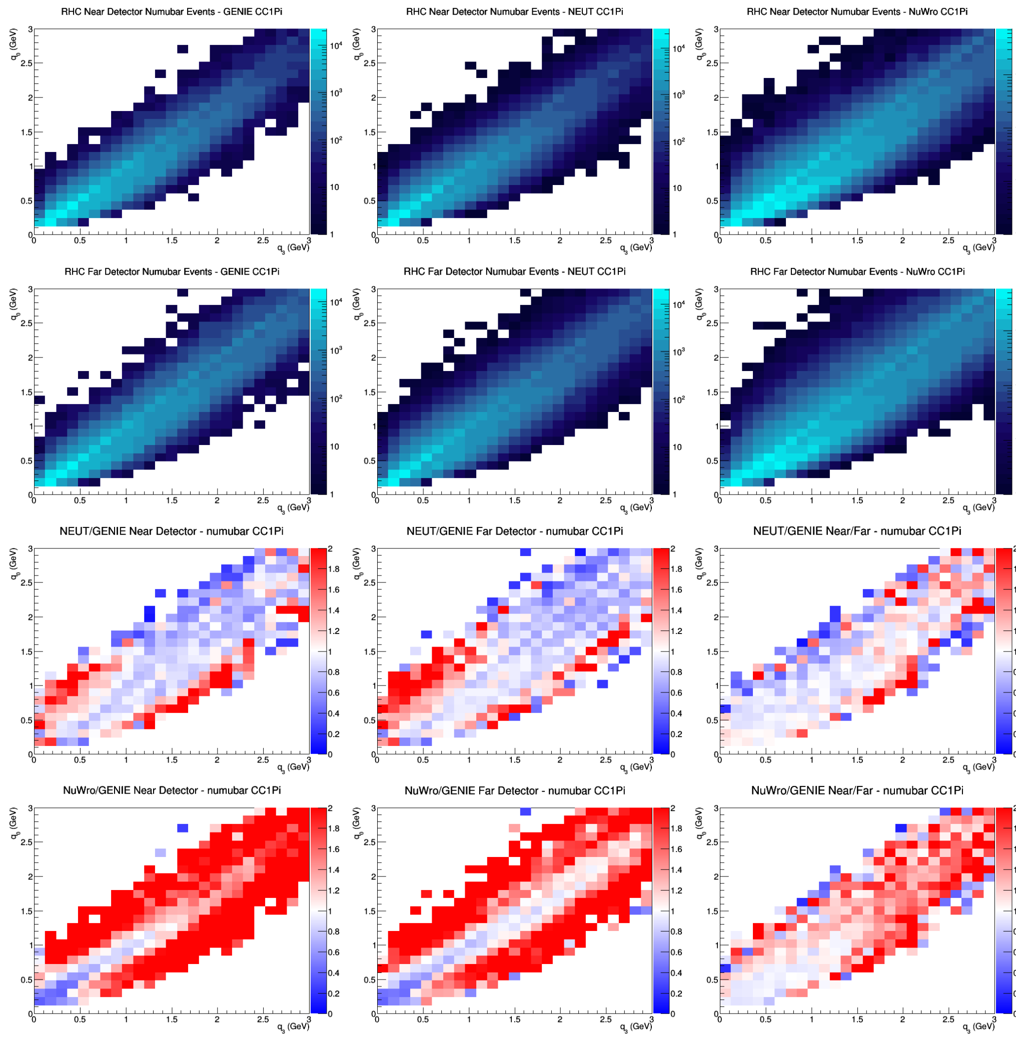

## C.32 numubar CC1Pi GAr efficiencies

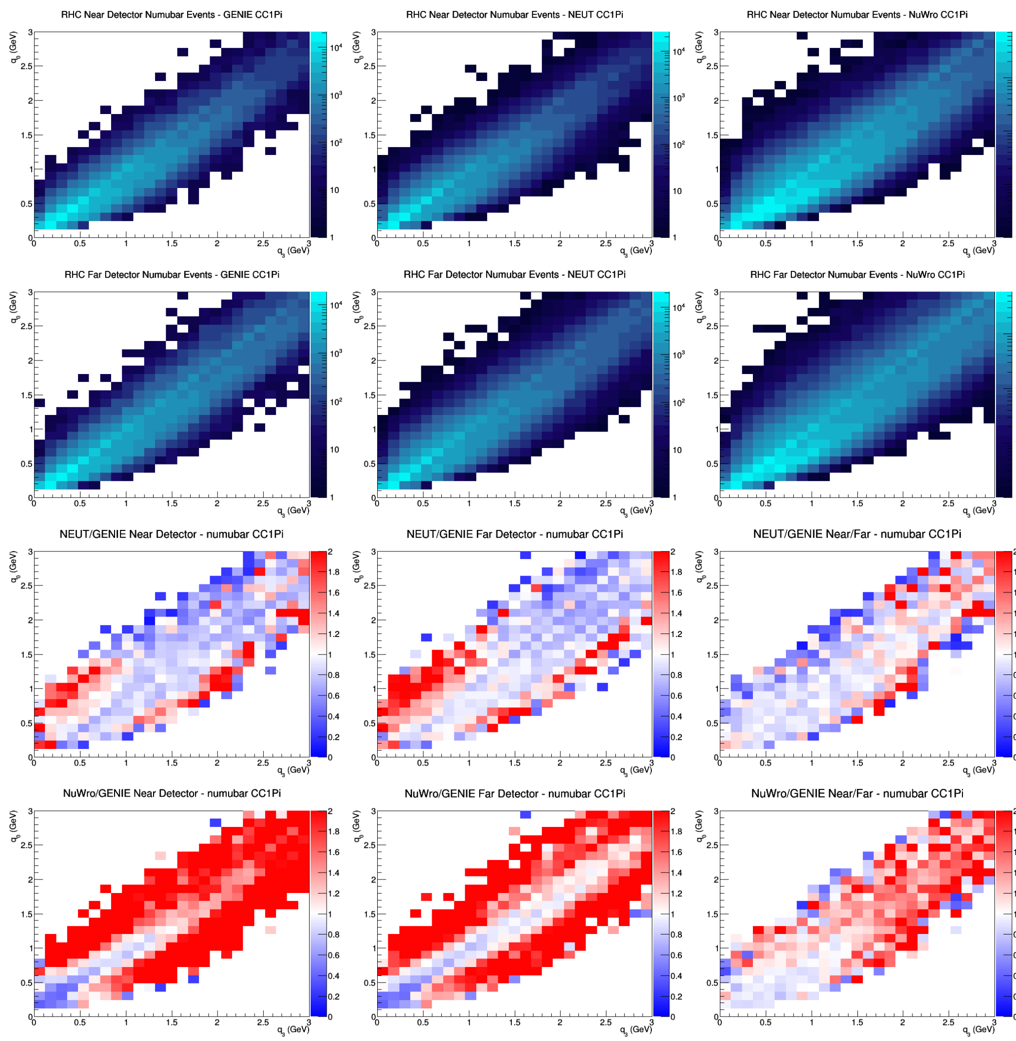

## C.33 numu CCOther no efficiencies

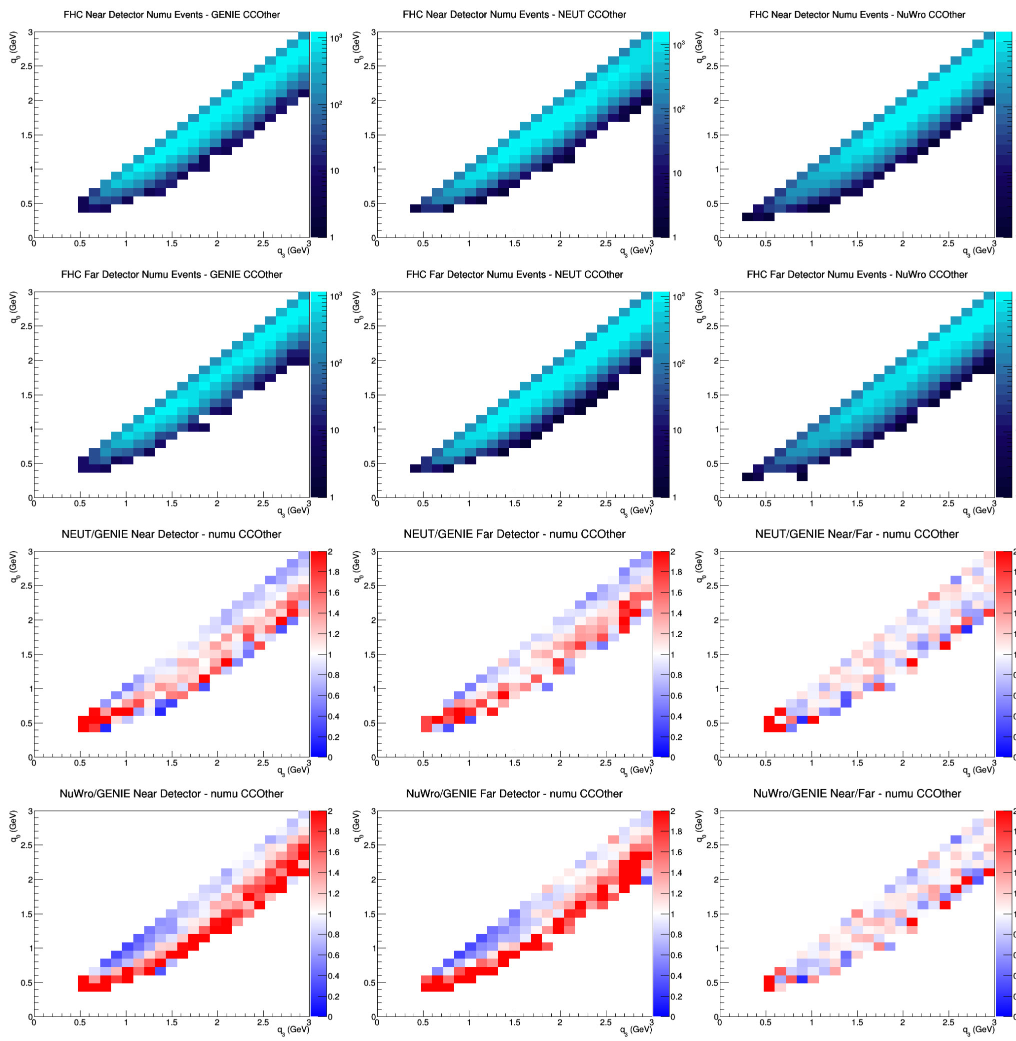

## C.34 numu CCOther FGT efficiencies

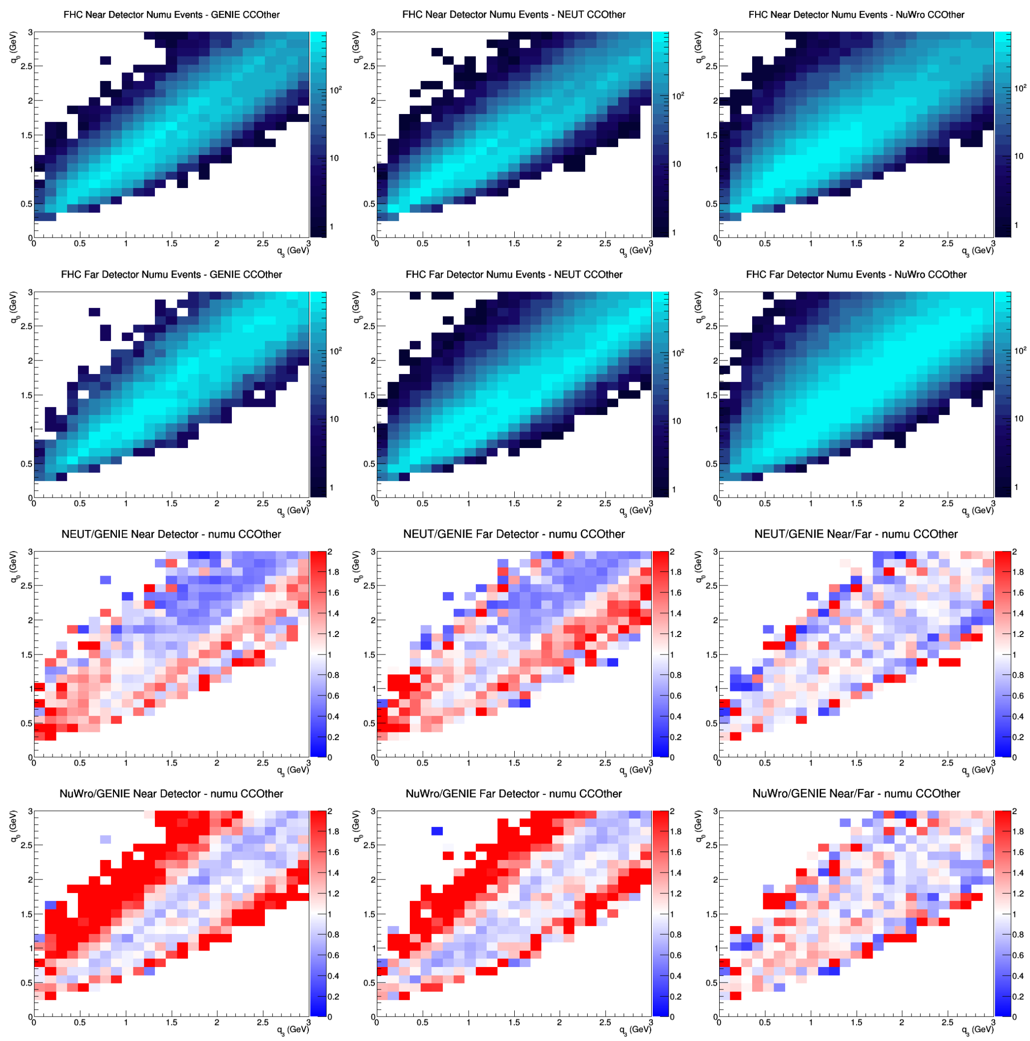

## C.35 numu CCOther LAr efficiencies

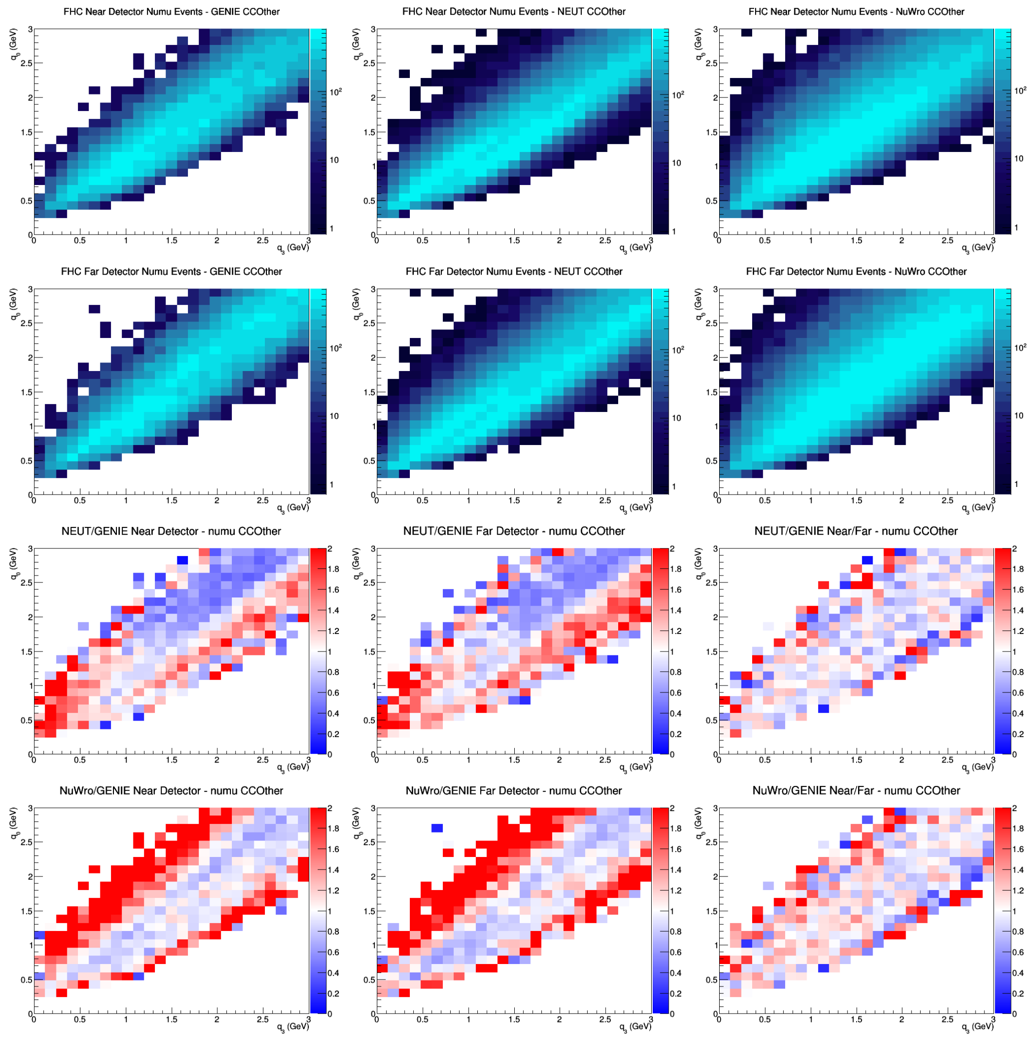

## C.36 numu CCOther GAr efficiencies

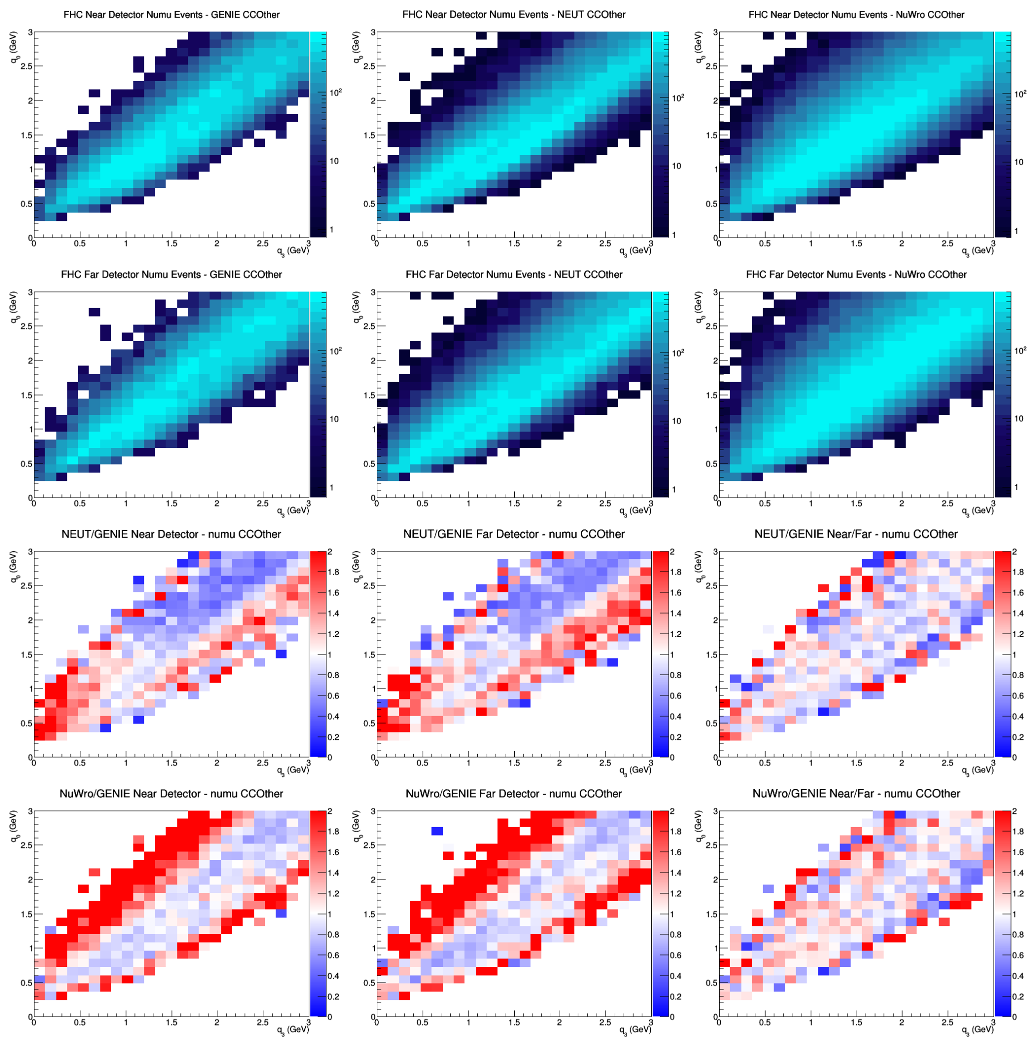

# C.37 numubar CCOther no efficiencies

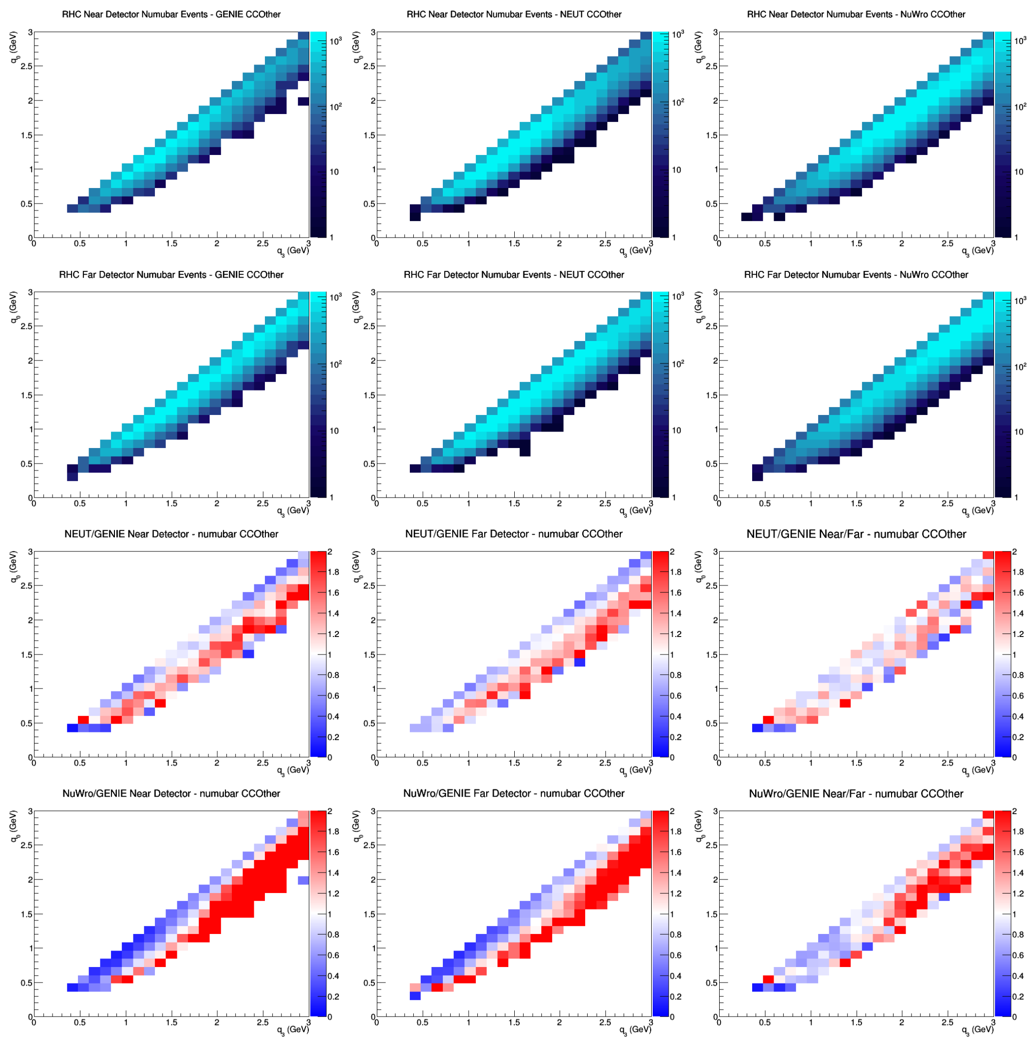

## C.38 numubar CCOther FGT efficiencies

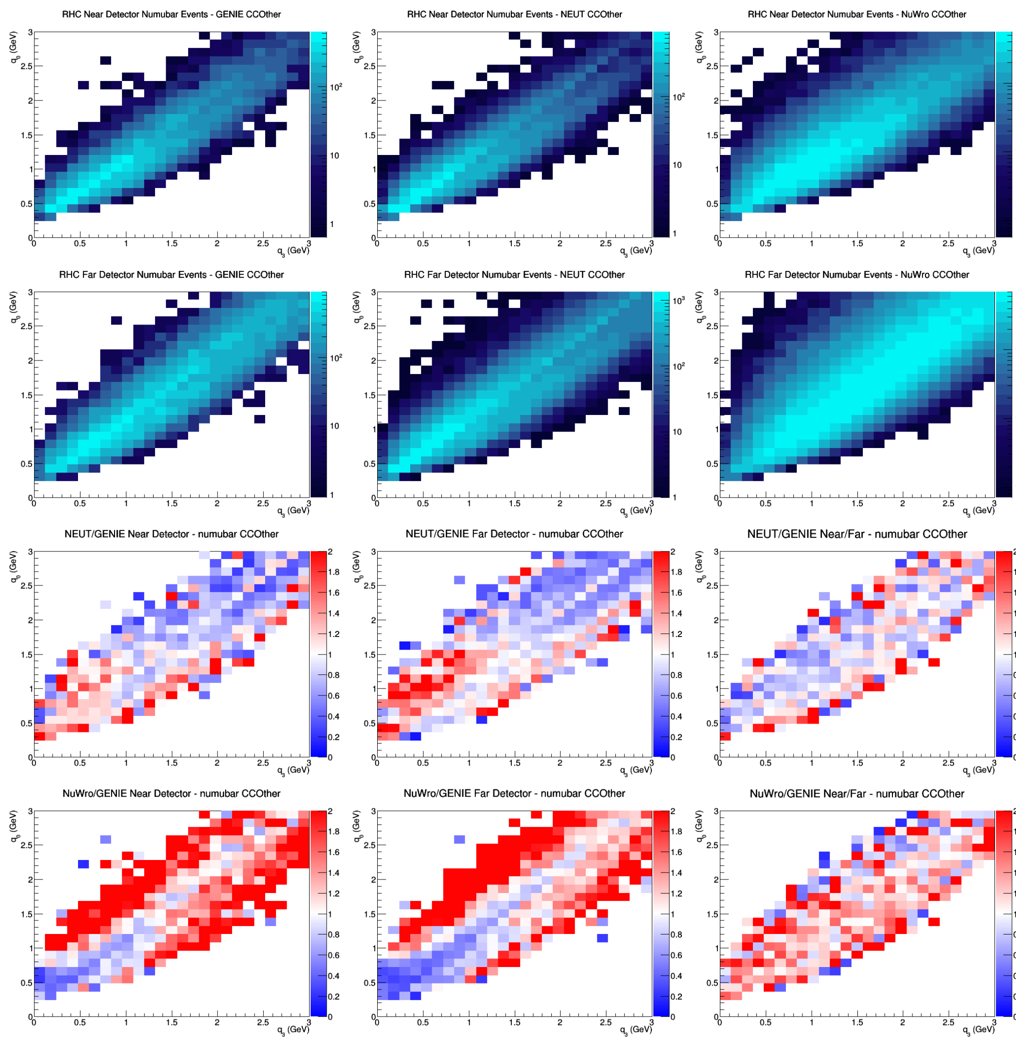

## C.39 numubar CCOther LAr efficiencies

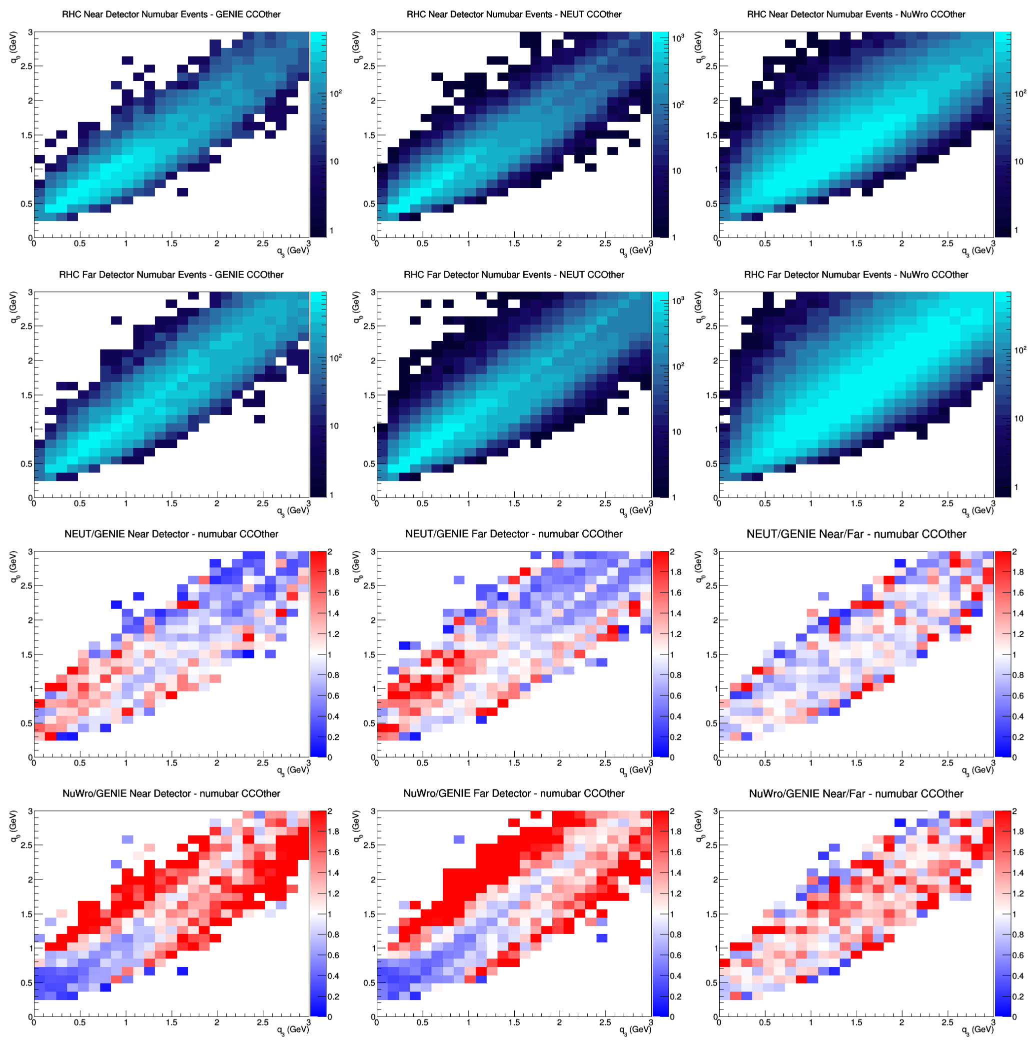

## C.40 numubar CCOther GAr efficiencies

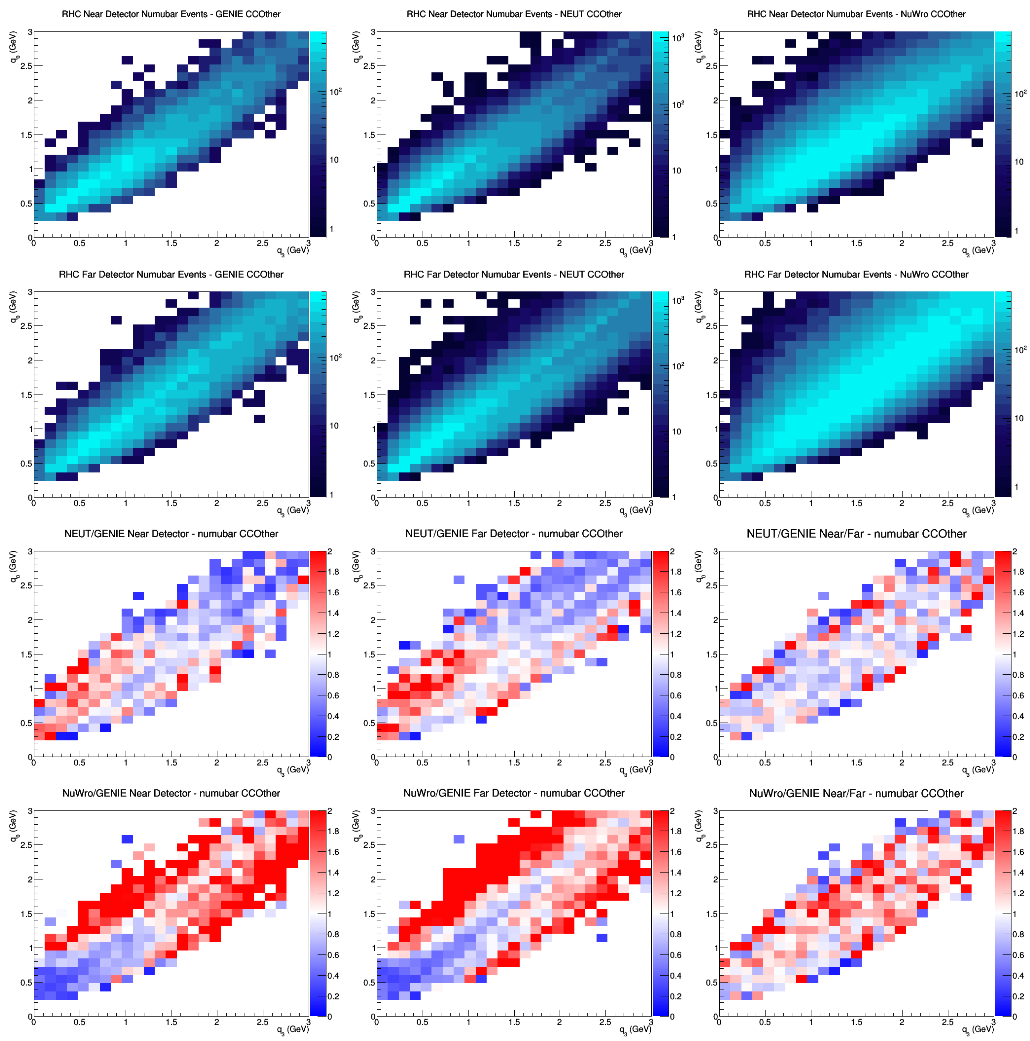

# D Neutron Multiplicities & Energy

This appendix includes all the plots not shown in Section 5.1. For full description of the files, please make reference to that section. The plots will be put in the same order as before.

## D.1 $\nu$ Plots

### D.1.1 CCQE

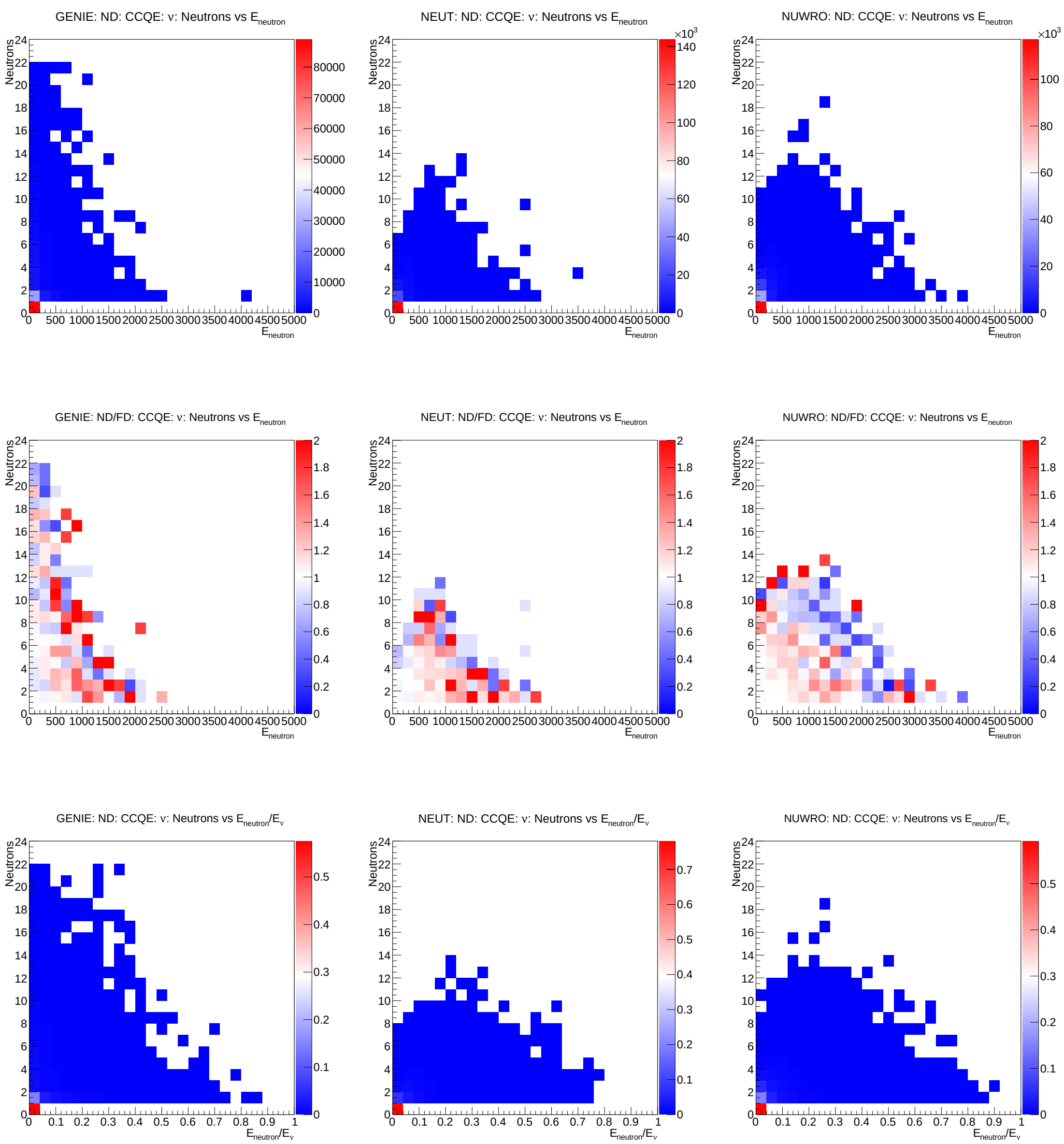


### D.1.2 2P2H

These are the same as shown in Section 5.1.

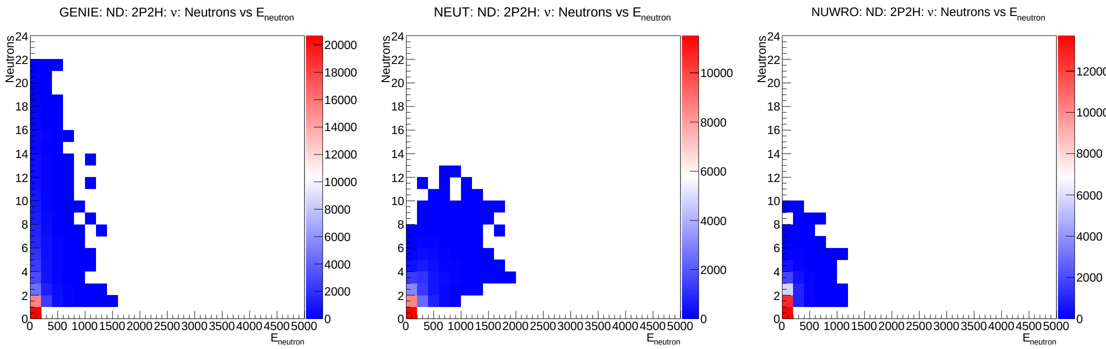
GENIE: ND: 2P2H: ν: Neutrons vs E_neutron
NEUT: ND: 2P2H: ν: Neutrons vs E_neutron
NUWRO: ND: 2P2H: ν: Neutrons vs E_neutron
Neutrons
E_neutron

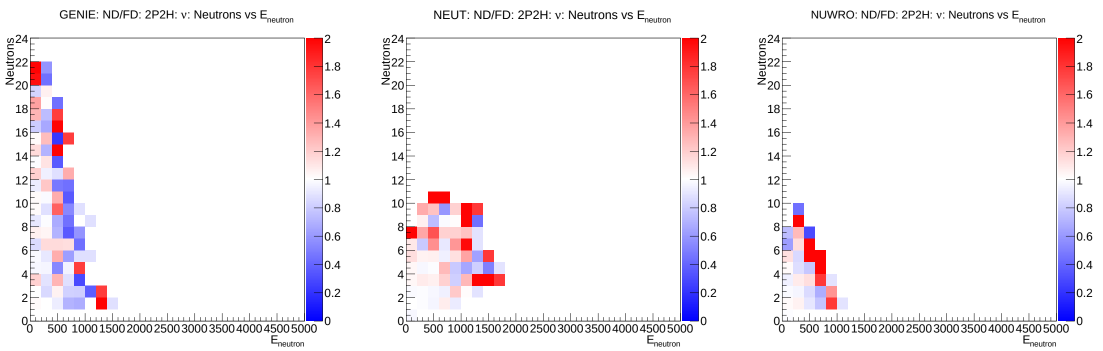
GENIE: ND/FD: 2P2H: ν: Neutrons vs E_neutron
NEUT: ND/FD: 2P2H: ν: Neutrons vs E_neutron
NUWRO: ND/FD: 2P2H: ν: Neutrons vs E_neutron
Neutrons
E_neutron

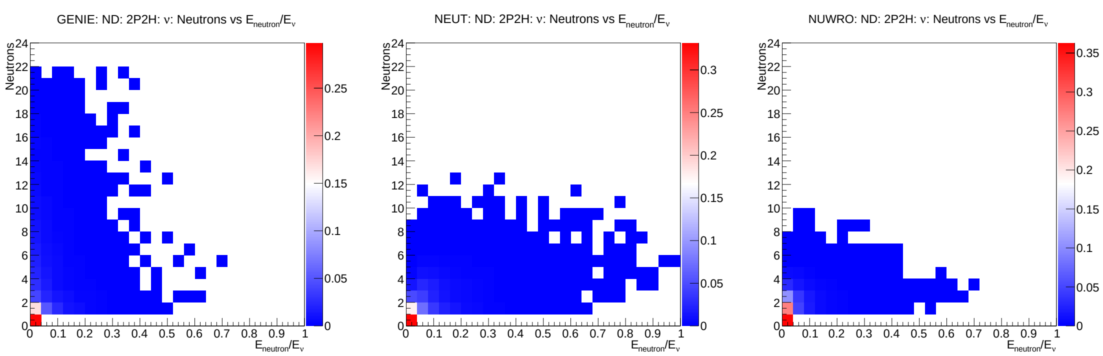
GENIE: ND: 2P2H: ν: Neutrons vs E_neutron/E_ν
NEUT: ND: 2P2H: ν: Neutrons vs E_neutron/E_ν
NUWRO: ND: 2P2H: ν: Neutrons vs E_neutron/E_ν
Neutrons
E_neutron/E_ν

### D.1.3 CC1$\pi$

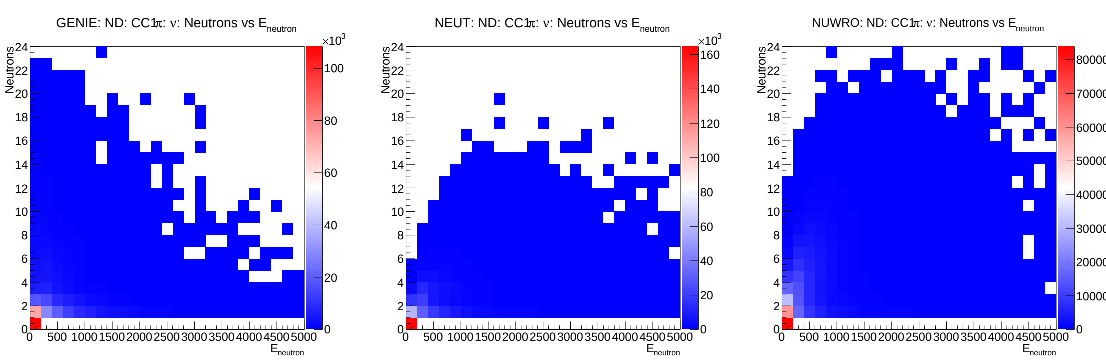
GENIE: ND: CC1π: ν: Neutrons vs E_neutron
NEUT: ND: CC1π: ν: Neutrons vs E_neutron
NUWRO: ND: CC1π: ν: Neutrons vs E_neutron
Neutrons
E_neutron

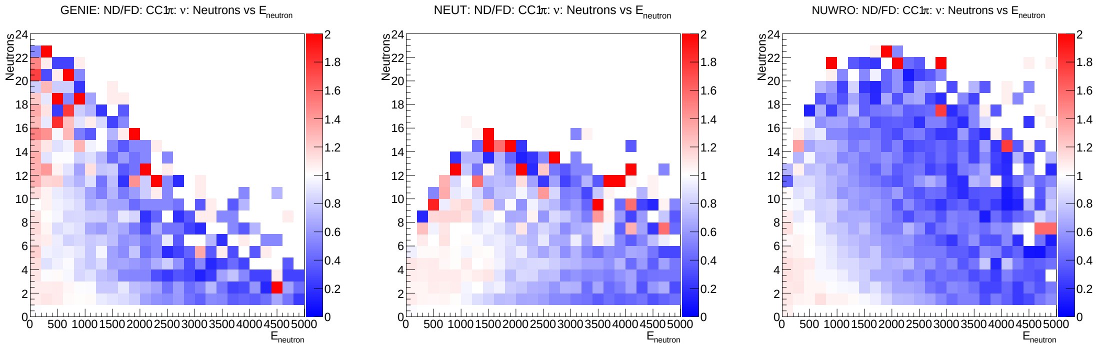
GENIE: ND/FD: CC1π: ν: Neutrons vs $E_{neutron}$
NEUT: ND/FD: CC1π: ν: Neutrons vs $E_{neutron}$
NUWRO: ND/FD: CC1π: ν: Neutrons vs $E_{neutron}$
Neutrons
$E_{neutron}$

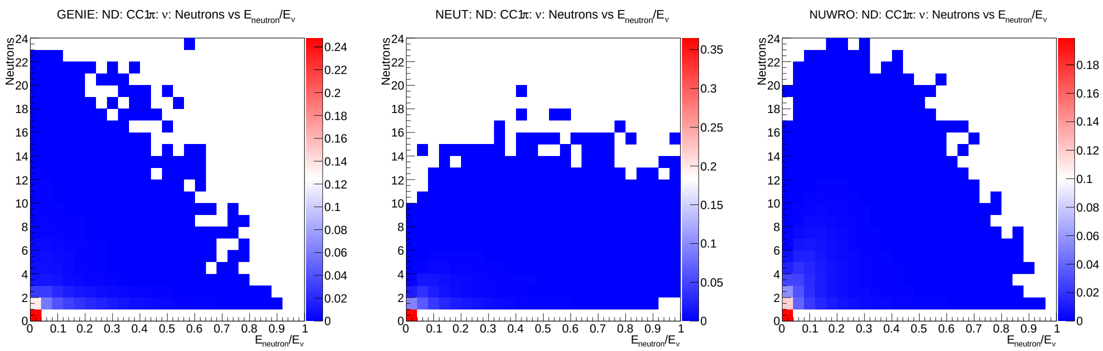
GENIE: ND: CC1π: ν: Neutrons vs $E_{neutron}/E_{\nu}$
NEUT: ND: CC1π: ν: Neutrons vs $E_{neutron}/E_{\nu}$
NUWRO: ND: CC1π: ν: Neutrons vs $E_{neutron}/E_{\nu}$
Neutrons
$E_{neutron}/E_{\nu}$

### D.1.4 CC-Other

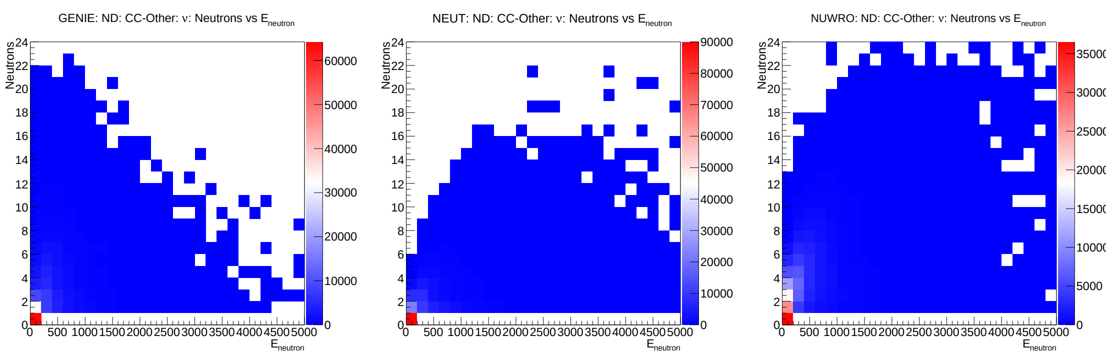
GENIE: ND: CC-Other: ν: Neutrons vs $E_{neutron}$
NEUT: ND: CC-Other: ν: Neutrons vs $E_{neutron}$
NUWRO: ND: CC-Other: ν: Neutrons vs $E_{neutron}$
Neutrons
$E_{neutron}$

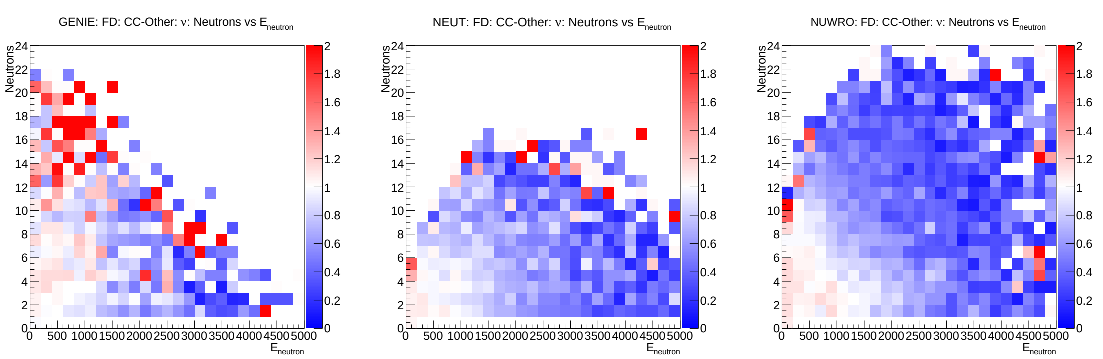
GENIE: FD: CC-Other: ν: Neutrons vs $E_{neutron}$
NEUT: FD: CC-Other: ν: Neutrons vs $E_{neutron}$
NUWRO: FD: CC-Other: ν: Neutrons vs $E_{neutron}$
Neutrons
$E_{neutron}$

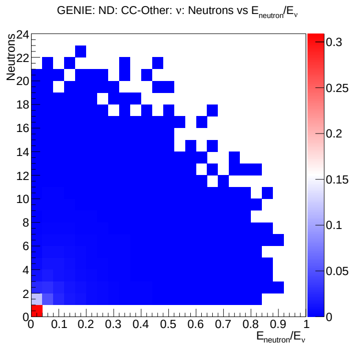

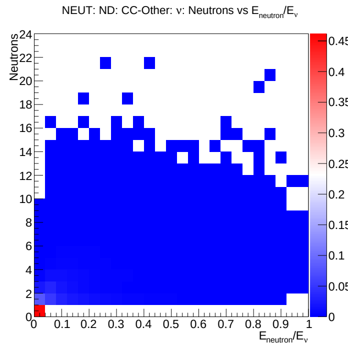

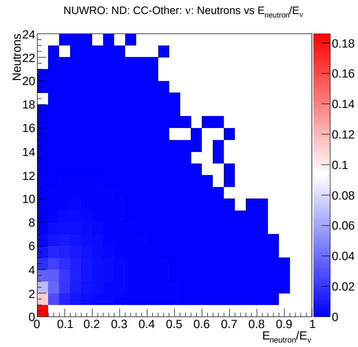


## D.2 $\bar{\nu}$ Plots

### D.2.1 CCQE

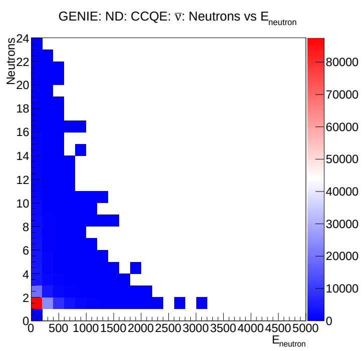

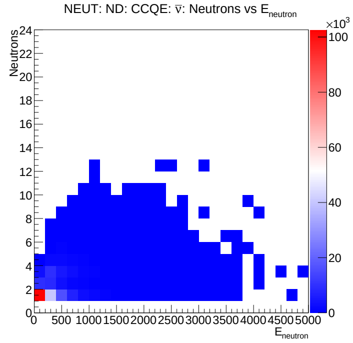

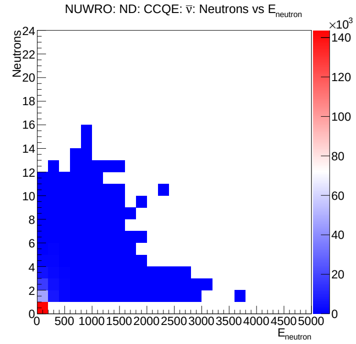


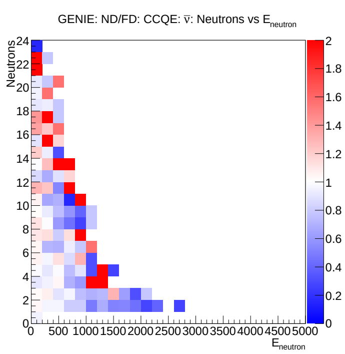

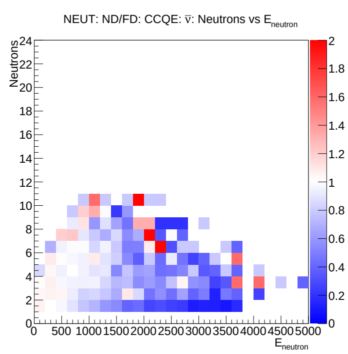

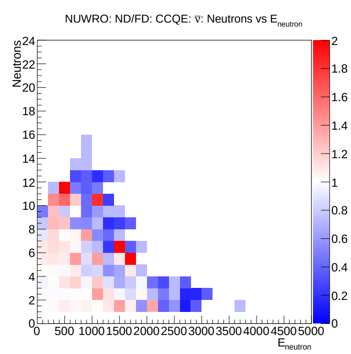

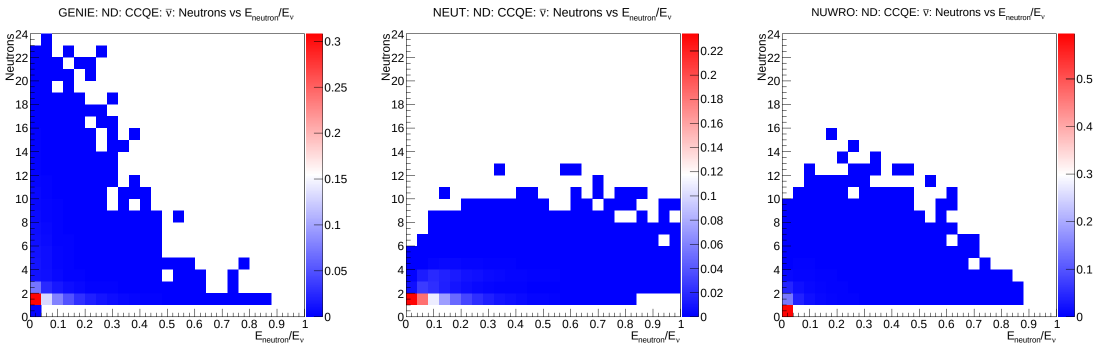


### D.2.2 2P2H

These are the same as shown in Section 5.1.

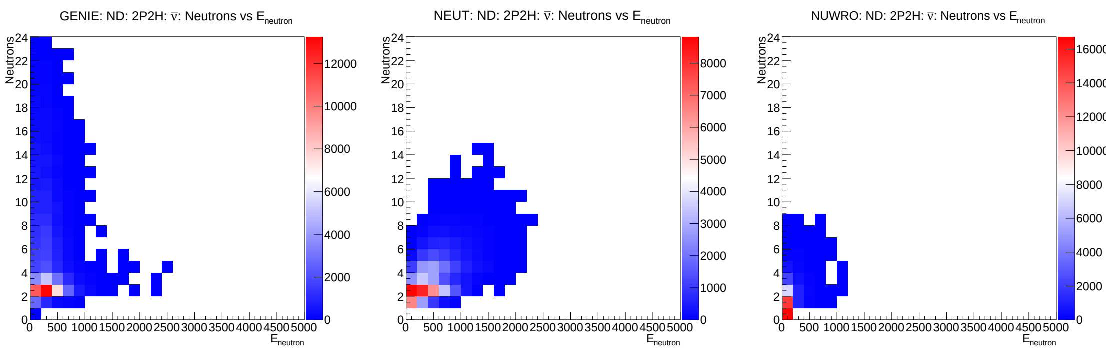


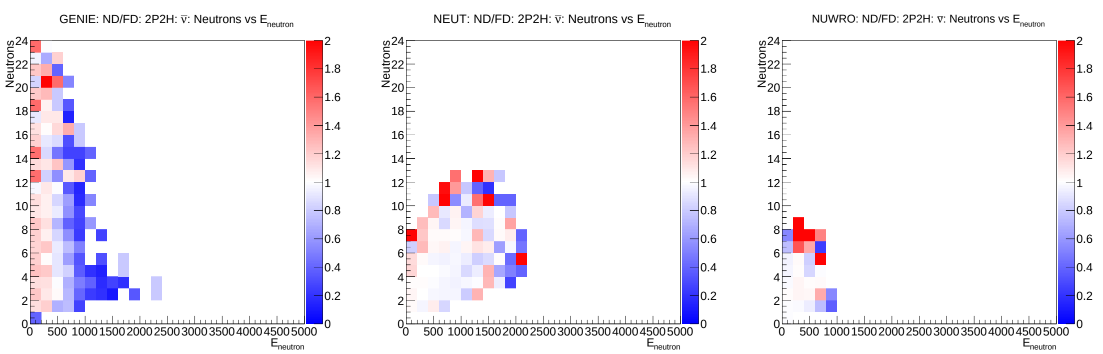

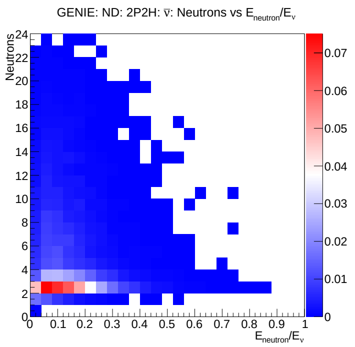
GENIE: ND: 2P2H: $\bar{\nu}$: Neutrons vs $E_{neutron}/E_{\nu}$
Neutrons
$E_{neutron}/E_{\nu}$

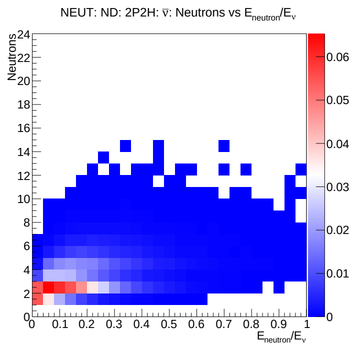
NEUT: ND: 2P2H: $\bar{\nu}$: Neutrons vs $E_{neutron}/E_{\nu}$
Neutrons
$E_{neutron}/E_{\nu}$

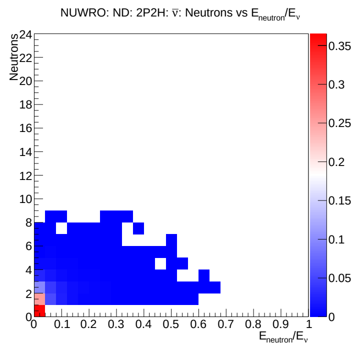
NUWRO: ND: 2P2H: $\bar{\nu}$: Neutrons vs $E_{neutron}/E_{\nu}$
Neutrons
$E_{neutron}/E_{\nu}$

### D.2.3 CC1$\pi$

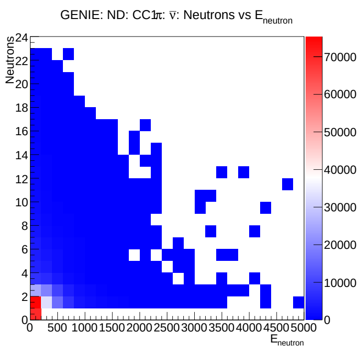
GENIE: ND: CC1$\pi$: $\bar{\nu}$: Neutrons vs $E_{neutron}$
Neutrons
$E_{neutron}$

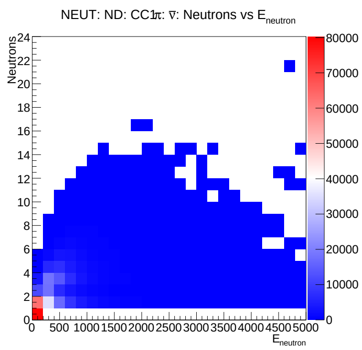
NEUT: ND: CC1$\pi$: $\bar{\nu}$: Neutrons vs $E_{neutron}$
Neutrons
$E_{neutron}$

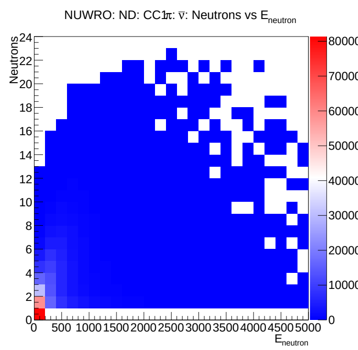
NUWRO: ND: CC1$\pi$: $\bar{\nu}$: Neutrons vs $E_{neutron}$
Neutrons
$E_{neutron}$

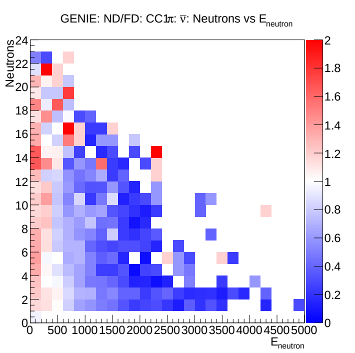
GENIE: ND/FD: CC1$\pi$: $\bar{\nu}$: Neutrons vs $E_{neutron}$
Neutrons
$E_{neutron}$

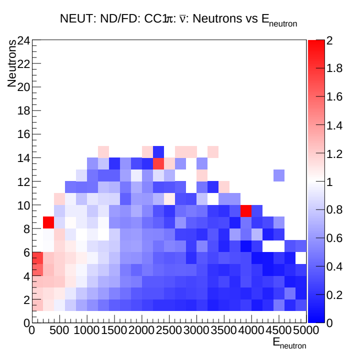
NEUT: ND/FD: CC1$\pi$: $\bar{\nu}$: Neutrons vs $E_{neutron}$
Neutrons
$E_{neutron}$

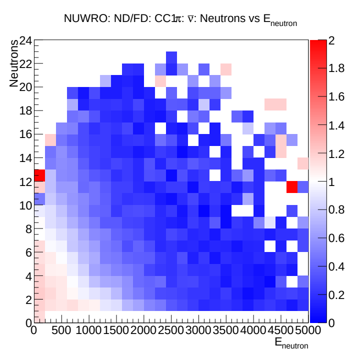
NUWRO: ND/FD: CC1$\pi$: $\bar{\nu}$: Neutrons vs $E_{neutron}$
Neutrons
$E_{neutron}$

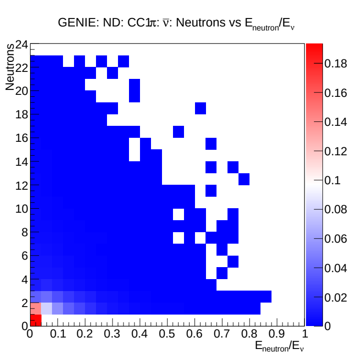
GENIE: ND: CC1$\pi$: $\bar{\nu}$: Neutrons vs $E_{neutron}/E_{\nu}$
Neutrons
$E_{neutron}/E_{\nu}$

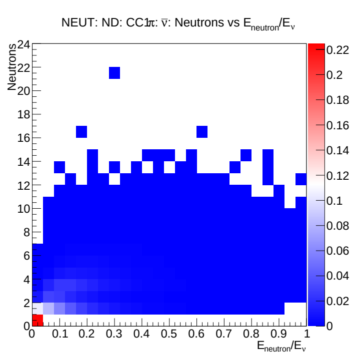
NEUT: ND: CC1$\pi$: $\bar{\nu}$: Neutrons vs $E_{neutron}/E_{\nu}$
Neutrons
$E_{neutron}/E_{\nu}$

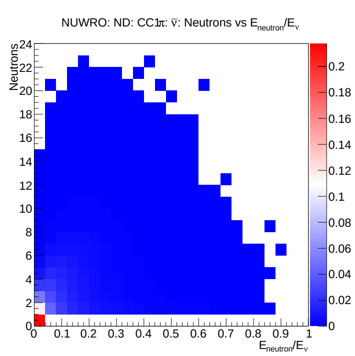
NUWRO: ND: CC1$\pi$: $\bar{\nu}$: Neutrons vs $E_{neutron}/E_{\nu}$
Neutrons
$E_{neutron}/E_{\nu}$

### D.2.4 CC-Other

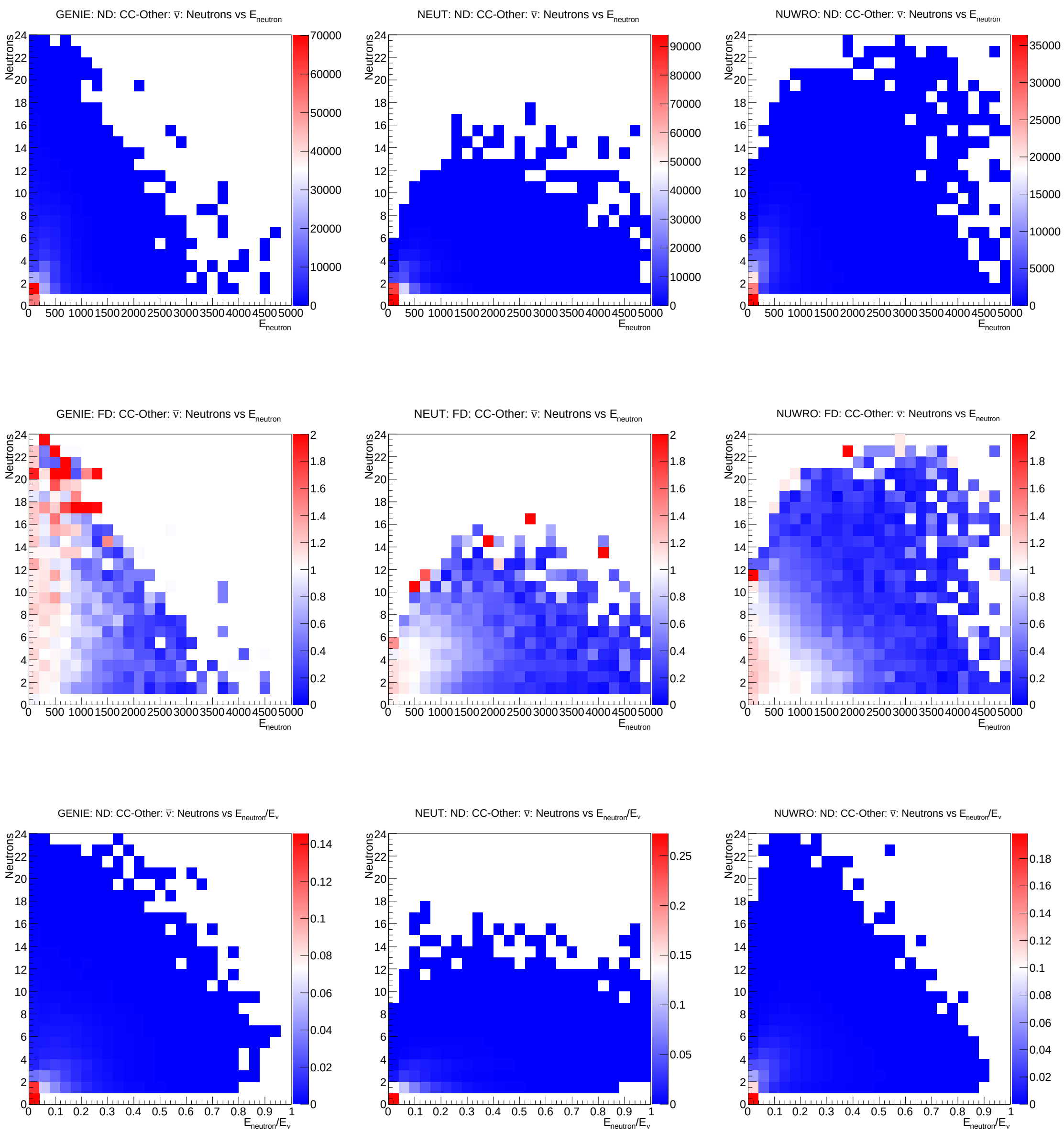


# E Proton Multiplicity vs Total Proton Momentum Plots

This appendix includes all the plots not show in Section 5.2. For full description of the files, please make reference to that section. The plots will be put in the same order as before.

## E.1 numu CCQE no efficiencies

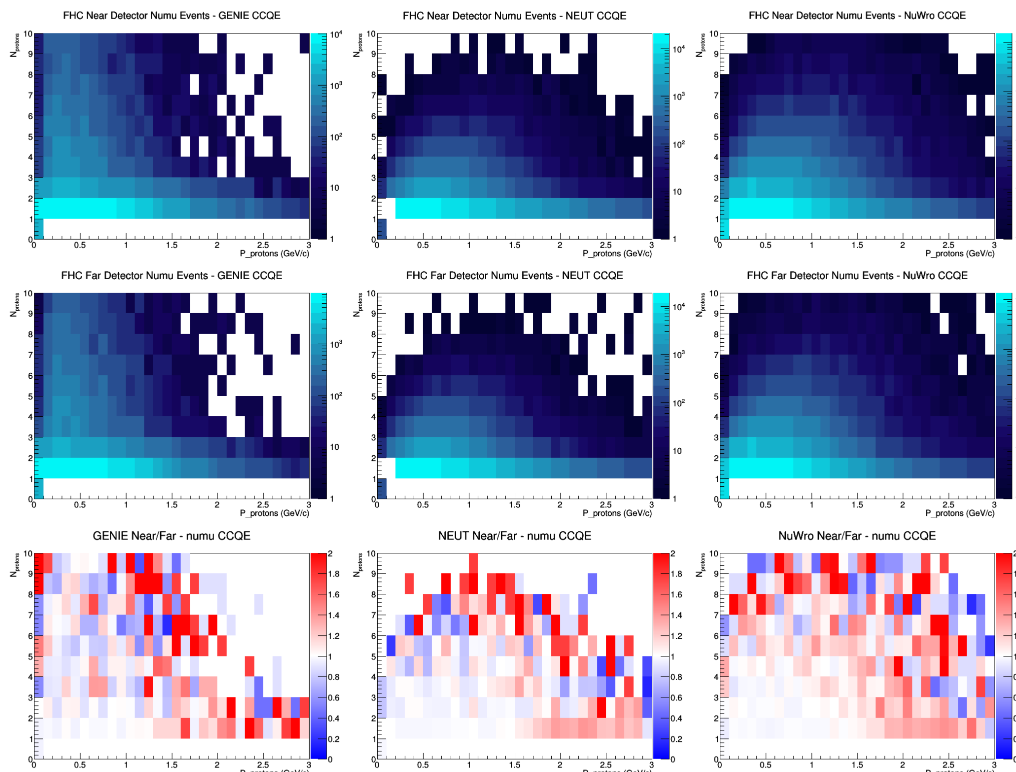
FHC Near Detector Numu Events - GENIE CCQE
FHC Near Detector Numu Events - NEUT CCQE
FHC Near Detector Numu Events - NuWro CCQE
FHC Far Detector Numu Events - GENIE CCQE
FHC Far Detector Numu Events - NEUT CCQE
FHC Far Detector Numu Events - NuWro CCQE
GENIE Near/Far - numu CCQE
NEUT Near/Far - numu CCQE
NuWro Near/Far - numu CCQE
N_protons
P_protons (GeV/c)

## E.2 numu CCQE FGT efficiencies

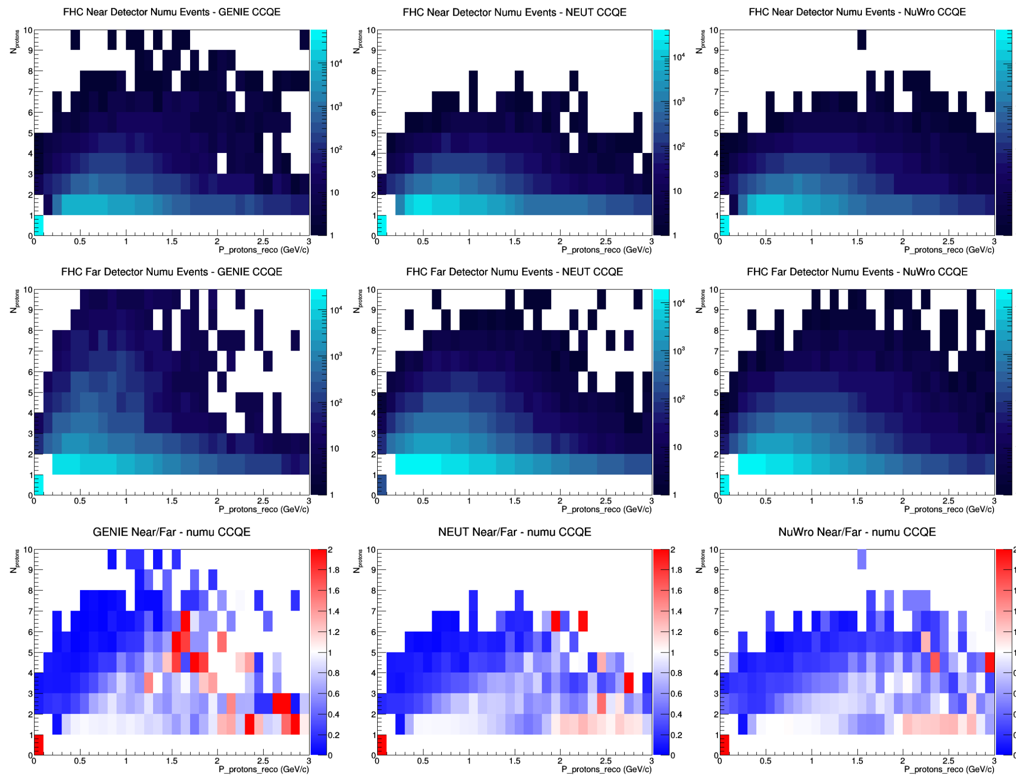

## E.3 numu CCQE LAr efficiencies

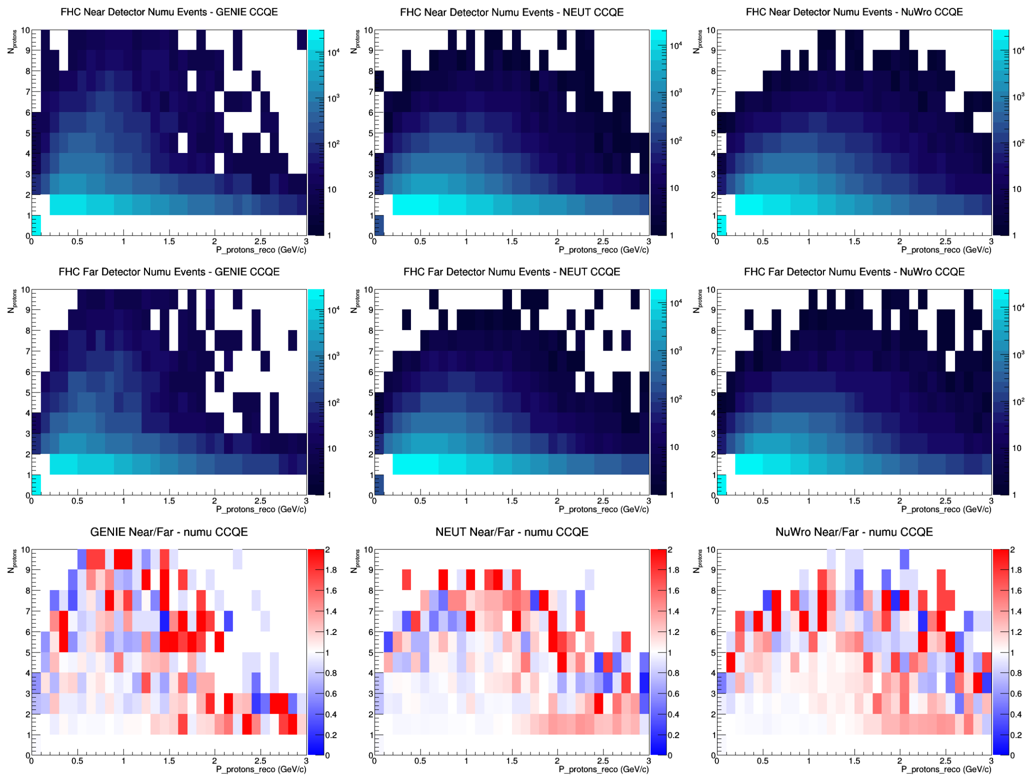

## E.4 numu CCQE GAr efficiencies

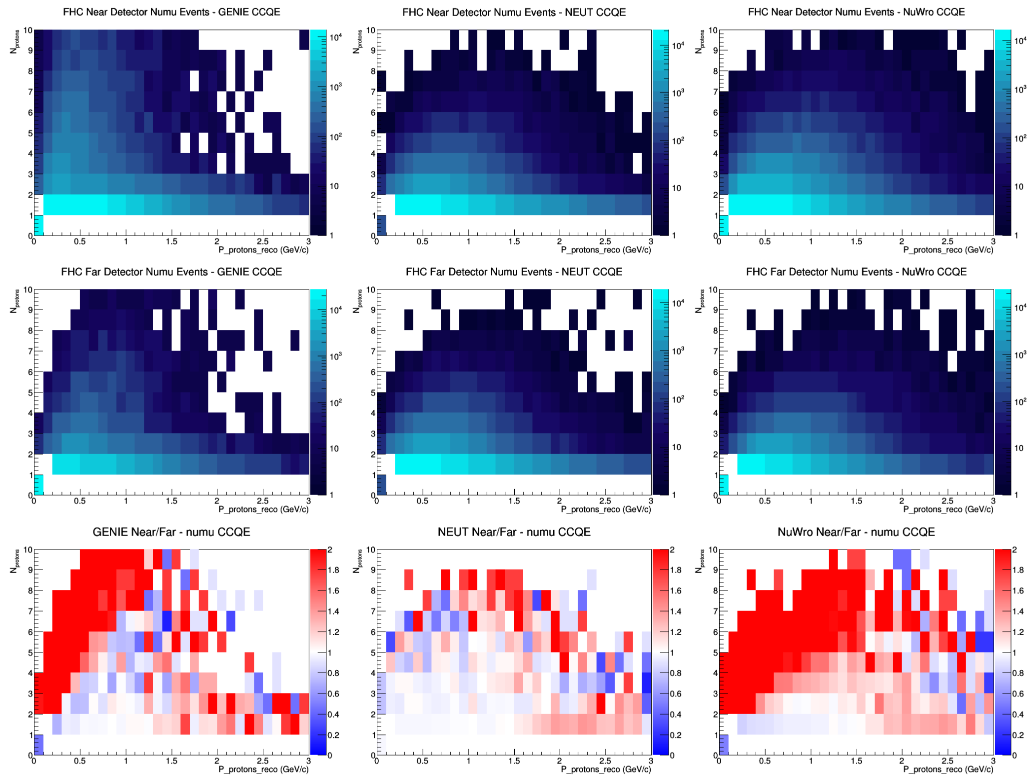

## E.5 numubar CCQE no efficiencies

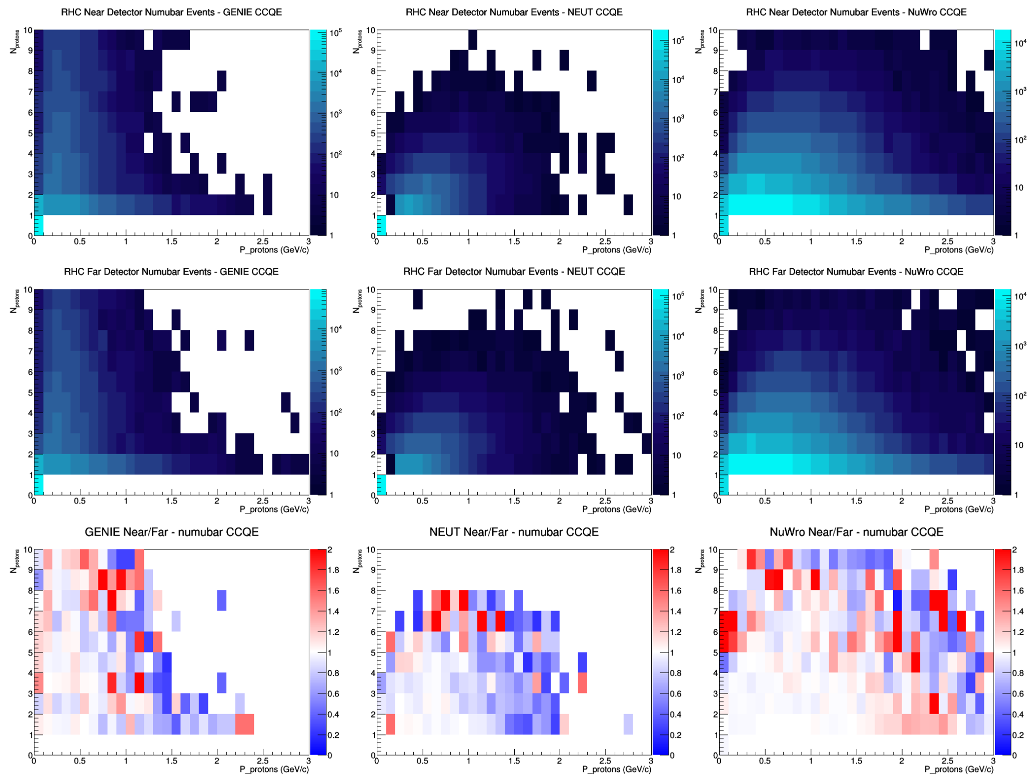

## E.6 numubar CCQE FGT efficiencies

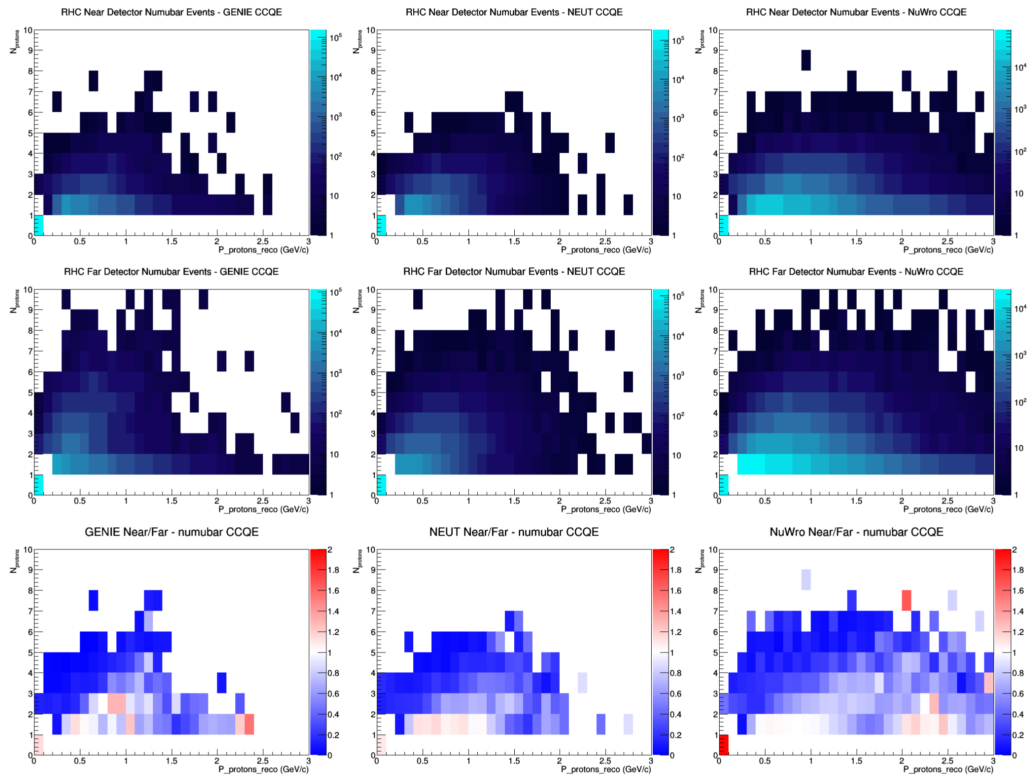

## E.7 numubar CCQE LAr efficiencies

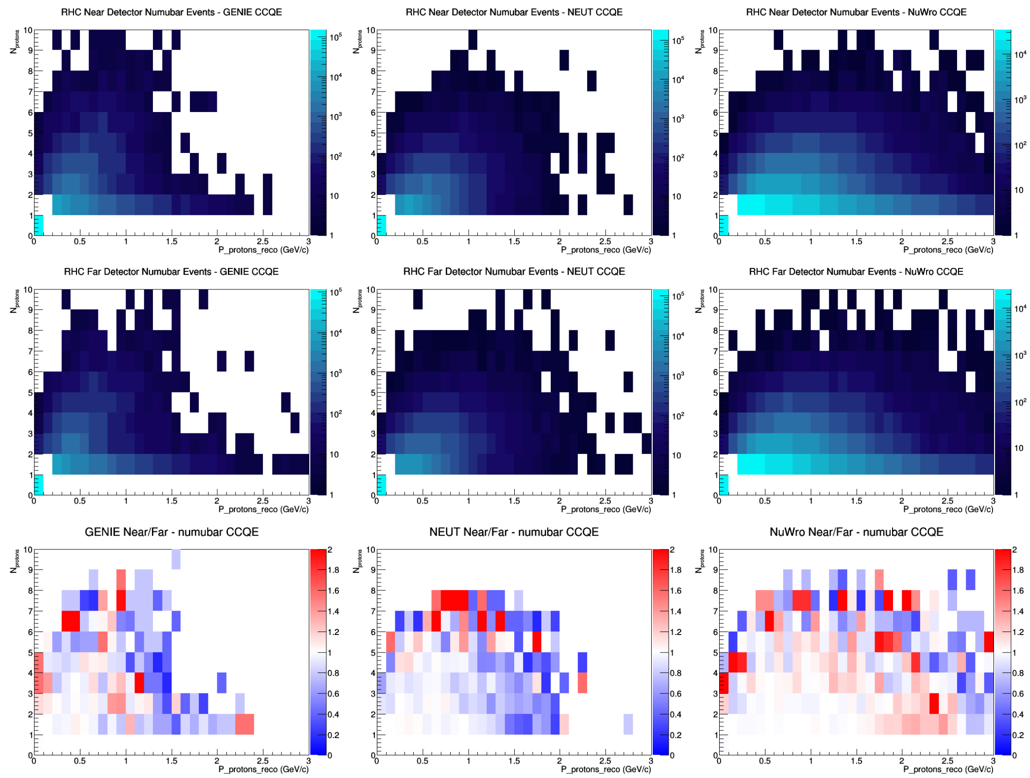

## E.8 numubar CCQE GAr efficiencies

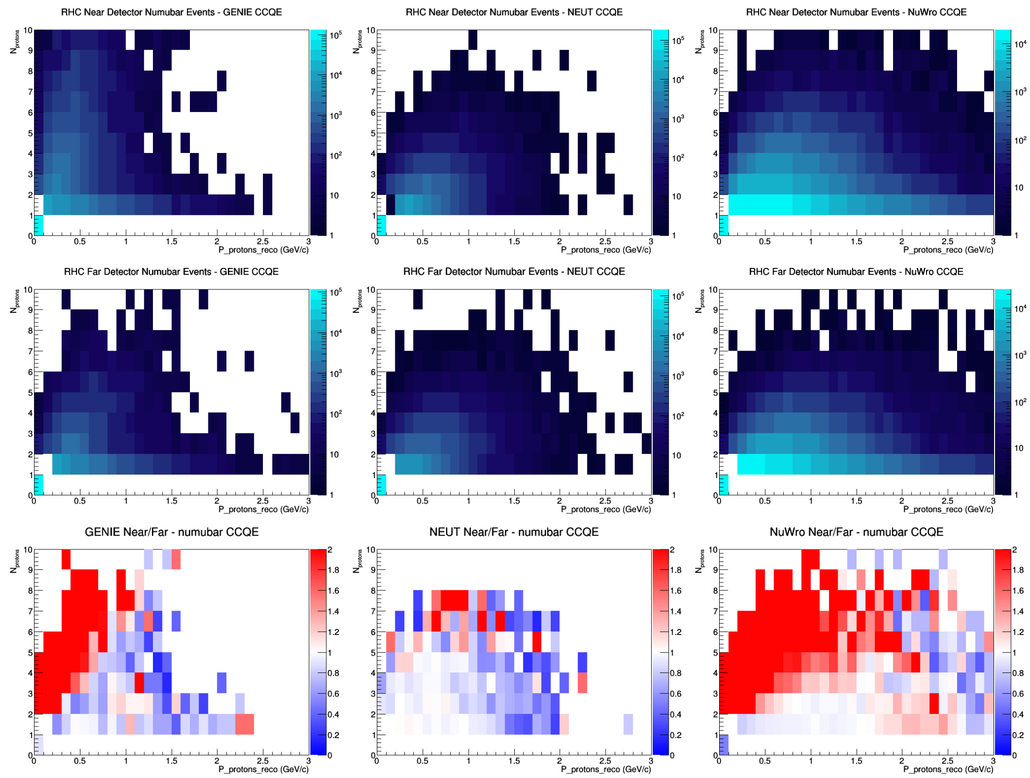

## E.9 numu 2p2h no efficiencies

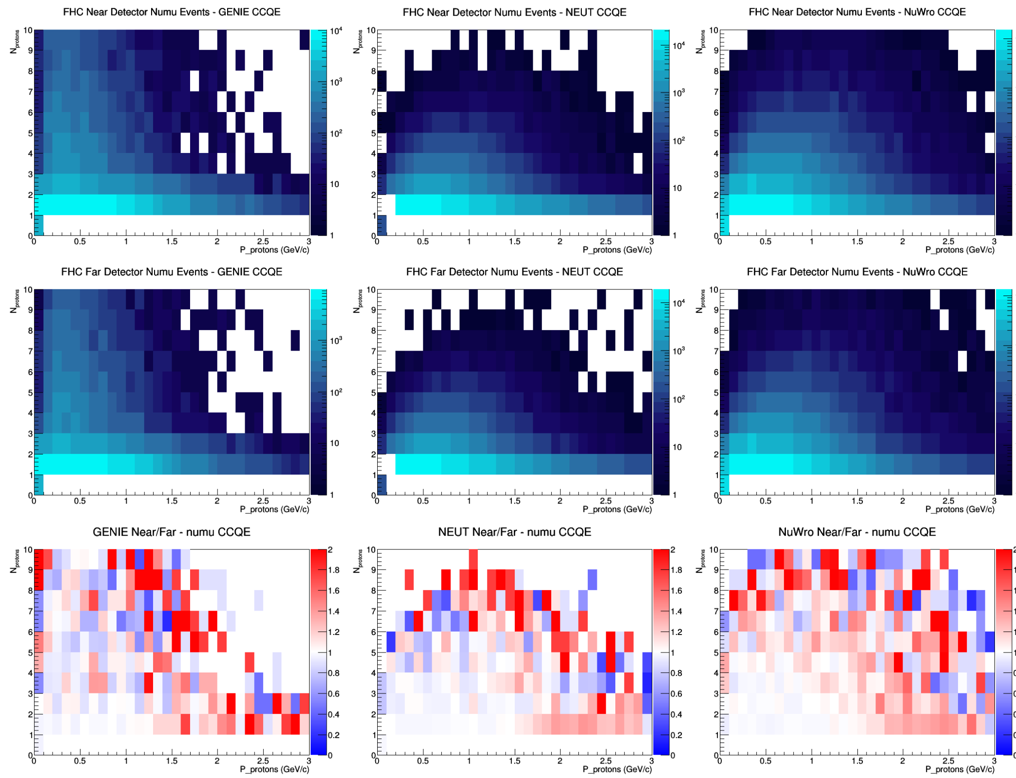

## E.10 numu 2p2h FGT efficiencies

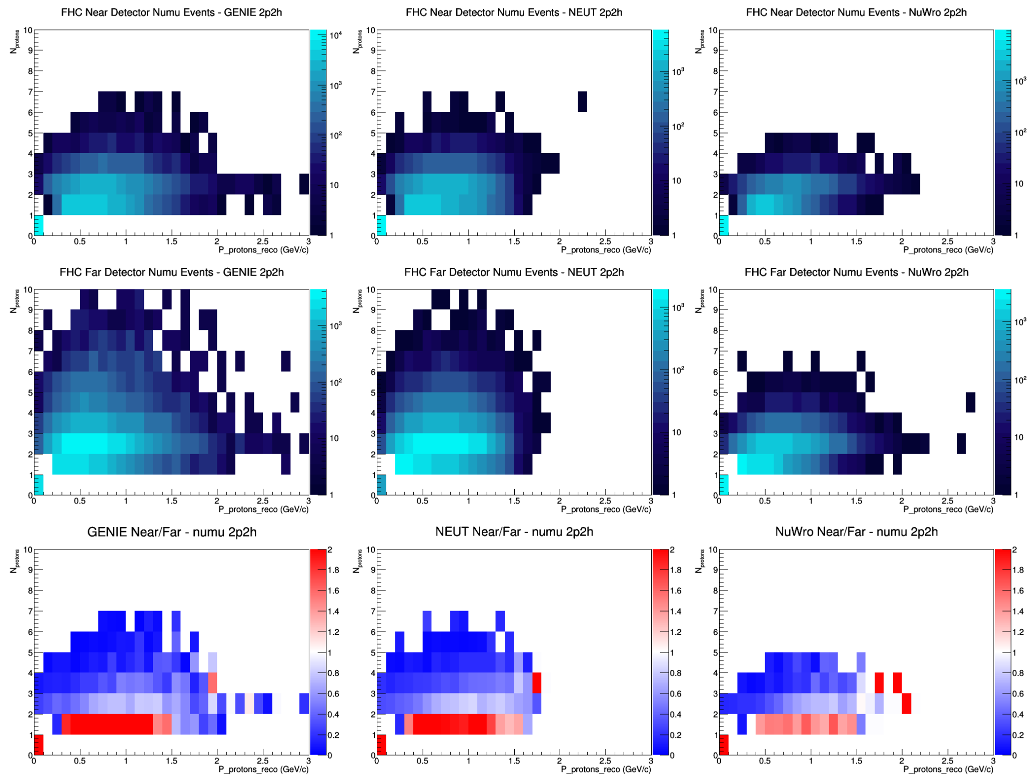

## E.11 numu 2p2h LAr efficiencies

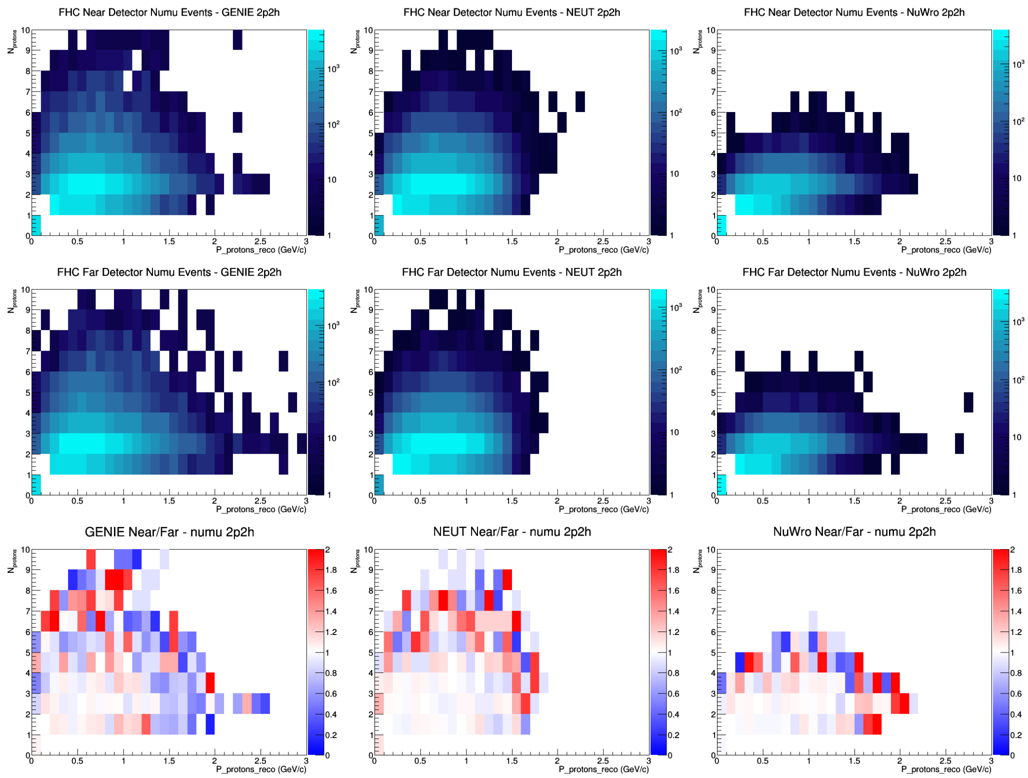

## E.12 numu 2p2h GAr efficiencies

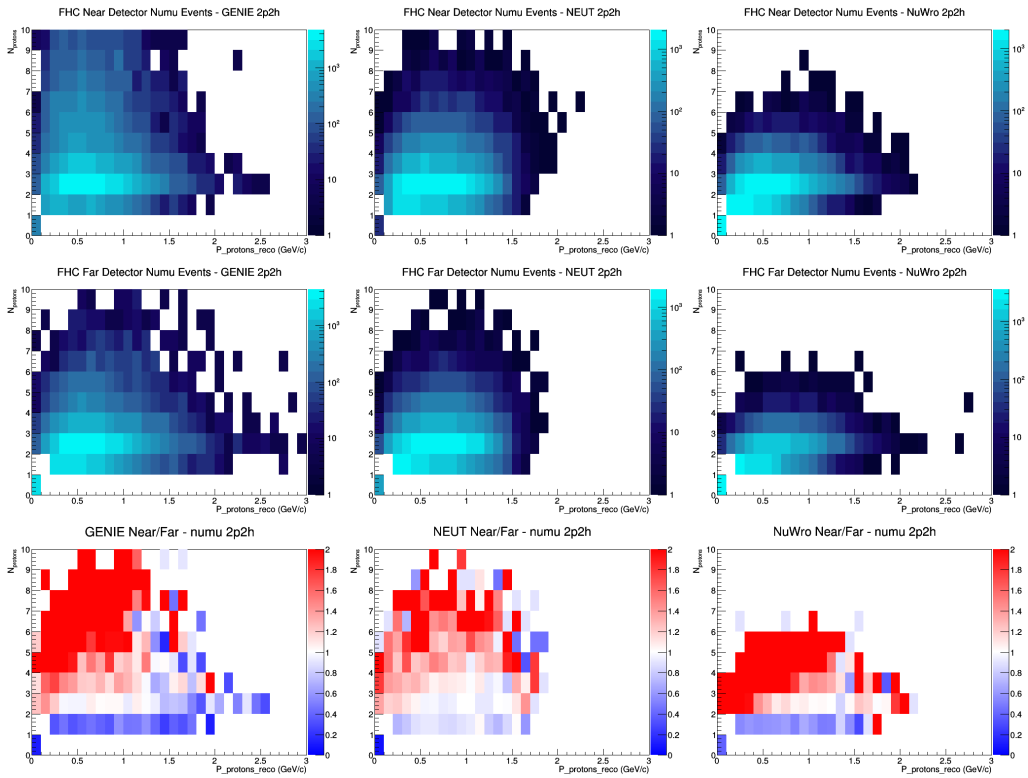

## E.13 numubar 2p2h no efficiencies

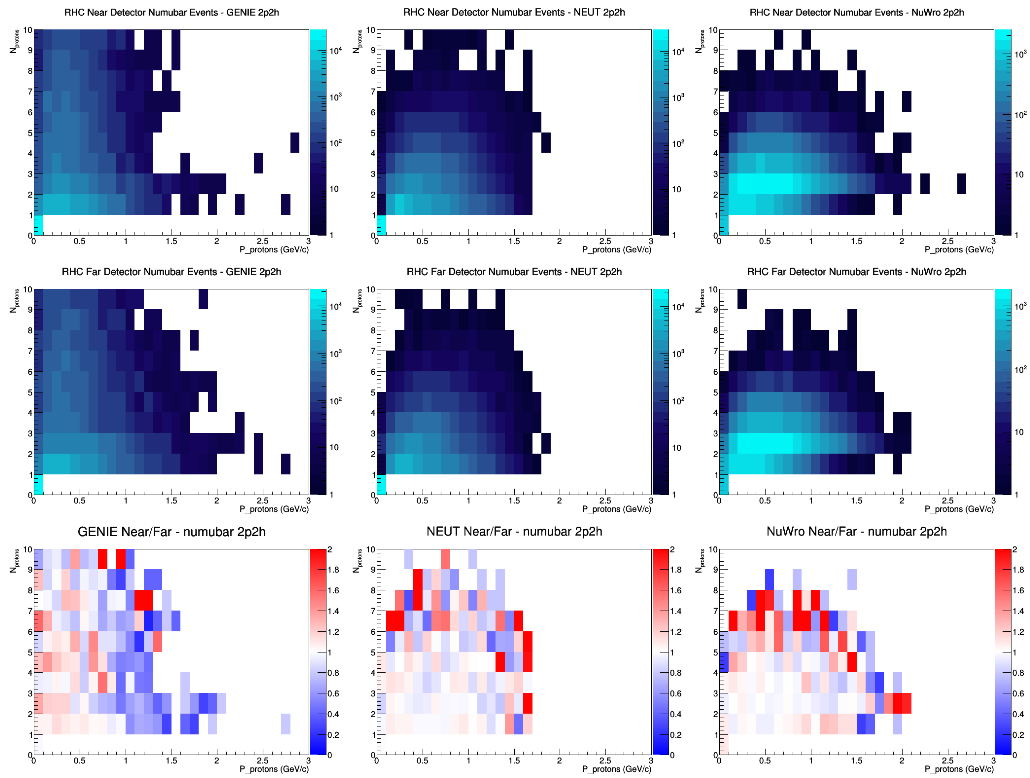

## E.14 numubar 2p2h FGT efficiencies

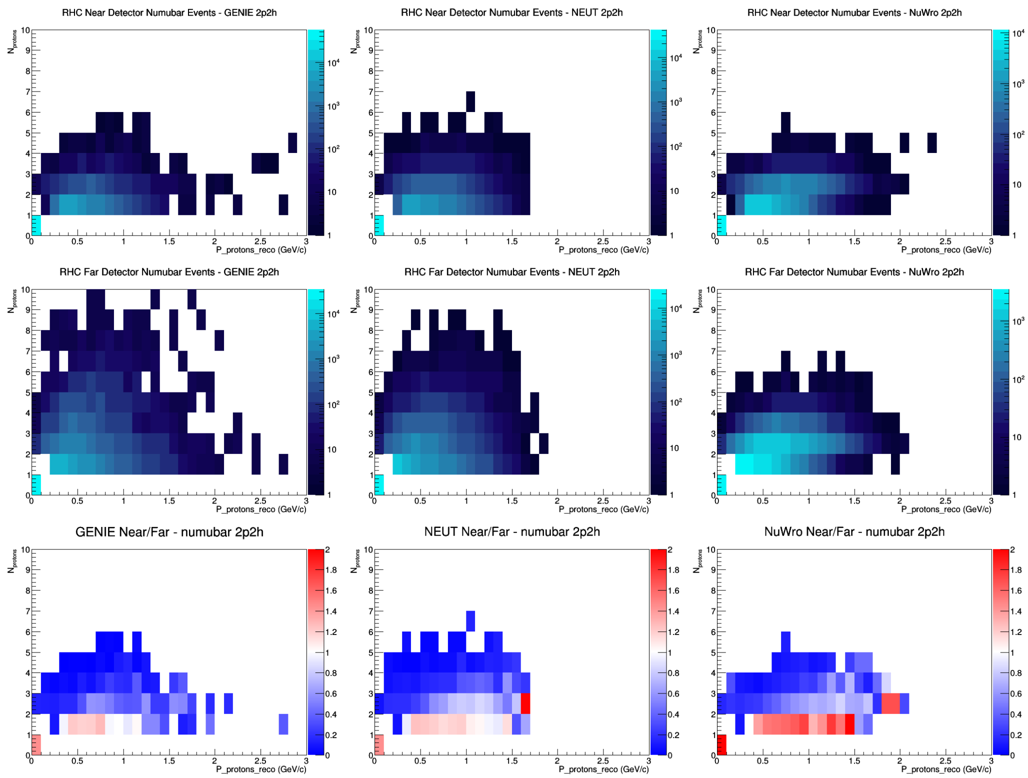

## E.15 numubar 2p2h LAr efficiencies

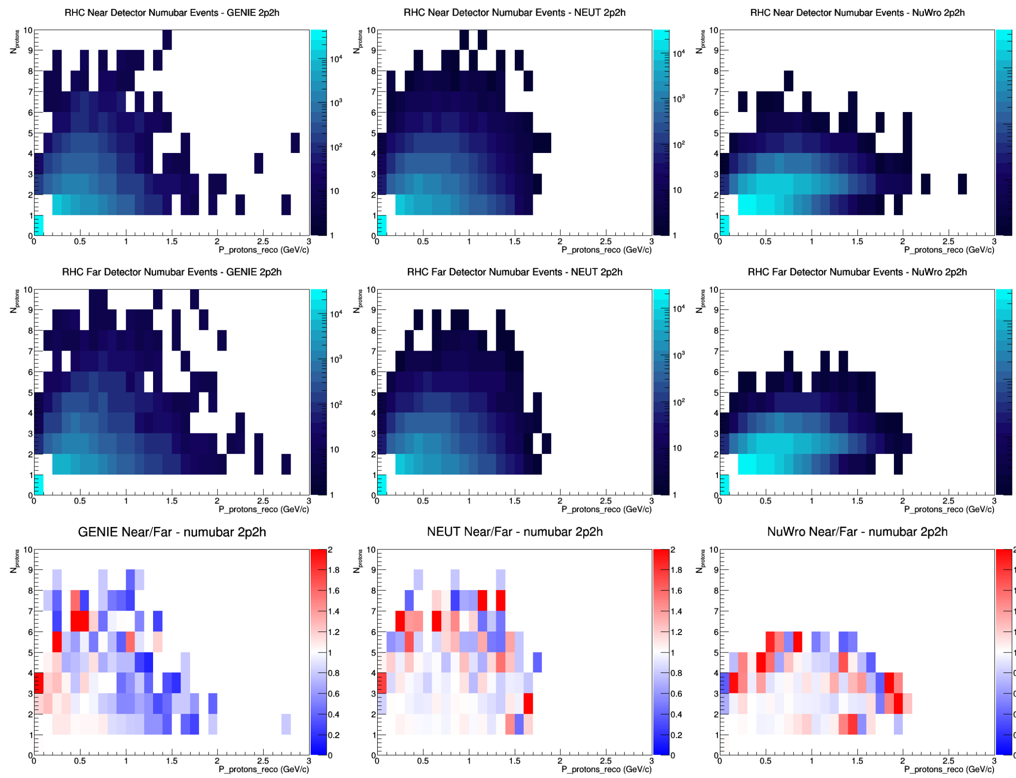

## E.16 numubar 2p2h GAr efficiencies

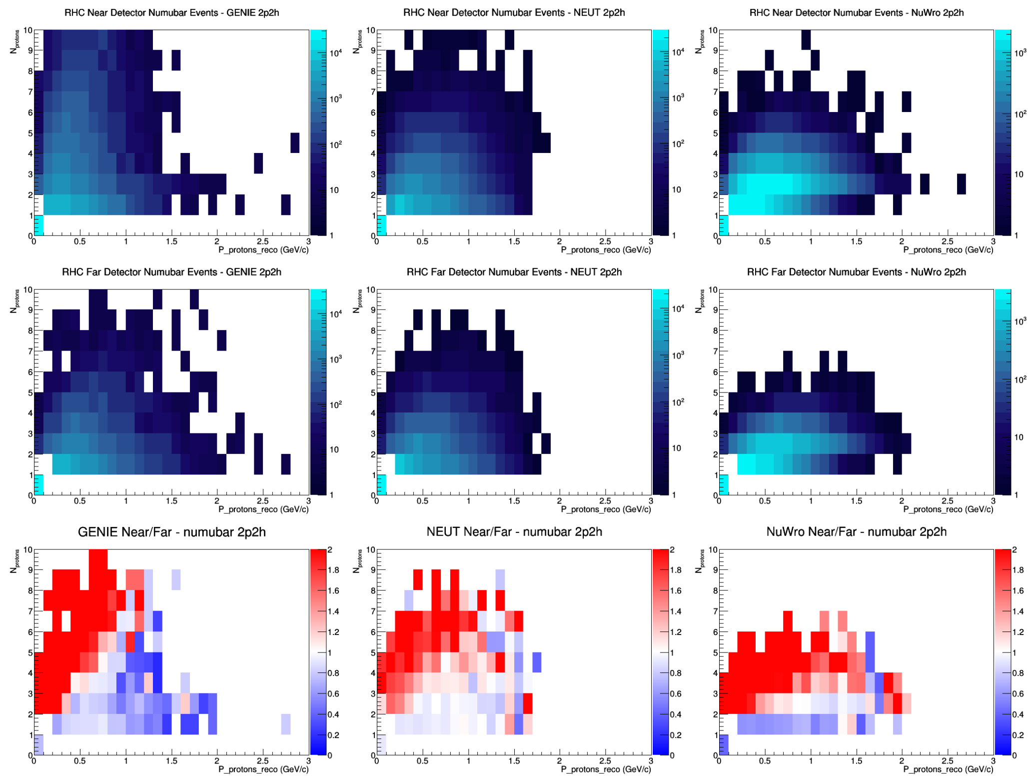

## E.17 numu CC0Pi no efficiencies

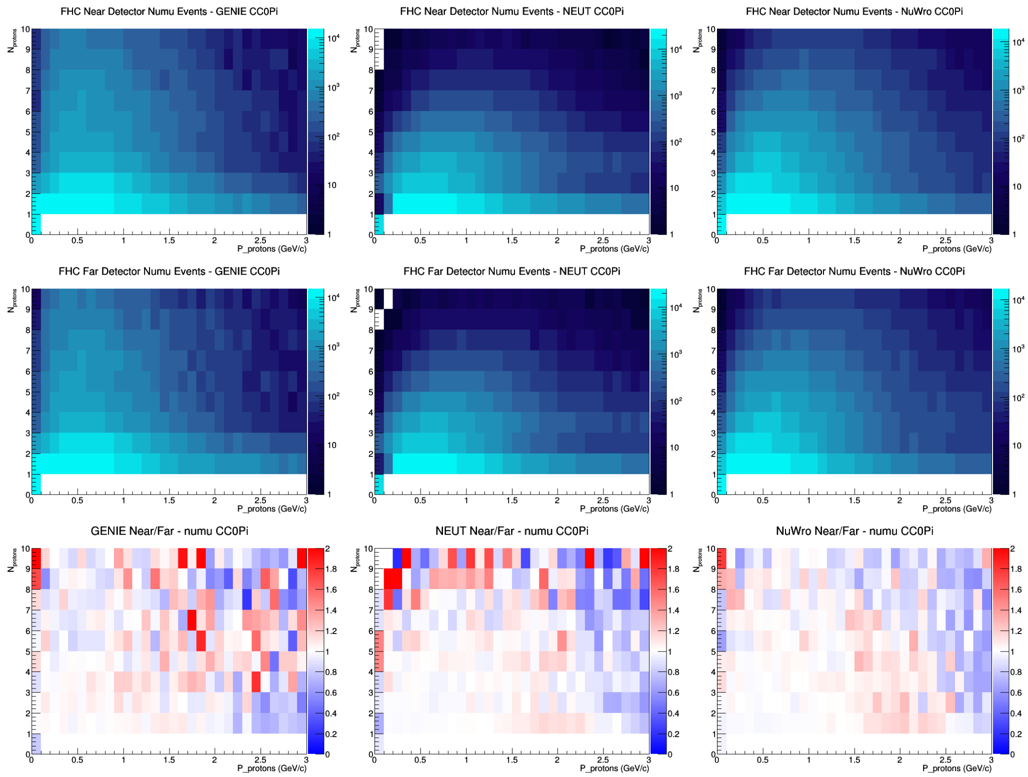

## E.18 numu CC0Pi FGT efficiencies

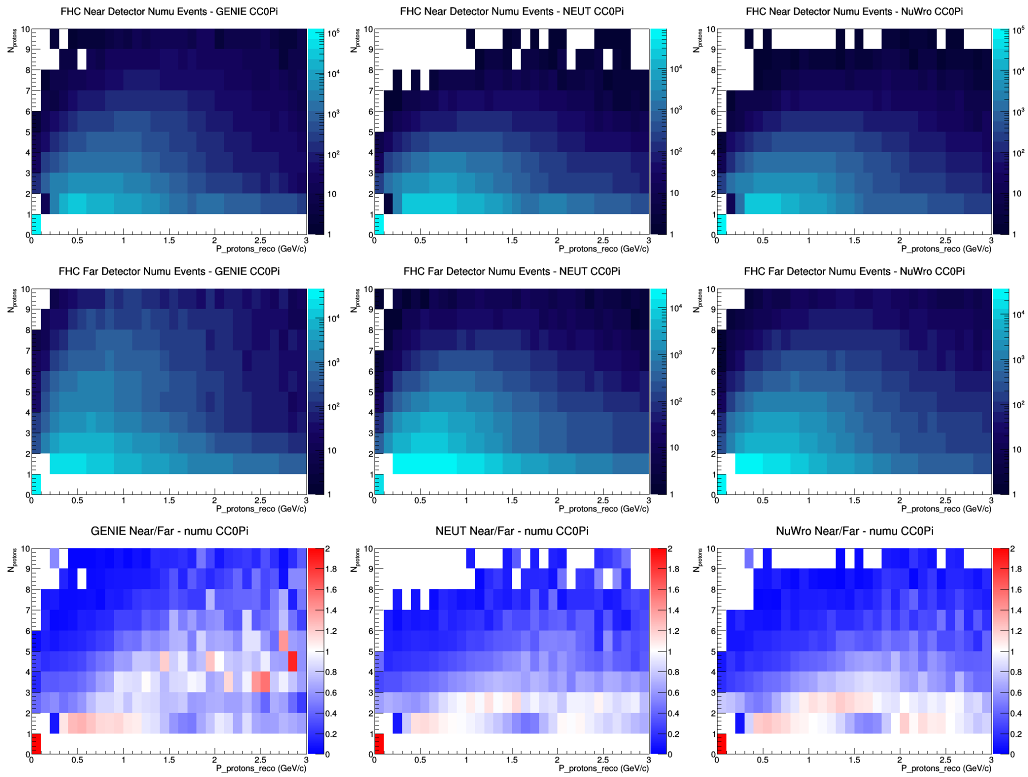

## E.19 numu CC0Pi LAr efficiencies

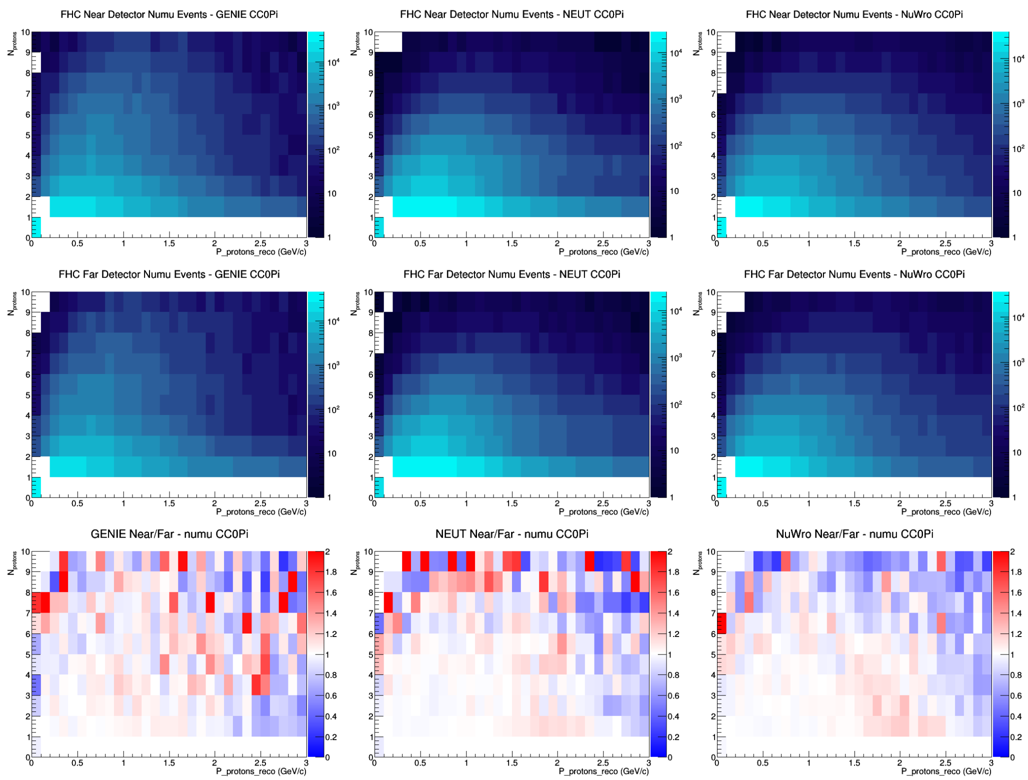

## E.20 numu CC0Pi GAr efficiencies

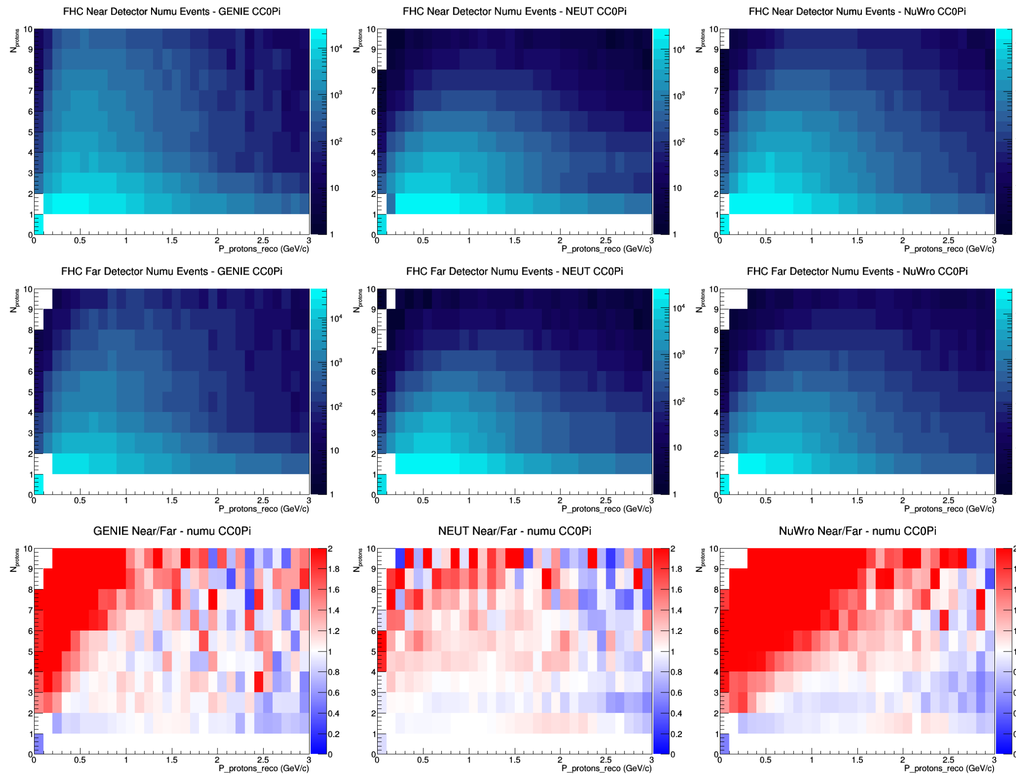

## E.21 numubar CC0Pi no efficiencies

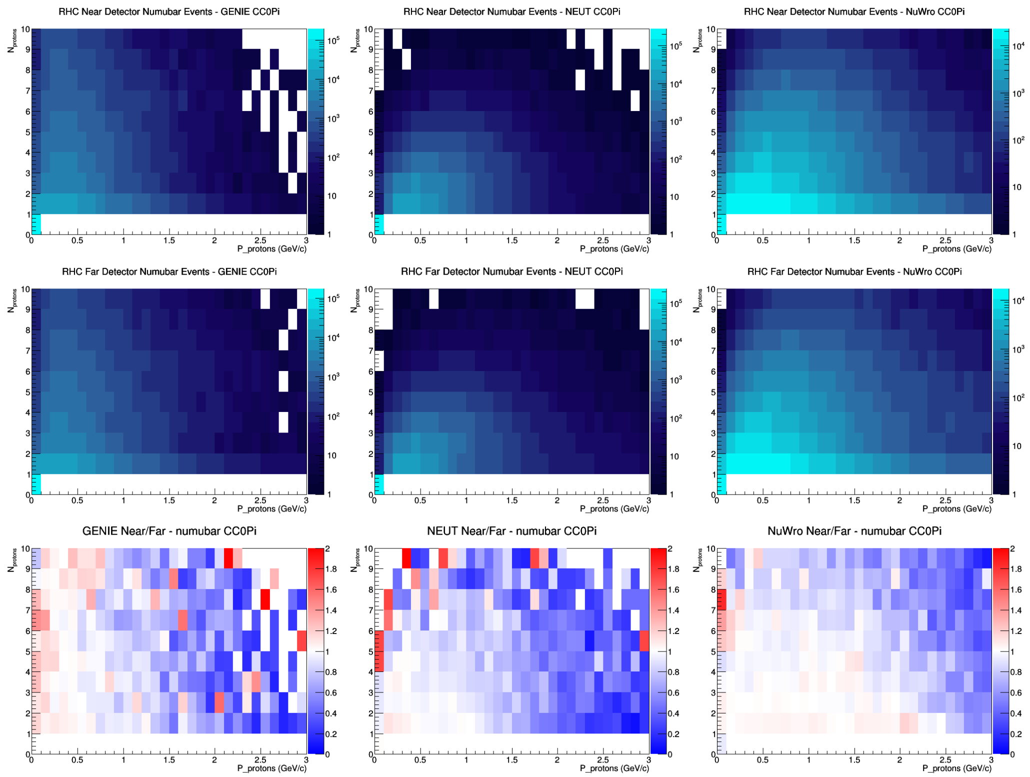

## E.22 numubar CC0Pi FGT efficiencies

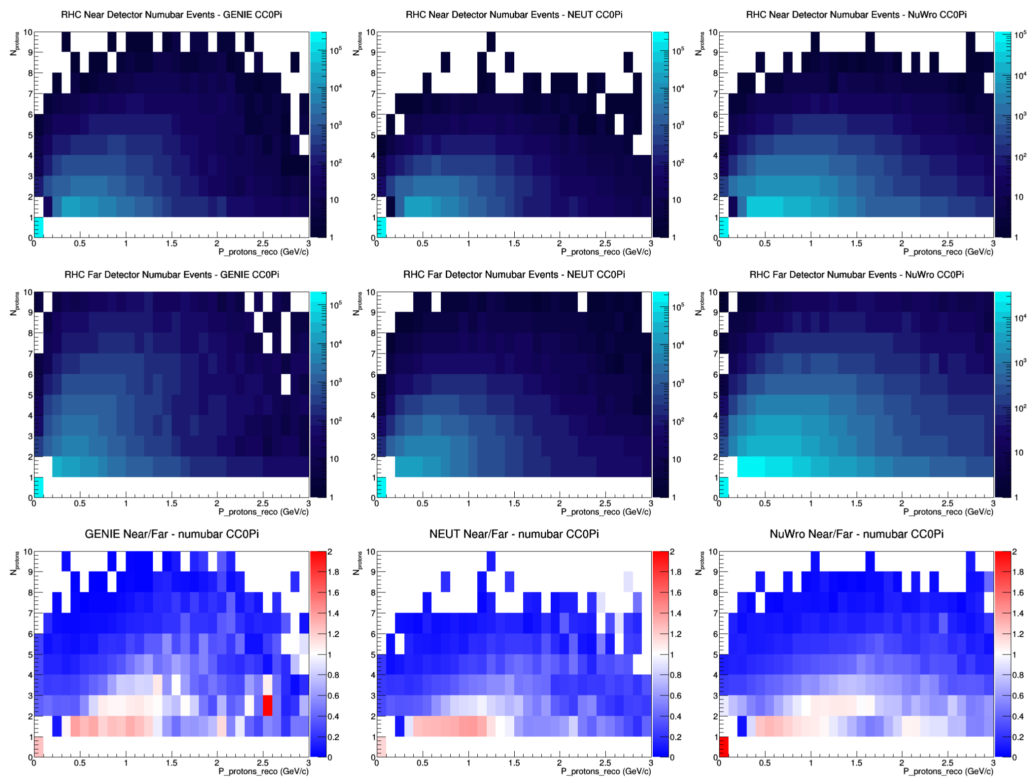

## E.23 numubar CC0Pi LAr efficiencies

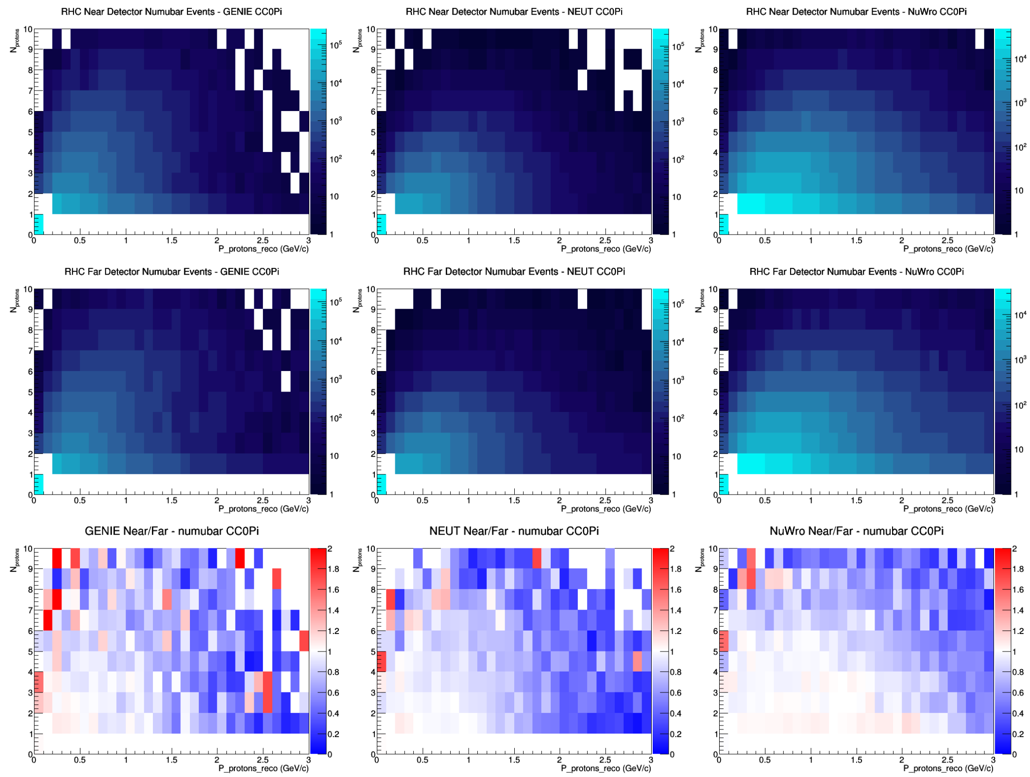

## E.24 numubar CC0Pi GAr efficiencies

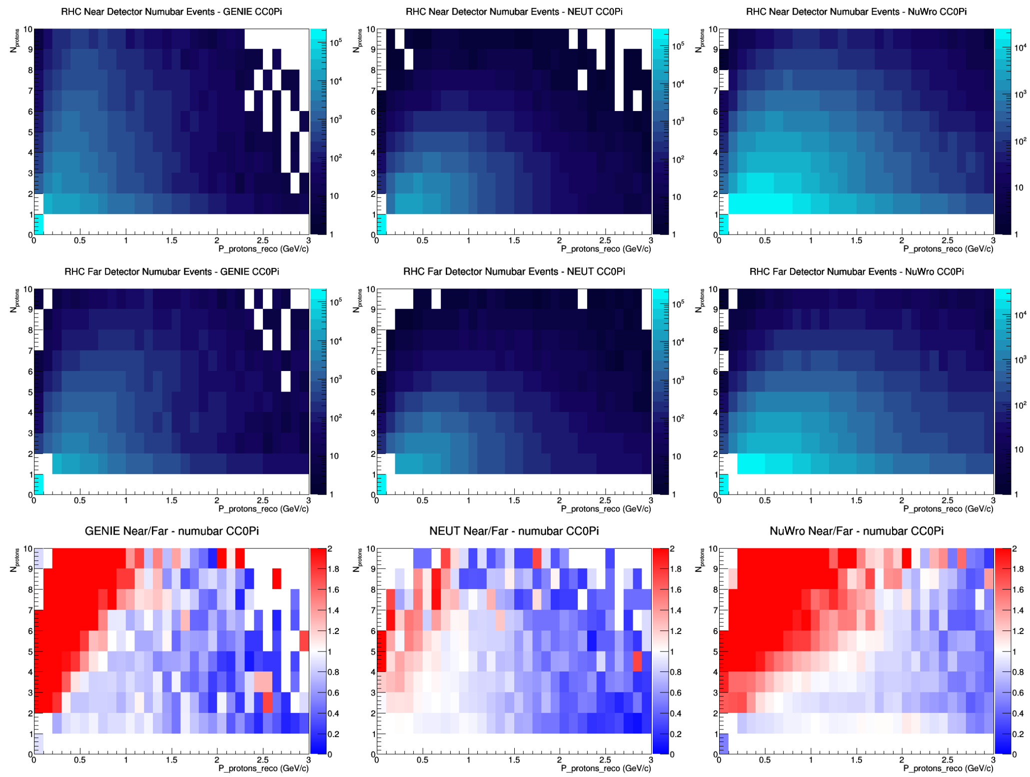

## E.25 numu CC1Pi no efficiencies

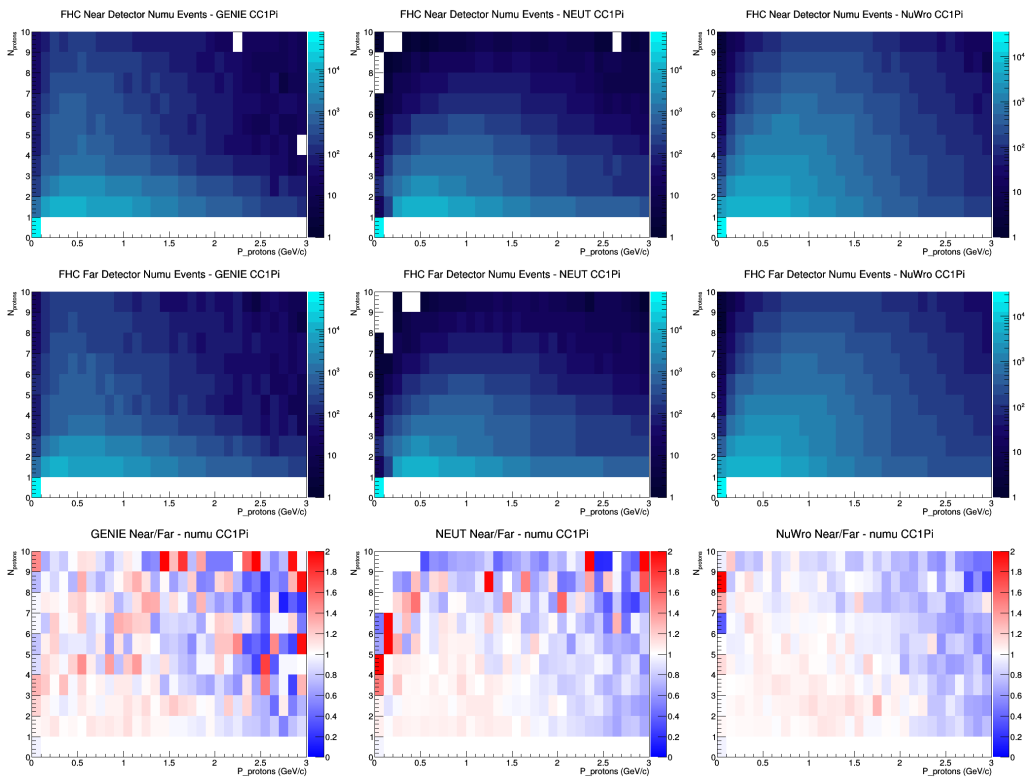

## E.26 numu CC1Pi FGT efficiencies

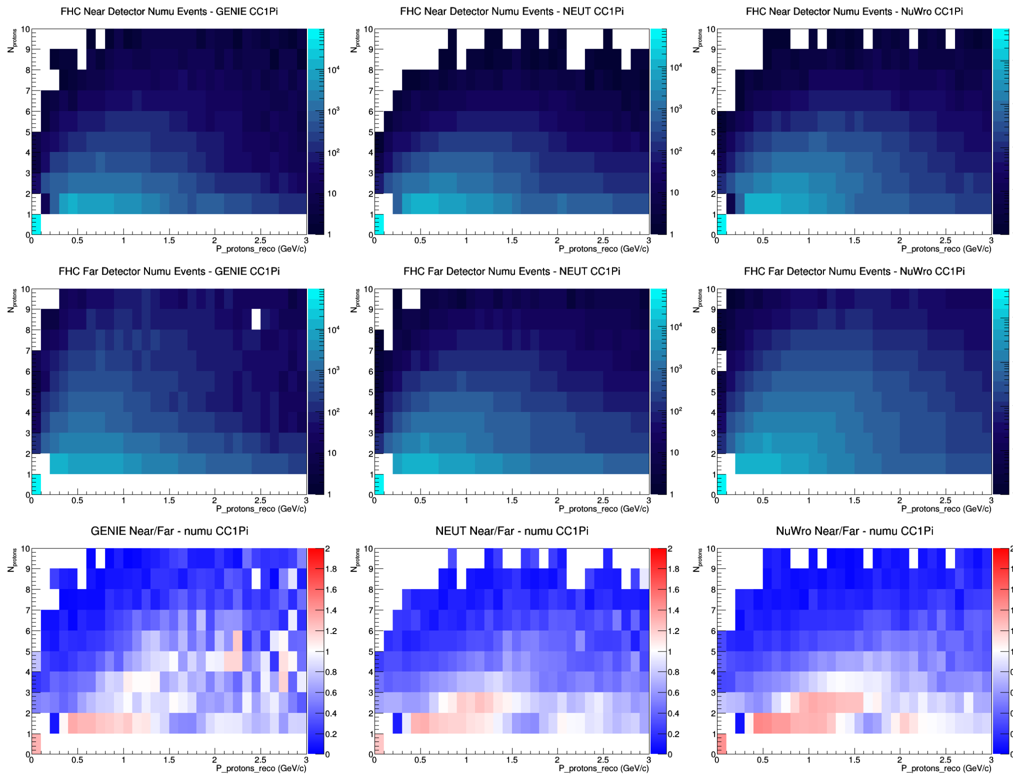

## E.27 numu CC1Pi LAr efficiencies

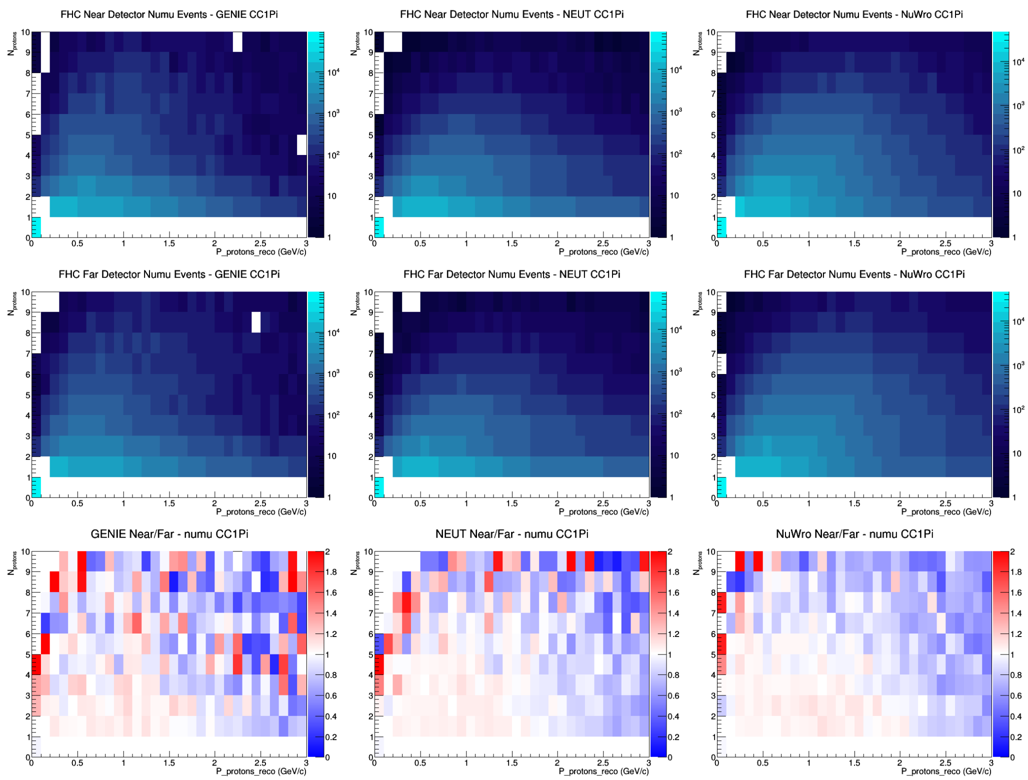

## E.28 numu CC1Pi GAr efficiencies

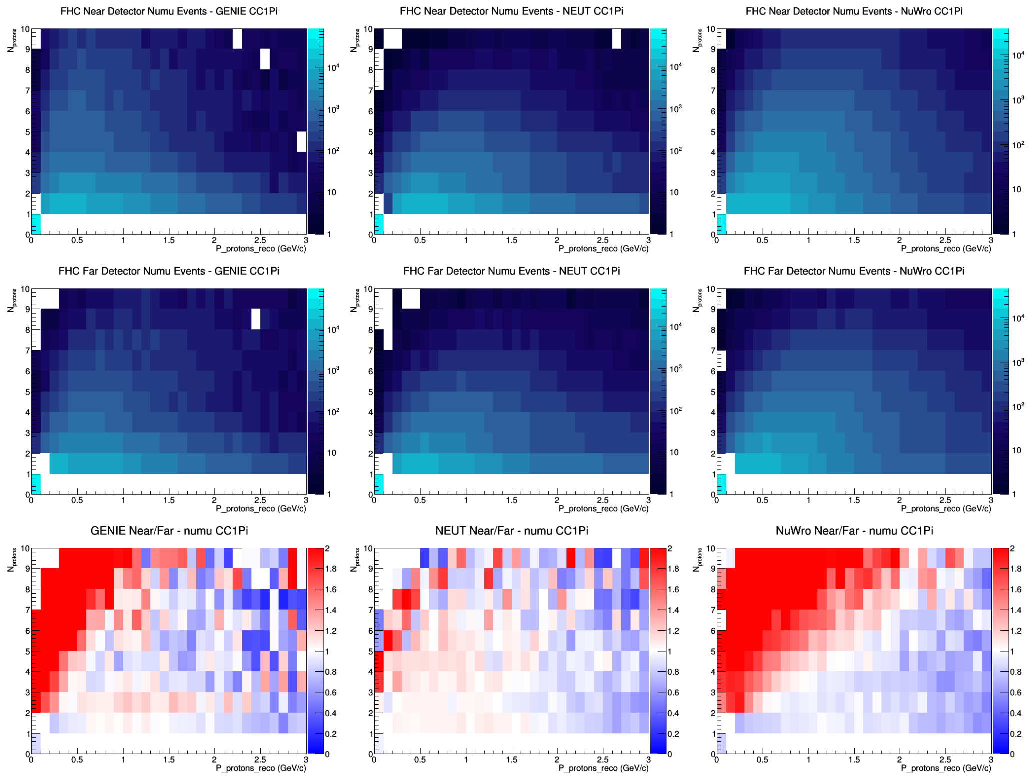

## E.29 numubar CC1Pi no efficiencies

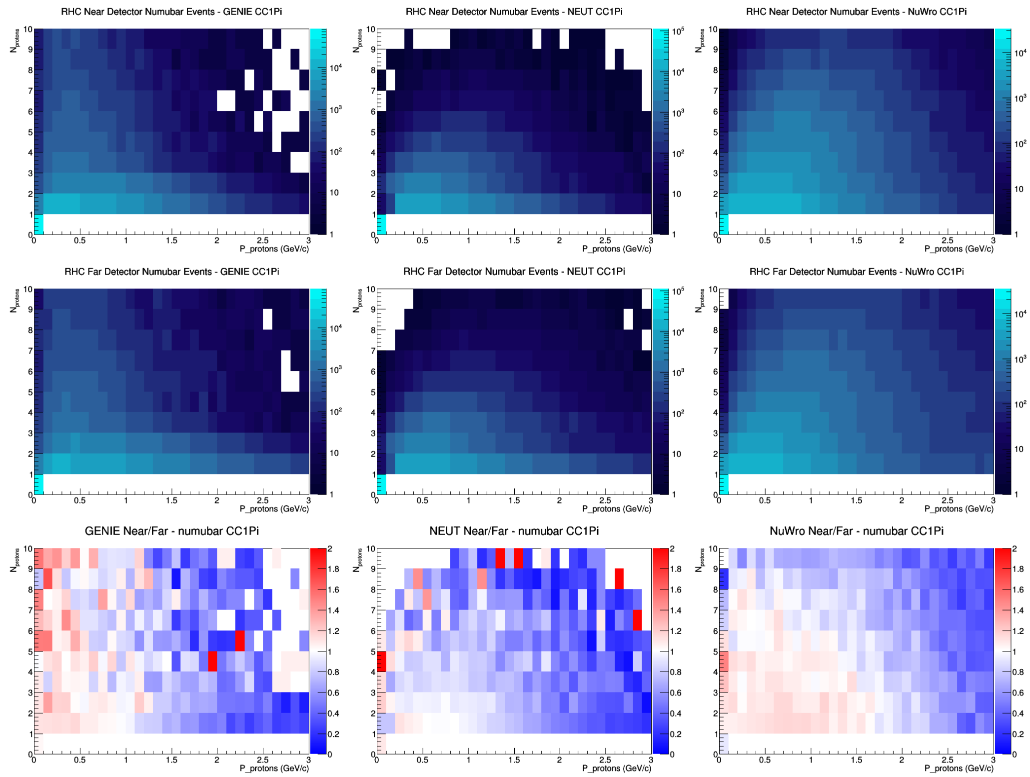

## E.30 numubar CC1Pi FGT efficiencies

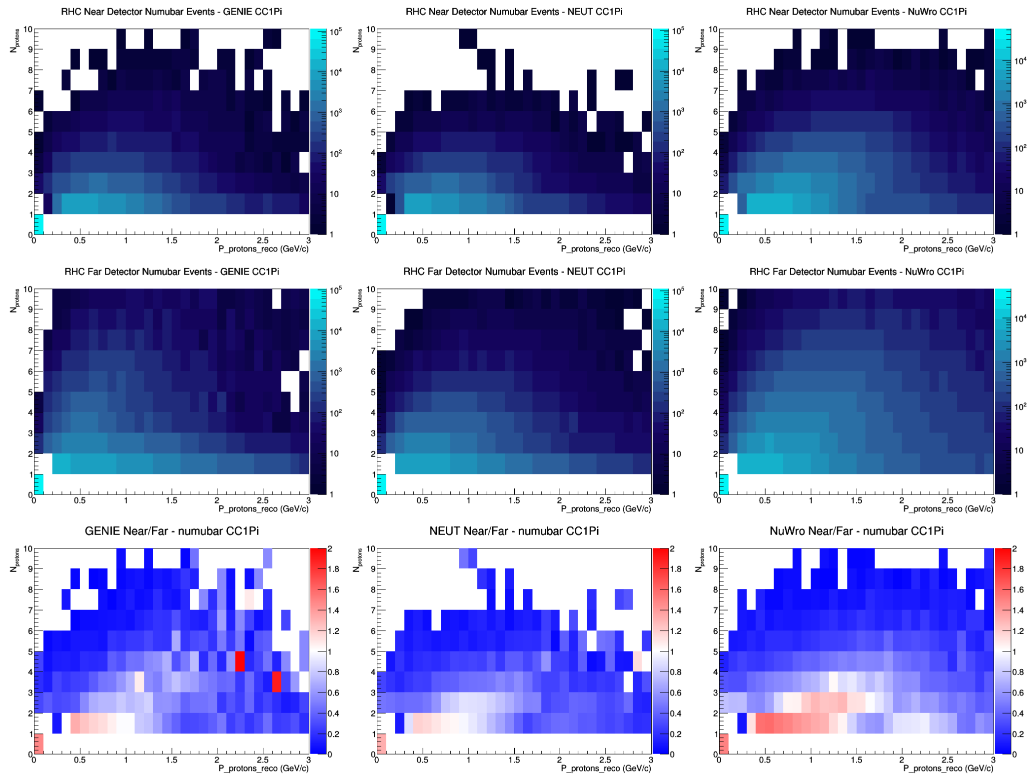

## E.31 numubar CC1Pi LAr efficiencies

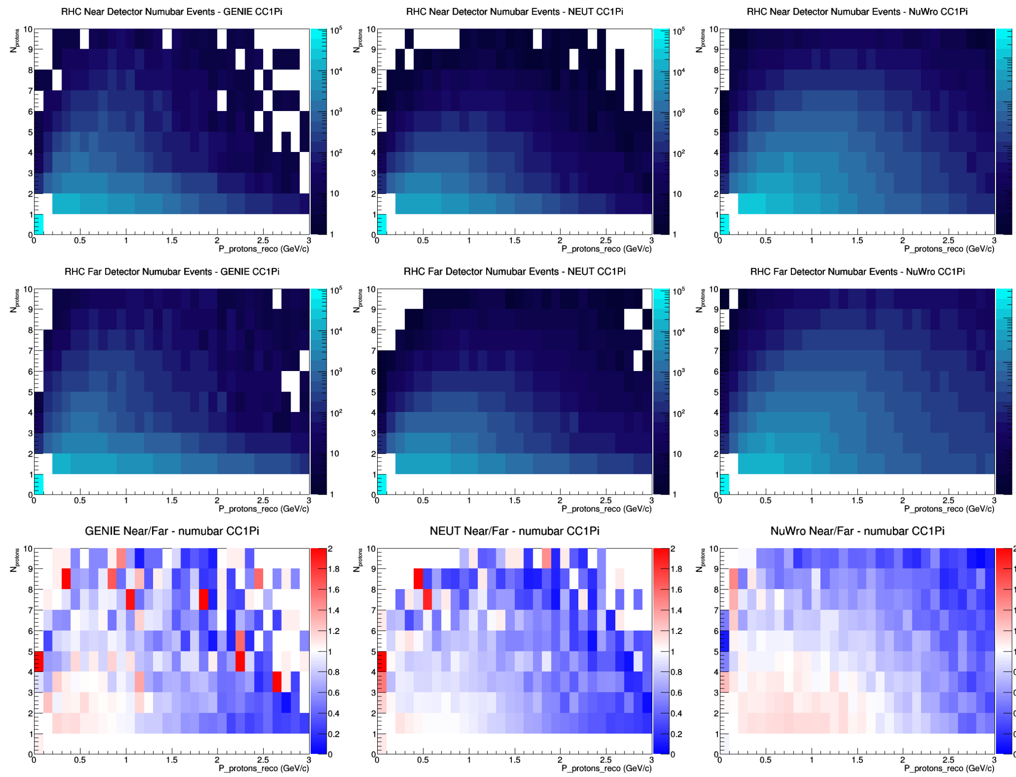

## E.32 numubar CC1Pi GAr efficiencies

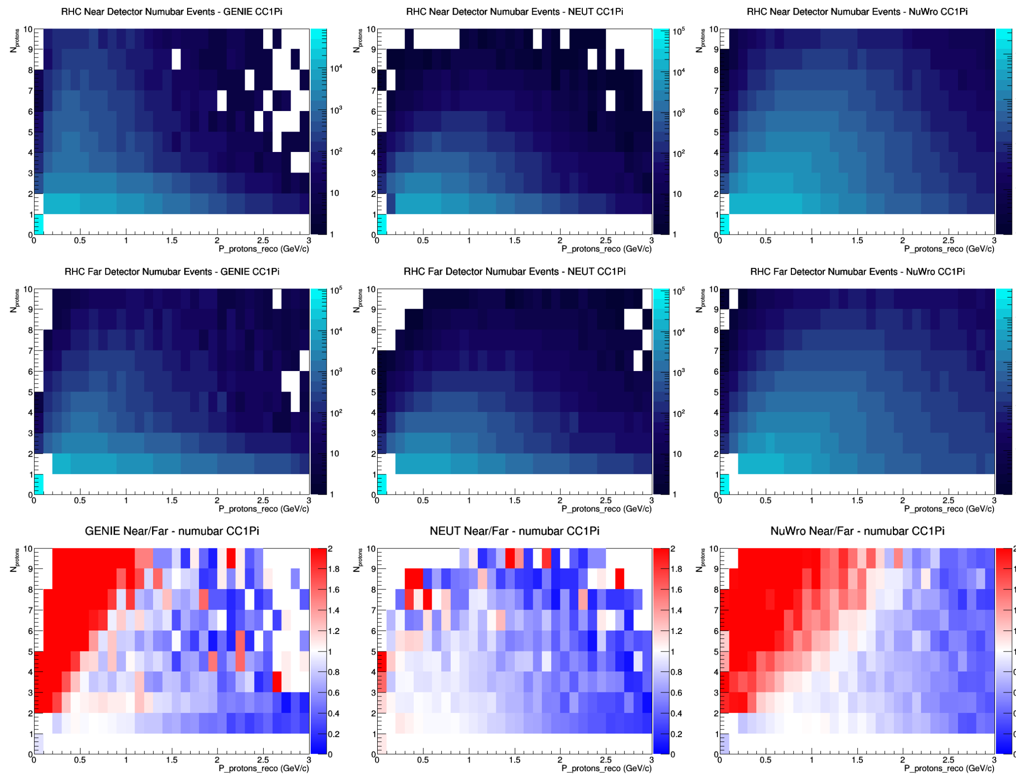

## E.33 numu CCOther FGT efficiencies

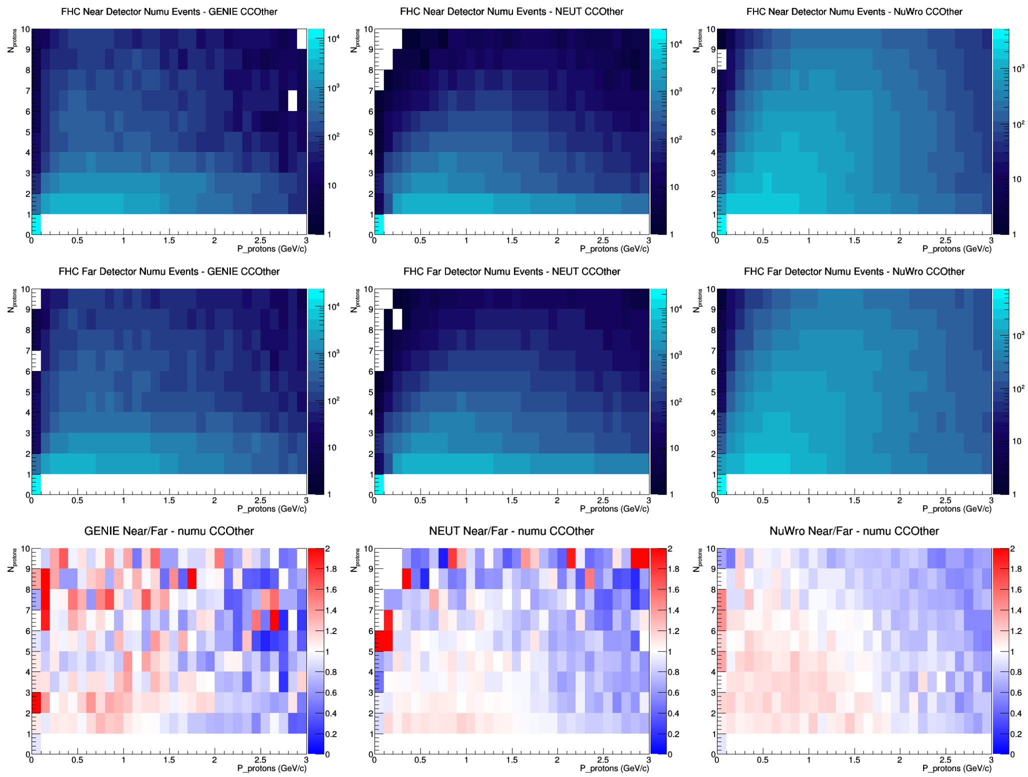

## E.34 numu CCOther FGT efficiencies

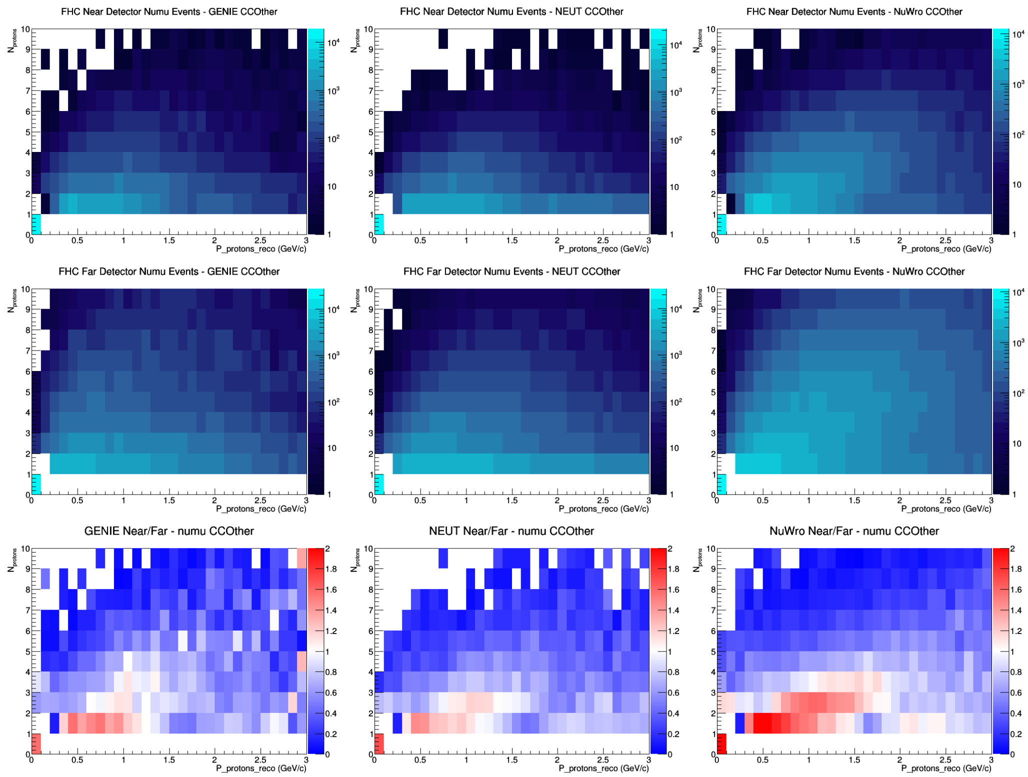

## E.35 numu CCOther LAr efficiencies

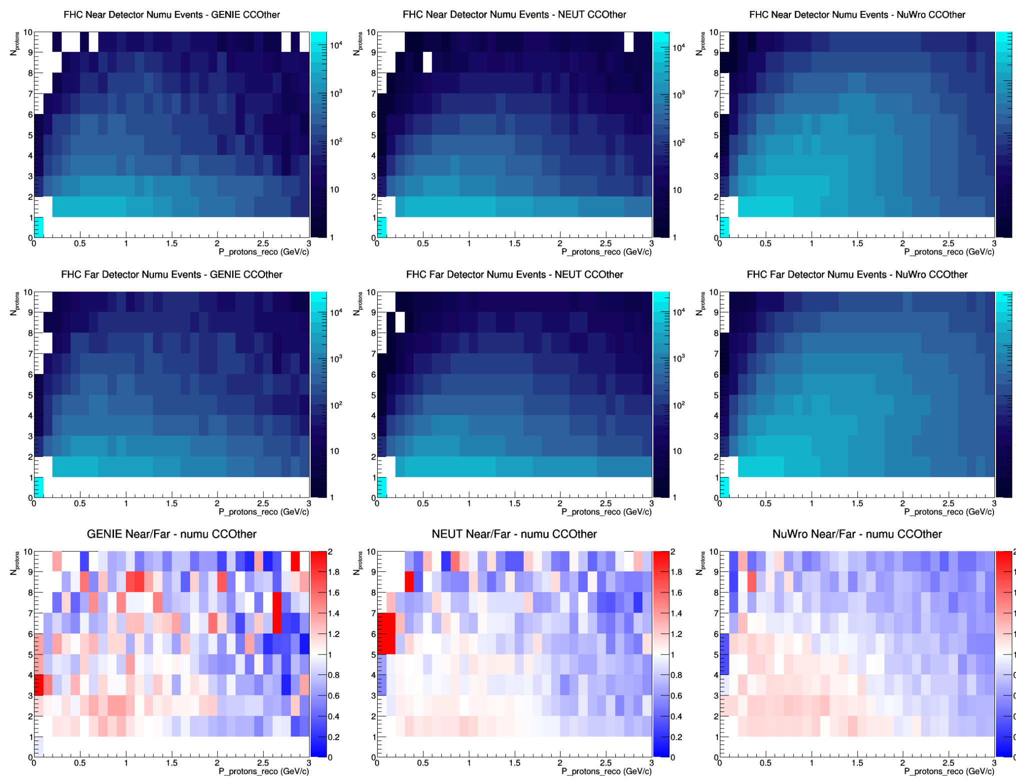

## E.36 numu CCOther GAr efficiencies

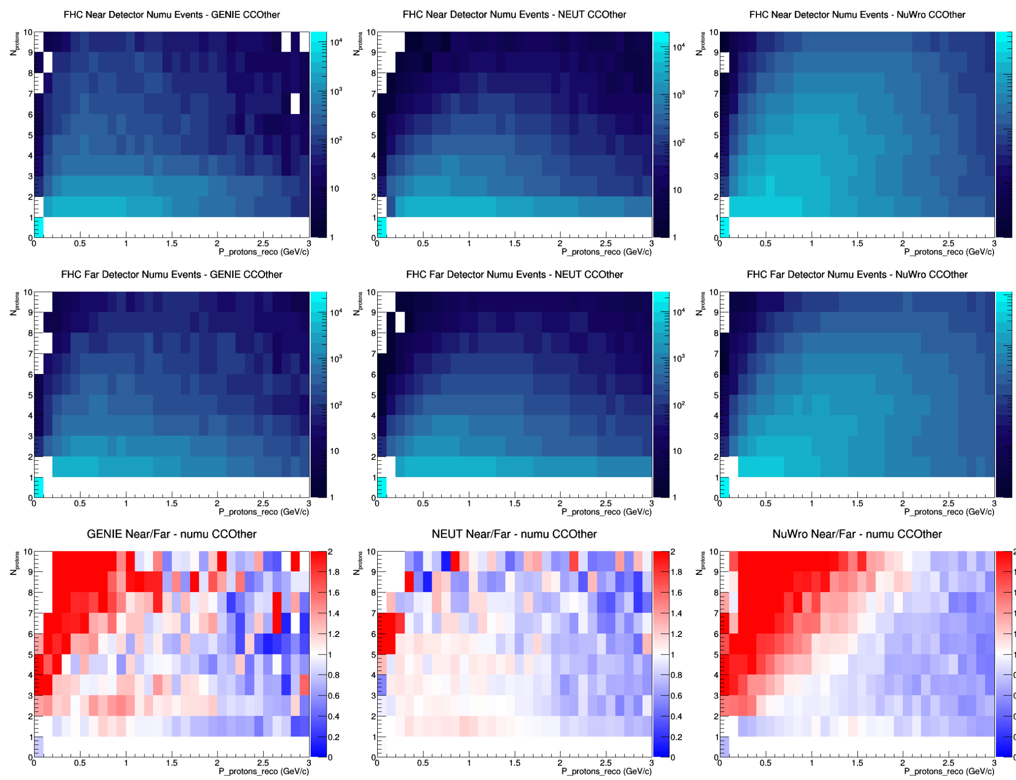

## E.37 numubar CCOther no efficiencies

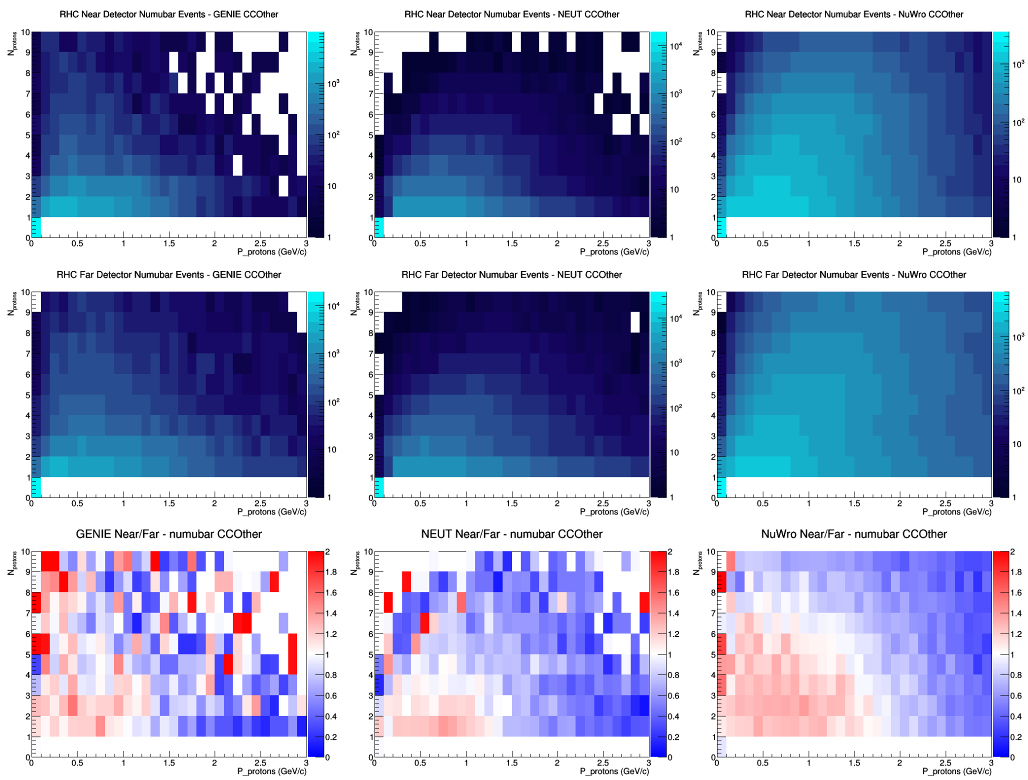

## E.38 numubar CCOther FGT efficiencies

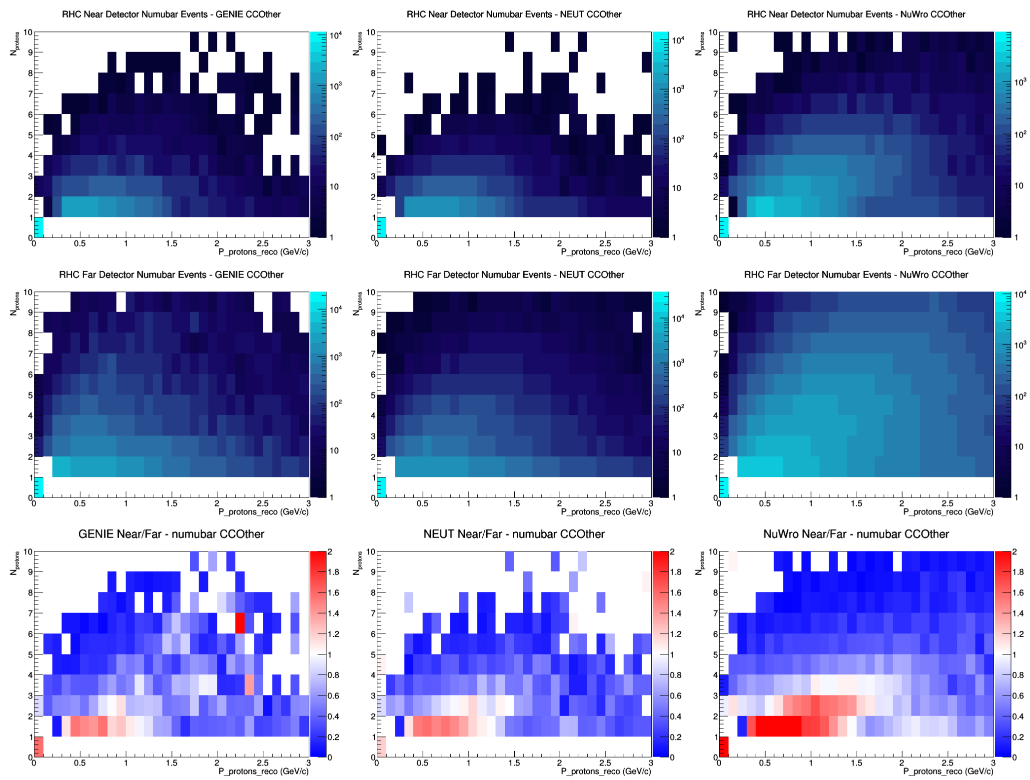

## E.39 numubar CCOther LAr efficiencies

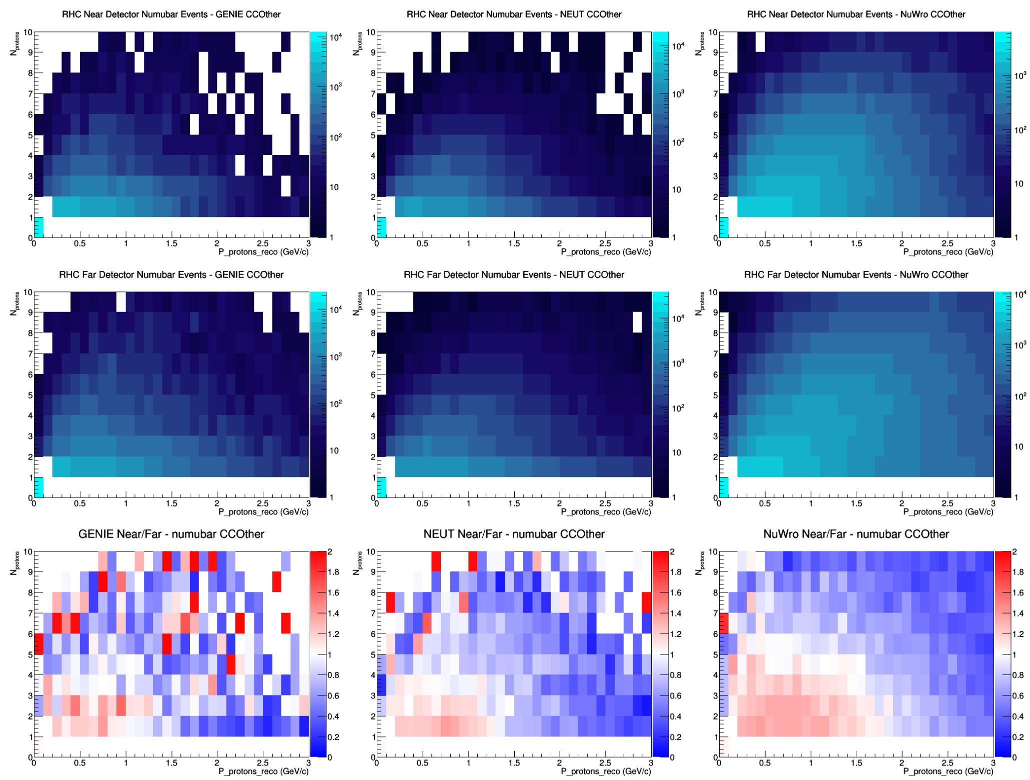

## E.40 numubar CCOther GAr efficiencies

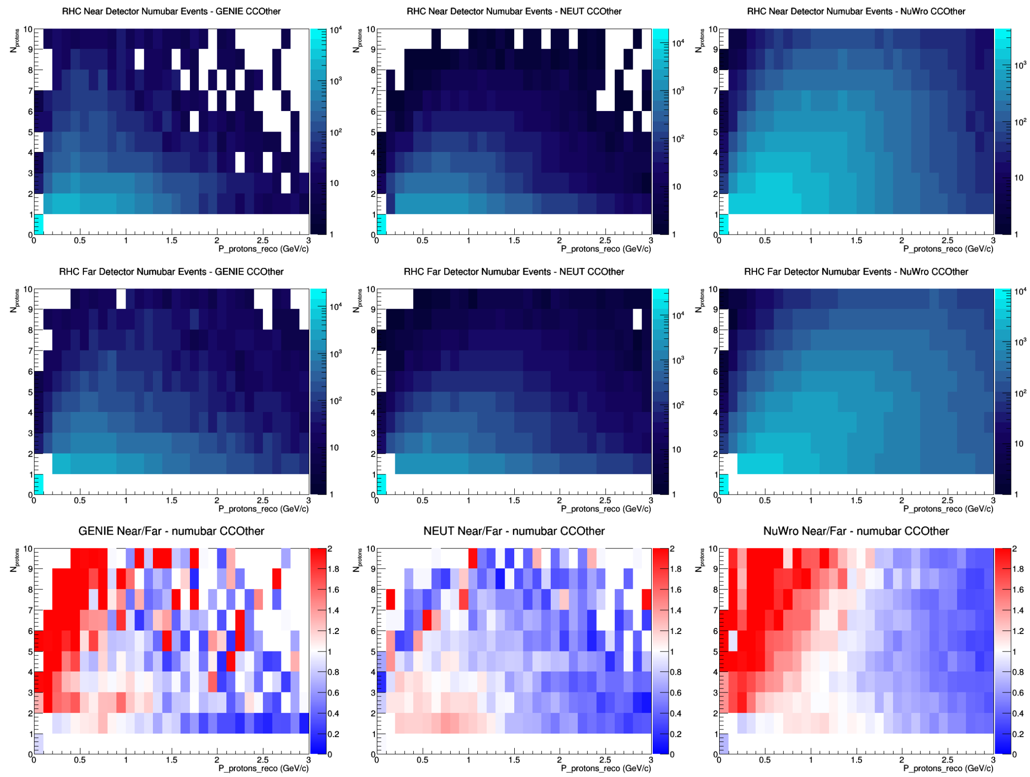

# F Etrue - Ereco Plots

This appendix includes all the plots not show in Section 5.3. For full description of the files, please make reference to that section. The plots will be put in the same order as before.

## F.1 numu

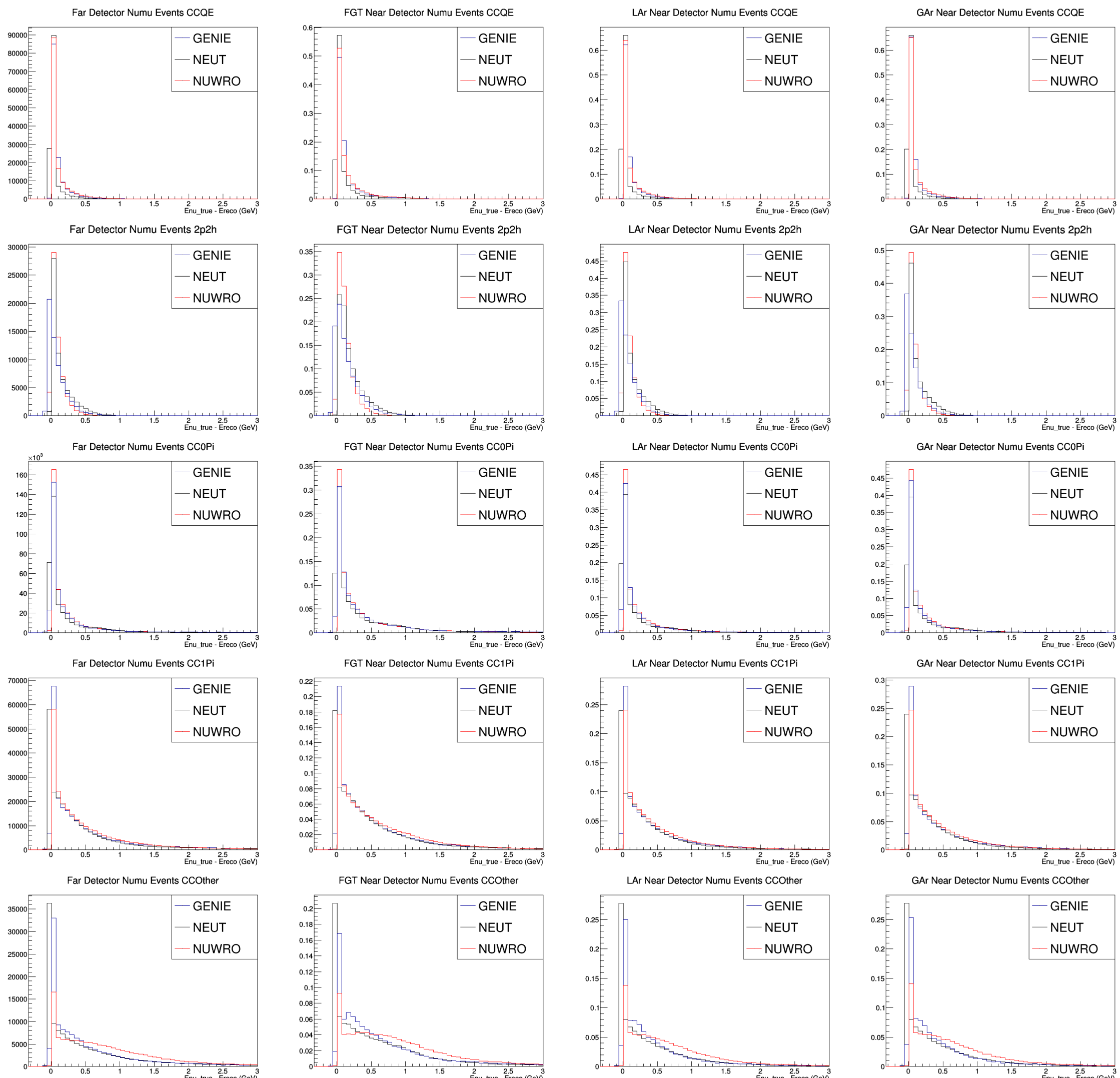

## F.2 numubar

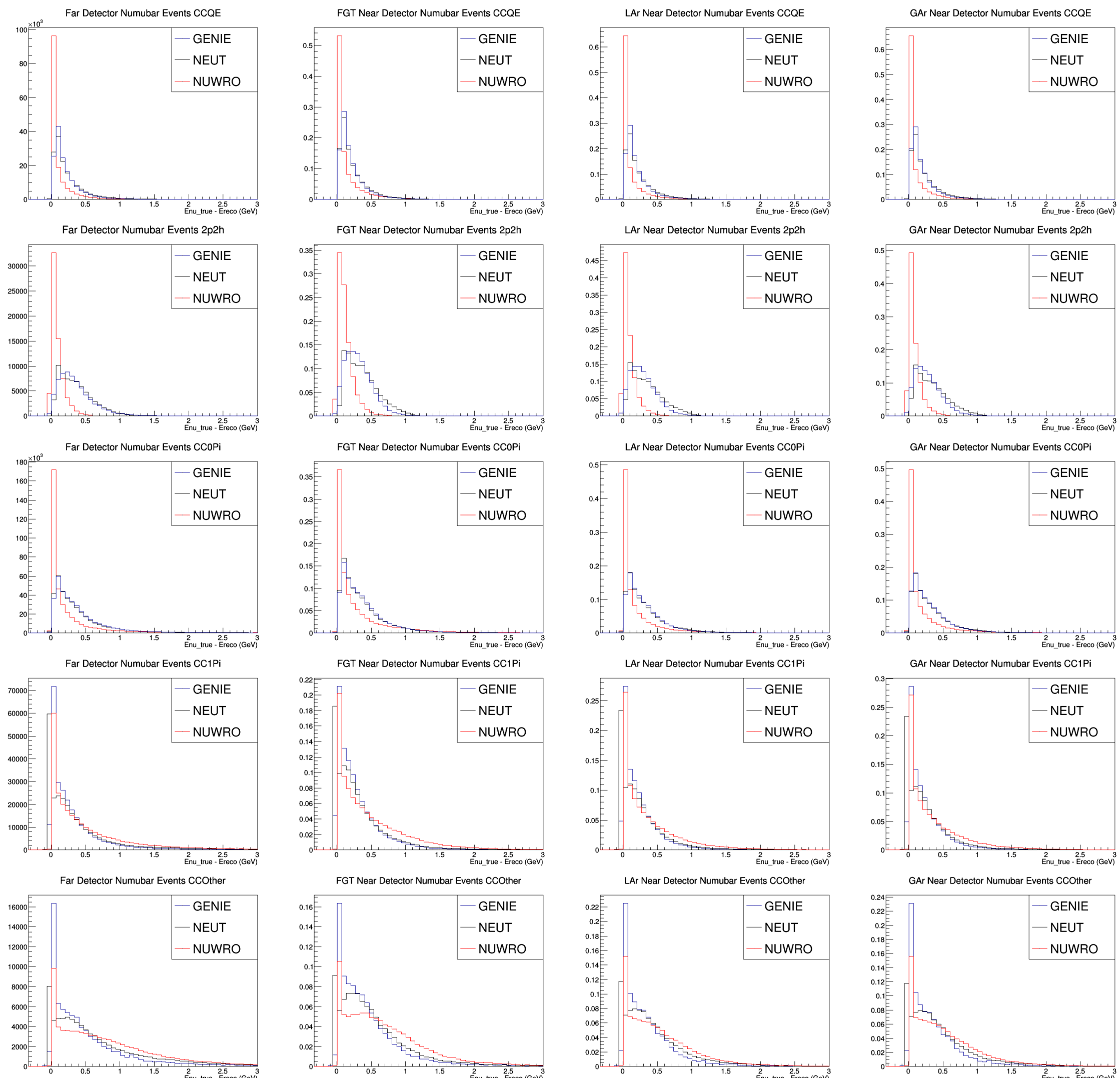

Far Detector Numubar Events CCQE
FGT Near Detector Numubar Events CCQE
LAr Near Detector Numubar Events CCQE
GAr Near Detector Numubar Events CCQE
Far Detector Numubar Events 2p2h
FGT Near Detector Numubar Events 2p2h
LAr Near Detector Numubar Events 2p2h
GAr Near Detector Numubar Events 2p2h
Far Detector Numubar Events CC0Pi
FGT Near Detector Numubar Events CC0Pi
LAr Near Detector Numubar Events CC0Pi
GAr Near Detector Numubar Events CC0Pi
Far Detector Numubar Events CC1Pi
FGT Near Detector Numubar Events CC1Pi
LAr Near Detector Numubar Events CC1Pi
GAr Near Detector Numubar Events CC1Pi
Far Detector Numubar Events CCOther
FGT Near Detector Numubar Events CCOther
LAr Near Detector Numubar Events CCOther
GAr Near Detector Numubar Events CCOther
GENIE
NEUT
NUWRO
Enu_true - Ereco (GeV)

# References

[1] The DUNE Collaboration *Long-Baseline Neutrino Facility (LBNF) and Deep Underground Neutrino Experiment (DUNE) Conceptual Design Report Volume 1: The LBNF and DUNE Projects* arXiv:1601.05471v1

[2] Maury Goodman *The Deep Underground Neutrino Experiment* Advances in High Energy Physics, vol. 2015, Article ID 256351, 9 pages, 2015. doi:10.1155/2015/256351

[3] Andreopoulos, C. *et al. The GENIE Neutrino Monte Carlo Generator*. Nucl.Instrum.Meth. A614 (2010) 87-104 arXiv:0905.2517 [hep-ph] FERMILAB-PUB-09-418-CD

[4] Hayato, Yoshinari *A neutrino interaction simulation program library NEUT*. Acta Phys.Polon. B40 (2009) 2477-2489

[5] T. Golan, J.T. Sobczyk, J. Zmuda *NuWro: the Wrocaw Monte Carlo Generator of Neutrino Interactions*. Nuclear Physics B - Proceedings Supplements 229 (2012) 499

[6] P. Stowell, C. Wret, C. Wilkinson, L. Pickering, S. Cartwright, Y. Hayato, K. Mahn, K.S. McFarland, J. Sobczyk, R. Terri, L. Thompson, M.O. Wascko, Y. Uchida *NUISANCE: a neutrino cross-section generator tuning and comparison framework* arXiv:1612:07393v2

[7] T. Alion, *et al. Experiment Simulation Configurations Used in DUNE CDR* arXiv:1606.09550

[8] Andreopoulos, *et al. VALOR DUNE Joint Oscillation and Systematics Constraint Fit*